UNIVERSITY OF MINNESOTA
ST. ANTHONY FALLS LABORATORY
Engineering, Environmental and Geophysical Fluid Dynamics

Project Report No. 417

Hydraulic Transient Analysis of TARP Phase II O'Hare Tunnel System under Different Operating Plans

by

Jianming He and Charles C. S. Song

Prepared for

U.S. ARMY CORPS OF ENGINEERS
Chicago District
111 No. Canal Street, Suite 600
Chicago, IL 60606

October 1997
Minneapolis, Minnesota

Prepared for: US Army Corps of Engineers, Chicago District
Last Revised: 2/26/98
Disk Locators: c:\PR417txt.doc;
(Disk #224: a:\PR417txt.doc; PR417cov.doc)

TABLE OF CONTENTS

TABLE OF CONTENTS i

LIST OF FIGURES iii

I. INTRODUCTION 1

1.1 STUDY OBJECTIVE 1
1.2 WORK SCOPE 1
1.3 STUDY PROGRESS 2

II. THE MIXED TRANSIENT FLOW MODEL 3

2.1 MODELING EQUATIONS 3
2.2 MODELING CONFIGURATION 4
2.3 TREATMENT OF THE DOWNSTREAM BOUNDARY CONDITION 4
2.4 OTHER INPUT DATA 5
2.5 INFLOW HYDROGRAPHS 6
2.6 TUNNEL INITIAL CONDITIONS 7

III. GENERAL HYDRAULIC TRANSIENT CHARACTERISTICS 8

3.1 GATED (AT DS-8) CASES 8
  Case 1: 4 inch 10 min storm event with an empty initial tunnel condition 8
  Case 3: 4 inch 10 min. storm event with tunnel initially at 67% full 9
  Case4-6: 4 inch 30 min. storm event with different initial tunnel conditions 9
  Case7-9: 4 inch 1 hour storm event with different initial tunnel conditions 9
  Other small rainfall and longer duration storm events 10
  Large rainfall magnitude and long duration events 10
3.2 UNGATED (DS-8) CASES 10
3.3 COMBINED (GATED AND UNGATED) INFLOW CASES 11
3.4 EFFECT OF AIR ENTRAINMENT 11

IV. CONCLUSIONS 13

4.1 GATED (DS-8) CASES: 13
4.2 UNGATED (DS-8) CASES: 14
4.3 COMBINED (GATED AND UNGATED) INFLOW CASES: 15
4.4 EFFECT OF AIR ENTRAINMENT 16

REFERENCES 17

Figures 1 through 105

LIST OF FIGURES

Fig. 1 TARP O'Hare System

Fig. 2 O'Hare tunnel system configuration for modeling purpose.

Fig. 3 Connection between the TARP Phase I tunnel system and the proposed terminal reservoir.

Fig. 4 A typical dropshaft structure (DS-4)

Fig. 5 Total inflow hydrodraphs to the tunnel system for 10 min storm events (gated at DS-8).

Fig. 6 Total inflow hydrodraphs to the tunnel system for 30 min storm events (gated at DS-8).

Fig. 7 Total inflow hydrodraphs to the tunnel system for 1 hour storm events (gated at DS-8).

Fig. 8 Total inflow hydrodraphs to the tunnel system for 2 hour storm events (gated at DS-8).

Fig. 9 Total inflow hydrodraphs to the tunnel system for 3 hour storm events (gated at DS-8).

Fig. 10 Total inflow hydrodraphs to the tunnel system for 6 to 24 hour storm events (gated at DS-8).

Fig. 11 Total inflow hydrodraphs to the tunnel system for 10 min storm events (ungated at DS-8).

Fig. 12 Total inflow hydrodraphs to the tunnel system for 30 min storm events (ungated at DS-8).

Fig. 13 Total inflow hydrodraphs to the tunnel system for 1 hour storm events (ungated at DS-8).

Fig. 14 Total inflow hydrodraphs to the tunnel system for 2 hour storm events (ungated at DS-8).

Fig. 15 Total inflow hydrodraphs to the tunnel system for 3 hour storm events (ungated at DS-8).

Fig. 16 Total inflow hydrodraphs to the tunnel system for 6 to 24 hour storm events (ungated at DS-8).

Fig. 17 Water elevation variations with time during 4 in 10 min storm event at 5 locations (DS-1, DS-5, DS-8, main shaft and reservoir), modeling conditions: empty initial tunnel condition and gated inflow at DS-8.

Fig. 18 Detailed water elevation variations with time in the surge process during 4 in 10 min storm event at 2 locations (DS-1 and DS-5), modeling conditions: empty initial tunnel condition and gated inflow at DS-8.

Fig. 19 Detailed water elevation variations with time in the surge process during 4 in 10 min storm event at 3 locations (DS-8, main shaft and reservoir), modeling conditions: empty initial tunnel condition and gated inflow at DS-8.

Fig. 20 Instantaneous water elevations in the main tunnel from DS-1 to the main shaft during 4 in 10 min storm event, modeling conditions: empty initial tunnel condition and gated inflow at DS-8.

Fig. 21 Maximum water elevations in the main tunnel from DS-1 to the main shaft during 4 in 10 min storm event, modeling conditions: empty initial tunnel condition and gated inflow at DS-8.

Fig. 22 Water elevation variations with time during 4 in 10 min storm event at 5 locations (DS-1, DS-5, DS-8, main shaft and reservoir), modeling conditions: 33% full initial tunnel condition and gated inflow at DS-8.

Fig. 23 Detailed water elevation variations with time in the surge process during 4 in 10 min storm event at 2 locations (DS-1 and DS-5), modeling conditions: 33% full initial tunnel condition and gated inflow at DS-8.

Fig. 24 Detailed water elevation variations with time in the surge process during 4 in 10 min storm event at 3 locations (DS-8, main shaft and reservoir), modeling conditions: 33% full initial tunnel condition and gated inflow at DS-8.

Fig. 25 Instantaneous water elevations in the main tunnel from DS-1 to the main shaft during 4 in 10 min storm event, modeling conditions: 33% full initial tunnel condition and gated inflow at DS-8.

Fig. 26 Maximum water elevations in the main tunnel from DS-1 to the main shaft during 4 in 10 min storm event, modeling conditions: 33% full initial tunnel condition and gated inflow at DS-8.

Fig. 27 Water elevation variations with time during 4 in 10 min storm event at 5 locations (DS-1, DS-5, DS-8, main shaft and reservoir), modeling conditions: 67% full initial tunnel condition and gated inflow at DS-8.

Fig. 28 Detailed water elevation variations with time in the surge process during 4 in 10 min storm event at 2 locations (DS-1 and DS-5), modeling conditions: 67% full initial tunnel condition and gated inflow at DS-8.

Fig. 29 Detailed water elevation variations with time in the surge process during 4 in 10 min storm event at 3 locations (DS-8, main shaft and reservoir), modeling conditions: 67% full initial tunnel condition and gated inflow at DS-8.

Fig. 30 Instantaneous water elevations in the main tunnel from DS-1 to the main shaft during 4 in 10 min storm event, modeling conditions: 67% full initial tunnel condition and gated inflow at DS-8.

Fig. 31 Maximum water elevations in the main tunnel from DS-1 to the main shaft during 4 in 10 min storm event, modeling conditions: 67% full initial tunnel condition and gated inflow at DS-8.

Fig. 32 Water elevation variations with time during 4 in 30 min storm event at 5 locations (DS-1, DS-5, DS-8, main shaft and reservoir), modeling conditions: empty initial tunnel condition and gated inflow at DS-8.

Fig. 33 Detailed water elevation variations with time in the surge process during 4 in 30 min storm event at 2 locations (DS-1 and DS-5), modeling conditions: empty initial tunnel condition and gated inflow at DS-8.

Fig. 34 Detailed water elevation variations with time in the surge process during 4 in 30 min storm event at 3 locations (DS-8, main shaft and reservoir), modeling conditions: empty initial tunnel condition and gated inflow at DS-8.

Fig. 35 Instantaneous water elevations in the main tunnel from DS-1 to the main shaft during 4 in 30 min storm event, modeling conditions: empty initial tunnel condition and gated inflow at DS-8.

Fig. 36 Maximum water elevations in the main tunnel from DS-1 to the main shaft during 4 in 30 min storm event, modeling conditions: empty initial tunnel condition and gated inflow at DS-8.

Fig. 37 Water elevation variations with time during 4 in 30 min storm event at 5 locations (DS-1, DS-5, DS-8, main shaft and reservoir), modeling conditions: 33% full initial tunnel condition and gated inflow at DS-8.

Fig. 38 Detailed water elevation variations with time in the surge process during 4 in 30 min storm event at 2 locations (DS-1 and DS-5), modeling conditions: 33% full initial tunnel condition and gated inflow at DS-8.

Fig. 39 Detailed water elevation variations with time in the surge process during 4 in 30 min storm event at 3 locations (DS-8, main shaft and reservoir), modeling conditions: 33% full initial tunnel condition and gated inflow at DS-8.

Fig. 40 Instantaneous water elevations in the main tunnel from DS-1 to the main shaft during 4 in 30 min storm event, modeling conditions: 33% full initial tunnel condition and gated inflow at DS-8.

Fig. 41 Maximum water elevations in the main tunnel from DS-1 to the main shaft during 4 in 30 min storm event, modeling conditions: 33% full initial tunnel condition and gated inflow at DS-8.

Fig. 42 Water elevation variations with time during 4 in 30 min storm event at 5 locations (DS-1, DS-5, DS-8, main shaft and reservoir), modeling conditions: 67% full initial tunnel condition and gated inflow at DS-8.

Fig. 43 Detailed water elevation variations with time in the surge process during 4 in 30 min storm event at 2 locations (DS-1 and DS-5), modeling conditions: 67% full initial tunnel condition and gated inflow at DS-8.

Fig. 44 Detailed water elevation variations with time in the surge process during 4 in 30 min storm event at 3 locations (DS-8, main shaft and reservoir), modeling conditions: 67% full initial tunnel condition and gated inflow at DS-8.

Fig. 45 Instantaneous water elevations in the main tunnel from DS-1 to the main shaft during 4 in 30 min storm event, modeling conditions: 67% full initial tunnel condition and gated inflow at DS-8.

Fig. 46 Maximum water elevations in the main tunnel from DS-1 to the main shaft during 4 in 30 min storm event, modeling conditions: 67% full initial tunnel condition and gated inflow at DS-8.

Fig. 47 Water elevation variations with time during 4 in 1 hour storm event at 5 locations (DS-1, DS-5, DS-8, main shaft and reservoir), modeling conditions: empty initial tunnel condition and gated inflow at DS-8.

Fig. 48 Detailed water elevation variations with time in the surge process during 4 in 1 hour storm event at 2 locations (DS-1 and DS-5), modeling conditions: empty initial tunnel condition and gated inflow at DS-8.

Fig. 49 Detailed water elevation variations with time in the surge process during 4 in 1 hour storm event at 3 locations (DS-8, main shaft and reservoir), modeling conditions: empty initial tunnel condition and gated inflow at DS-8.

Fig. 50 Instantaneous water elevations in the main tunnel from DS-1 to the main shaft during 4 in 1 hour storm event, modeling conditions: empty initial tunnel condition and gated inflow at DS-8.

Fig. 51 Maximum water elevations in the main tunnel from DS-1 to the main shaft during 4 in 1 hour storm event, modeling conditions: empty initial tunnel condition and gated inflow at DS-8.

Fig. 52 Water elevation variations with time during 4 in 1 hour storm event at 5 locations (DS-1, DS-5, DS-8, main shaft and reservoir), modeling conditions: 33% full initial tunnel condition and gated inflow at DS-8.

Fig. 53 Detailed water elevation variations with time in the surge process during 4 in 1 hour storm event at 2 locations (DS-1 and DS-5), modeling conditions: 33% full initial tunnel condition and gated inflow at DS-8.

Fig. 54 Detailed water elevation variations with time in the surge process during 4 in 1 hour storm event at 3 locations (DS-8, main shaft and reservoir), modeling conditions: 33% full initial tunnel condition and gated inflow at DS-8.

Fig. 55 Instantaneous water elevations in the main tunnel from DS-1 to the main shaft during 4 in 1 hour storm event, modeling conditions: 33% full initial tunnel condition and gated inflow at DS-8.

Fig. 56 Maximum water elevations in the main tunnel from DS-1 to the main shaft during 4 in 1 hour storm event, modeling conditions: 33% full initial tunnel condition and gated inflow at DS-8.

Fig. 57 Water elevation variations with time during 4 in 1 hour storm event at 5 locations (DS-1, DS-5, DS-8, main shaft and reservoir), modeling conditions: 67% full initial tunnel condition and gated inflow at DS-8.

Fig. 58 Detailed water elevation variations with time in the surge process during 4 in 1 hour storm event at 2 locations (DS-1 and DS-5), modeling conditions: 67% full initial tunnel condition and gated inflow at DS-8.

Fig. 59 Detailed water elevation variations with time in the surge process during 4 in 1 hour storm event at 3 locations (DS-8, main shaft and reservoir), modeling conditions: 67% full initial tunnel condition and gated inflow at DS-8.

Fig. 60 Instantaneous water elevations in the main tunnel from DS-1 to the main shaft during 4 in 1 hour storm event, modeling conditions: 67% full initial tunnel condition and gated inflow at DS-8.

Fig. 61 Maximum water elevations in the main tunnel from DS-1 to the main shaft during 4 in 1 hour storm event, modeling conditions: 67% full initial tunnel condition and gated inflow at DS-8.

Fig. 62 Water elevation variations with time during 4 in 2 hour storm event at 5 locations (DS-1, DS-5, DS-8, main shaft and reservoir), modeling conditions: empty initial tunnel condition and gated inflow at DS-8.

Fig. 63 Detailed water elevation variations with time in the surge process during 4 in 2 hour storm event at 2 locations (DS-1 and DS-5), modeling conditions: empty initial tunnel condition and gated inflow at DS-8.

Fig. 64 Detailed water elevation variations with time in the surge process during 4 in 2 hour storm event at 3 locations (DS-8, main shaft and reservoir), modeling conditions: empty initial tunnel condition and gated inflow at DS-8.

Fig. 65 Instantaneous water elevations in the main tunnel from DS-1 to the main shaft during 4 in 2 hour storm event, modeling conditions: empty initial tunnel condition and gated inflow at DS-8.

Fig. 66 Maximum water elevations in the main tunnel from DS-1 to the main shaft during 4 in 2 hour storm event, modeling conditions: empty initial tunnel condition and gated inflow at DS-8.

Fig. 67 Water elevation variations with time during 3 in 10 min storm event at 5 locations (DS-1, DS-5, DS-8, main shaft and reservoir), modeling conditions: empty initial tunnel condition and gated inflow at DS-8.

Fig. 68 Detailed water elevation variations with time in the surge process during 3 in 10 min storm event at 2 locations (DS-1 and DS-5), modeling conditions: empty initial tunnel condition and gated inflow at DS-8.

Fig. 69 Detailed water elevation variations with time in the surge process during 3 in 10 min storm event at 3 locations (DS-8, main shaft and reservoir), modeling conditions: empty initial tunnel condition and gated inflow at DS-8.

Fig. 70 Instantaneous water elevations in the main tunnel from DS-1 to the main shaft during 3 in 10 min storm event, modeling conditions: empty initial tunnel condition and gated inflow at DS-8.

Fig. 71 Maximum water elevations in the main tunnel from DS-1 to the main shaft during 3 in 10 min storm event, modeling conditions: empty initial tunnel condition and gated inflow at DS-8.

Fig. 72 Water elevation variations with time during 6 in 12 hour storm event at 5 locations (DS-1, DS-5, DS-8, main shaft and reservoir), modeling conditions: 67% full initial tunnel condition and gated inflow at DS-8.

Fig. 73 Instantaneous water elevations in the main tunnel from DS-1 to the main shaft during 6 in 12 hour storm event, modeling conditions: 67% full initial tunnel condition and gated inflow at DS-8.

Fig. 74 Maximum water elevations in the main tunnel from DS-1 to the main shaft during 6 in 12 hour storm event, modeling conditions: 67% full initial tunnel condition and gated inflow at DS-8.

Fig. 75 Water elevation variations with time during 6 in 24 hour storm event at 5 locations (DS-1, DS-5, DS-8, main shaft and reservoir), modeling conditions: 67% full initial tunnel condition and gated inflow at DS-8.

Fig. 76 Instantaneous water elevations in the main tunnel from DS-1 to the main shaft during 6 in 24 hour storm event, modeling conditions: 67% full initial tunnel condition and gated inflow at DS-8.

Fig. 77 Maximum water elevations in the main tunnel from DS-1 to the main shaft during 6 in 24 hour storm event, modeling conditions: 67% full initial tunnel condition and gated inflow at DS-8.

Fig. 78 Water elevation variations with time during 6 in 12 hour storm event at 5 locations (DS-1, DS-5, DS-8, main shaft and reservoir), modeling conditions: empty full initial tunnel condition and ungated inflow at DS-8.

Fig. 79 Instantaneous water elevations in the main tunnel from DS-1 to the main shaft during 6 in 12 hour storm event, modeling conditions: empty full initial tunnel condition and ungated inflow at DS-8.

Fig. 80 Maximum water elevations in the main tunnel from DS-1 to the main shaft during 6 in 12 hour storm event, modeling conditions: empty full initial tunnel condition and ungated inflow at DS-8.

Fig. 81 Water elevation variations with time during 6 in 12 hour storm event at 5 locations (DS-1, DS-5, DS-8, main shaft and reservoir), modeling conditions: 67% full initial tunnel condition and ungated inflow at DS-8.

Fig. 82 Instantaneous water elevations in the main tunnel from DS-1 to the main shaft during 6 in 12 hour storm event, modeling conditions: 67% full initial tunnel condition and ungated inflow at DS-8.

Fig. 83 Maximum water elevations in the main tunnel from DS-1 to the main shaft during 6 in 12 hour storm event, modeling conditions: 67% full initial tunnel condition and ungated inflow at DS-8.

Fig. 84 Water elevation variations with time during 6 in 24 hour storm event at 5 locations (DS-1, DS-5, DS-8, main shaft and reservoir), modeling conditions: empty full initial tunnel condition and ungated inflow at DS-8.

Fig. 85 Instantaneous water elevations in the main tunnel from DS-1 to the main shaft during 6 in 24 hour storm event, modeling conditions: empty full initial tunnel condition and ungated inflow at DS-8.

Fig. 86 Maximum water elevations in the main tunnel from DS-1 to the main shaft during 6 in 24 hour storm event, modeling conditions: empty full initial tunnel condition and ungated inflow at DS-8.

Fig. 87 Water elevation variations with time during 6 in 24 hour storm event at 5 locations (DS-1, DS-5, DS-8, main shaft and reservoir), modeling conditions: 67% full initial tunnel condition and ungated inflow at DS-8.

Fig. 88 Instantaneous water elevations in the main tunnel from DS-1 to the main shaft during 6 in 24 hour storm event, modeling conditions: 67% full initial tunnel condition and ungated inflow at DS-8.

Fig. 89 Maximum water elevations in the main tunnel from DS-1 to the main shaft during 6 in 24 hour storm event, modeling conditions: 67% full initial tunnel condition and ungated inflow at DS-8.

Fig. 90 Total inflow hydrodraphs to the tunnel system for 10 min storm events (combined inflow at DS-8).

Fig. 91 Total inflow hydrodraphs to the tunnel system for 30 min storm events (combined inflow at DS-8).

Fig. 92 Total inflow hydrodraphs to the tunnel system for 1 hour storm events (combined inflow at DS-8).

Fig. 93 Total inflow hydrodraphs to the tunnel system for 2 hour storm events (combined inflow at DS-8).

Fig. 94 Total inflow hydrodraphs to the tunnel system for 3 hour storm events (combined inflow at DS-8).

Fig. 95 Total inflow hydrodraphs to the tunnel system for 6 to 24 hour storm events (combined inflow at DS-8).

Fig. 96 Water elevation variations with time during 4 in 10 min storm event at 5 locations (DS-1, DS-5, DS-8, main shaft and reservoir), modeling conditions: empty initial tunnel condition, wave speed=400 ft/s, and combined inflow at DS-8.

Fig. 97 Detailed water elevation variations with time in the surge process during 4 in 10 min storm event at 2 locations (DS-1 and DS-5), modeling conditions: empty initial tunnel condition, wave speed=400 ft/s, and combined inflow at DS-8.

Fig. 98 Detailed water elevation variations with time in the surge process during 4 in 10 min storm event at 3 locations (DS-8, main shaft and reservoir), modeling conditions: empty initial tunnel condition, wave speed=400 ft/s, and combined inflow at DS-8.

Fig. 99 Instantaneous water elevations in the main tunnel from DS-1 to the main shaft during 4 in 10 min storm event, modeling conditions: empty initial tunnel condition, wave speed=400 ft/s, and combined inflow at DS-8.

Fig. 100 Maximum water elevations in the main tunnel from DS-1 to the main shaft during 4 in 10 min storm event, modeling conditions: empty initial tunnel condition, wave speed=400 ft/s, and combined inflow at DS-8.

Fig. 101 Water elevation variations with time during 4 in 10 min storm event at 5 locations (DS-1, DS-5, DS-8, main shaft and reservoir), modeling conditions: initially 85% full tunnel condition, wave speed=400 ft/s, and combined inflow at DS-8.

Fig. 102 Detailed water elevation variations with time in the surge process during 4 in 10 min storm event at 2 locations (DS-1 and DS-5), modeling conditions: initially 85% full tunnel condition, wave speed=400 ft/s, and combined inflow at DS-8.

Fig. 103 Detailed water elevation variations with time in the surge process during 4 in 10 min storm event at 3 locations (DS-8, main shaft and reservoir), modeling conditions: initially 85% full tunnel condition, wave speed=400 ft/s, and combined inflow at DS-8.

Fig. 104 Instantaneous water elevations in the main tunnel from DS-1 to the main shaft during 4 in 10 min storm event, modeling conditions: initially 85% full tunnel condition, wave speed=400 ft/s, and combined inflow at DS-8.

Fig. 105 Maximum water elevations in the main tunnel from DS-1 to the main shaft during 4 in 10 min storm event, modeling conditions: initially 85% full tunnel condition, wave speed=400 ft/s, and combined inflow at DS-8.

I. INTRODUCTION

1.1 Study Objective

The O'Hare System of the Tunnel and Reservoir Plan (TARP), which serves 11.2 square miles of combined sewers, as shown in Fig. 1, is the smallest of the four systems comprising the 352-square mile combined sewer services area operated by the Metropolitan Water Reclamation District of Greater Chicago (MWRDGC).

The potential for surge type problems within the Chicago Area TARP tunnels was demonstrated early after the initial construction and operation of the mainstream tunnel system by storms of September and October 1986. A previous study conducted by Song et al. [1]* analyzed the surge phenomena within the main tunnel system and recommended potential solutions to its control. MWRDGC developed an operating plan to regulate inflows with the dropshaft gates to deal with the phenomena. The phenomena of the surge exists in the main stream tunnel system because the system, under uncontrolled conditions, can produce upstream inflows which exceed tunnel conveyance capacity during the process of tunnel pressurization. The tunnel oscillations of this condition can further be amplified within existing drop shafts. The potential for this phenomena was determined to exist within the CUP O'Hare Tunnel system based on a study by Guo and Song [2] using a designed hydrograph for the Chicago District.

The purpose of this phase of study is to determine the surge magnitudes associated with different tunnel initial conditions for specified storm events. Based on the results of the simulation runs, strong surges which may negatively affect the tunnel safety, should be identified and an appropriate operation procedure, such as limiting the inflow using the dropshaft gates, is to be suggested.

1.2 Work Scope

For the purpose described above, the following three major tasks are carried out:

a. Analyze a series of synthetic storm rainfall runoff events with the Mixed Transient Model (MXTRAN) previously developed by Dr. Charles Song's group of the University of Minnesota. This model was previously used for the CUP O'Hare system [2] in 1988. However, since the original code was developed and run on an old VAX

---

* Numbers in brackets indicate references on page 17.

machine, which no longer exists, the new version of the MXTRAN will be developed for the CUP O'Hare system.

b. Set up and analyze the impacts of tunnel oscillation and surge within drop shafts using a separate math model as described in [1].

c. From the data analysis of the steps above, develop an operation schedule of inflow control method, if necessary.

1.3 Study Progress

The study was initiated after Mr. David Moughton of the U.S. Army Corps of Engineers visited the St. Anthony Falls Laboratory, University of Minnesota, when he transferred the hydrograph data to Dr. Song's group in April 1997.

This report discusses the significant modeling results based on the runs described above.

II. THE MIXED TRANSIENT FLOW MODEL

2.1 Modeling Equations

The flow to be simulated is very unsteady and features highly dynamic phenomena such as pressurization surge and geysering. The transient flow model used, then, must be able to simultaneously calculate unsteady open channel flows and unsteady pressurized flows, including the abrupt change that occurs at the shock or the surge front.

The well-known St. Venant equations:

$$\frac{\partial y}{\partial t}+v\frac{\partial y}{\partial x}+\frac{c^2}{g}\frac{\partial v}{\partial x}=0 \tag{1}$$

$$g\frac{\partial y}{\partial x}+\frac{\partial y}{\partial t}+v\frac{\partial v}{\partial x}+g(S_f-S_o)=0 \tag{2}$$

are used to represent the unsteady open channel flow. In the above equations, y is the flow depth, v is the flow velocity, c is the gravity wave speed, S_o is the channel slope, S_f is the energy slope, and g is the acceleration due to gravity, x is the distance along a tunnel, and t is time.

The corresponding equations for unsteady pressurized flow are:

$$\frac{\partial y}{\partial t}+v\frac{\partial y}{\partial x}+\frac{a^2}{g}\frac{\partial v}{\partial x}=0 \tag{3}$$

$$g\frac{\partial y}{\partial x}+\frac{\partial y}{\partial t}+v\frac{\partial v}{\partial x}+g(S_f-S_o)=0 \tag{4}$$

in which a is the pressure wave speed, while y takes the meaning of piezometric head measured from the tunnel invert. The systems of the equations (1) - (4) are solved by the method of Characteristics [3].

Because the transition from the open channel flow condition to pressurized flow condition must be abrupt, as in the case of a hydraulic jump, the special shock boundary conditions must be applied. It was shown by Cardle and Song [3], for a pressurization surge or a positive surge, that three characteristic equations plus two shock boundary conditions can be used to calculate five unknowns at the interface. These five unknowns are v and y on both sides of the interface and the speed of the interface movement. The model can also simulate the negative surge which occurs during the depressurization process. The detailed physical nature of the process has been discussed by Guo and Song [4].

A number of other boundary conditions representing junctions, dropshafts, upstream ends, downstream end, reservoirs, pump stations, and other accessories are also provided in the model. Inflow hydrographs, outflow conditions, and other active or passive control methods can also be included in the input data file. Flow velocity, depth, discharge, and other variables at any locations and any time may be specified as outputs.

For more than twenty years, the above dynamic transient mixed flow mathematical model has been applied to a number of large sewer tunnel systems as a problem solver or design tool. These tunnel systems include Rochester City Sewer System, NY [5], Chicago TARP Phase I [1, 6] and Phase II [7], Phoenix I-10 Tunnel System, AZ [8], Milwaukee In-line Storage System, WI [9, 10], New York Passaic River Flood Protection Tunnel, NY [11], Fall River Tunnel System, MA [12] and Narragansett Bay Commission Tunnel System, RI [13].

2.2 Modeling Configuration

For the mathematical modeling purpose, the simplified O'Hare tunnel system configuration, as shown in Fig. 2, is used. Numbers shown in Fig. 2 are the station numbers used in the model for the purpose of defining different segments of the system. Each junction is represented by three stations for identification of three connecting segments. The entire system is divided into 76 segments of 500 feet each. Locations of eight dropshafts or inflow points are also shown in Fig. 2. Each dropshaft is assumed to be directly attached to the tunnel, and the detailed geometry including the shift tube is ignored in the tunnel model. The effects of the drift tube of each dropshaft are considered separately using the dropshaft dynamic model. Dropshaft No. 6 is lumped into the junction represented by Station Nos. 25, 41, and 42. The O'Hare Water Reclamation Plant (WRP) is combined into Dropshaft No. 7 by imposing a negative inflow.

2.3 Treatment of the Downstream Boundary Condition

The existing TARP phase 1 tunnel system is connected to the downstream reservoir through a 170-foot long concrete conduit at the main shaft, as shown in Fig. 3. The hydraulics of the terminal reservoir, the connecting conduit, and the main shaft are represented by a downstream boundary condition. There are three different flow regimes possible at the downstream end. When the water level in the main shaft is below the crown of the tunnel, the main shaft acts as a reservoir, and there is a free surface flow at the downstream end. If the water level in the main shaft is above the crown of the tunnel but below the water level in the reservoir, there is a pressurized flow at the downstream end and the main shaft is still treated as reservoir. If the water level in the main shaft exceeds the water level in the terminal reservoir, the water is conveyed to the terminal reservoir according to the following equation,

$$Q = cA\sqrt{2g(H_t - H_r)} \tag{5}$$

where Q is the flow rate from the tunnel to the reservoir; A is the area of connecting conduit (10'x10'); H_t is the water level in the tunnel system at the main shaft; H_r is the water level in the terminal reservoir, and c is the discharge coefficient, estimated to be equal to 0.524.

2.4 Other Input Data

The main tunnel that extends from St. 1, through Sts. 20 and 50, to St. 76, as shown in Fig. 2, is a 20-foot diameter tunnel. The branch tunnel between St. 26 and St. 49 is a 16-foot diameter tunnel. The numbering in Fig. 2 is the stationing used in the model. Finally, the diameter of the branch between St. 21 and St. 25 is 9 feet. The tunnel slope is 0.001 everywhere except for the last four segments (from St. 71 to St. 76), where an adverse slope of -0.002 exists, and a small sudden drop between St. 18 to St. 19. The Manning's coefficient (n) is assumed to be equal to 0.013.

There are eight dropshafts in the tunnel system, as shown in Figs. 1 and 2. A typical dropshaft structure (DS-4) is shown in Fig. 4. The dropshaft diameter, outfall level, and other dropshaft parameters are summarized in Table 1.

Table 1 Dropshaft Parameters

No.	Diameter (ft)	Invert Ele. (ft)	Outflow Ele. (ft)	Ground Ele.(ft)	Drift Tube Length(ft)	Drift Tube Size (ftxft)	Deaeration Chamber
1	9'x9'	-58.06	+73.80	+95.00	65'		13'x28'
2	5'	-61.17	+62.08	+84.00	80'	5'x5'	8'x11'
3	7'2"	-65.07	+48.00	+80.50	80'	9'x11'	9'x16'
4	9'	-66.16	+64.60	+81.50	106'	11'x15'	11'x25'
5	9'	-56.14	+61.50	+73.00	65'		12'x28'
6	7'2"	-65.08	+60.81	+73.50	74'	9'x9'	9'x10'
7	5'	-79.68	+79.50	+79.50	108'	5'x5'	8'x11'
8	9'	-57.23	+61.75	+74.50	64'		12'x24'
The elevation data are based on Chicago City Datum (CCD) system.							

The terminal reservoir size is 1,050 acre-feet. The reservoir area is calculated by assuming cylindrical volume and by knowing the total depth. The diameter of the main shaft at the lower level is 25 feet. The O'Hare Treatment Plant capacity is taken to be 170 cfs during the whole filling process.

2.5 Inflow Hydrographs

Hydrographs due to a total of 30 storm events provided by Corps of Engineers were tested. They are

1. 0.5 inch rainfall 10 minute duration event.
2. 0.5 inch rainfall 30 minute duration event.
3. 0.5 inch rainfall 1 hour duration event.
4. 0.5 inch rainfall 2 hour duration event.
5. 0.5 inch rainfall 3 hour duration event.
6. 1.0 inch rainfall 10 minute duration event.
7. 1.0 inch rainfall 30 minute duration event.
8. 1.0 inch rainfall 1 hour duration event.
9. 1.0 inch rainfall 2 hour duration event.
10. 1.0 inch rainfall 3 hour duration event.
11. 2.0 inch rainfall 10 minute duration event.
12. 2.0 inch rainfall 30 minute duration event.
13. 2.0 inch rainfall 1 hour duration event.
14. 2.0 inch rainfall 2 hour duration event.
15. 2.0 inch rainfall 3 hour duration event.
16. 3.0 inch rainfall 10 minute duration event.
17. 3.0 inch rainfall 30 minute duration event.
18. 3.0 inch rainfall 1 hour duration event.
19. 3.0 inch rainfall 2 hour duration event.
20. 3.0 inch rainfall 3 hour duration event.
21. 3.0 inch rainfall 6 hour duration event.
22. 4.0 inch rainfall 10 minute duration event.
23. 4.0 inch rainfall 30 minute duration event.
24. 4.0 inch rainfall 1 hour duration event.
25. 4.0 inch rainfall 2 hour duration event.
26. 4.0 inch rainfall 3 hour duration event.
27. 4.0 inch rainfall 6 hour duration event.
28. 4.0 inch rainfall 12 hour duration event.
29. 6.0 inch rainfall 12 hour duration event.
30. 6.0 inch rainfall 24 hour duration event.

In Addition, the inflow to DS-8 may be considered as controllable or uncontrollable. Therefore, for each storm event, the hydrograph to DS-8 has two possible conditions: gated and ungated inflows. Combining the two possible conditions for each storm event with the inflows to the other dropshafts results in 60 possible inflow hydrographs to the tunnel system.

The total inflow hydrographs to the tunnel system for each storm event listed above plus the gated and ungated condition at DS-8 are plotted in Figs. 5 to 16. As shown in the figures, the gated inflows have higher peaks but smaller steady flows at the end of storm events which are higher than 2 inches. The hydrograph with the highest peak is that of 4 inch 10 minute storm event when DS-8 is gated.

2.6 Tunnel Initial Conditions

As defined in the contract, three different initial tunnel water level conditions (0/33/67/ percent full) for each storm event should be tested. Therefore, the total of the simulation runs could be as many as 180 (3 initial tunnel conditions times 60 possible inflow conditions).

III. GENERAL HYDRAULIC TRANSIENT CHARACTERISTICS

Based on the modeling configurations and the hydrographs described before with the three different tunnel initial conditions, the simulation results show that most of the cases do not cause any transient problem. In this report, only the significant transient characteristics identified out of all the cases tested are discussed.

3.1 Gated (at DS-8) Cases

Case 1: 4 inch 10 min storm event with an empty initial tunnel condition

Among all the 30 storm events, 4 inch 10 minute storm event (DS-8 gated) has the highest inflow peak and could cause the most severe transient problem.

Fig. 17 shows the water level at DS-1, DS-5, DS-8, the main shaft, and the downstream end reservoir as functions of time due to the 4 in 10 min storm event assuming that the tunnel and reservoir are initially empty. The reservoir bottom elevation is at -4.0 CCD. The tunnel starts to pressurize at the main shaft at about t=2.0 hours. At t=2.9 hours, the water level at the main shaft rises above the reservoir bottom elevation, and the reservoir starts to receive the water. But by this time the tunnel has completed its pressurization and the water at DS-1, DS-5, and DS-8 reaches the maximum values. The results are plotted in Fig. 17, and replotted in Fig. 18 and Fig. 19 using different scales. These figures show that the water level at all the three upstream ends oscillates severely as the water in the shafts rises. For an example, the water level in DS-8 surges up about 100 feet during its first surge and 70 feet during its second surge. The second surge reaches the elevation of 65 CCD which is slightly higher than the outfall elevation of 61.75 CCD. However, this is still somewhat below the ground surface elevation of 74.5 CCD. The surge produces maximum overflow rate of 165.4 cfs and the total overflow volume of 3,129 cubic feet.

The condition described above is marginally critical in terms of geysering possibilities. Therefore, the semi-empirical stability parameters (see [2]) are calculated and obtained N_f=0.31 (N_f is free oscillation number) N_s=0.12 (N_s is surge tank oscillation number), and N_w=0.07 (N_w is water hammer oscillation). These values are all sufficiently less than 1 so that further dynamic modeling for the dropshaft was deemed unnecessary.

Fig. 20 shows the instantaneous hydraulic gradelines at different time instances in the main tunnel from DS-1 to the main shaft. The stationing in this figure excludes Stations 21 to 49 (the branches) in Fig. 2. Therefore, the numbering along Elmhurst Rd.

section is different from those in Fig. 2. The same change also occurs in similar figures to be described below. The bottom solid line represents the tunnel invert elevation, and the top solid line indicates the ground surface elevation. The dropshafts and their outfall elevation are also plotted as the dashed lines. This figure indicates that the water level rises very rapidly from t=2 hours to t=3 hours but the hydraulic gradeline settles down to a very flat line of a steady flow.

Fig. 21 shows the maximum water elevation in the main tunnel during the entire storm event. The maximum value is obtained by sorting through the storm time period for each station. Therefore, it may not happen at the same time at a different location. The results indicates that the maximum water in the main tunnel is below the outfall level, and far below the ground level.

Case 3: 4 inch 10 min. storm event with tunnel initially at 67% full

Figs. 27 to 31 show the simulation results for the case of a 4 in. 10 min. storm event with the tunnel initially 67 % full. The corresponding initial water level at the main shaft is - 54.2 CCD which is 20.8 feet higher than the tunnel invert. As shown in Fig. 27, the water level oscillations due to the surges are weaker in this case than those in the previous cases. But because of the reduced available storage volume, the overflow at DS-3 is substantially increased. As shown in Fig. 31, the maximum water level at DS-3 is higher than the outfall elevation. The computed overflow lasts for 15 minutes and the total volume is 8,770 cubic feet. DS-3 is the only place where overflow occurs, and there is no geysering problem indicated.

Case4-6: 4 inch 30 min. storm event with different initial tunnel conditions

The simulation results for the 4 in. 30 min. storm event with initially empty tunnel are shown in Figs. 32 to 36. Since the inflow hydrographs in this case are very similar to those of the 4 in. 10 min. event, the transient conditions are also very similar to those of Case 1. The total amount of overflow is 3,445 cubic feet in this case.

The simulation results for the same storm event but with the tunnel initially 33% full are shown in Figs. 37 to 41. Both the surge intensity and the overflow volume are reduced due to the increased initial storage. Unlike the previous cases, a small amount of overflow (186 cubic feet) is predicted at DS-5.

The simulation results for the case of the tunnel initially 67 % full are shown in Figs. 42 to 46. The surge intensity is further reduced, and no overflow is predicted.

Case7-9: 4 inch 1 hour storm event with different initial tunnel conditions

The simulated results for the three cases are shown in Figs. 47 to 61. Due to reduced peak inflow rates as compared with the previous cases, the surge intensities are less and overflows are also reduced. Only in the case of an initially empty tunnel, is there an overflow of 1,828 cubic feet occurring at DS-8.

Other small rainfall and longer duration storm events

Figs. 62 to 66 show the simulation results for the 4 in. 2 hour storm event with initially empty tunnel. These figures show that there is further reduction in the surge intensity and no geysering problem is expected. No overflow is predicted in this case. In fact, for duration equal to or greater than 2 hours, there are no geysering or overflow problems for all three assumed initial tunnel conditions.

Figs. 67 to 71 show the simulation results for the 3 in. 10 min. storm event with initially empty tunnel. Since the 3 inch storm generates significantly less intensive runoff, surges generated are relatively weak and cause no overflow. In fact for all storm events with less than 3 inch magnitude, no significant surge and overflow conditions are predicted.

Large rainfall magnitude and long duration events

It has been shown that any storm less than 3 inches or duration longer than 2 hours causes no significant surge or overflow. Even with the 6 inch storm (DS-8 gated), the reservoir has sufficient capacity to capture all the inflow. Therefore, as long as the duration is long so that the peak inflow rate is small, there should be no surge or overflow problems. Figs. 72 to 77 show the simulation results for the 6 in. 12 hour and the 6 in. 24 hour storms with the tunnel initially 67 % full. It can be observed that the surges are very weak and the water level is below the lowest outfall level.

3.2 Ungated (DS-8) Cases

By comparing the hydrographs shown in Figs. 5 through 16, it is clear that the hydrographs for the ungated cases have somewhat lower peak values than the corresponding gated cases. On the other hand, they have higher flow at the tail end of the hydrographs.

Since the surge problem for the O'Hare Tunnel System is highly related to the peak inflow intensity, the ungated cases generate slightly smaller surges than the corresponding gated cases. Otherwise the results are quite similar between the gated and the ungated cases. For this reason, it appears unnecessary to repeat the presentation of the individual ungated cases.

Because of the relatively large flow rate at the tail end of the hydrographs, the 6 in. 12 hour and the 6 in. 24 hour storm events will cause the reservoir to fill up to 48 CCD level within 36 hours and cause water to flow out of the tunnel at DS-3 (back flow). Back flow is inevitable because the steady inflow rate is greater than the pumping rate of

170 cfs. The simulation results due to the 6 in. 12 hour and the 6 in. 24 hour storm events at different initial tunnel conditions are shown in Figs. 78 to 89.

However, if the outfall at DS-3 is closed (no overflow is allowed), the reservoir level can rise to 63.50 CCD and 59.18 CCD for 6 in. 12 hour and 6 in. 2 hour storm events at the end of 36 hours with tunnel initially at 67% full, respectively.

3.3 Combined (Gated and Ungated) Inflow Cases

The combined (gated and ungated) total inflows to the tunnel system are shown in Figs. 90 to 95. The same cases as shown above have been simulated with the combined inflows. The simulated results shows that the difference due to the inflow change is very small compared with the corresponding cases described above. There is no geysering problem identified in all the simulated cases.

3.4 Effect of Air Entrainment

A well designed dropshaft can return most of the air entrained by the falling water to the atmosphere and minimize the air content of the water in the tunnel. The effect of air Entrainment is two fold: 1) increase the gross volume causing a relative decrease in the storage capacity and 2) decrease the pressure wave speed causing a reduction in transient intensity. The dropshafts used in the O'Hare Tunnel System were designed to minimize air concentration. Therefore, 1% to 4% air concentration by volume is believed to be a good estimate for this system.

Previous analysis by Guo and Song [2] assumed 1% air concentration which corresponds to the pressure wave speed of 400 ft/s. That analysis indicated marginal problem with surges when the water initially stored in the tunnel is smaller than 50% full for a 100 year 6 hour hydrograph. We think that 1% air concentration assumption is most conservative, especially considering the low frequency inflow. Normally, a strong inflow to a tunnel system will generate higher air concentration. Therefore, the analysis described above was based on the assumption that the air concentration is 4% and the corresponding pressure wave velocity is 200 ft/s. Generally speaking, the effect of the wave speed on surge condition is small. However, due to the critical condition for the most strong inflow cases, there are some critical differences due to the different wave speed.

To compare with the results due to Guo and Song [2], 400 ft/s was also used in the case of 4 in. 10 min. hydrograph. The simulated results show similar hydraulic surge features that were displayed in [2], i.e., when the initial water in the tunnel is lower, potential geysering problems may occur. Figs. 96 to 100 show the simulated results with a 4 in. 10 min. hydrograph when the tunnel is initially empty. Due to the higher wave speed, the surge during the pressurization process becomes stronger. When the tunnel is initially 85% full, a potential geysering problem disappears. The results are shown in Figs. 101 to 105.

IV. CONCLUSIONS

In this study, 30 different storm events with three initial tunnel conditions (0/33/67% full) in the O'Hare tunnel system were investigated for the hydraulic transient characteristics. For each storm event, the inflow to DS-8 can be gated. Therefore, two inflow conditions (gated and ungated) to the tunnel at DS-8 were also studied. The main hydraulic transient characteristics based on the study are summarized as follows

4.1 Gated (DS-8) Cases:

The modeling results for the gated inflow condition at DS-8 are summarized as the following table:

Rainfall (inches)	Duration	Tunnel Full(%)	Overflow V (ft^3)	Max overflow Rate(ft^3/s)	Overflow Location	Back flow	Geyser
4	10 min	0	3129	165.4	DS-8	no	no
4	10 min	33	0	0	none	no	no
4	10 min	67	8770	15.2	DS-3	no	no
4	30 min	0	4391	182.5	DS-8	no	no
4	30 min	33	186	68.3	DS-5	no	no
4	30 min	67	0	0	none	no	no
4	1 hour	0	1828	111.0	DS-8	no	no
4	1 hour	33	0	0	none	no	no
4	1 hour	67	0	0	none	no	no
4	2 hour	0	0	0	none	no	no
4	2 hour	33	0	0	none	no	no
4	2 hour	67	0	0	none	no	no
3	10 min	0	0	0	none	no	no
3	10 min	33	0	0	none	no	no
3	10 min	67	0	0	none	no	no
6	12 hour	67	0	0	none	no	no
6	24 hour	67	0	0	none	no	no
The other combined cases with different rainfalls, duration, and tunnel full percentages result in no overflow and geyser problems.							

It appears that most of the cases do not have a severe transient problem. There are no backflow and geyser problems in all the gated cases. Small amounts of overflows in the 4 in.-10 min., 4 in.-30 min., and 4 in.-1 hour cases are identified. Hence, when storm duration is longer than 2 hours, or rainfall is 3 inches or less, there is no overflow problem.

We think that the overflow conditions are not serious since they are relatively small compared with the inflow rate and it only lasts a few seconds, except in the 67% full case. Note that overflow is the part of run-off that cannot get into the tunnel while backflow is the flow coming out of the tunnel.

4.2 Ungated (DS-8) Cases:

When DS-8 is ungated, the hydrograph to the tunnel from DS-8 is reduced significantly during the storm event, and increased after the storm due to the leakage. The main hydraulic transient characteristics of the ungated cases are shown in the following table.

Rainfall (inches)	**Duration**	**Tunnel Full(%)**	**Overflow V (ft^3)**	**Max overflow Rate(ft^3/s)**	**Overflow Location**	**Back flow**	**Geyser**
4	10 min	0	473	60.1	DS-8	no	no
4	10 min	33	1460	157.3	DS-8	no	no
4	10 min	67	0	0	none	no	no
4	30 min	0	6	1.8	DS-8	no	no
4	30 min	33	140	39.3	DS-5	no	no
4	30 min	67	0	0	none	no	no
4	1 hour	0	862	148.9	DS-5	no	no
4	1 hour	33	313	70.0	DS-5	no	no
4	1 hour	67	0	0	none	no	no
4	2 hour	0	0	0	none	no	no
4	2 hour	33	0	0	none	no	no
4	2 hour	67	0	0	none	no	no
3	10 min	0	0	0	none	no	no
3	10 min	33	0	0	none	no	no
3	10 min	67	0	0	none	no	no
6	12 hour	0	7.71x10^6	281.9	DS-3	yes	no
6	12 hour	33	8.76x10^6	280.3	DS-3	yes	no
6	12 hour	67	9.81x10^6	278.6	DS-3	yes	no
6	24 hour	0	3.40x10^6	289.5	DS-3	yes	no
6	24 hour	33	4.27x10^6	288.8	DS-3	yes	no
6	24 hour	67	5.13x10^6	288.0	DS-3	yes	no
The other combined cases with different rainfalls, duration, and tunnel full percentages result in no overflow and geyser problems.							

Note: the overflow volume is accounted for in the first 36 hours for the 6 inch rainfall cases.

Due to less inflow to the tunnel during the storm period, the surge oscillations become relatively weaker compared with the corresponding gated cases. However, since there is larger inflow to the tunnel after the storm, the water stage at the reservoir can reach the level of the lowest outfall elevation at DS-3. As a result, most of the inflow becomes backflow from DS-3 after that.

If no overflow is allowed from the dropshaft outfalls, at the end of 36 hours, the water level in the tunnel and reservoir can reach 63.58 CCD for a 6 in. 12 hour storm event, and 59.18 CCD for a 6 in. 24 hour storm event when the tunnel is initially 67% full. The levels are still lower than the lowest ground elevation among the dropshafts.

4.3 Combined (Gated and Ungated) Inflow Cases:

Since the combined inflow at DS-8 does not increase too much, the results due to the combined inflow show little difference from the gated and ungated cases described above. The main hydraulic transient characteristics of the combined inflow cases are shown in the following table.

Rainfall (inches)	Duration	Tunnel Full(%)	Overflow V (ft^3)	Max overflow Rate(ft^3/s)	Overflow Location	Back flow	Geyser
4	10 min	0	2724	144.9	DS-8	no	no
4	10 min	33	0	0	none	no	no
4	10 min	67	0	0	none	no	no
4	30 min	0	2279	123.3	DS-8	no	no
4	30 min	33	0	0	none	no	no
4	30 min	67	0	0	none	no	no
4	1 hour	0	0	0	none	no	no
4	1 hour	33	0	0	none	no	no
The other combined cases with different rainfalls, duration, and tunnel full percentages result in no overflow and geyser problems.							

The results due to 6 inch rainfall events are the same as those in the similar ungated cases.

Based on the above simulation results, it is concluded that the surge condition in the tunnel system is not impacted by operation of the DS-8 gate.

4.4 Effect of Air Entrainment

The above simulation is based on an assumption that the water volume in the tunnel contains 4% air, which results in a wave speed of 200 ft/s. The authors believe this assumption to be relevant considering the strong inflow at the low frequency case. However, if the air concentration is 1%, which results in a wave speed of 400 ft/s (used in [2]), the potential geysering problem may occur at DS-1, DS-5, and DS-8 for the 4 inch rainfall events. But if the tunnel is initially at 85%, the geysering problem can be avoided, even assuming only 1% air concentration.

REFERENCES

1. Song, C.C.S., Guo, Q., and Zheng, Y., "Hydraulic Transient Modeling of TARP Systems," St. Anthony Falls Hydraulic Laboratory, University of Minnesota, Project Report No. 270 , March 1988.

2. Guo, Q., and Song, C.C.S., "Hydraulic Transient Analysis of TARP Phase II O'Hare System," St. Anthony Falls Hydraulic Laboratory, University of Minnesota, Project Report No. 276, July 1988.

3. Cardle, J.A., and Song, C.C.S., "Mathematical Modeling of Unsteady Flow in Storm Sewers, " *International Journal of Engineering Fluid Mechanics*, Vol. 1, No. 4, 1988.

4. Guo, Q., and Song, C.C.S., "Surging in Urban Storm Drainage Systems," *Journal of Hydraulic Engineering, ASCE*, Vol. 116, No. 12, June, 1989.

5. Song, C.C.S., Cardle, J.A., and Gavali, S., "Mathematical Modeling of the Genesee River Storage - Conveyance System Rochester, NY," St. Anthony Falls Hydraulic Laboratory, University of Minnesota, Project Report No. 215 , July 1982.

6. Song, C.C.S., Lin, W., and Gong, C., "Hydraulic Transient Modeling of TARP Systems," St. Anthony Falls Hydraulic Laboratory, University of Minnesota, Project Report No. 332, March 1992.

7. Song, C.C.S., He, J., Liu, Y., and Gong, C., "Hydraulic Transient Study of Mainstream & Des Plaines TARP Phase II Systems," St. Anthony Falls Hydraulic Laboratory, University of Minnesota, Project Report No. 353, July 1994.

8. Song, C.C.S., "Mathematical Modeling of I-10 Inner Loop Drainage System," St. Anthony Falls Hydraulic Laboratory, University of Minnesota, Project Report No. 235, Aug. 1984.

9. Song, C.C.S., and Lin, W., "Study of Potential Hydraulic Transient for Milwaukee In-line Storage System," St. Anthony Falls Hydraulic Laboratory, University of Minnesota, Project Report No. 297 , July 1990.

10. Lin, W., and Song, C.C.S., "Hydraulic Transient Analysis of Tunnels and Dropshafts for Milwaukee In-line Storage System," St. Anthony Falls Hydraulic Laboratory, University of Minnesota, Project Report No. 340, July 1993.

11. He, J., Song, C.C.S., and Liu, Y., "Hydraulic Transient Study of Passaic River Flood Protection Tunnel," St. Anthony Falls Hydraulic Laboratory, University of Minnesota, Project Report No. 354, July 1994.

12. He, J., Song, C.C.S., and Liu, Y., "Hydraulic Transient Study of Narragansett Bay Commission Tunnel System," St. Anthony Falls Hydraulic Laboratory, University of Minnesota, Project Report No. 368, August 1995.

13. Streeter V. L., and Wylie, E. B., *Hydraulic Transients*, McGraw-Hill Book Company, New York, 1967.

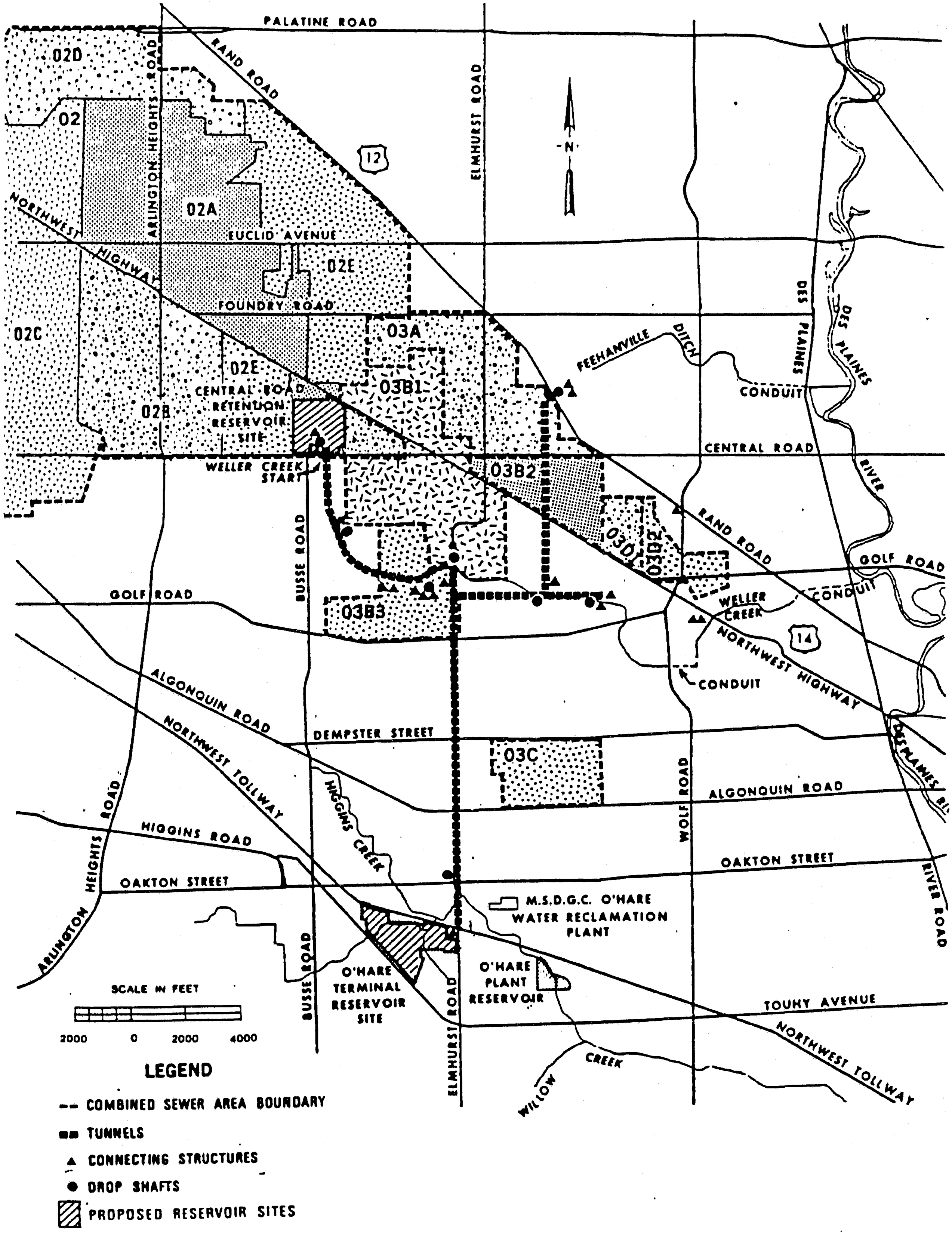

Fig. 1. TARP O'Hare System.

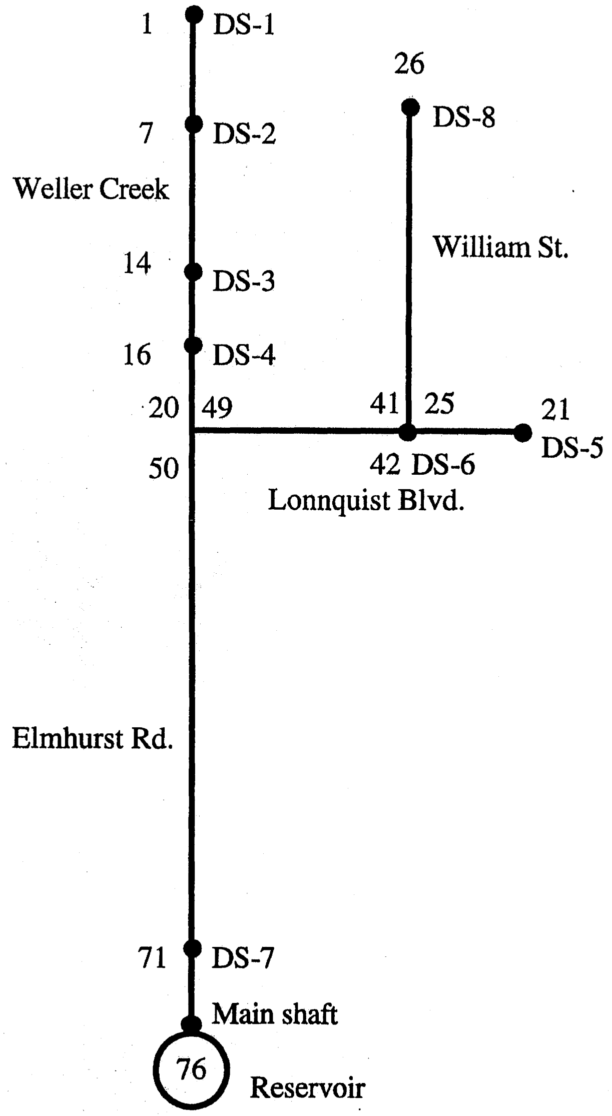

Fig. 2 O'Hare tunnel system configuration for modeling purpose.

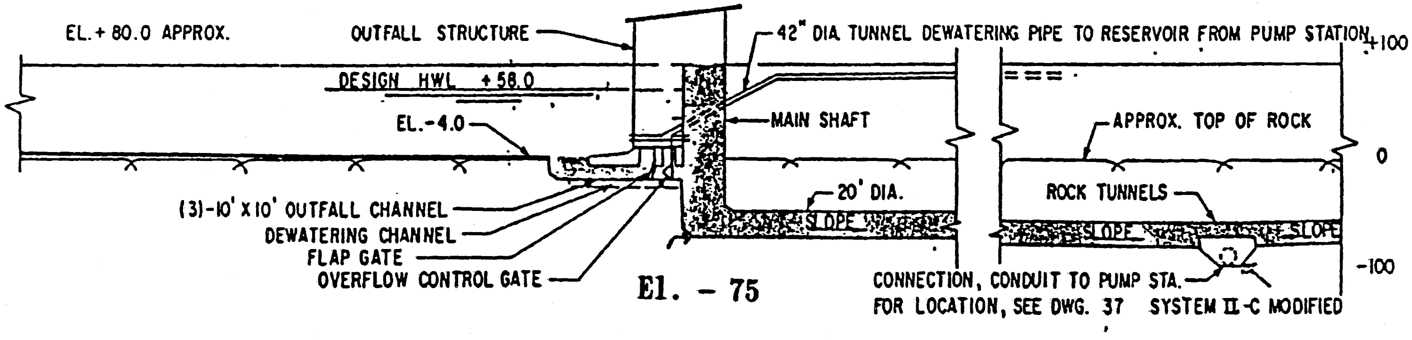

Fig. 3. Connection between the TARP Phase I tunnel system and the proposed terminal reservoir.

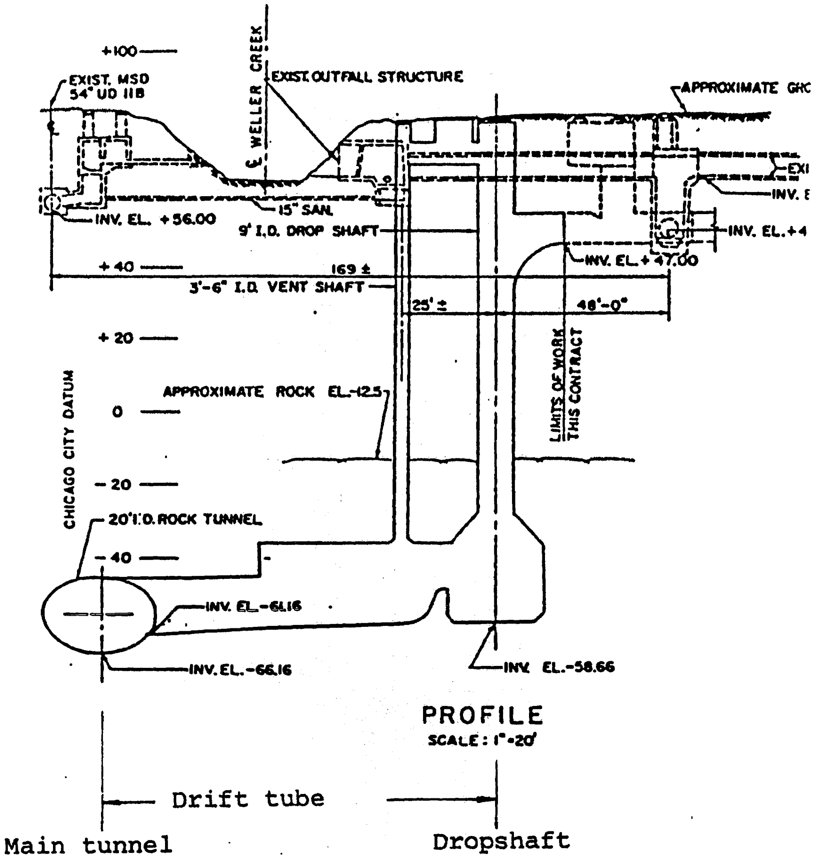

Fig. 4. A typical dropshaft structure (DS–4).

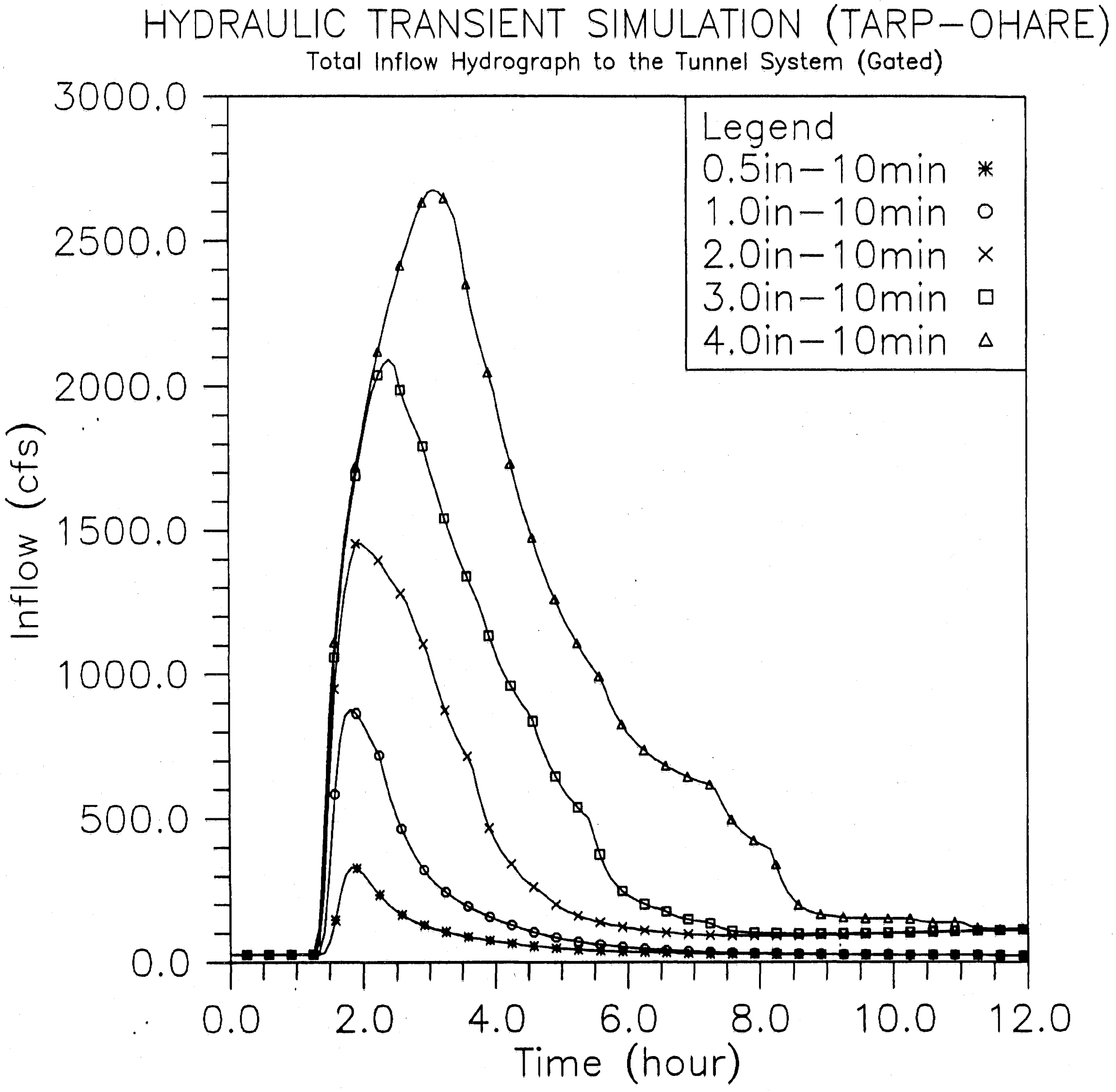

Fig. 5 Total inflow hydrodraphs to the tunnel system for 10 min storm events (gated at DS-8).

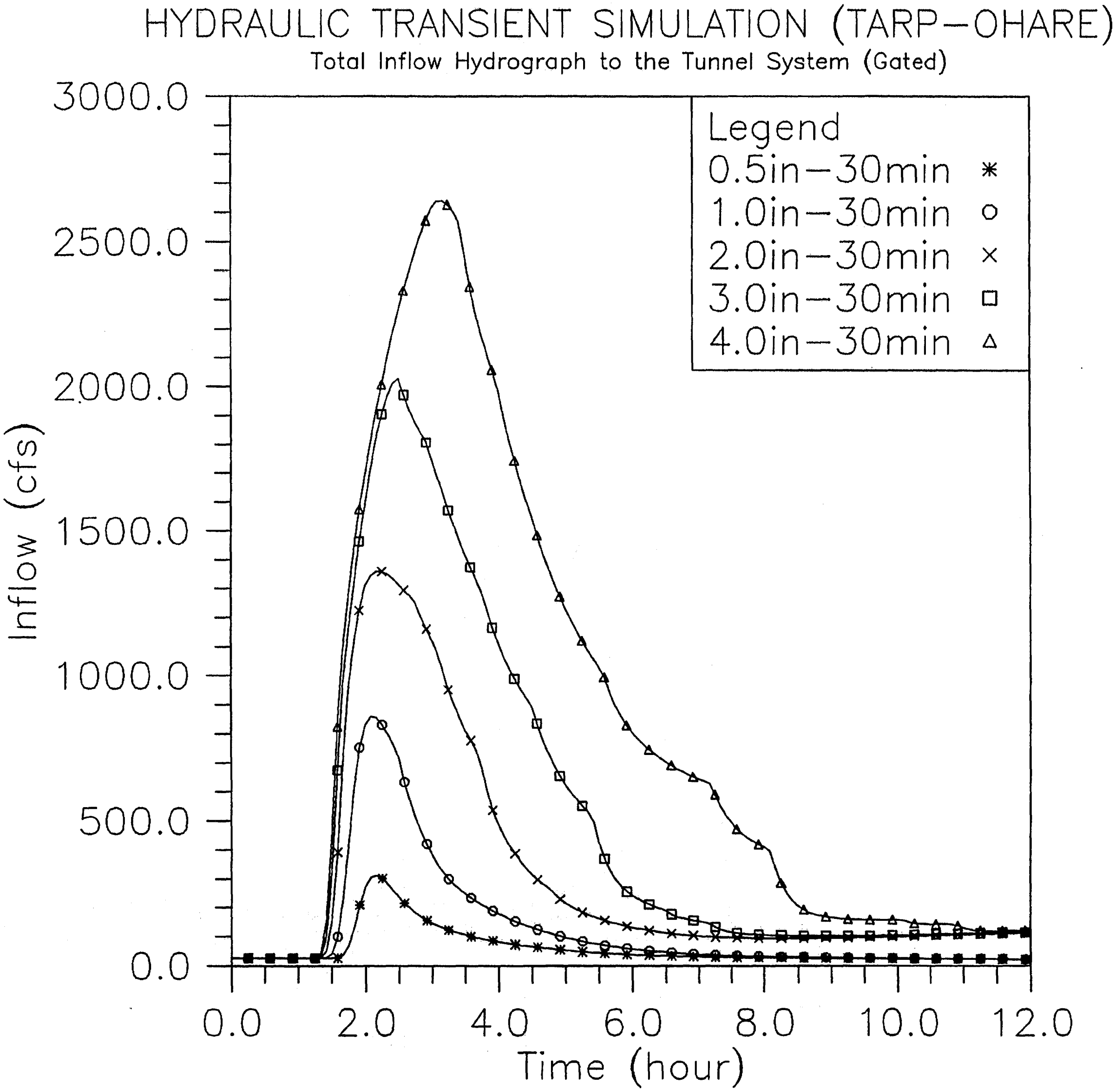

Fig. 6 Total inflow hydrodraphs to the tunnel system for 30 min storm events (gated at DS-8).

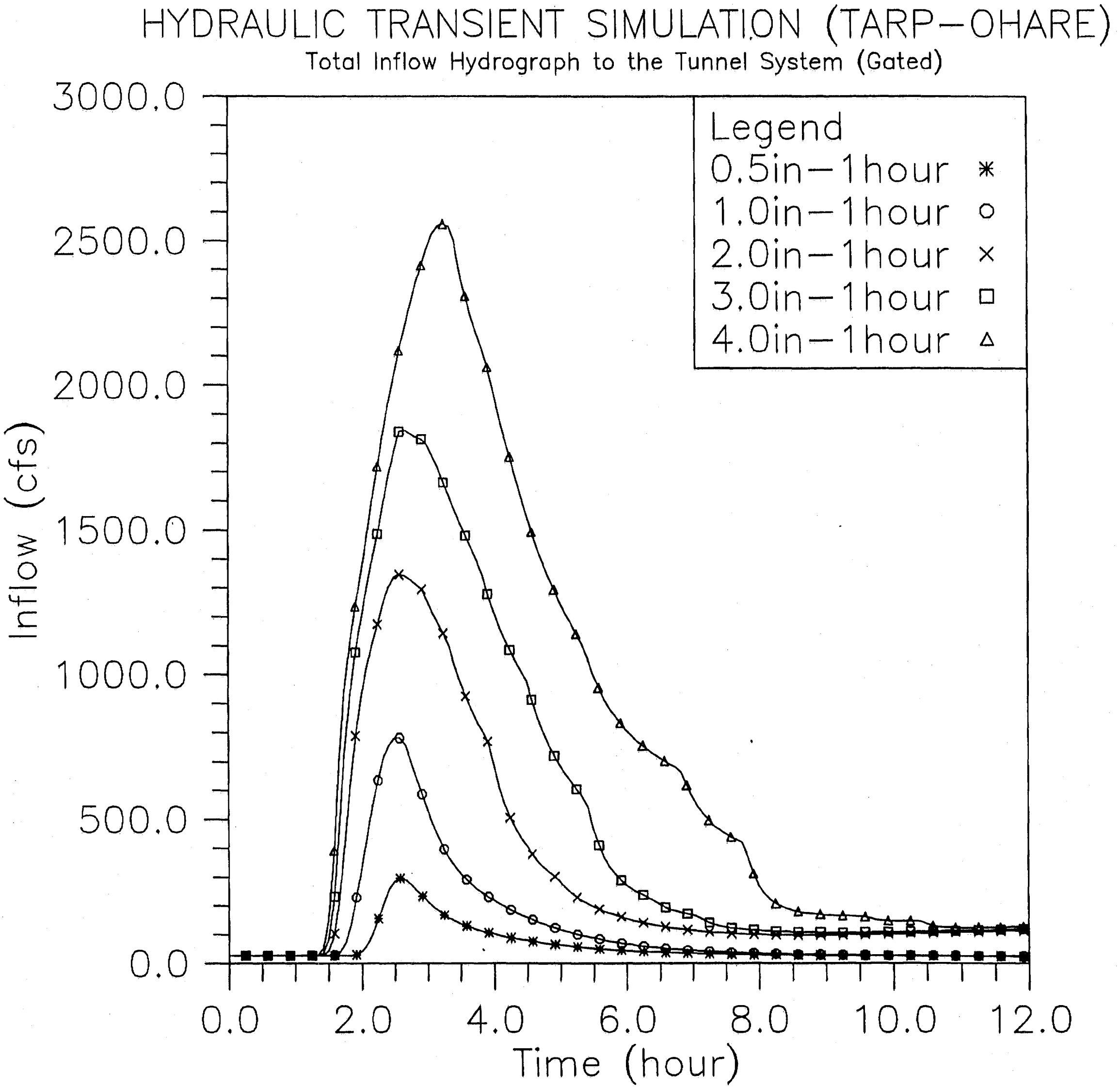

Fig. 7 Total inflow hydrodraphs to the tunnel system for 1 hour storm events (gated at DS-8).

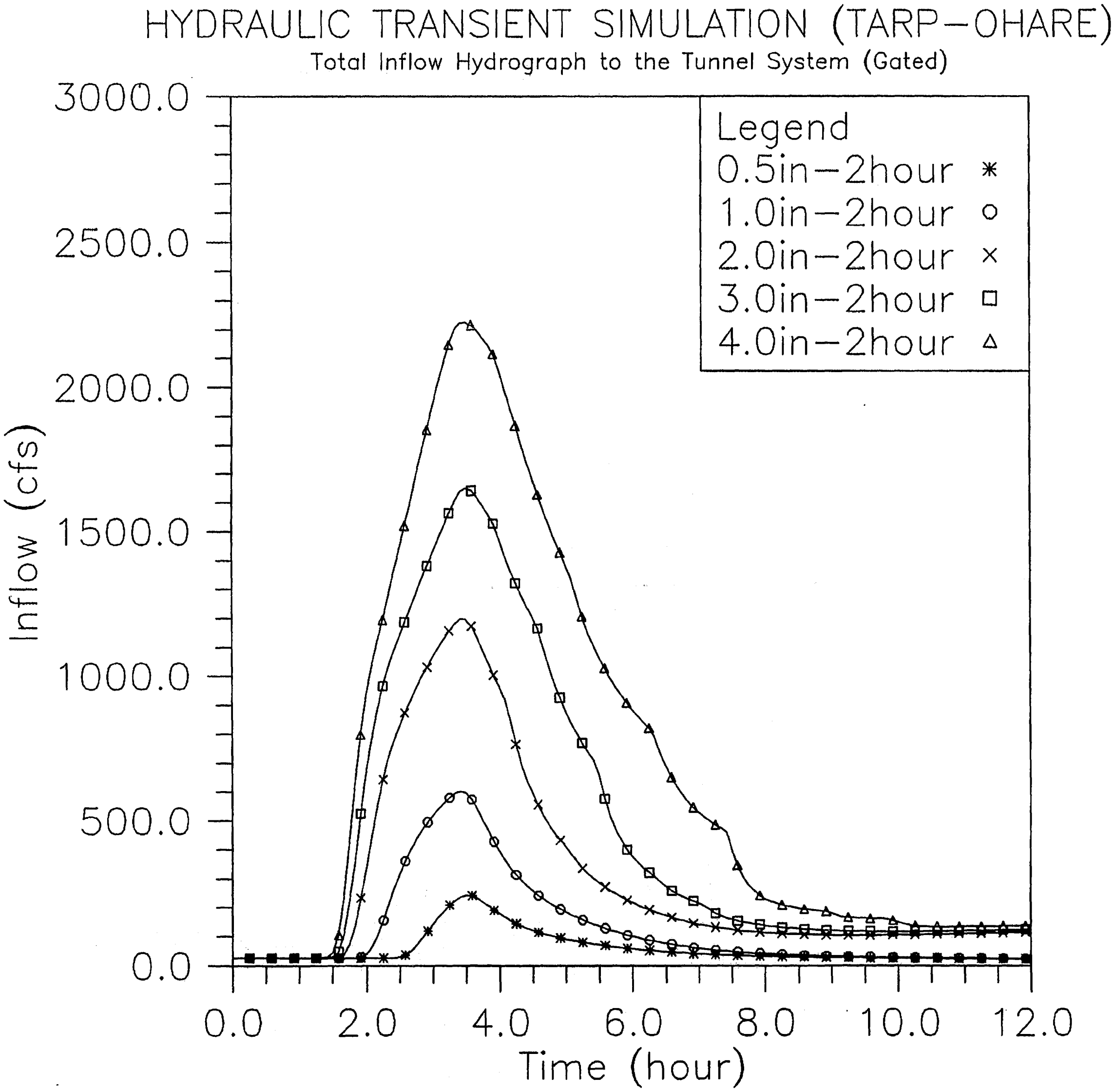

Fig. 8 Total inflow hydrodraphs to the tunnel system for 2 hour storm events (gated at DS-8).

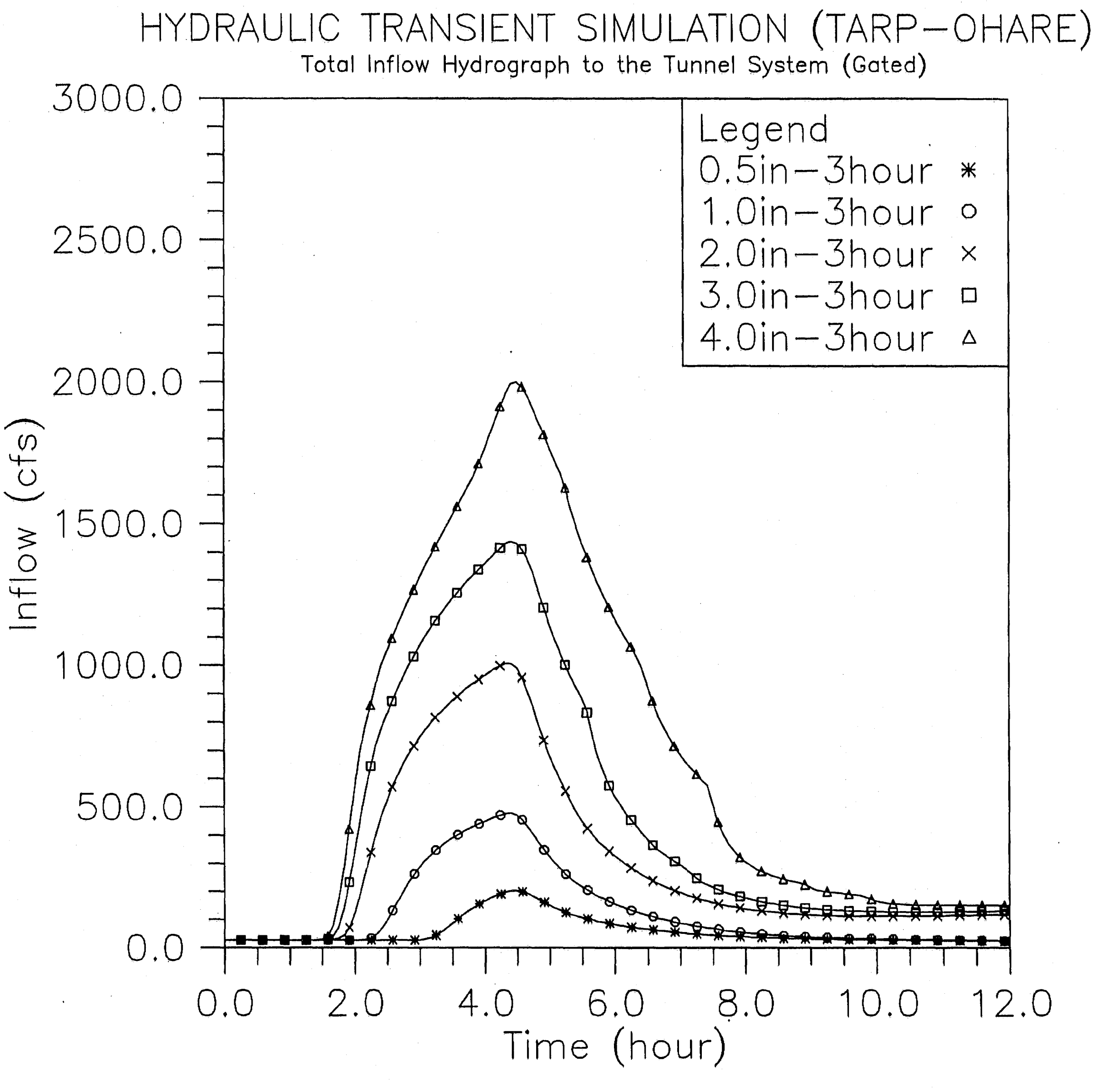

Fig. 9 Total inflow hydrodraphs to the tunnel system for 3 hour storm events (gated at DS-8).

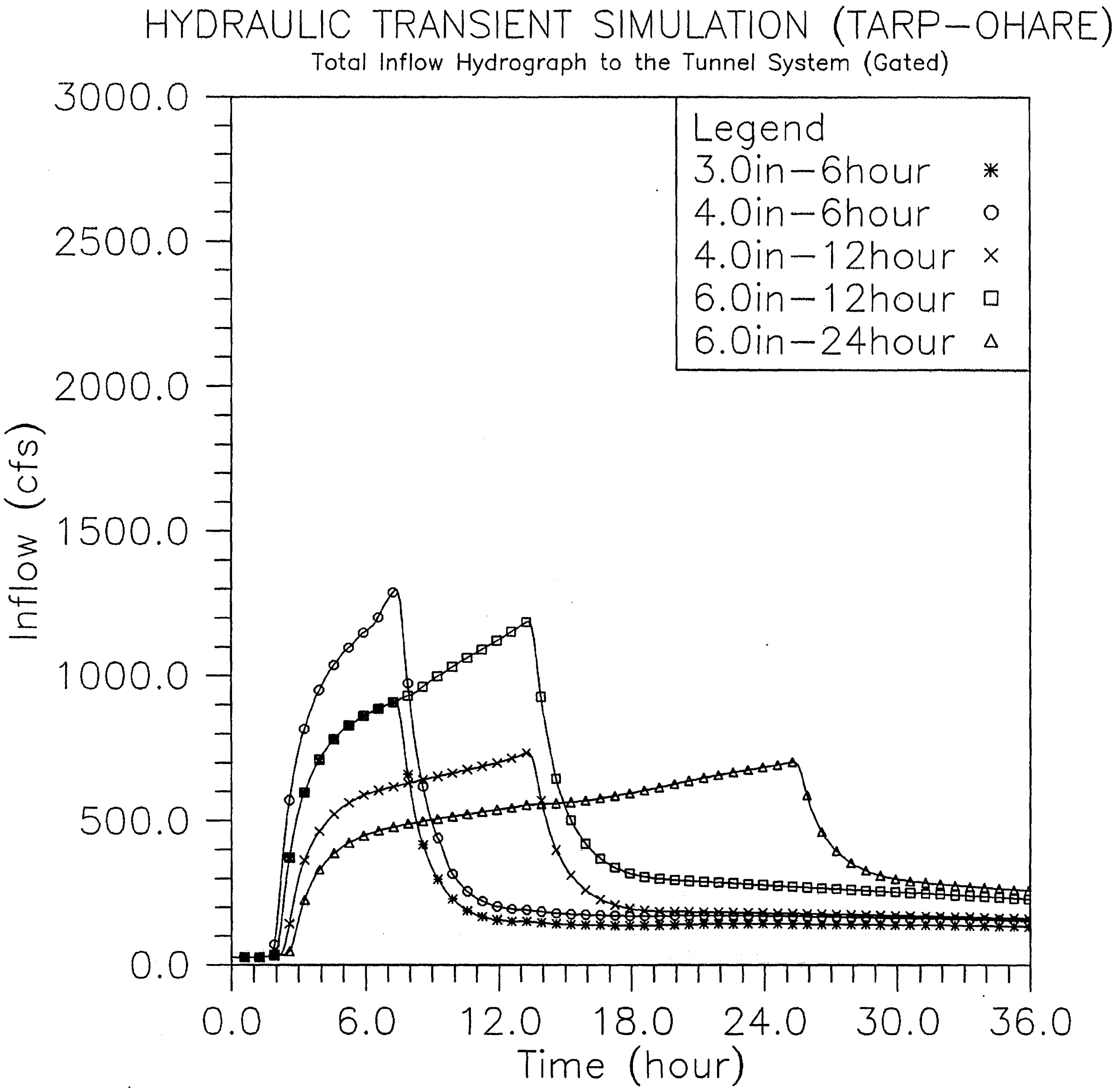

Fig. 10 Total inflow hydrodraphs to the tunnel system for 6 to 24 hour storm events (gated at DS-8).

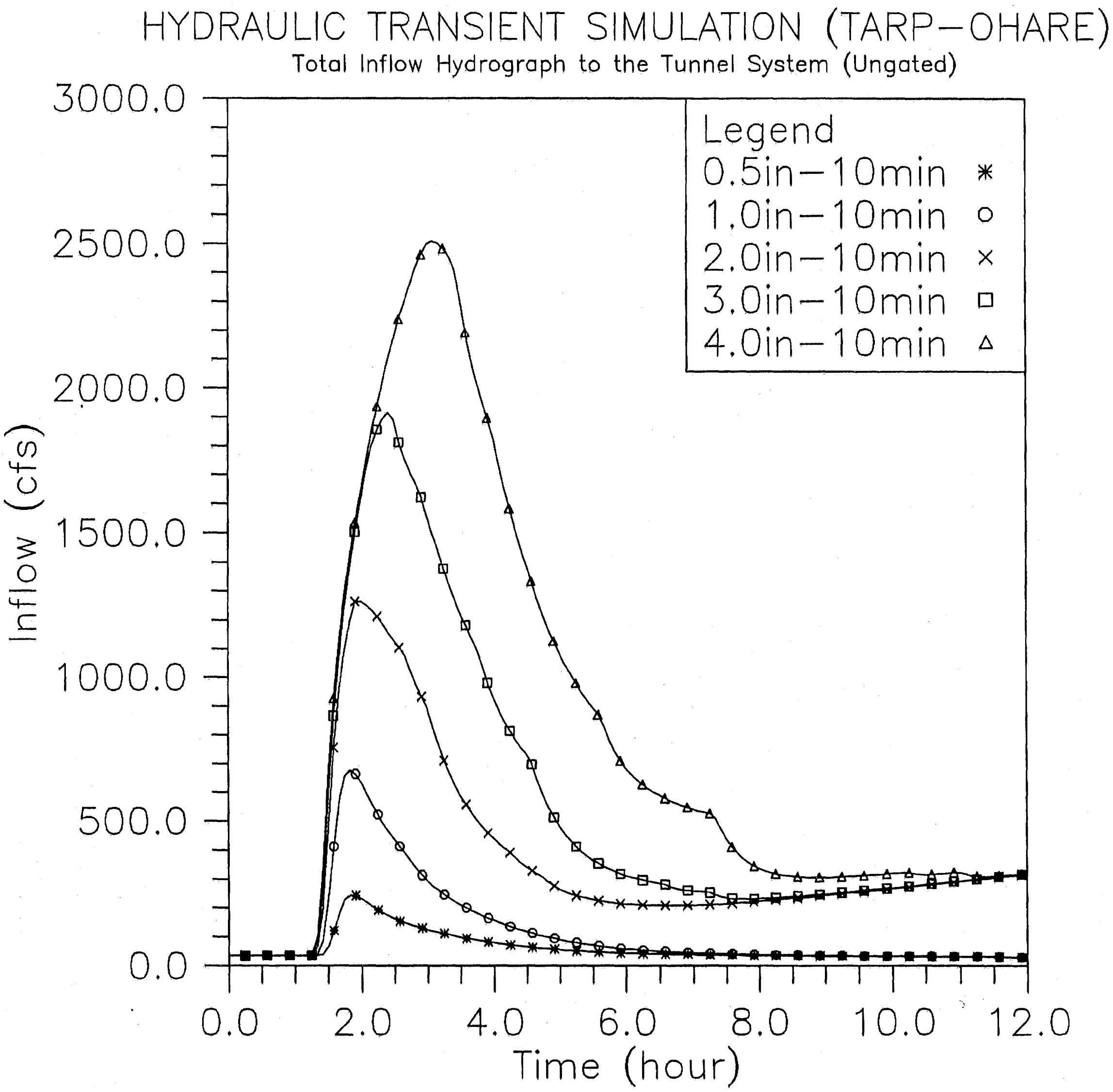

Fig. 11 Total inflow hydrodraphs to the tunnel system for 10 min storm events (ungated at DS-8).

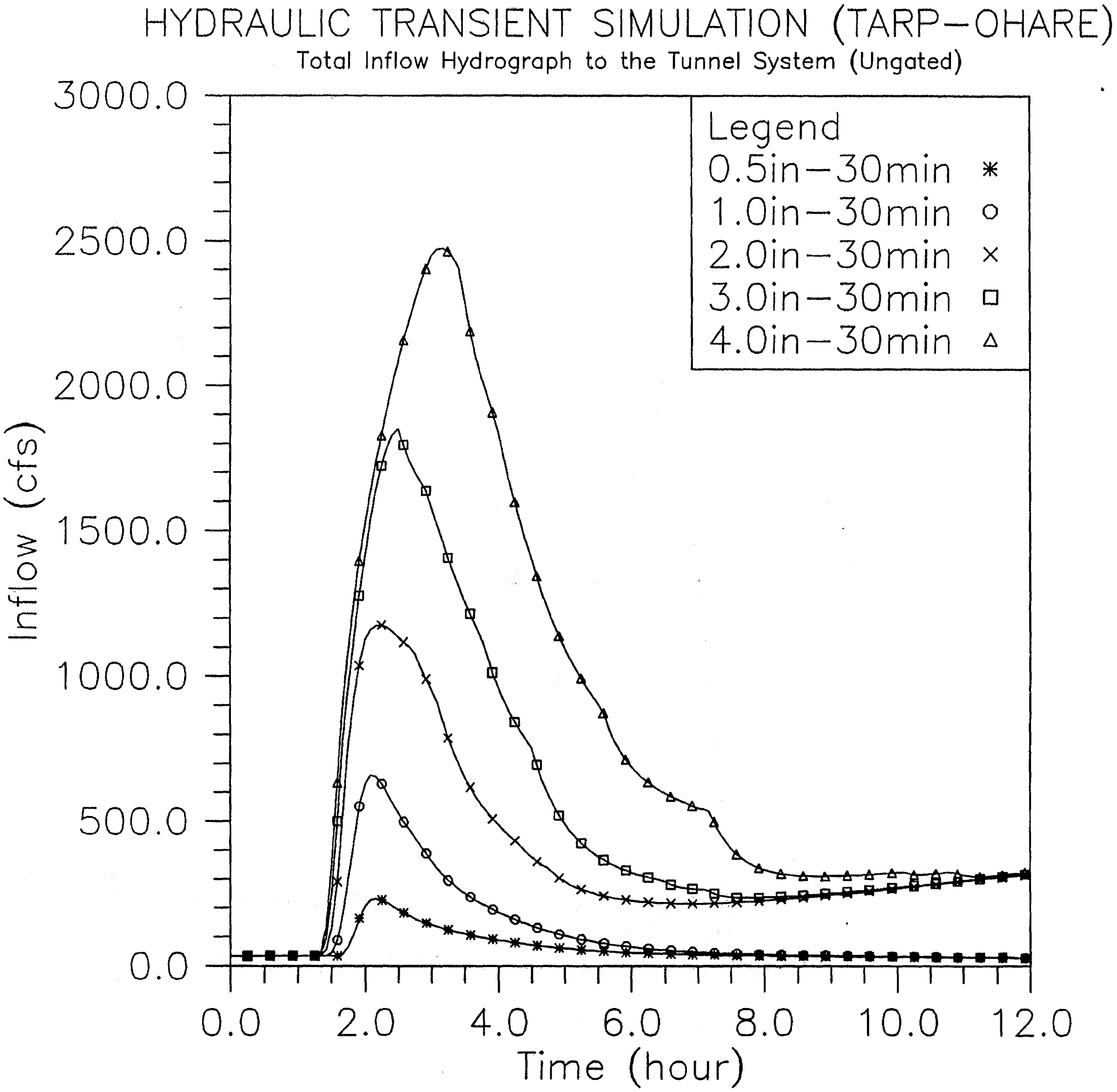

Fig. 12 Total inflow hydrodraphs to the tunnel system for 30 min storm events (ungated at DS-8).

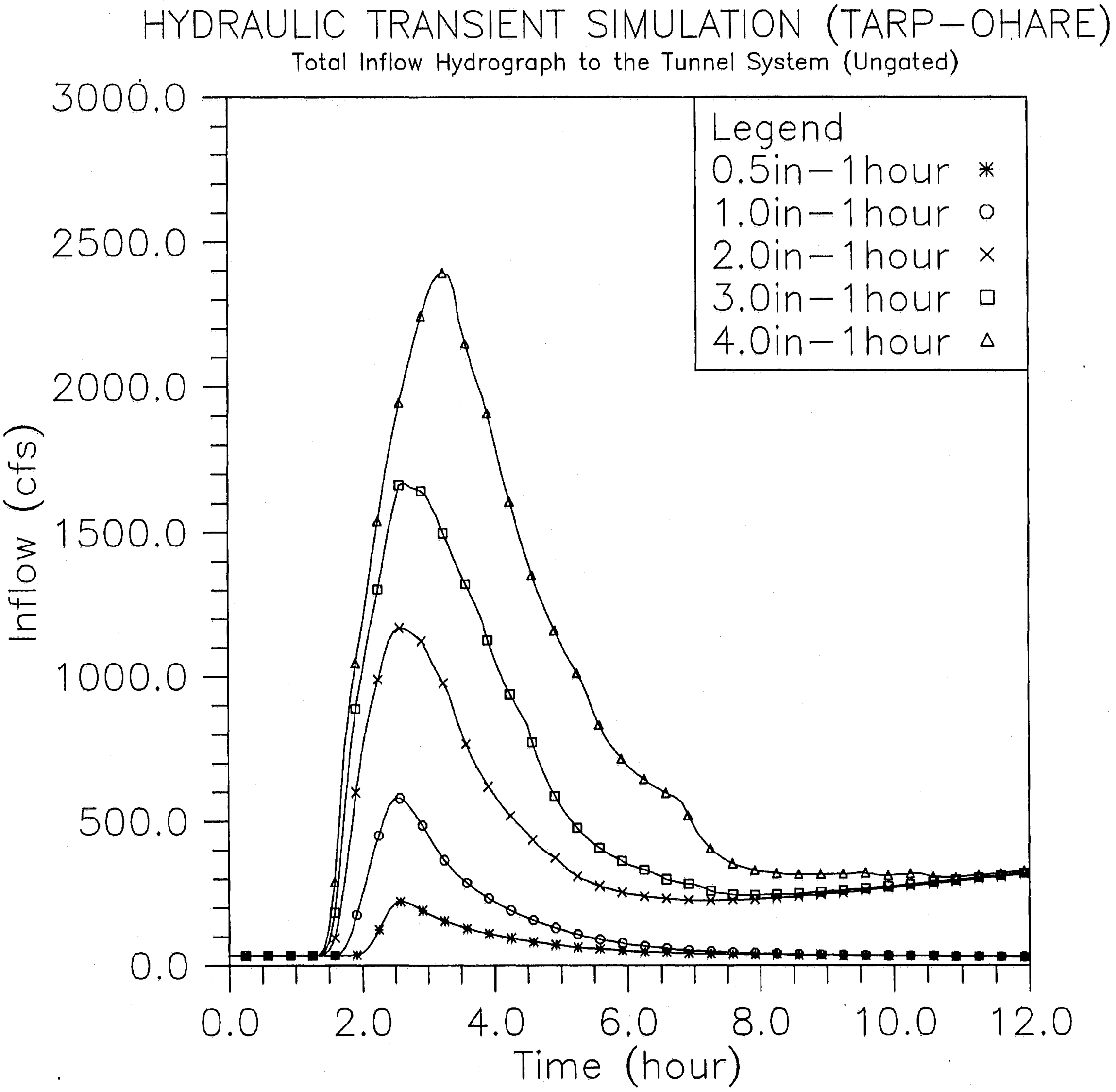

Fig. 13 Total inflow hydrodraphs to the tunnel system for 1 hour storm events (ungated at DS-8).

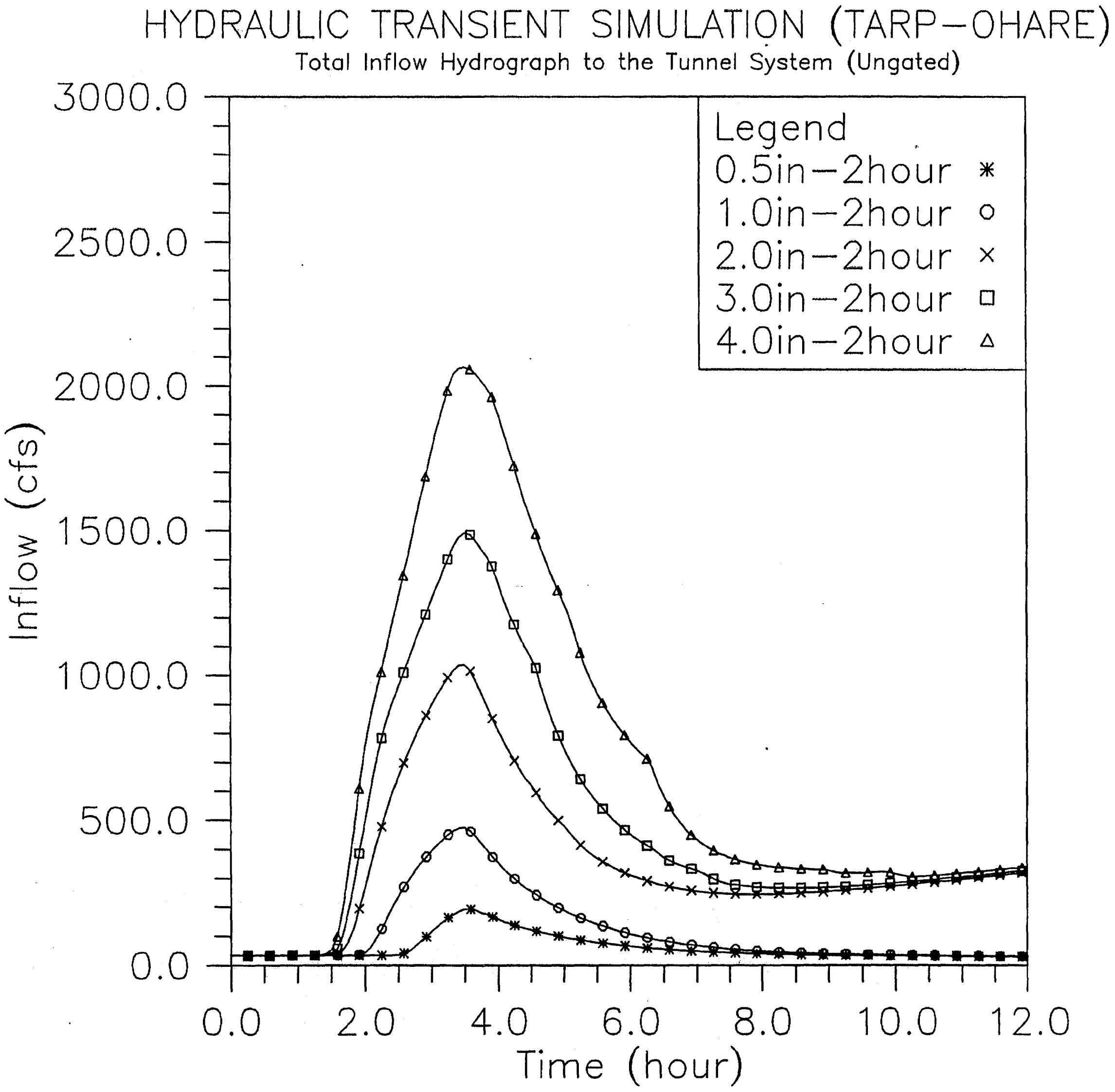

Fig. 14 Total inflow hydrodraphs to the tunnel system for 2 hour storm events (ungated at DS-8).

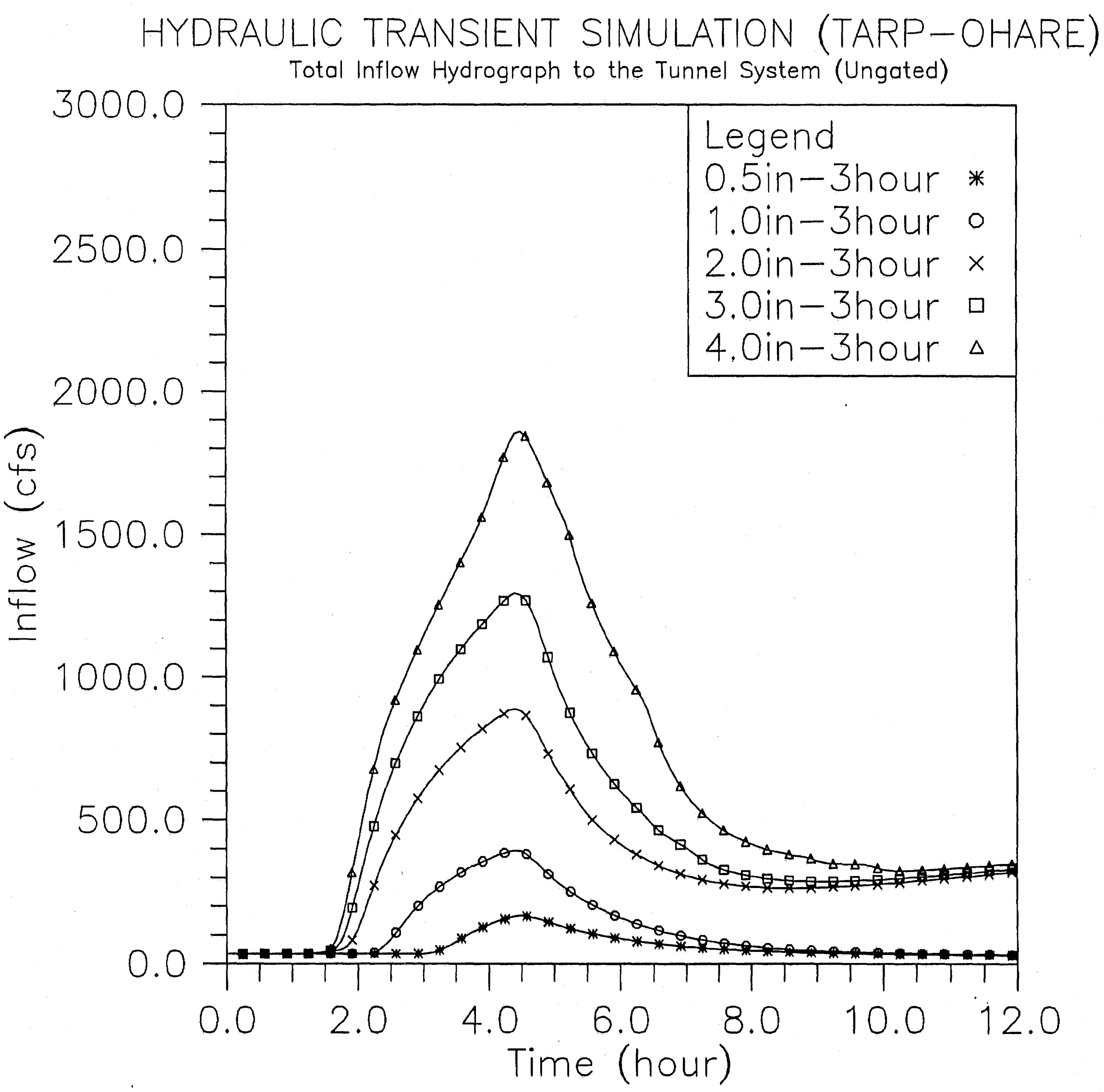

Fig. 15 Total inflow hydrodraphs to the tunnel system for 3 hour storm events (ungated at DS-8).

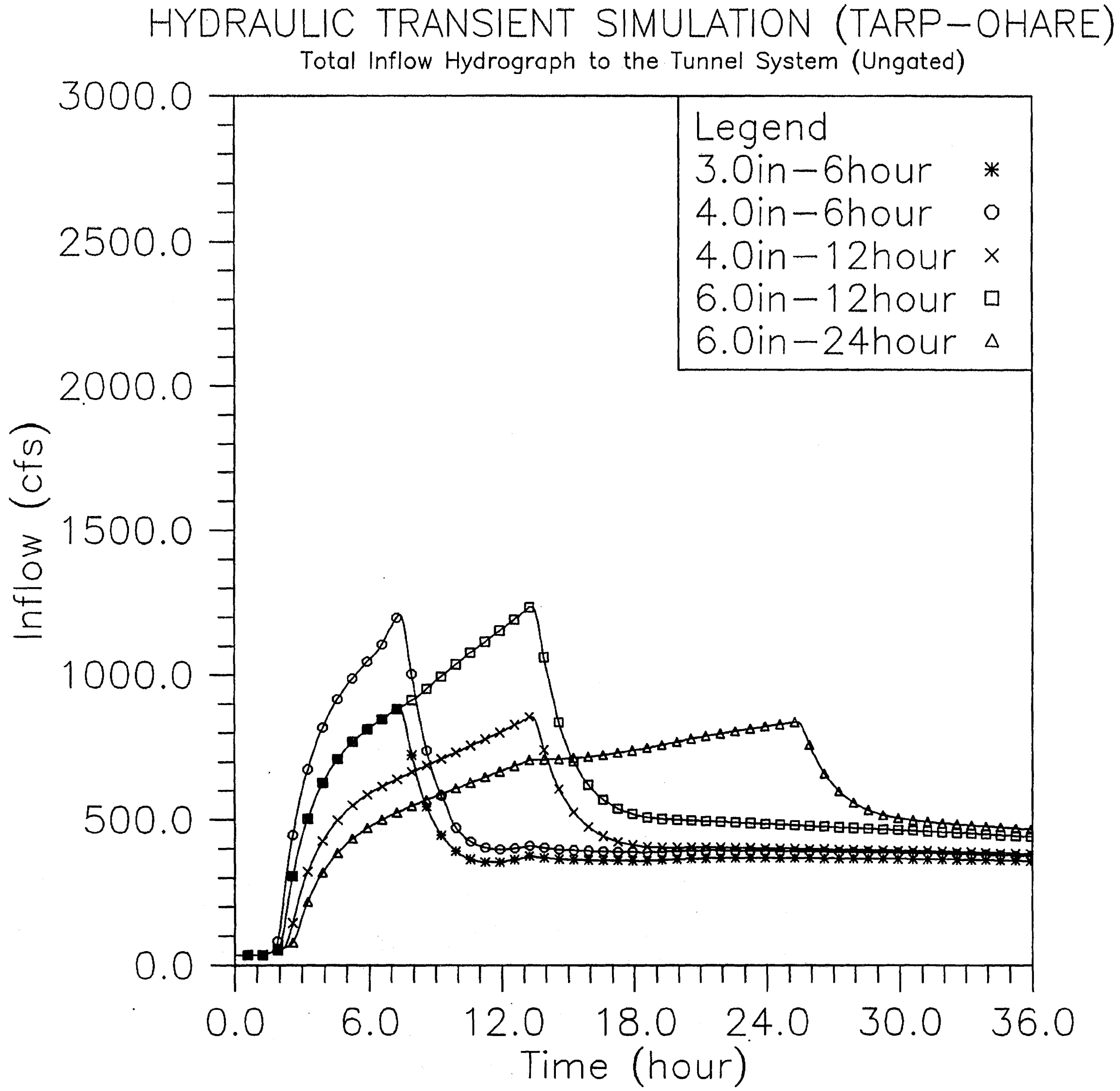

Fig. 16 Total inflow hydrodraphs to the tunnel system for 6 to 24 hour storm events (ungated at DS-8).

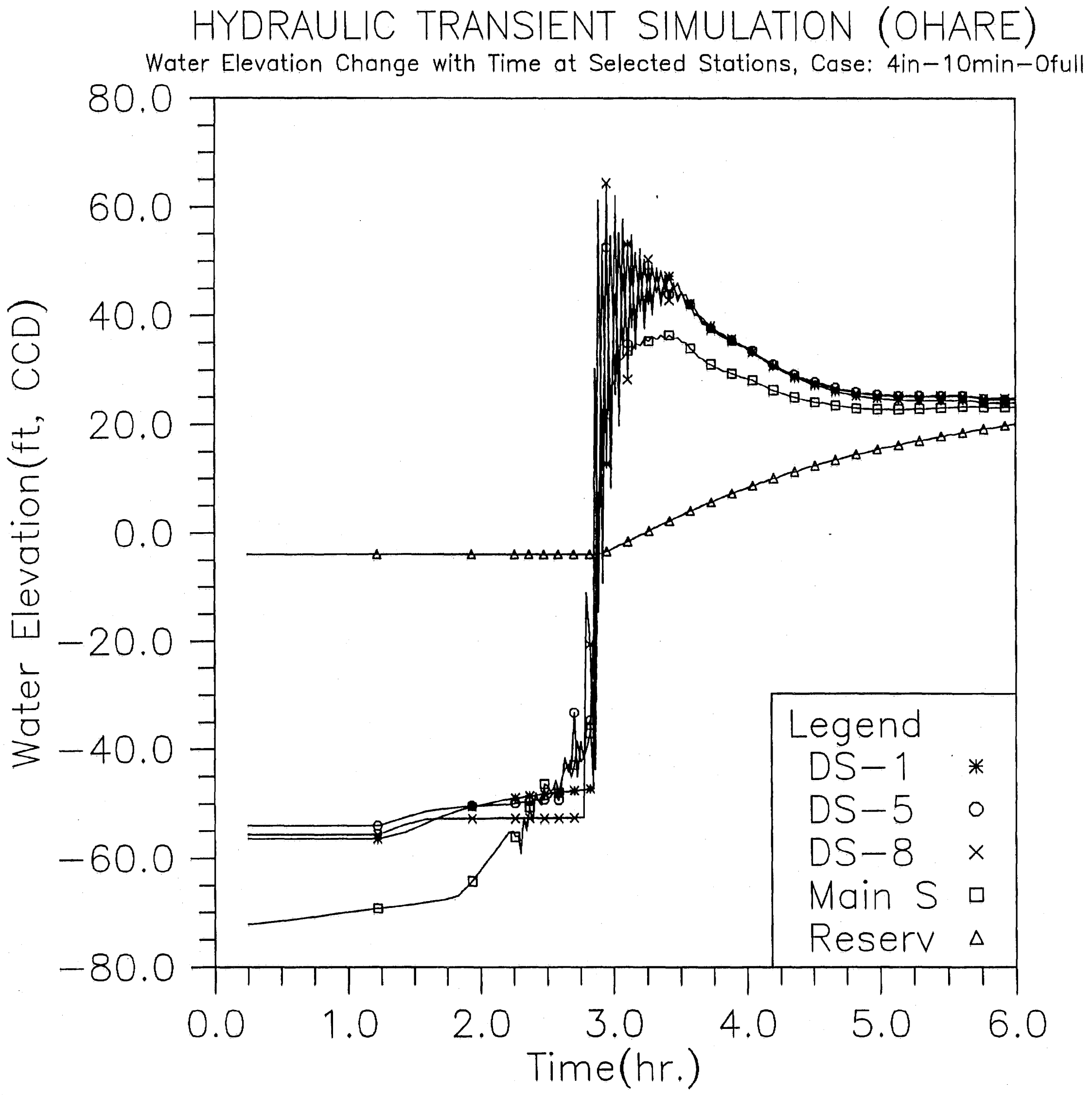

Fig. 17 Water elevation variations with time during 4 in 10 min storm event at 5 locations (DS-1, DS-5, DS-8, main shaft and reservoir), modeling conditions: empty initial tunnel condition and gated inflow at DS-8.

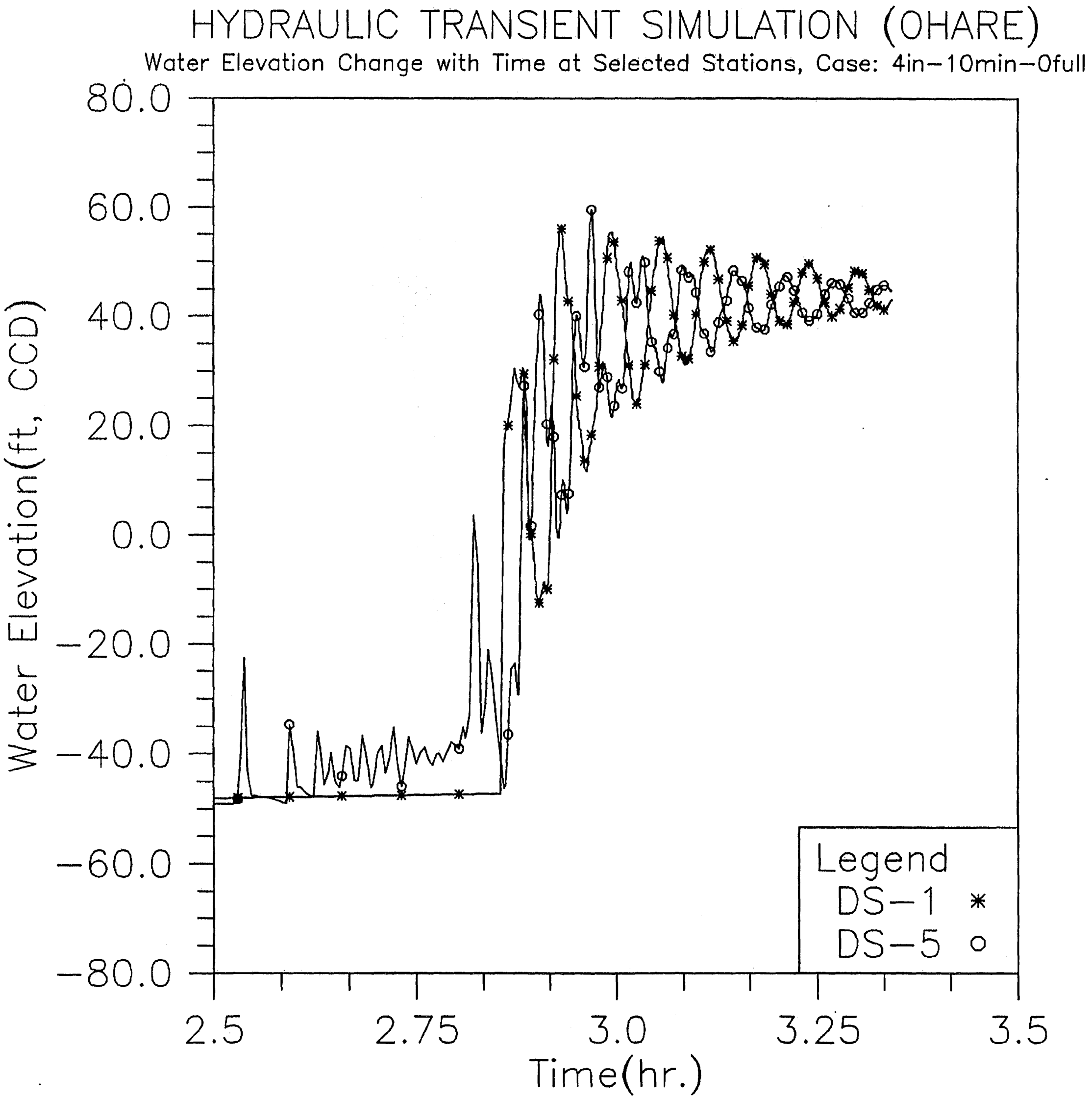

Fig. 18 Detailed water elevation variations with time in the surge process during 4 in 10 min storm event at 2 locations (DS-1 and DS-5), modeling conditions: empty initial tunnel condition and gated inflow at DS-8.

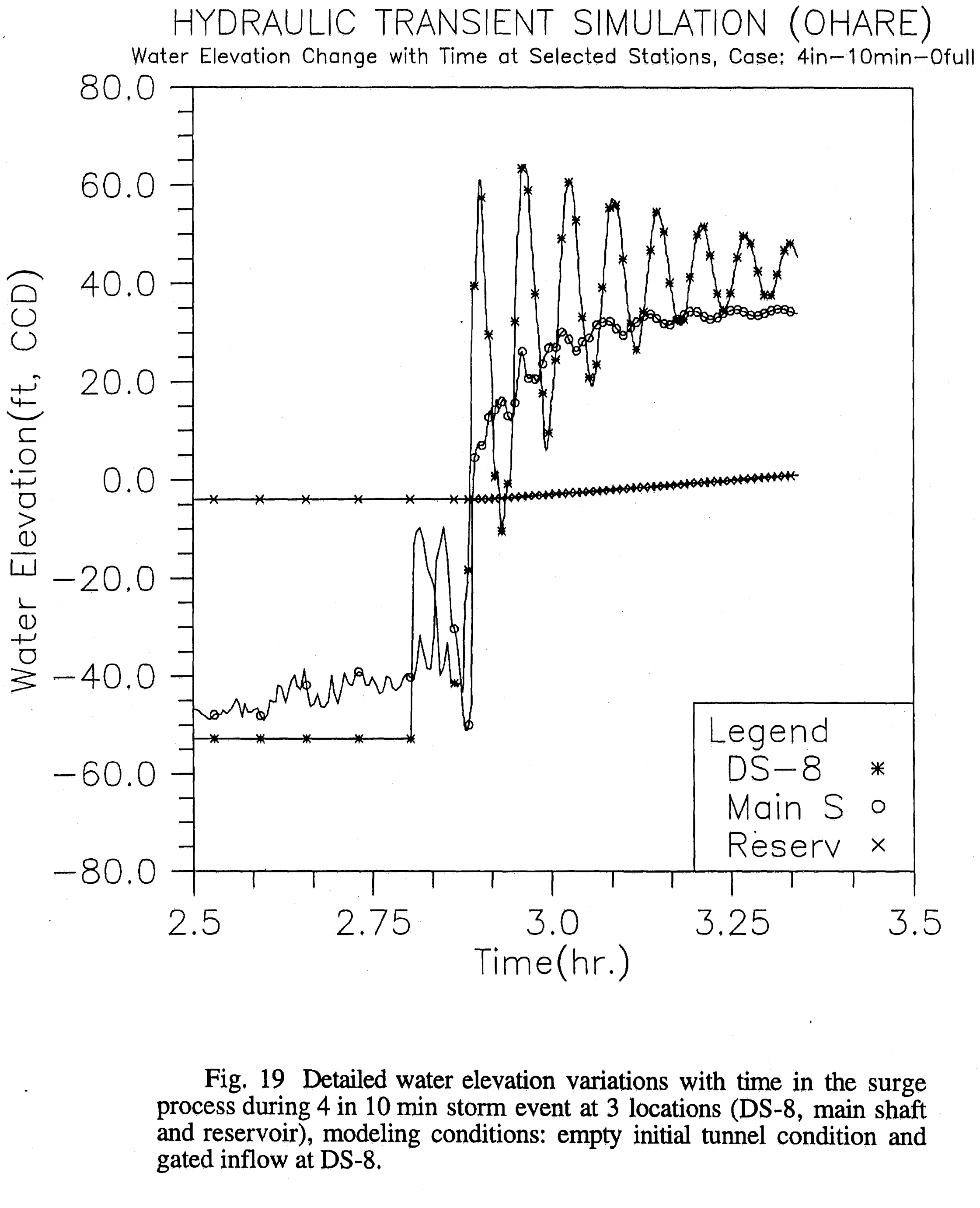

Fig. 19 Detailed water elevation variations with time in the surge process during 4 in 10 min storm event at 3 locations (DS-8, main shaft and reservoir), modeling conditions: empty initial tunnel condition and gated inflow at DS-8.

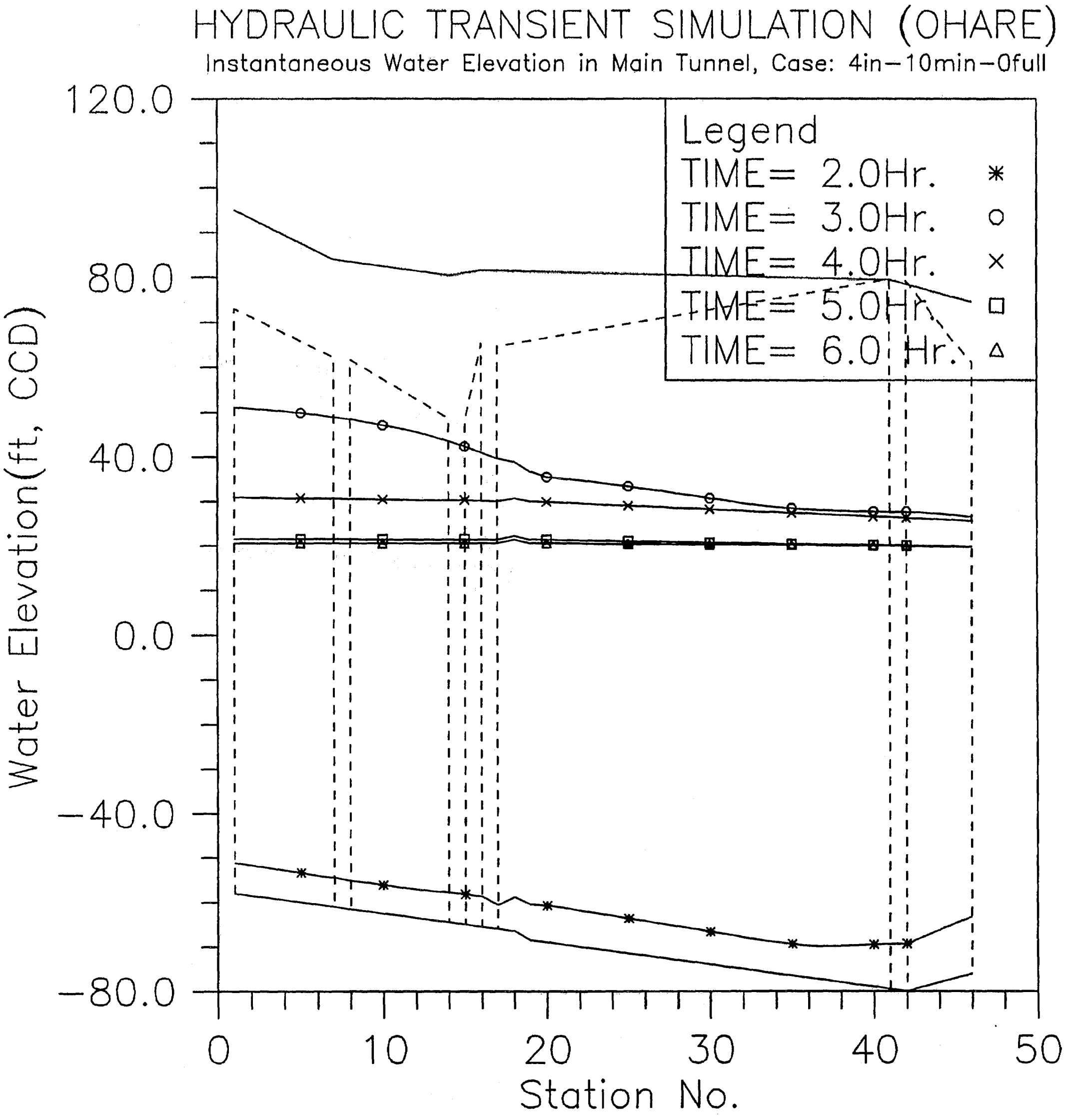

Fig. 20 Instantaneous water elevations in the main tunnel from DS-1 to the main shaft during 4 in 10 min storm event, modeling conditions: empty initial tunnel condition and gated inflow at DS-8.

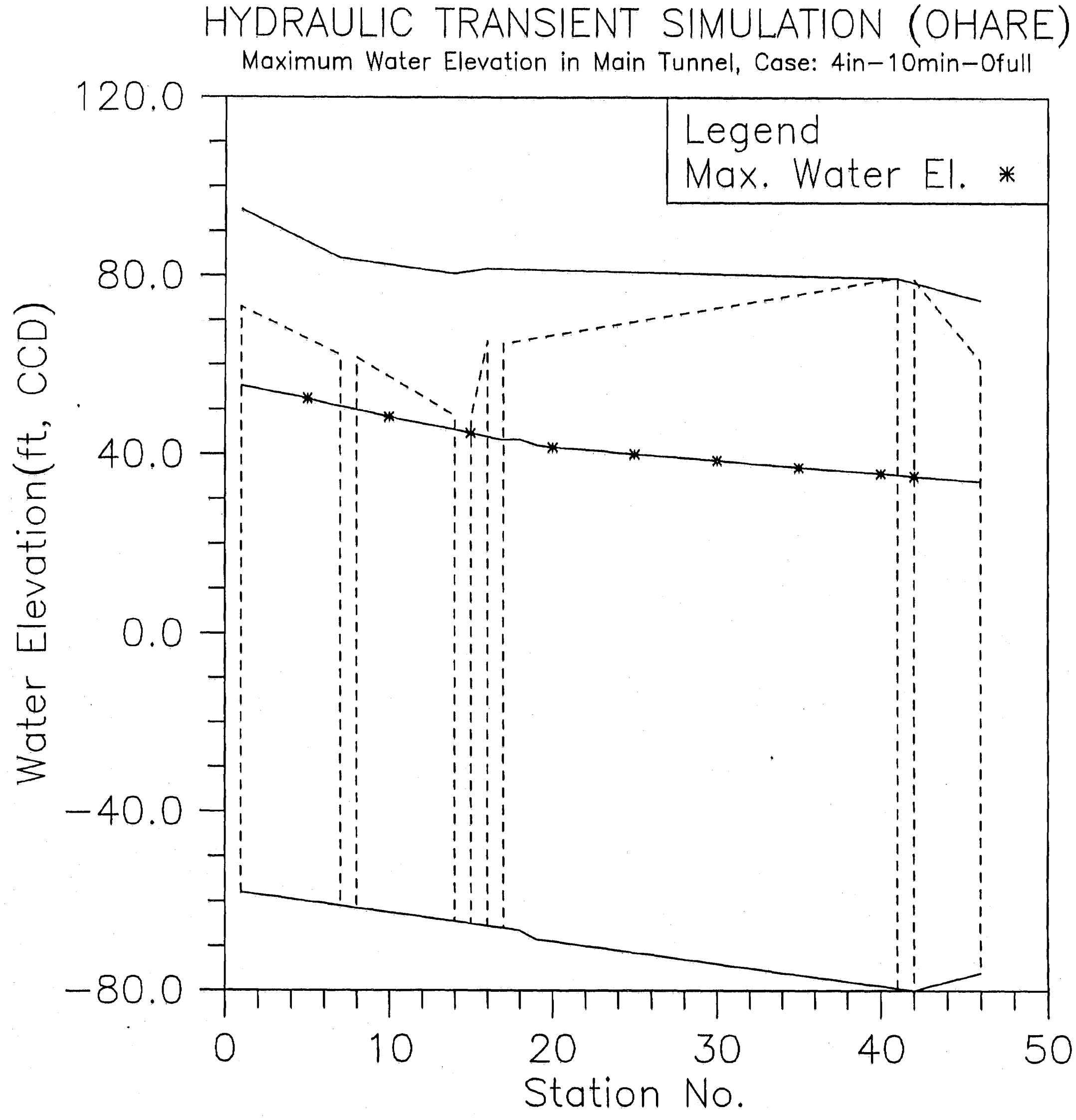

Fig. 21 Maximum water elevations in the main tunnel from DS-1 to the main shaft during 4 in 10 min storm event, modeling conditions: empty initial tunnel condition and gated inflow at DS-8.

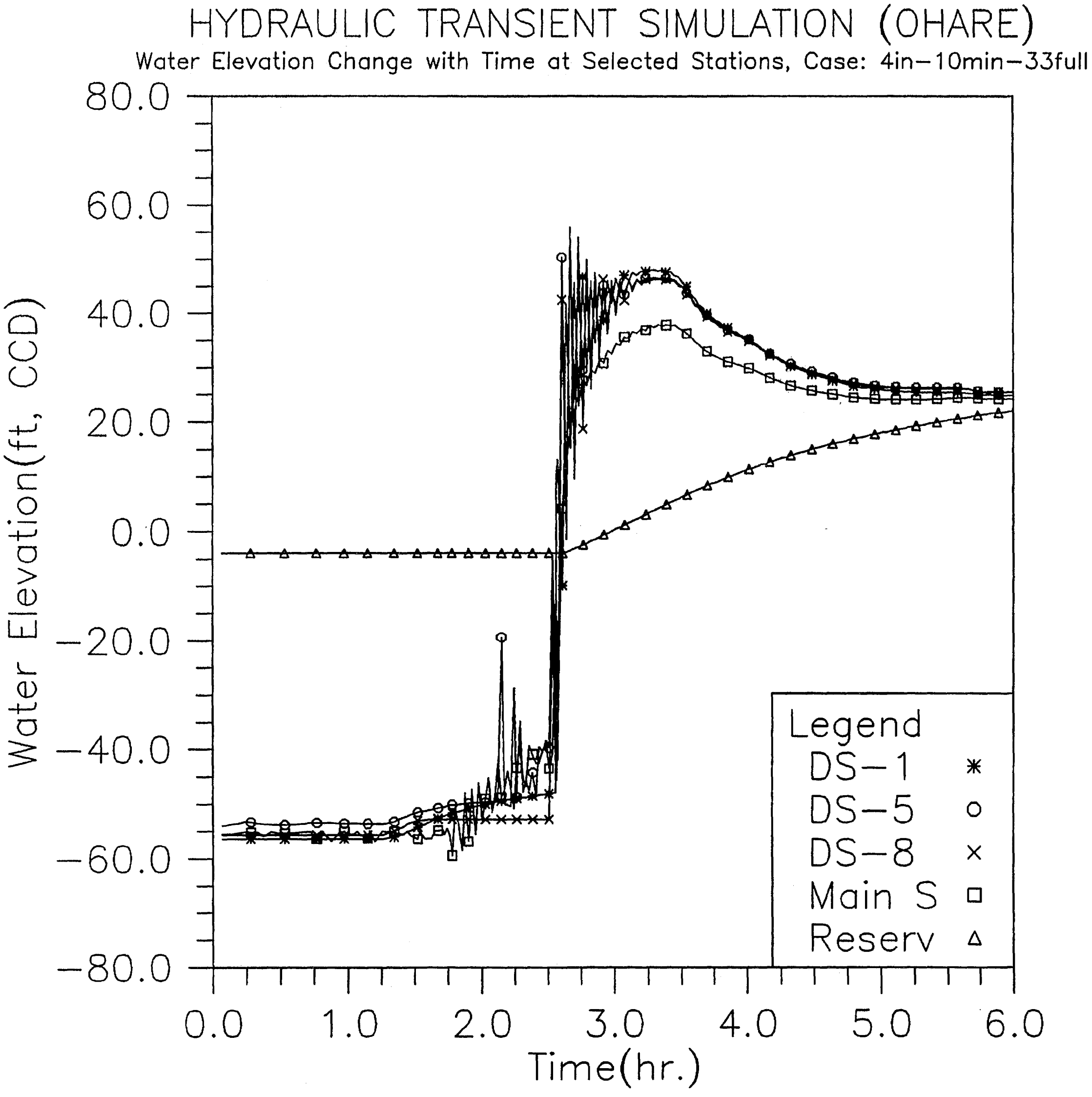

Fig. 22 Water elevation variations with time during 4 in 10 min storm event at 5 locations (DS-1, DS-5, DS-8, main shaft and reservoir), modeling conditions: 33% full initial tunnel condition and gated inflow at DS-8.

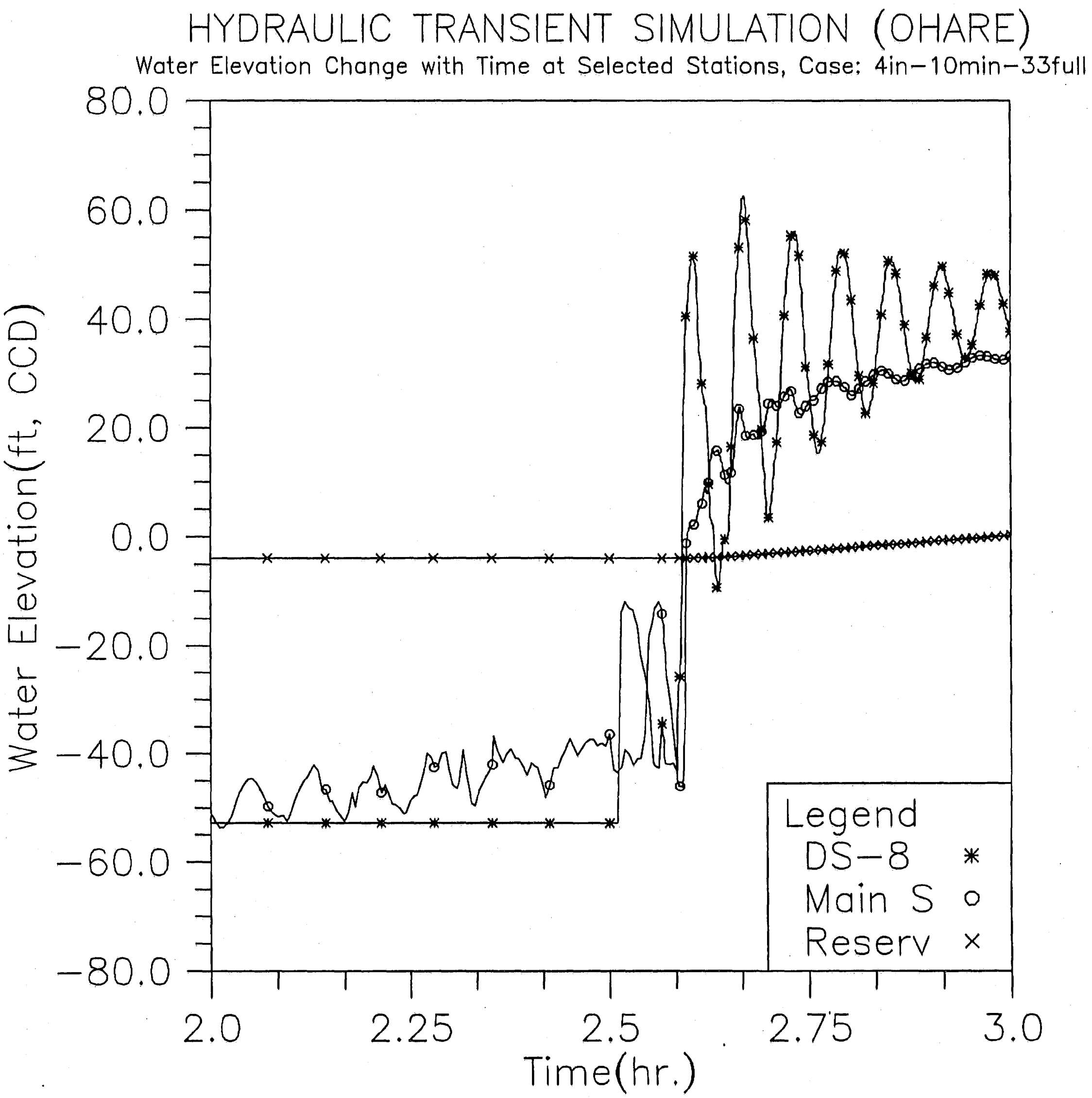

Fig. 23 Detailed water elevation variations with time in the surge process during 4 in 10 min storm event at 2 locations (DS-1 and DS-5), modeling conditions: 33% full initial tunnel condition and gated inflow at DS-8.

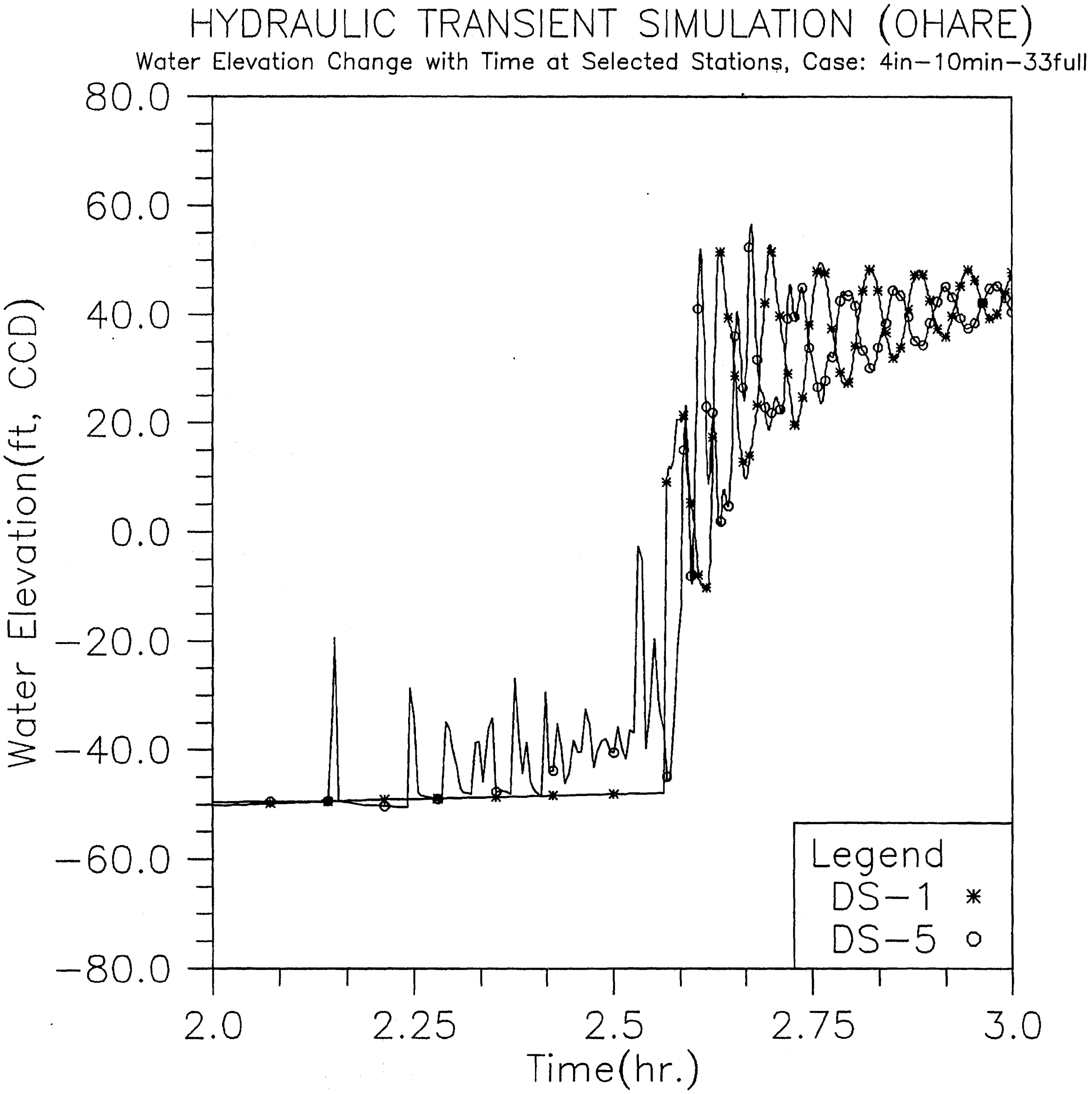

Fig. 24 Detailed water elevation variations with time in the surge process during 4 in 10 min storm event at 3 locations (DS-8, main shaft and reservoir), modeling conditions: 33% full initial tunnel condition and gated inflow at DS-8.

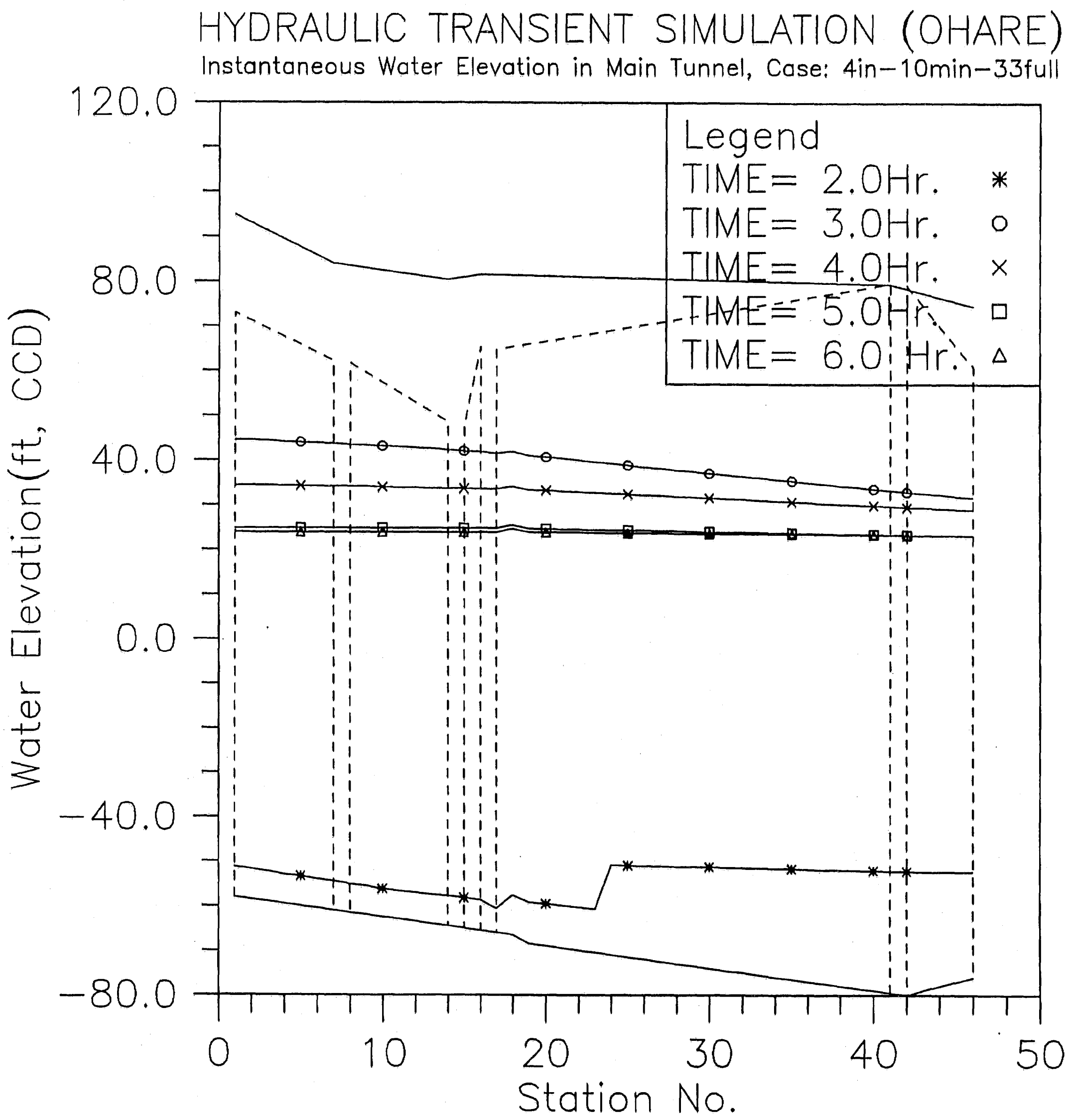

Fig. 25 Instantaneous water elevations in the main tunnel from DS-1 to the main shaft during 4 in 10 min storm event, modeling conditions: 33% full initial tunnel condition and gated inflow at DS-8.

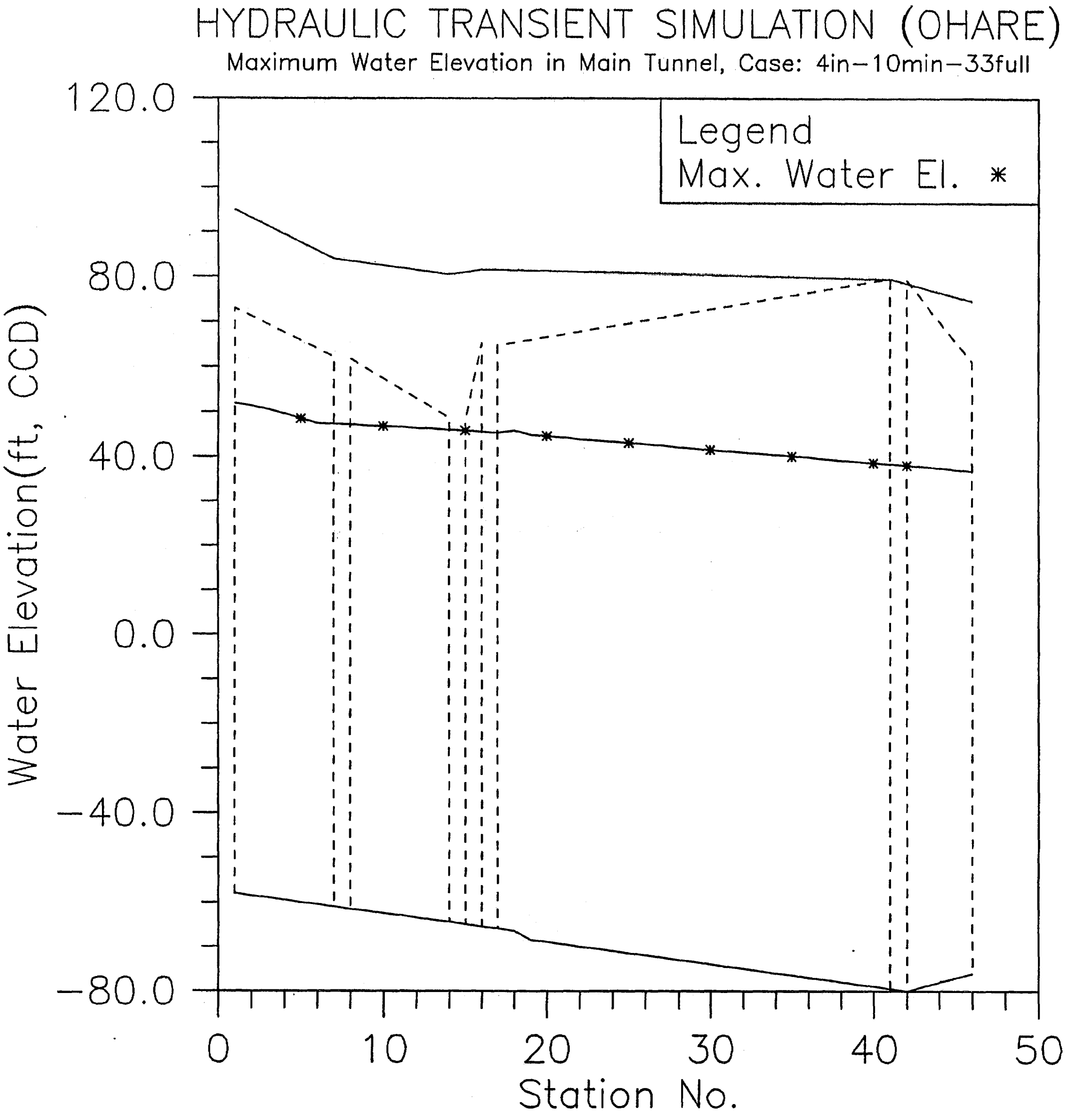

Fig. 26 Maximum water elevations in the main tunnel from DS-1 to the main shaft during 4 in 10 min storm event, modeling conditions: 33% full initial tunnel condition and gated inflow at DS-8.

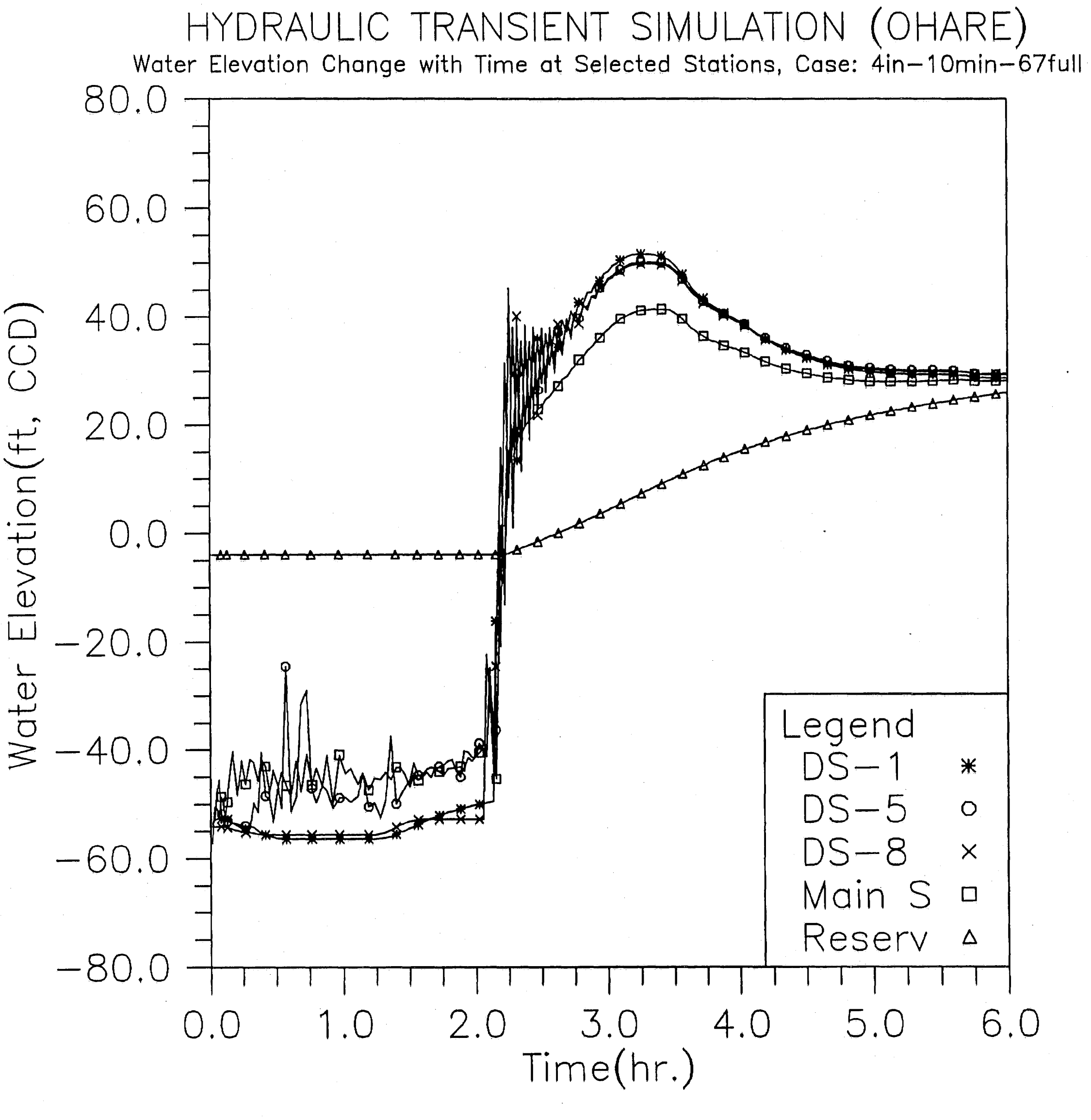

Fig. 27 Water elevation variations with time during 4 in 10 min storm event at 5 locations (DS-1, DS-5, DS-8, main shaft and reservoir), modeling conditions: 67% full initial tunnel condition and gated inflow at DS-8.

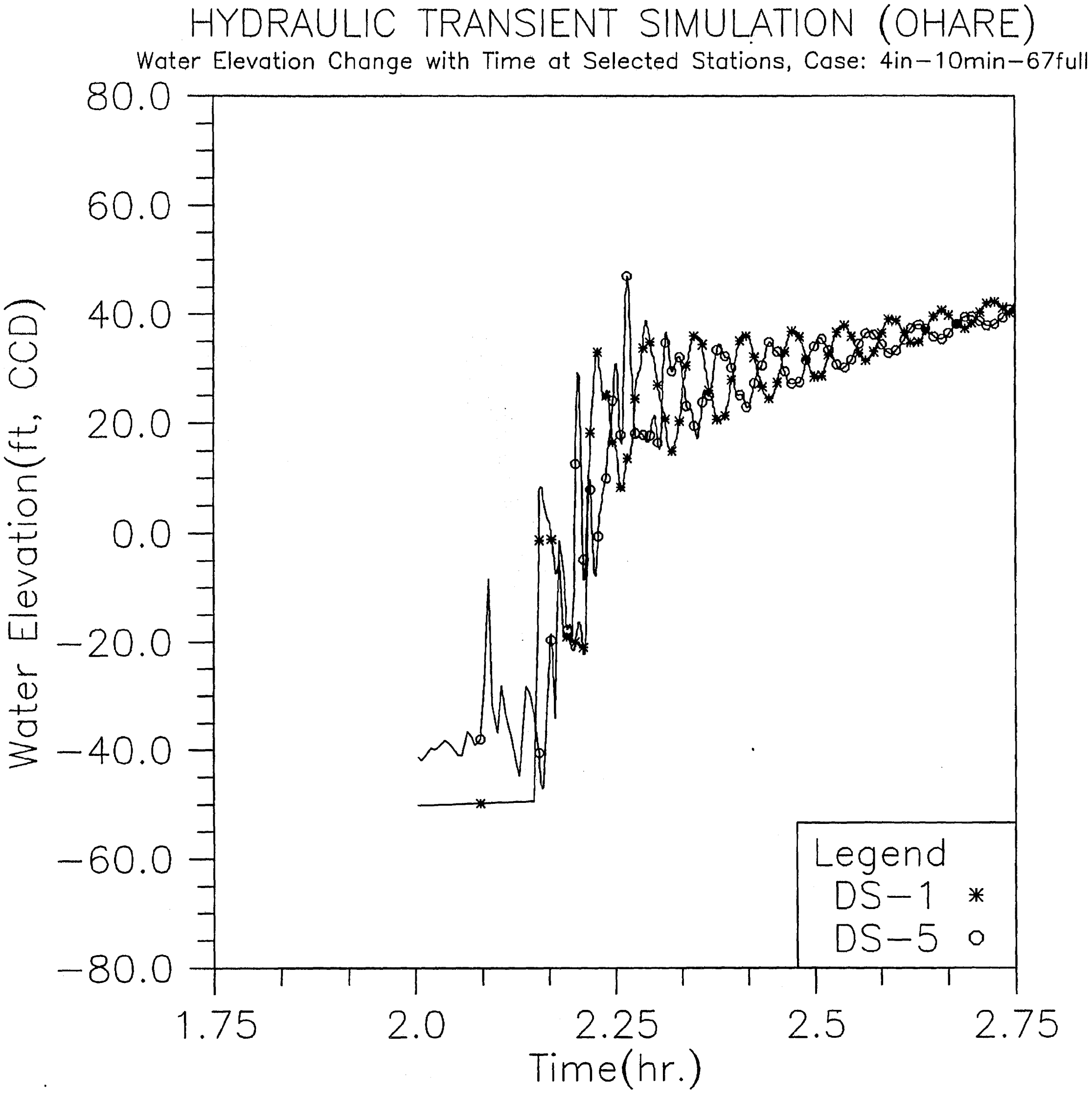

Fig. 28 Detailed water elevation variations with time in the surge process during 4 in 10 min storm event at 2 locations (DS-1 and DS-5), modeling conditions: 67% full initial tunnel condition and gated inflow at DS-8.

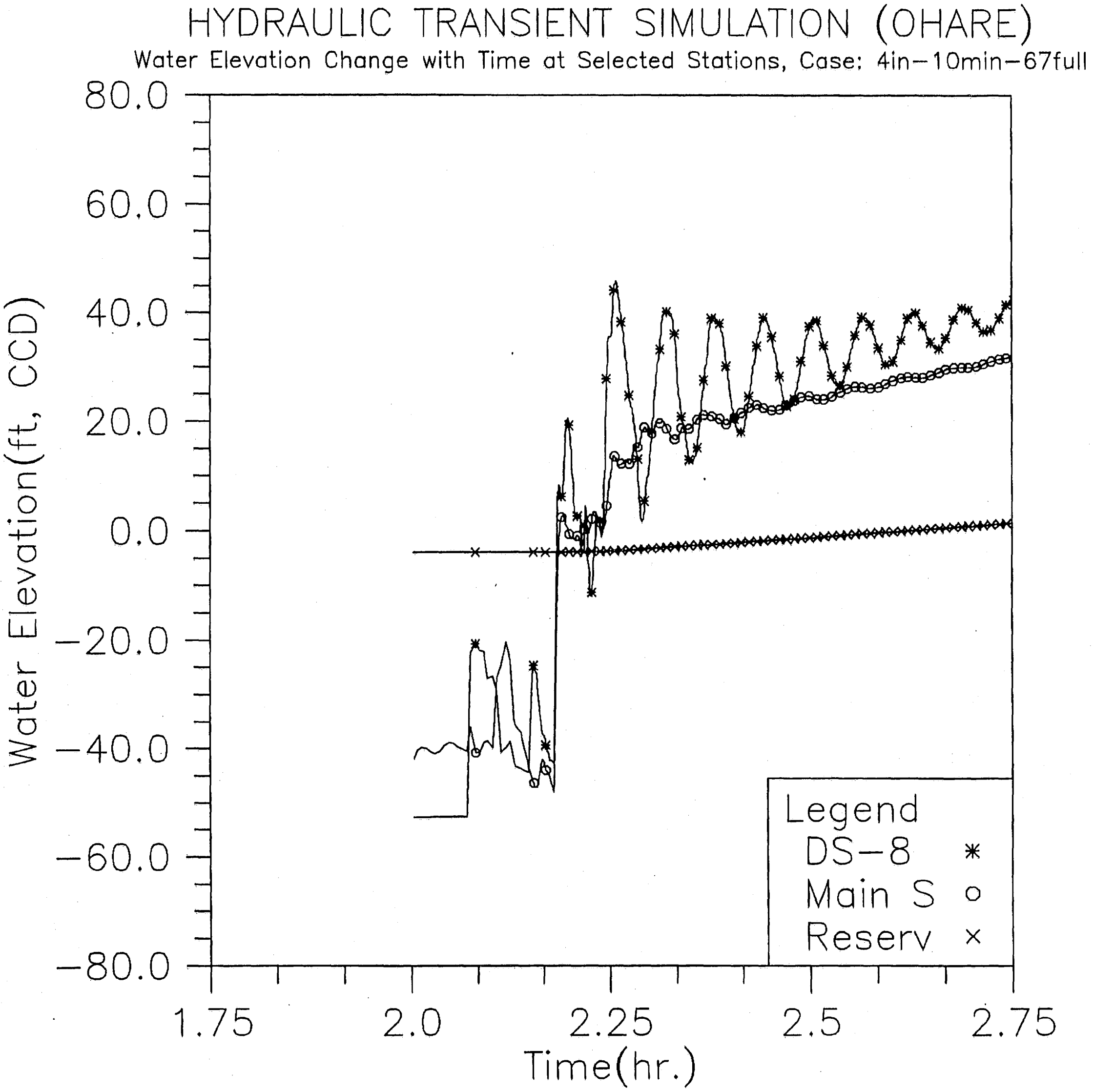

Fig. 29 Detailed water elevation variations with time in the surge process during 4 in 10 min storm event at 3 locations (DS-8, main shaft and reservoir), modeling conditions: 67% full initial tunnel condition and gated inflow at DS-8.

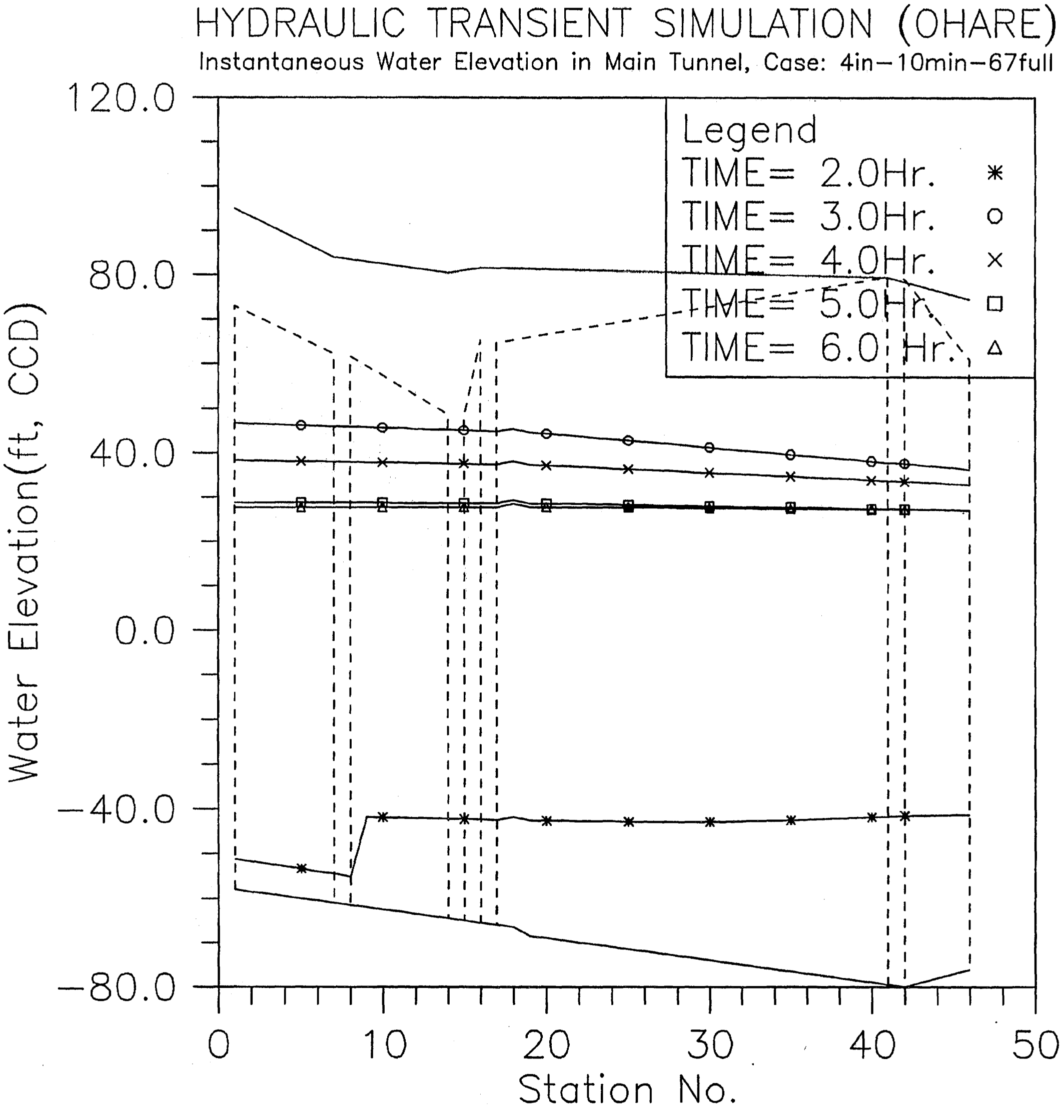

Fig. 30 Instantaneous water elevations in the main tunnel from DS-1 to the main shaft during 4 in 10 min storm event, modeling conditions: 67% full initial tunnel condition and gated inflow at DS-8.

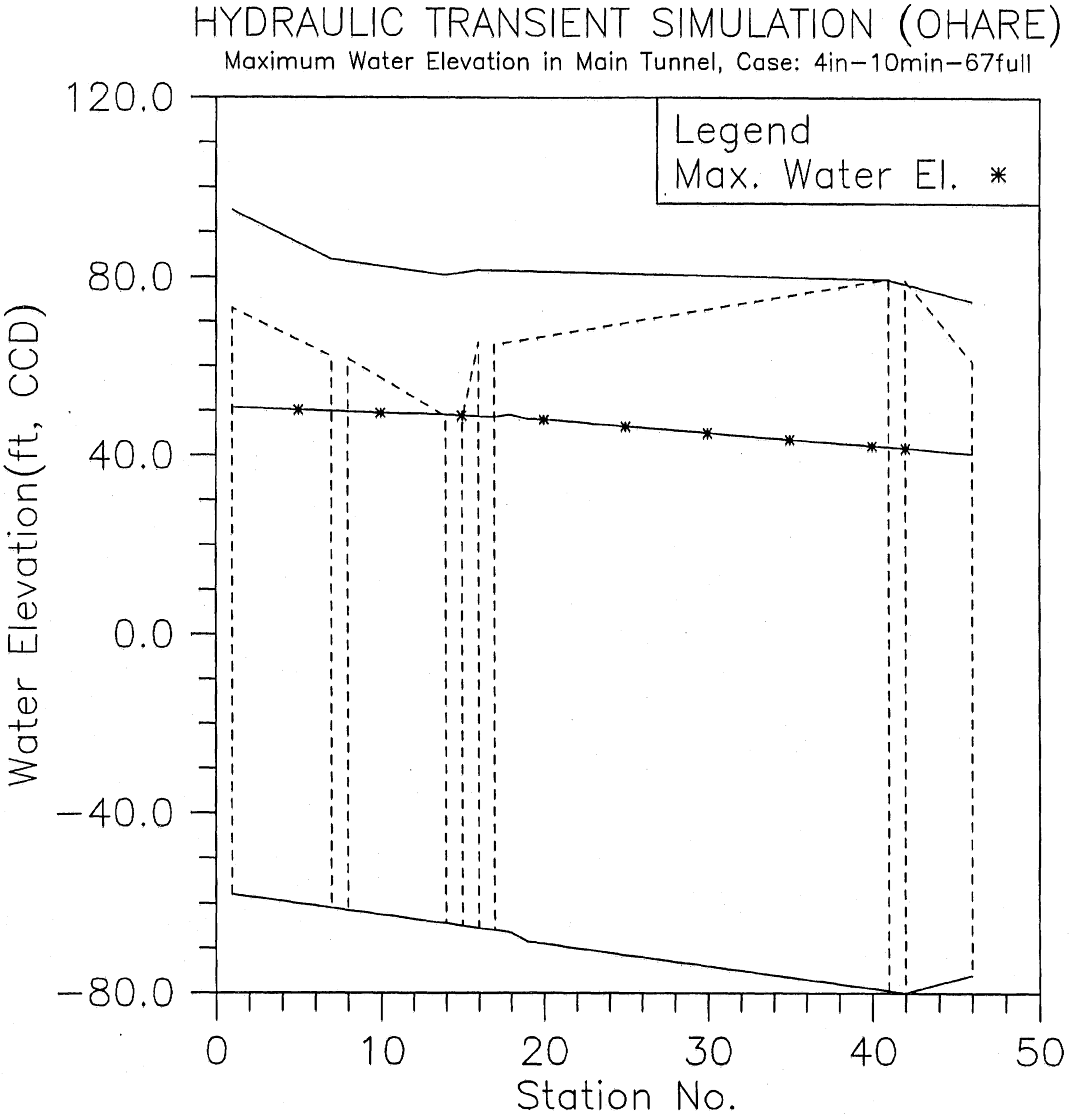

Fig. 31 Maximum water elevations in the main tunnel from DS-1 to the main shaft during 4 in 10 min storm event, modeling conditions: 67% full initial tunnel condition and gated inflow at DS-8.

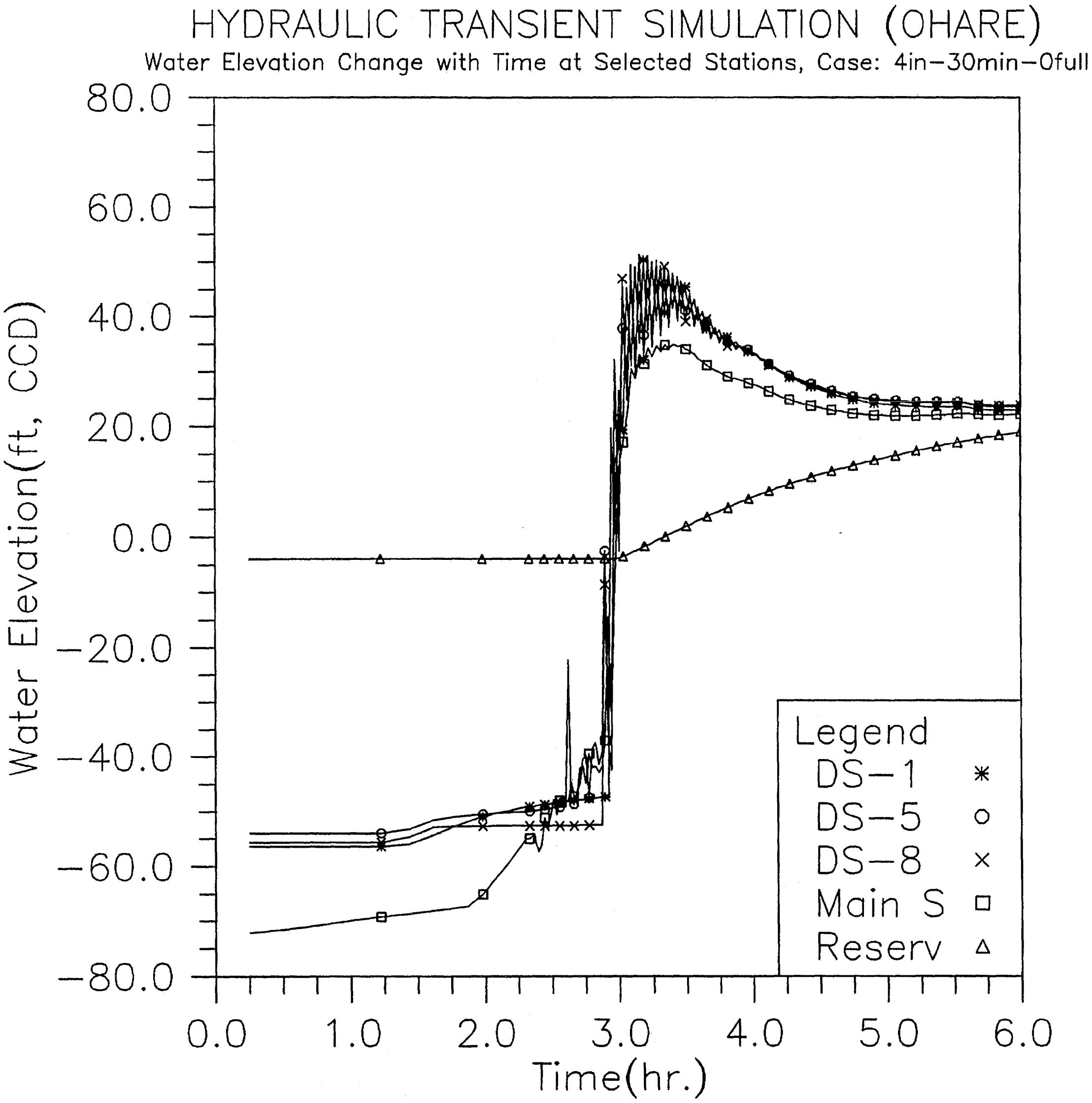

Fig. 32 Water elevation variations with time during 4 in 30 min storm event at 5 locations (DS-1, DS-5, DS-8, main shaft and reservoir), modeling conditions: empty initial tunnel condition and gated inflow at DS-8.

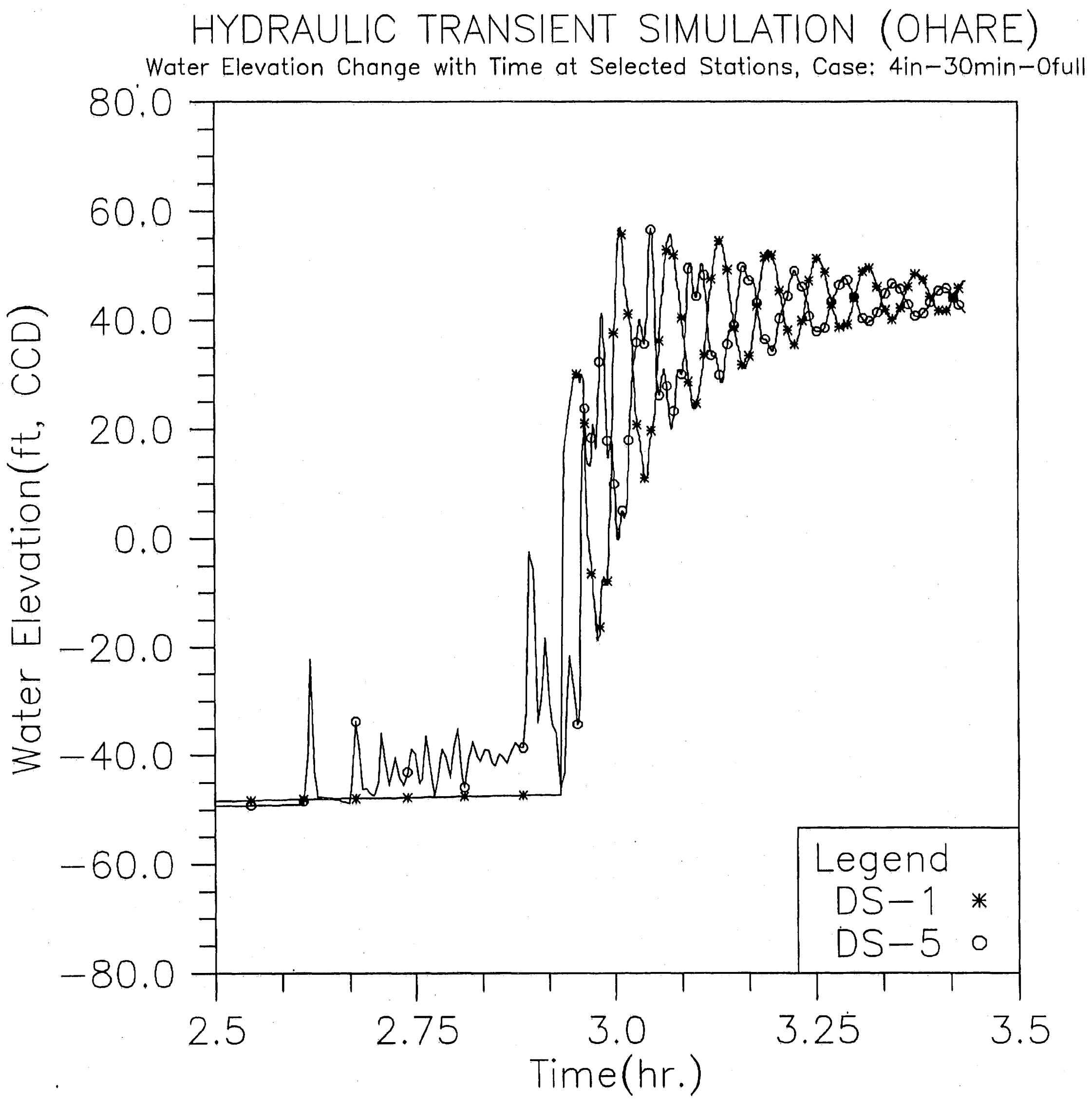

Fig. 33 Detailed water elevation variations with time in the surge process during 4 in 30 min storm event at 2 locations (DS-1 and DS-5), modeling conditions: empty initial tunnel condition and gated inflow at DS-8.

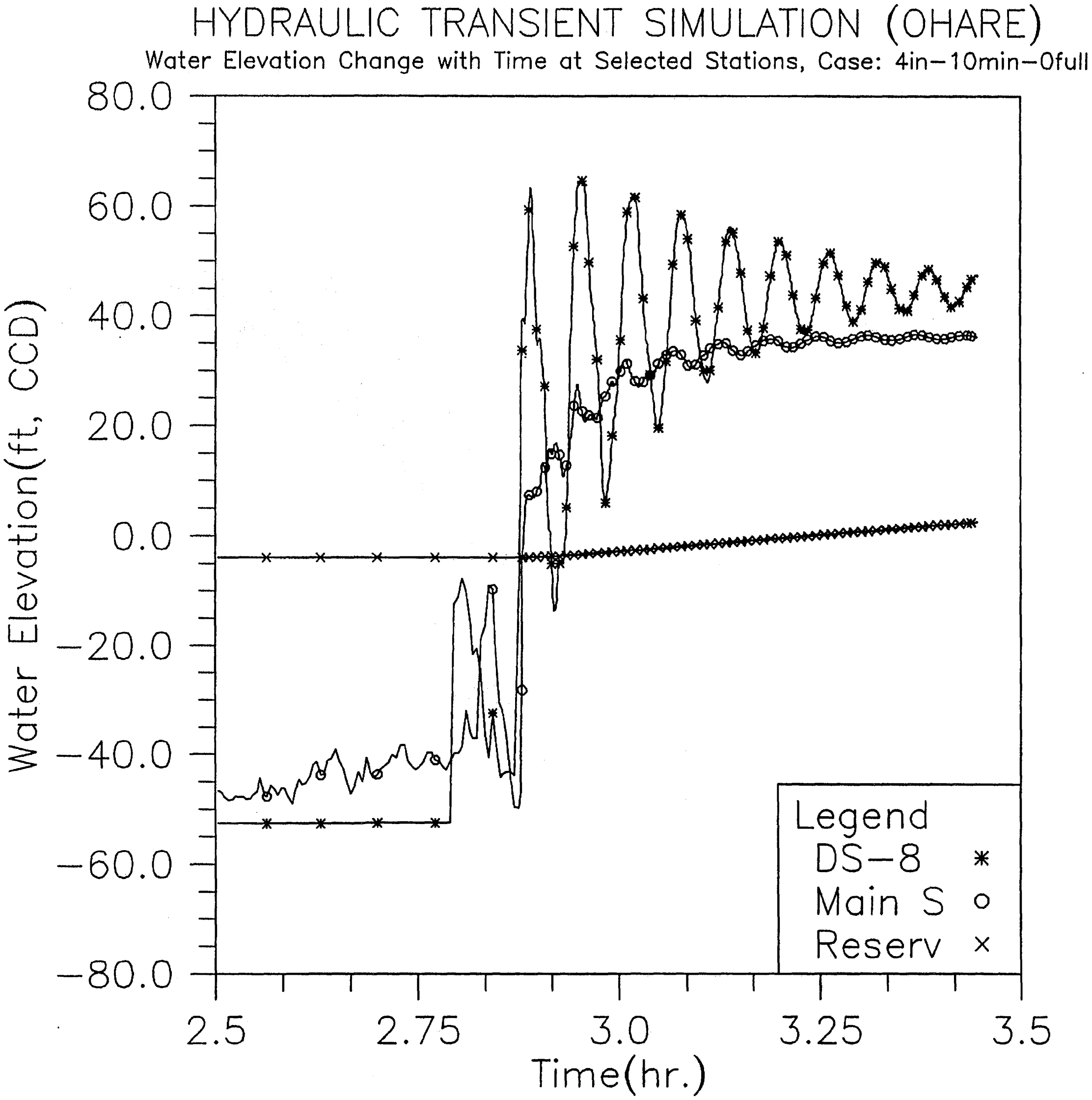

Fig. 34 Detailed water elevation variations with time in the surge process during 4 in 30 min storm event at 3 locations (DS-8, main shaft and reservoir), modeling conditions: empty initial tunnel condition and gated inflow at DS-8.

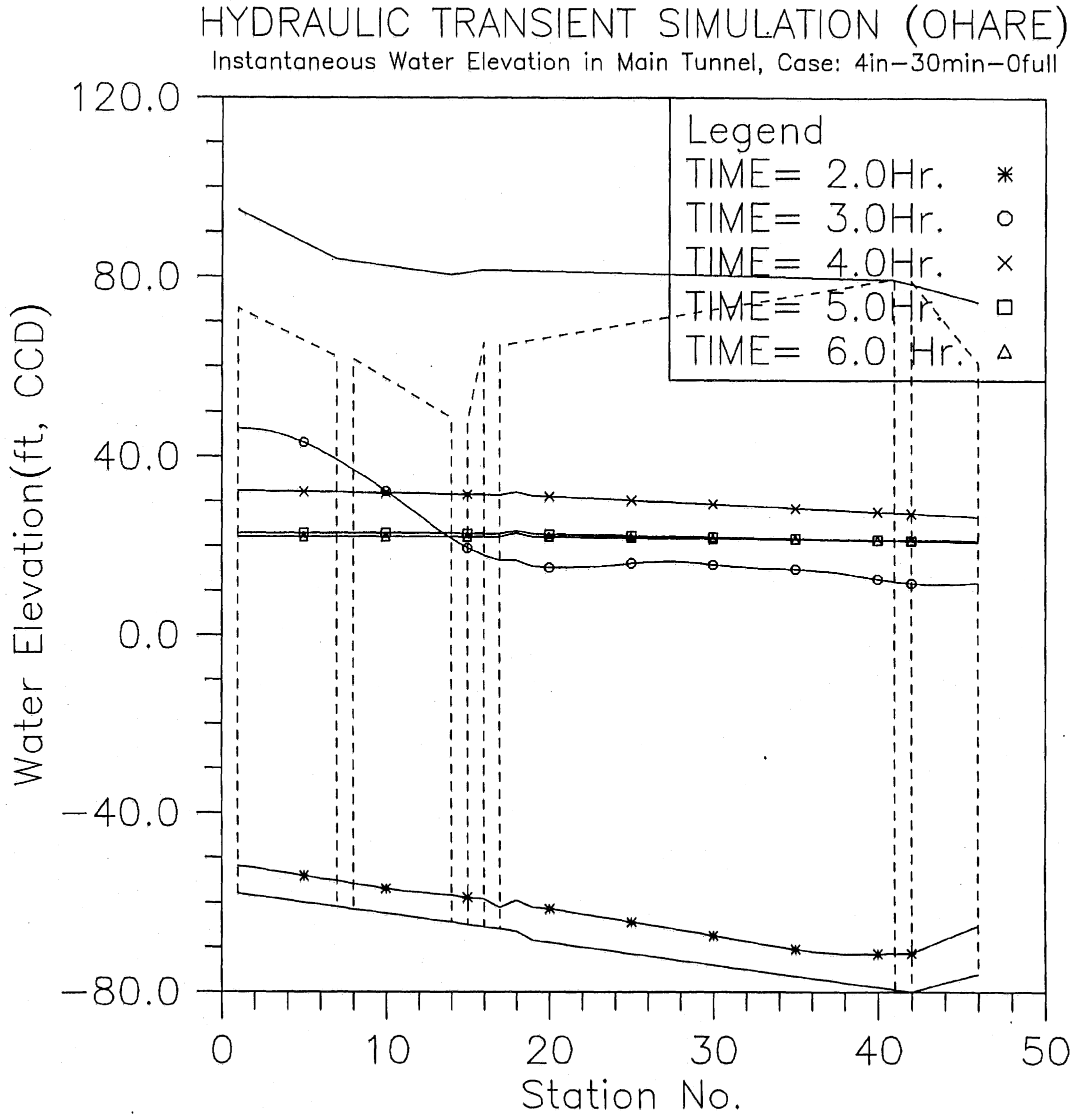

Fig. 35 Instantaneous water elevations in the main tunnel from DS-1 to the main shaft during 4 in 30 min storm event, modeling conditions: empty initial tunnel condition and gated inflow at DS-8.

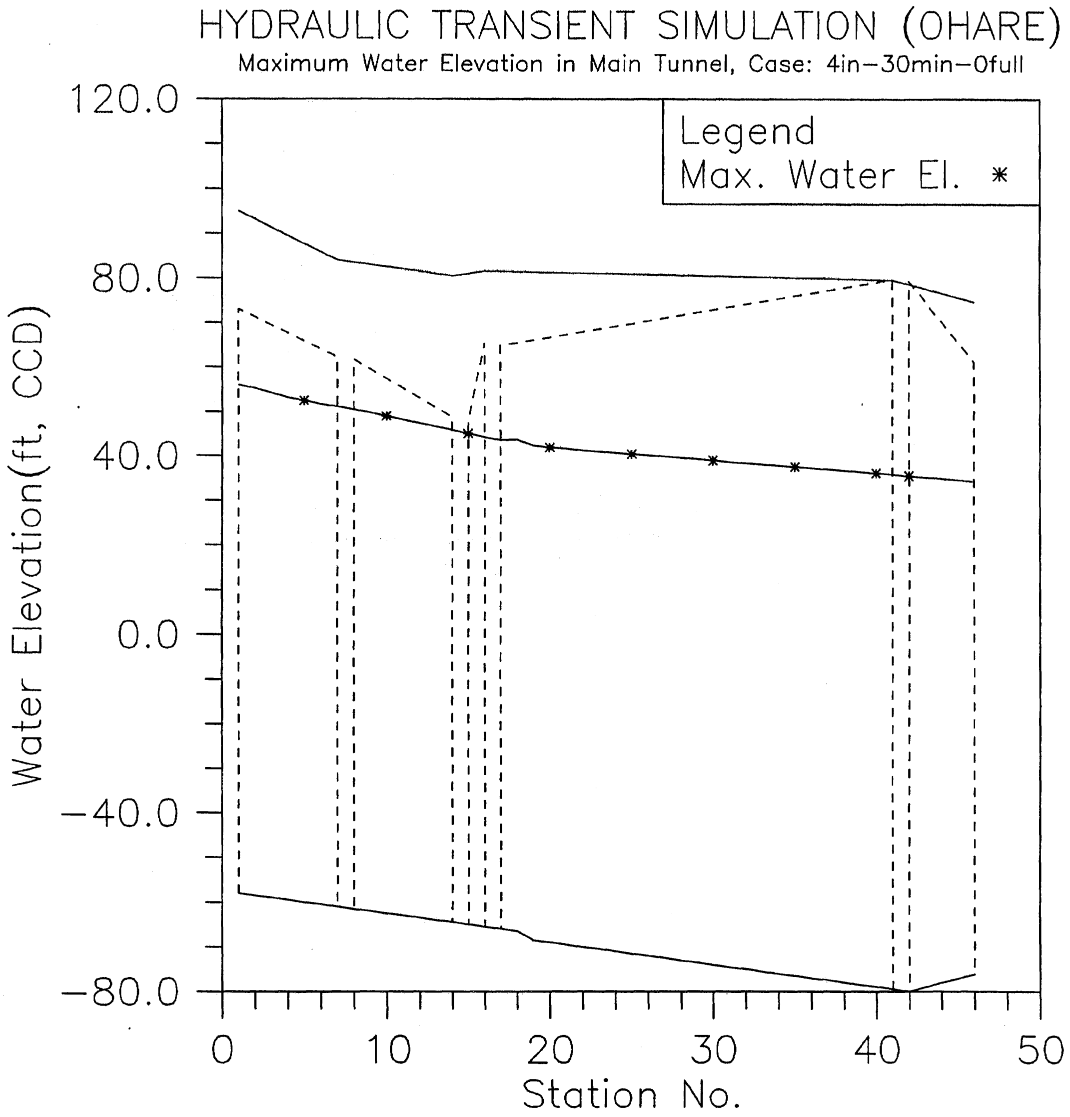

Fig. 36 Maximum water elevations in the main tunnel from DS-1 to the main shaft during 4 in 30 min storm event, modeling conditions: empty initial tunnel condition and gated inflow at DS-8.

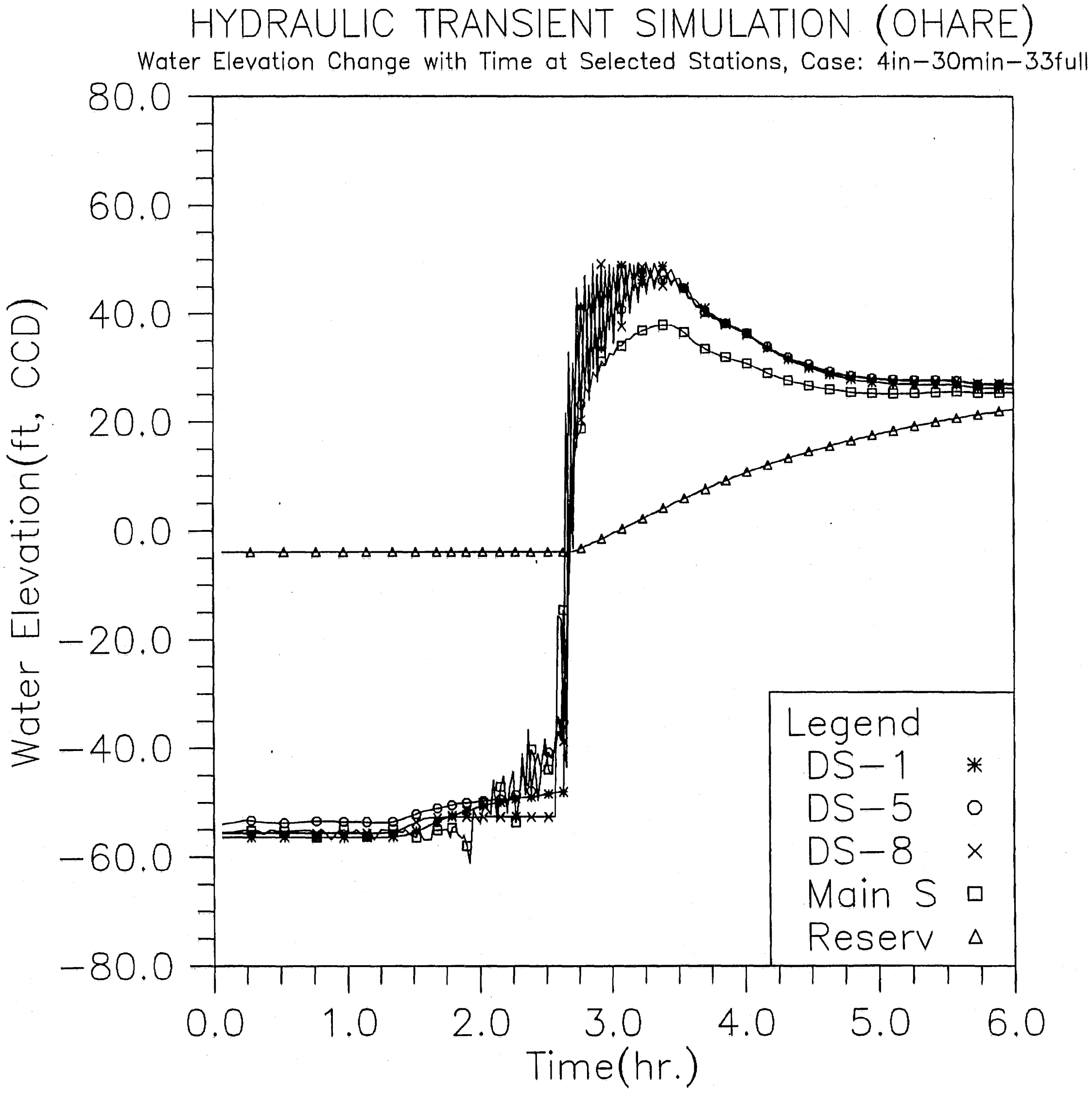

Fig. 37 Water elevation variations with time during 4 in 30 min storm event at 5 locations (DS-1, DS-5, DS-8, main shaft and reservoir), modeling conditions: 33% full initial tunnel condition and gated inflow at DS-8.

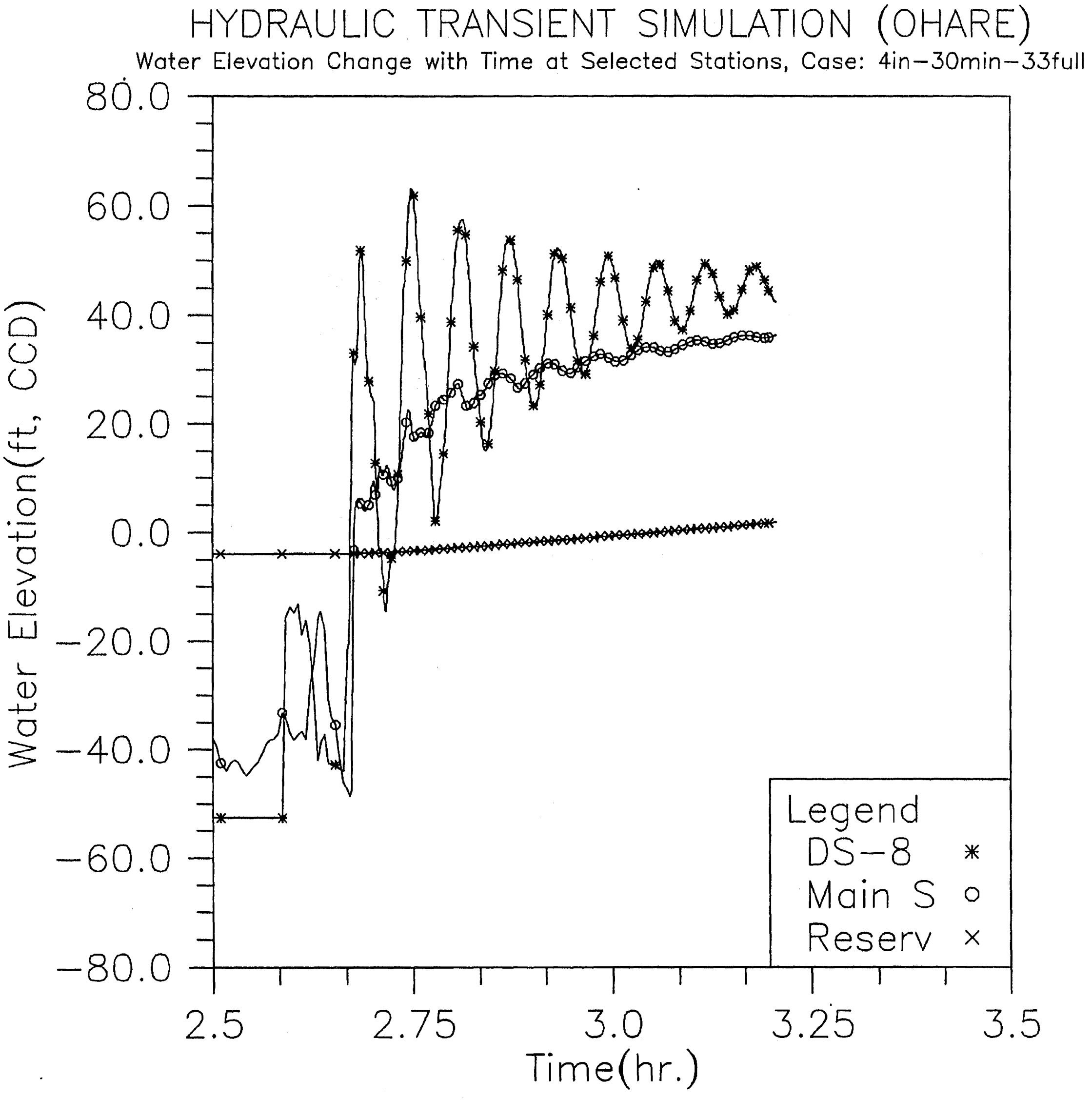

Fig. 38 Detailed water elevation variations with time in the surge process during 4 in 30 min storm event at 2 locations (DS-1 and DS-5), modeling conditions: 33% full initial tunnel condition and gated inflow at DS-8.

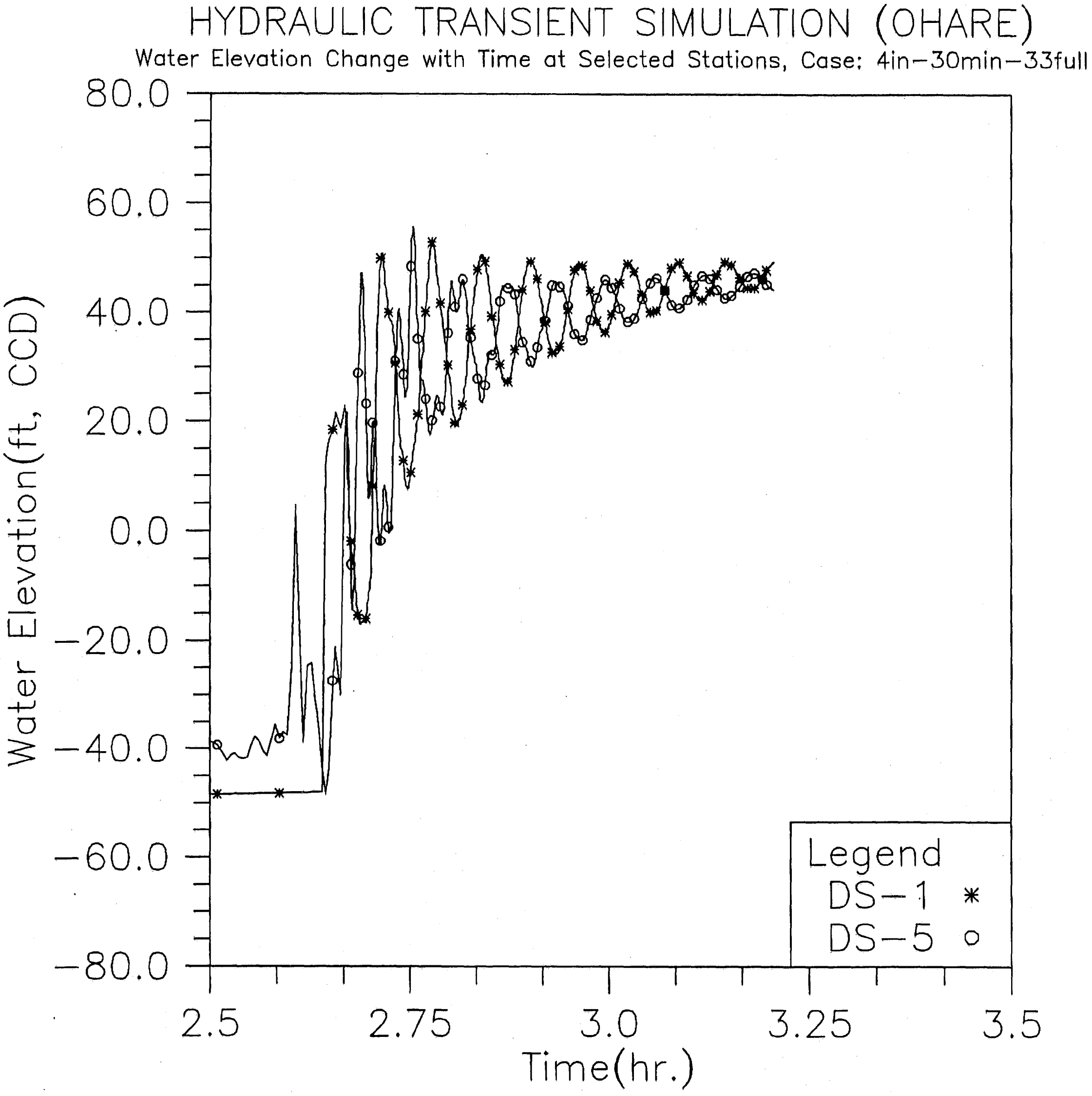

Fig. 39 Detailed water elevation variations with time in the surge process during 4 in 30 min storm event at 3 locations (DS-8, main shaft and reservoir), modeling conditions: 33% full initial tunnel condition and gated inflow at DS-8.

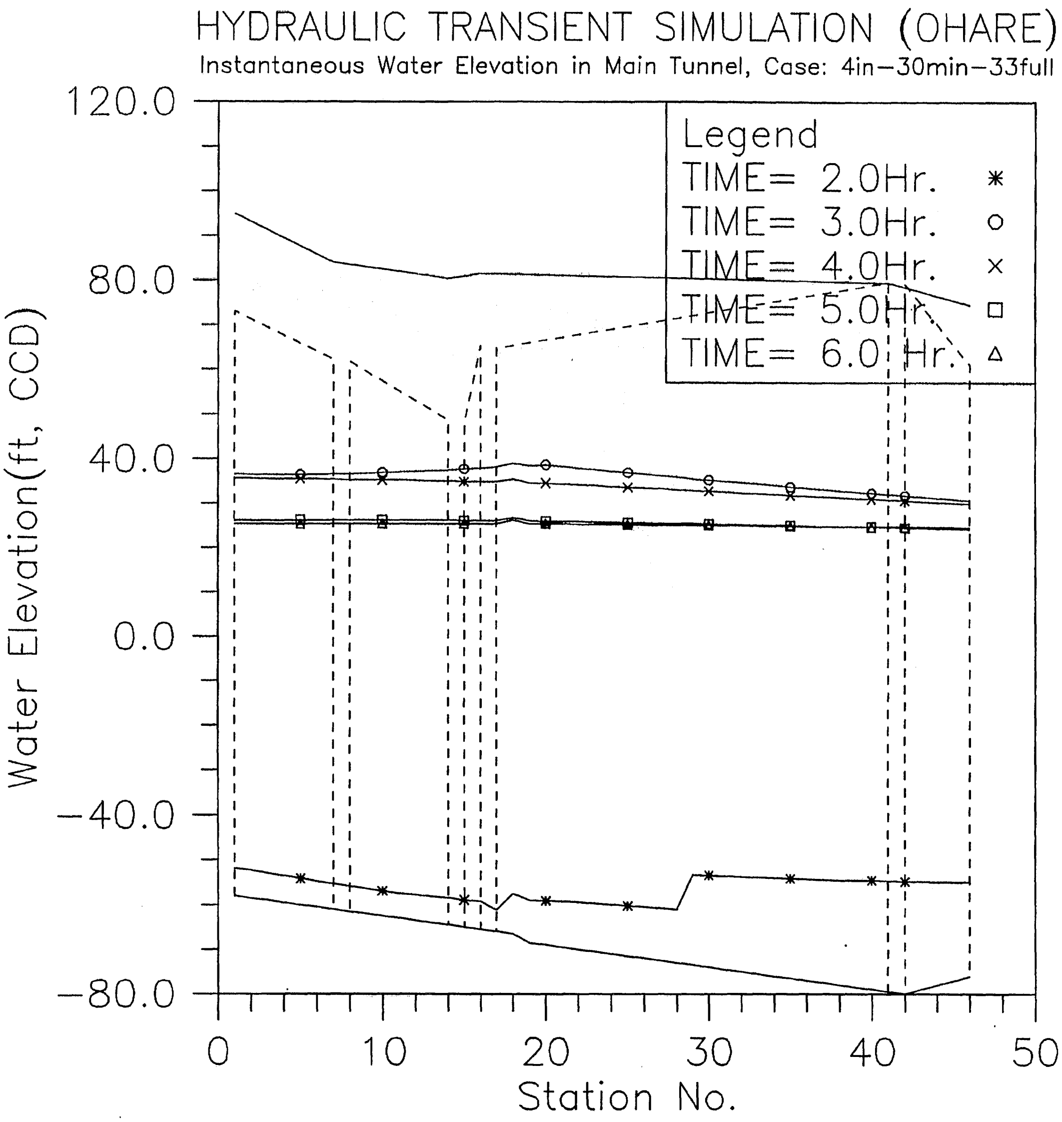

Fig. 40 Instantaneous water elevations in the main tunnel from DS-1 to the main shaft during 4 in 30 min storm event, modeling conditions: 33% full initial tunnel condition and gated inflow at DS-8.

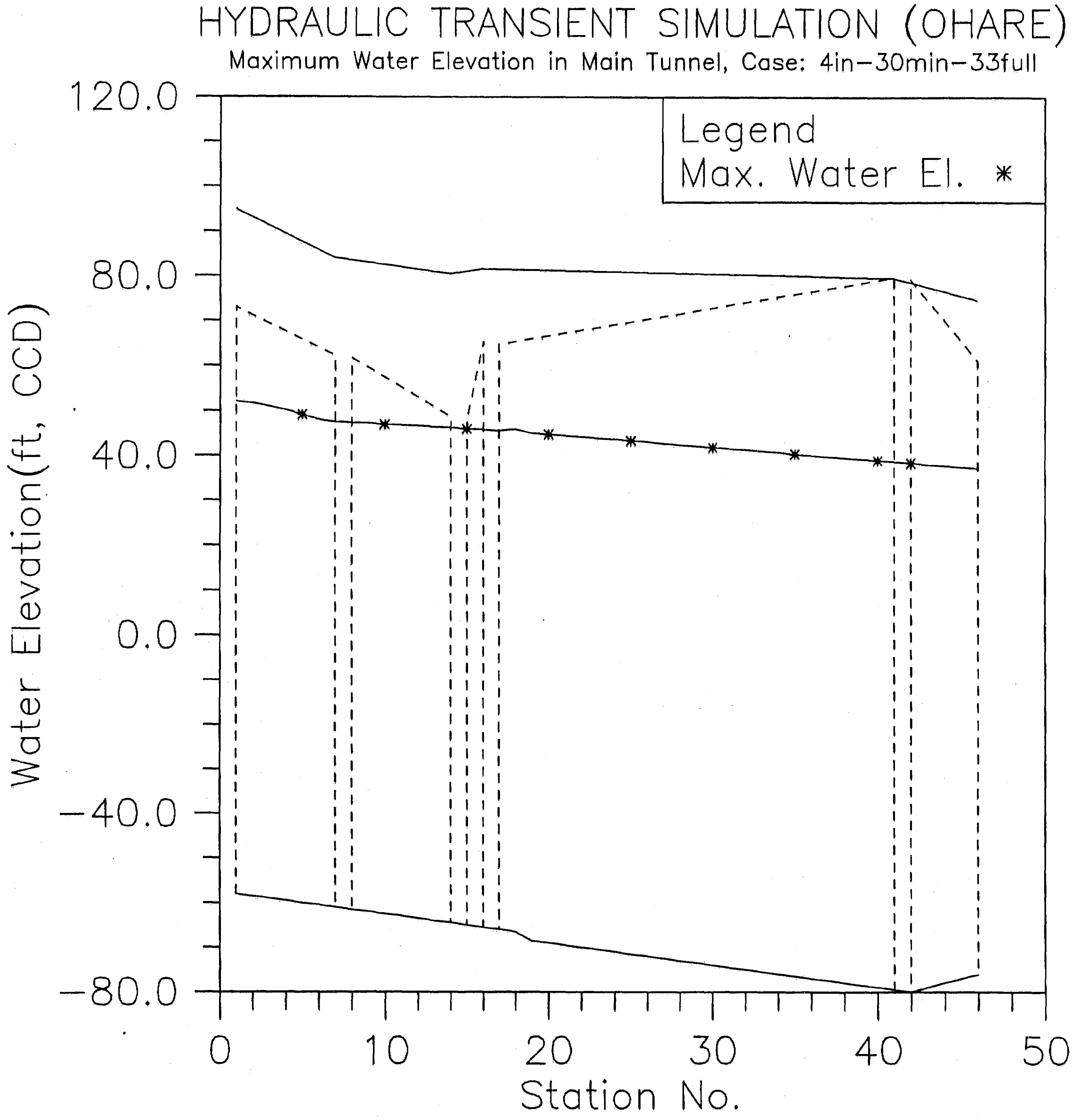

Fig. 41 Maximum water elevations in the main tunnel from DS-1 to the main shaft during 4 in 30 min storm event, modeling conditions: 33% full initial tunnel condition and gated inflow at DS-8.

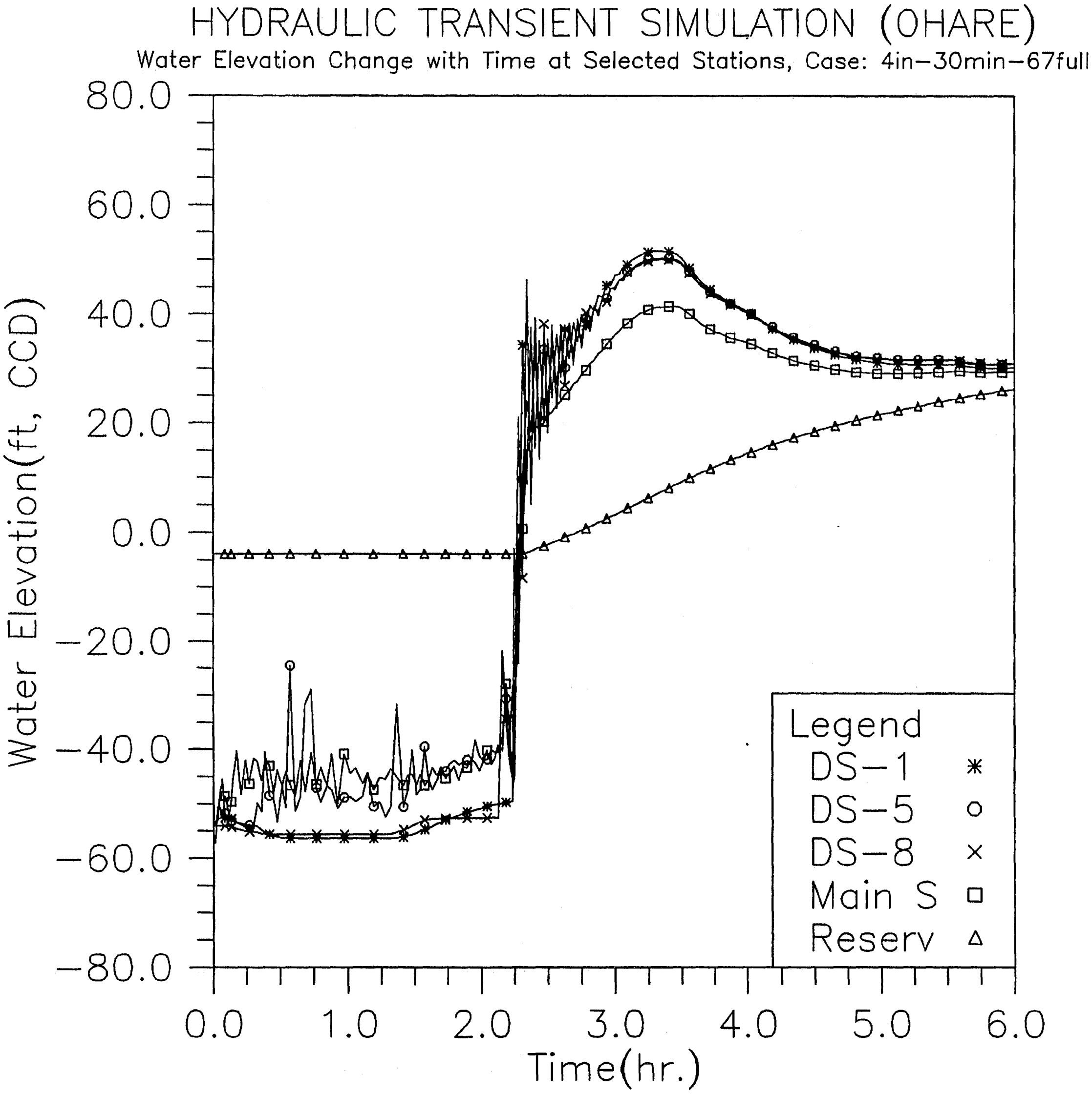

Fig. 42 Water elevation variations with time during 4 in 30 min storm event at 5 locations (DS-1, DS-5, DS-8, main shaft and reservoir), modeling conditions: 67% full initial tunnel condition and gated inflow at DS-8.

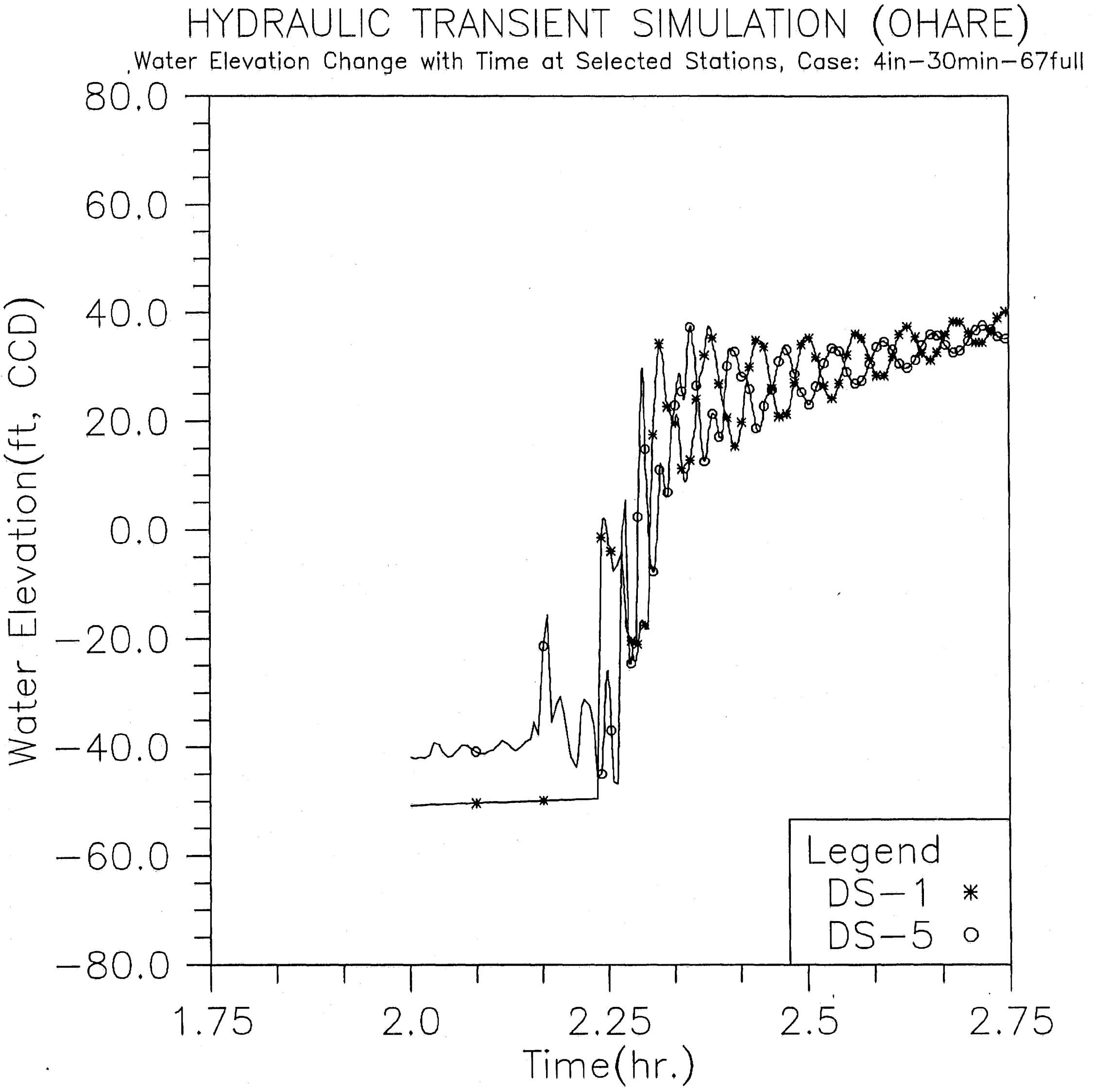

Fig. 43 Detailed water elevation variations with time in the surge process during 4 in 30 min storm event at 2 locations (DS-1 and DS-5), modeling conditions: 67% full initial tunnel condition and gated inflow at DS-8.

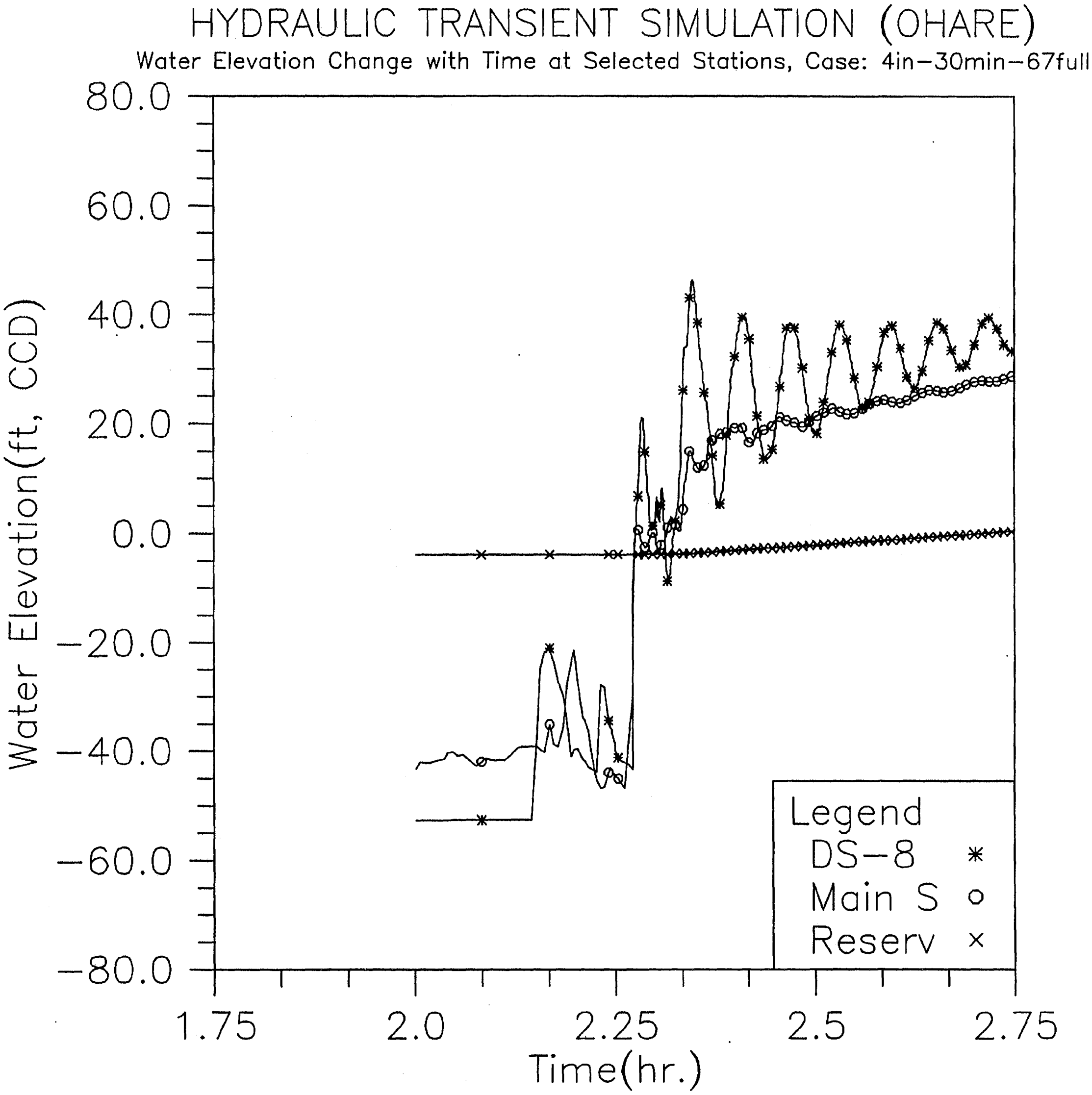

Fig. 44 Detailed water elevation variations with time in the surge process during 4 in 30 min storm event at 3 locations (DS-8, main shaft and reservoir), modeling conditions: 67% full initial tunnel condition and gated inflow at DS-8.

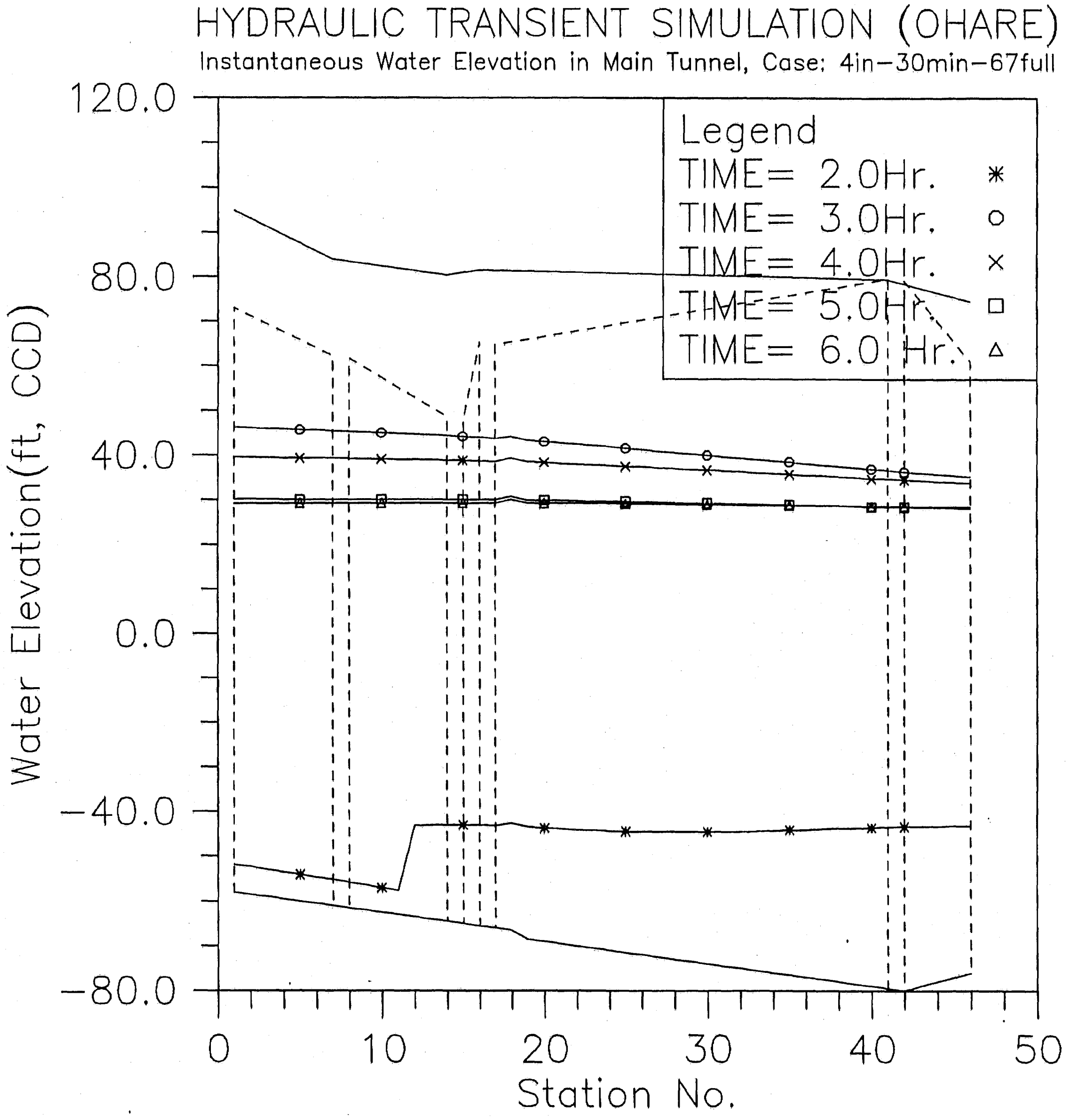

Fig. 45 Instantaneous water elevations in the main tunnel from DS-1 to the main shaft during 4 in 30 min storm event, modeling conditions: 67% full initial tunnel condition and gated inflow at DS-8.

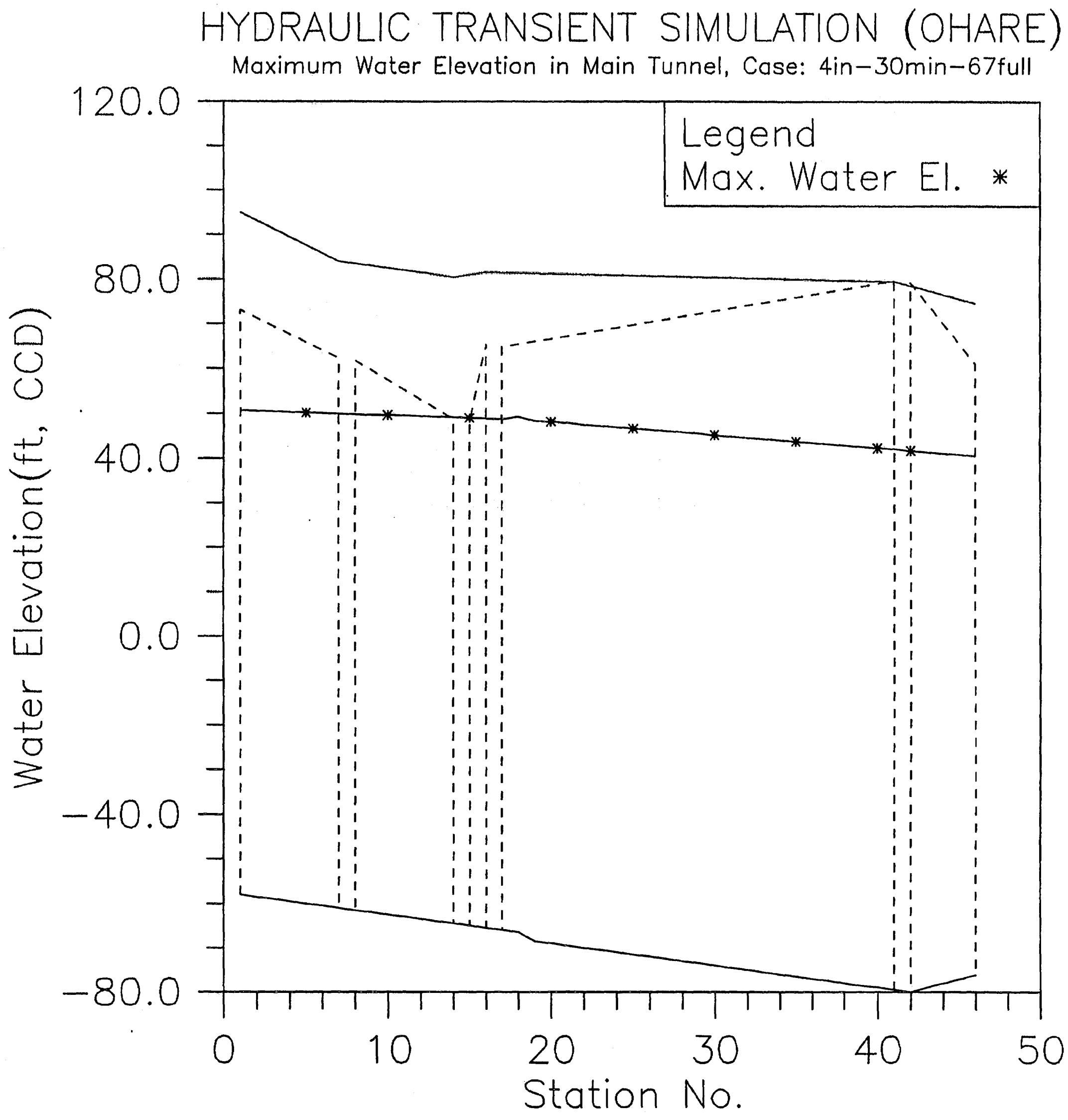

Fig. 46 Maximum water elevations in the main tunnel from DS-1 to the main shaft during 4 in 30 min storm event, modeling conditions: 67% full initial tunnel condition and gated inflow at DS-8.

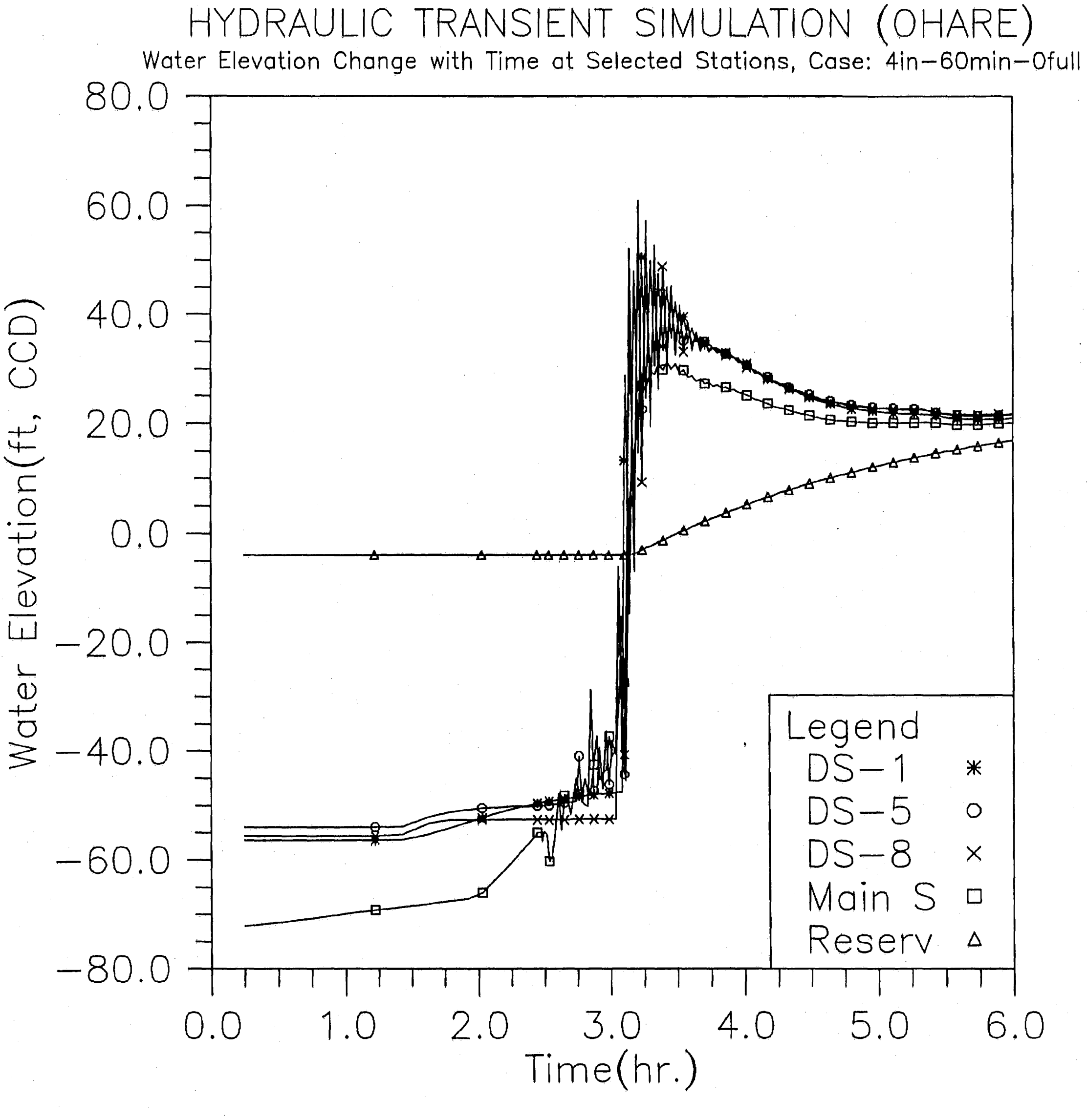

Fig. 47 Water elevation variations with time during 4 in 1 hour storm event at 5 locations (DS-1, DS-5, DS-8, main shaft and reservoir), modeling conditions: empty initial tunnel condition and gated inflow at DS-8.

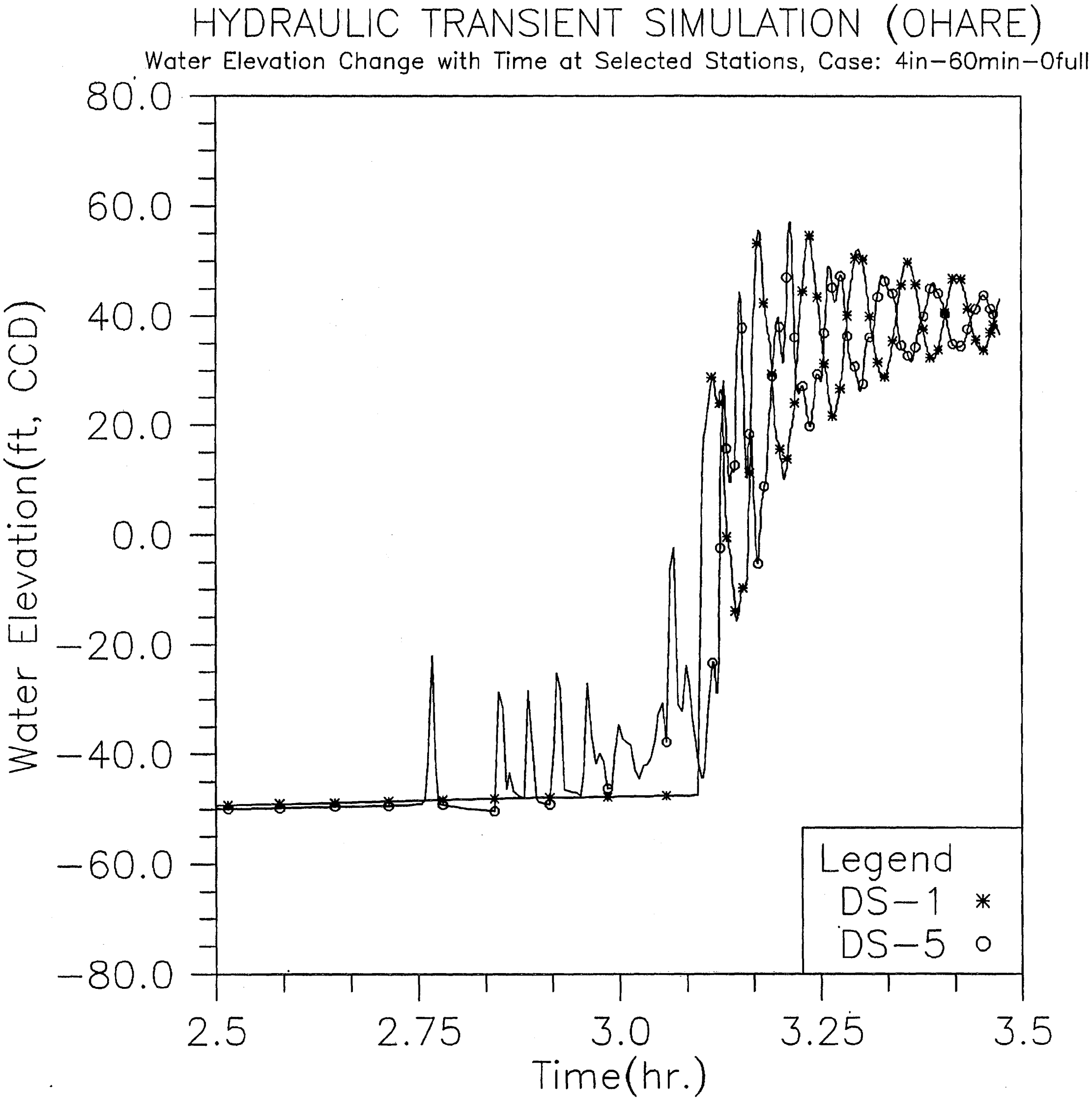

Fig. 48 Detailed water elevation variations with time in the surge process during 4 in 1 hour storm event at 2 locations (DS-1 and DS-5), modeling conditions: empty initial tunnel condition and gated inflow at DS-8.

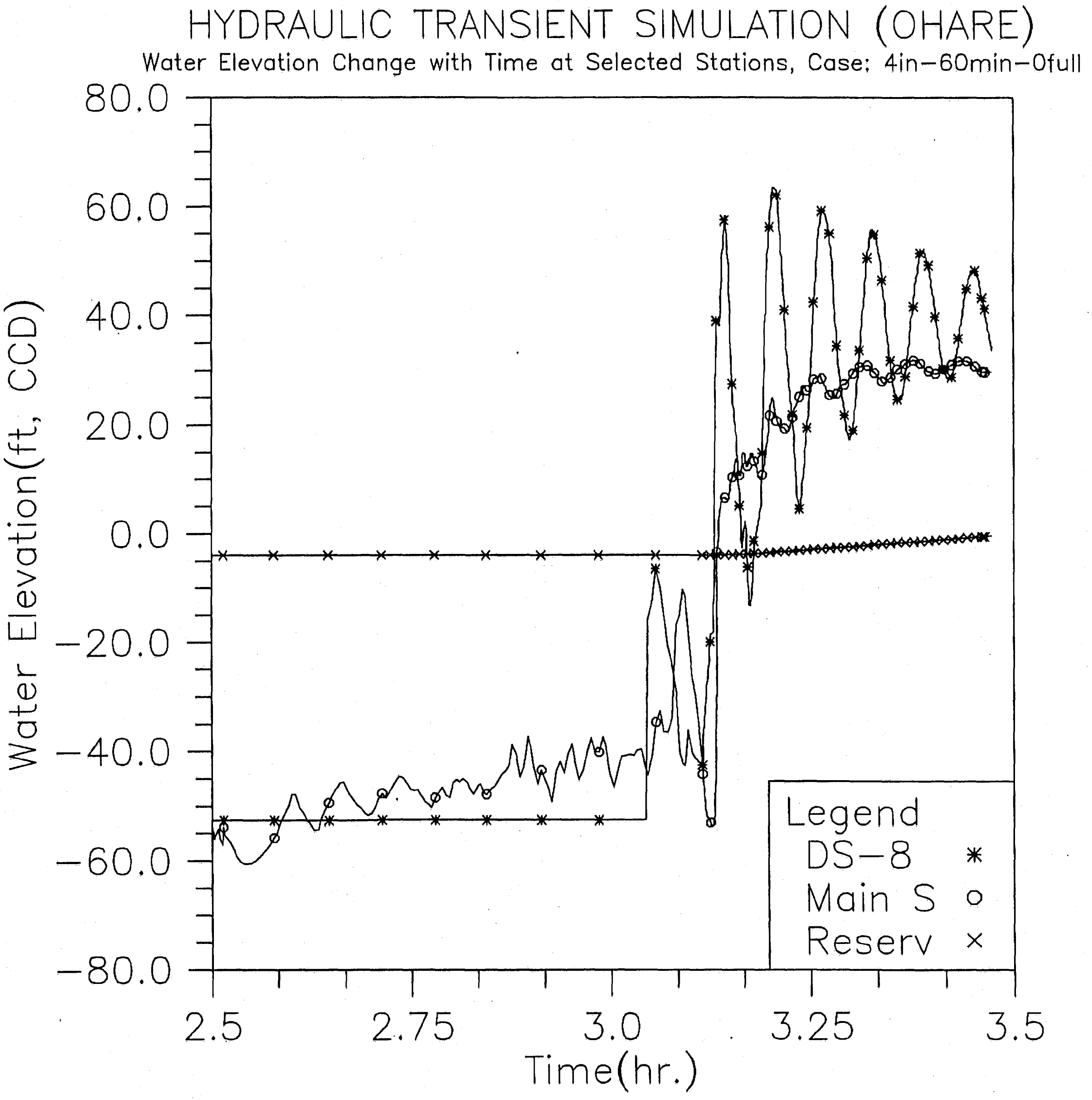

Fig. 49 Detailed water elevation variations with time in the surge process during 4 in 1 hour storm event at 3 locations (DS-8, main shaft and reservoir), modeling conditions: empty initial tunnel condition and gated inflow at DS-8.

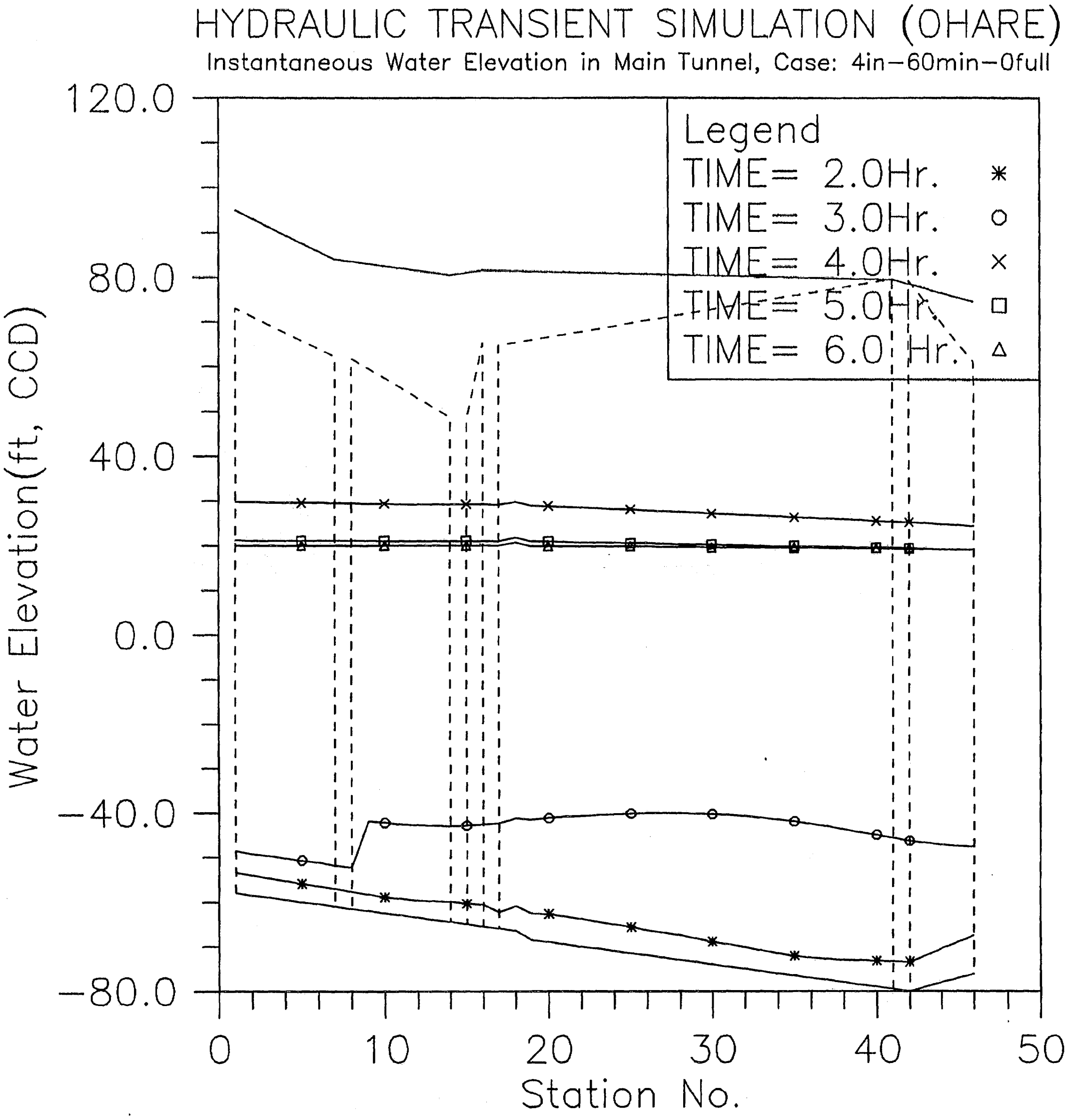

Fig. 50 Instantaneous water elevations in the main tunnel from DS-1 to the main shaft during 4 in 1 hour storm event, modeling conditions: empty initial tunnel condition and gated inflow at DS-8.

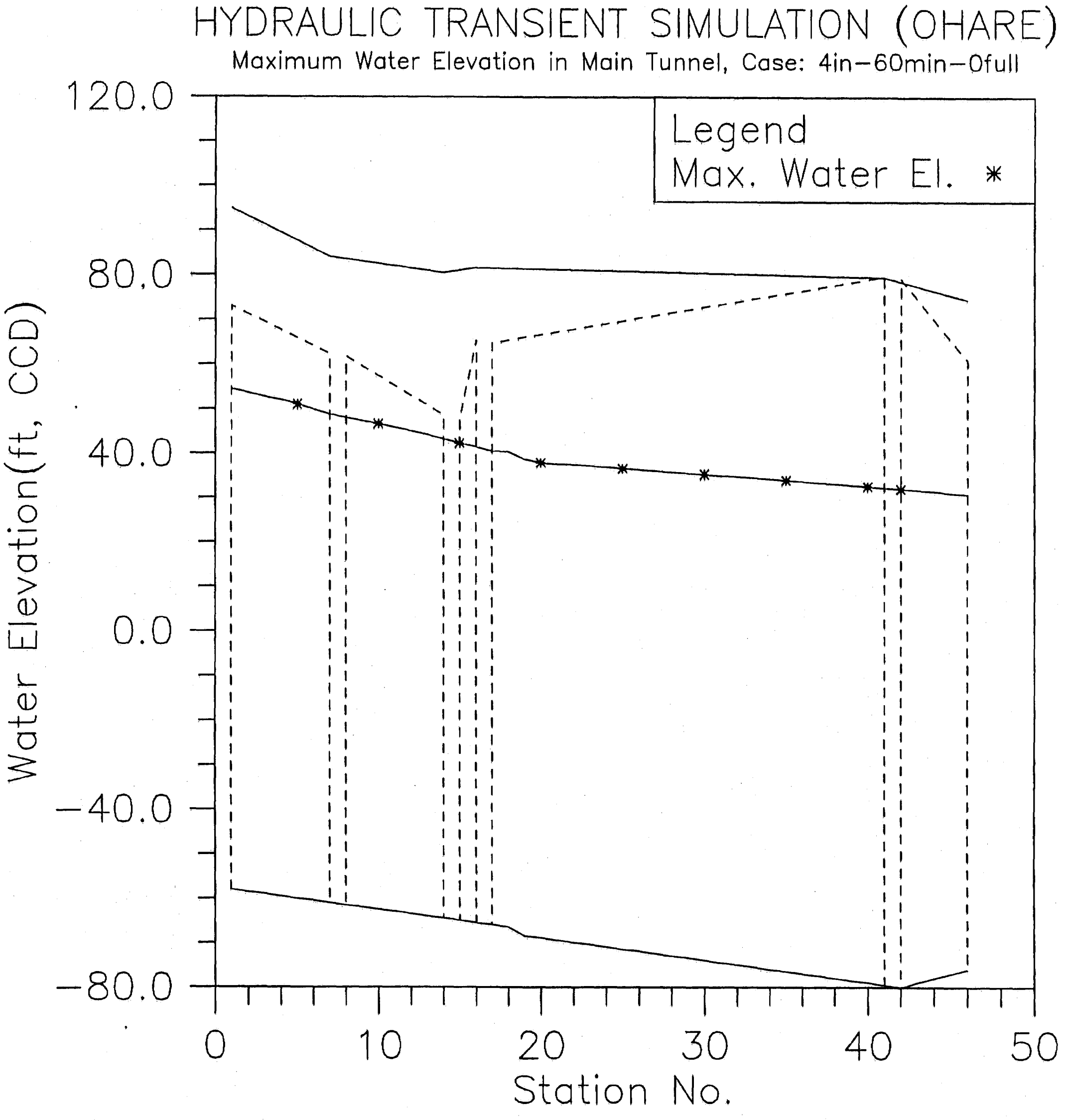

Fig. 51 Maximum water elevations in the main tunnel from DS-1 to the main shaft during 4 in 1 hour storm event, modeling conditions: empty initial tunnel condition and gated inflow at DS-8.

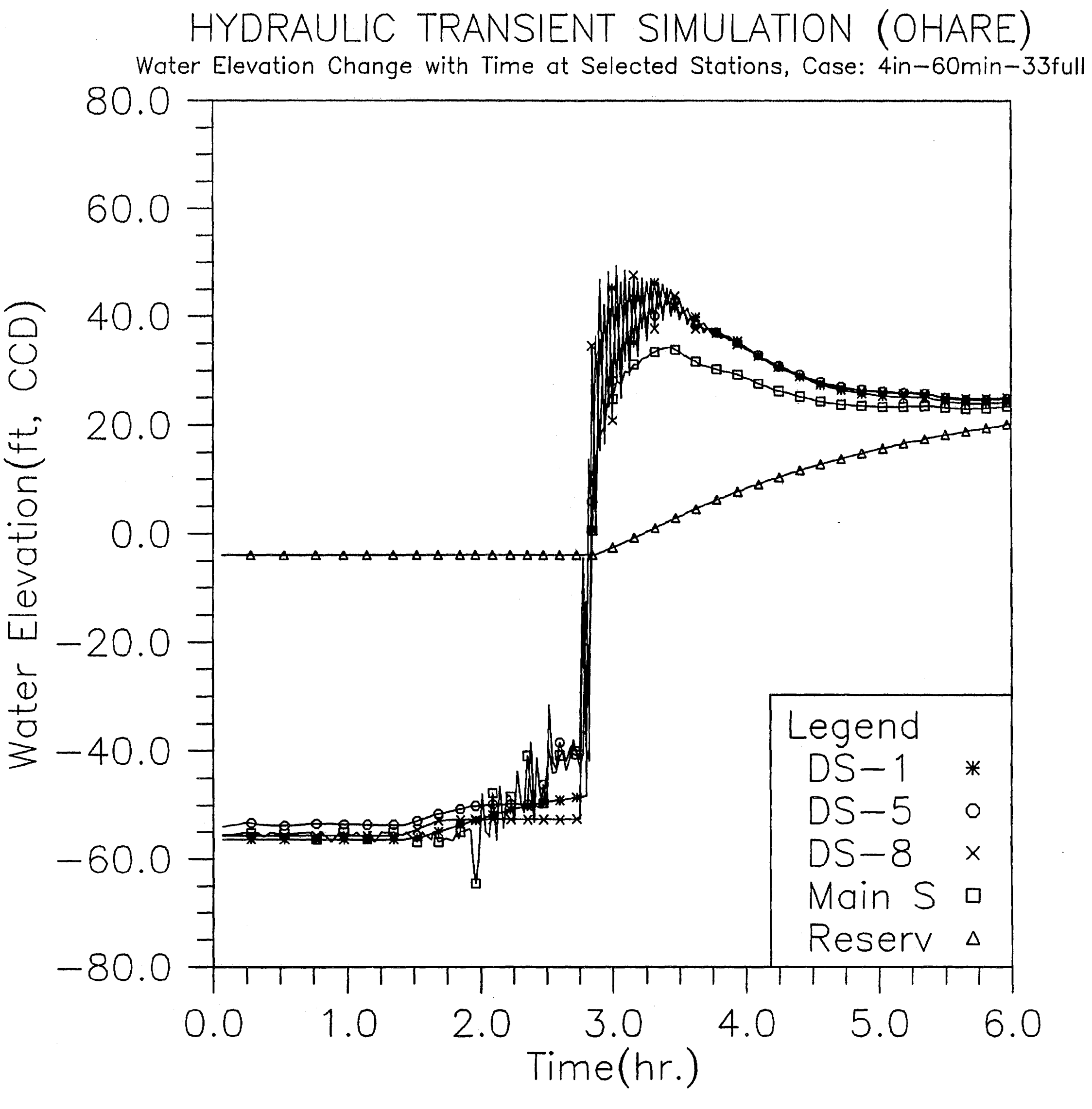

Fig. 52 Water elevation variations with time during 4 in 1 hour storm event at 5 locations (DS-1, DS-5, DS-8, main shaft and reservoir), modeling conditions: 33% full initial tunnel condition and gated inflow at DS-8.

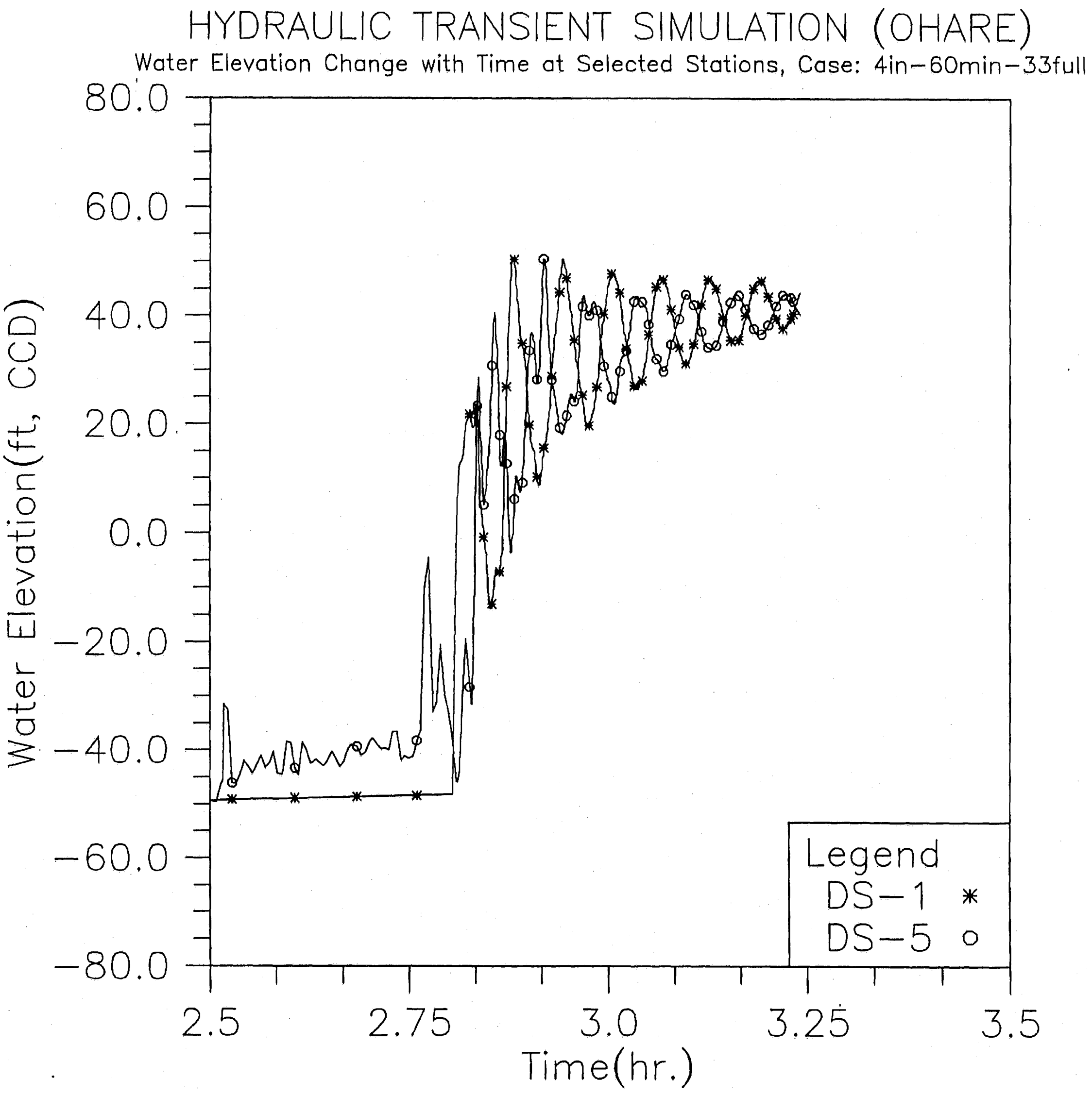

Fig. 53 Detailed water elevation variations with time in the surge process during 4 in 1 hour storm event at 2 locations (DS-1 and DS-5), modeling conditions: 33% full initial tunnel condition and gated inflow at DS-8.

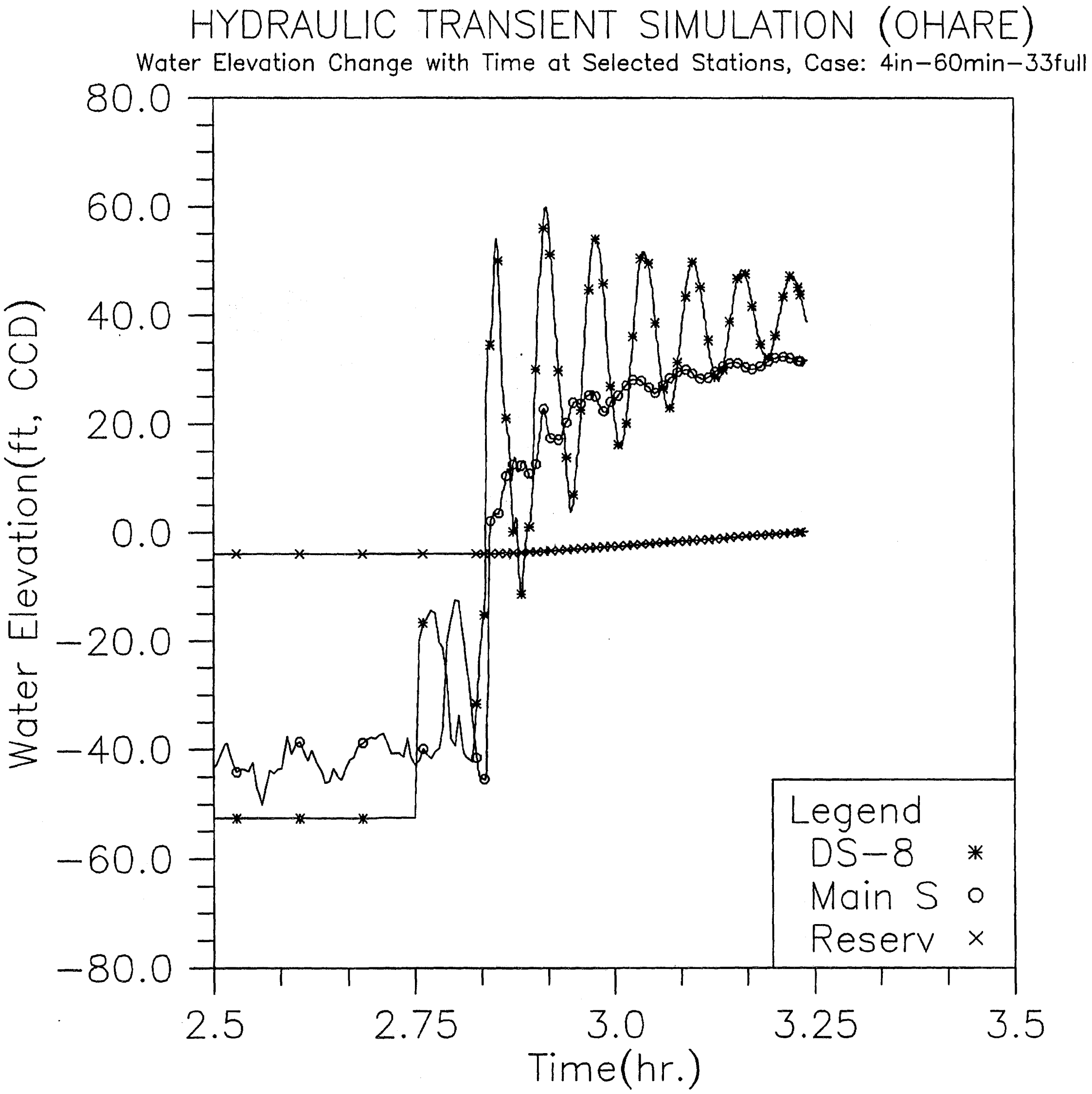

Fig. 54 Detailed water elevation variations with time in the surge process during 4 in 1 hour storm event at 3 locations (DS-8, main shaft and reservoir), modeling conditions: 33% full initial tunnel condition and gated inflow at DS-8.

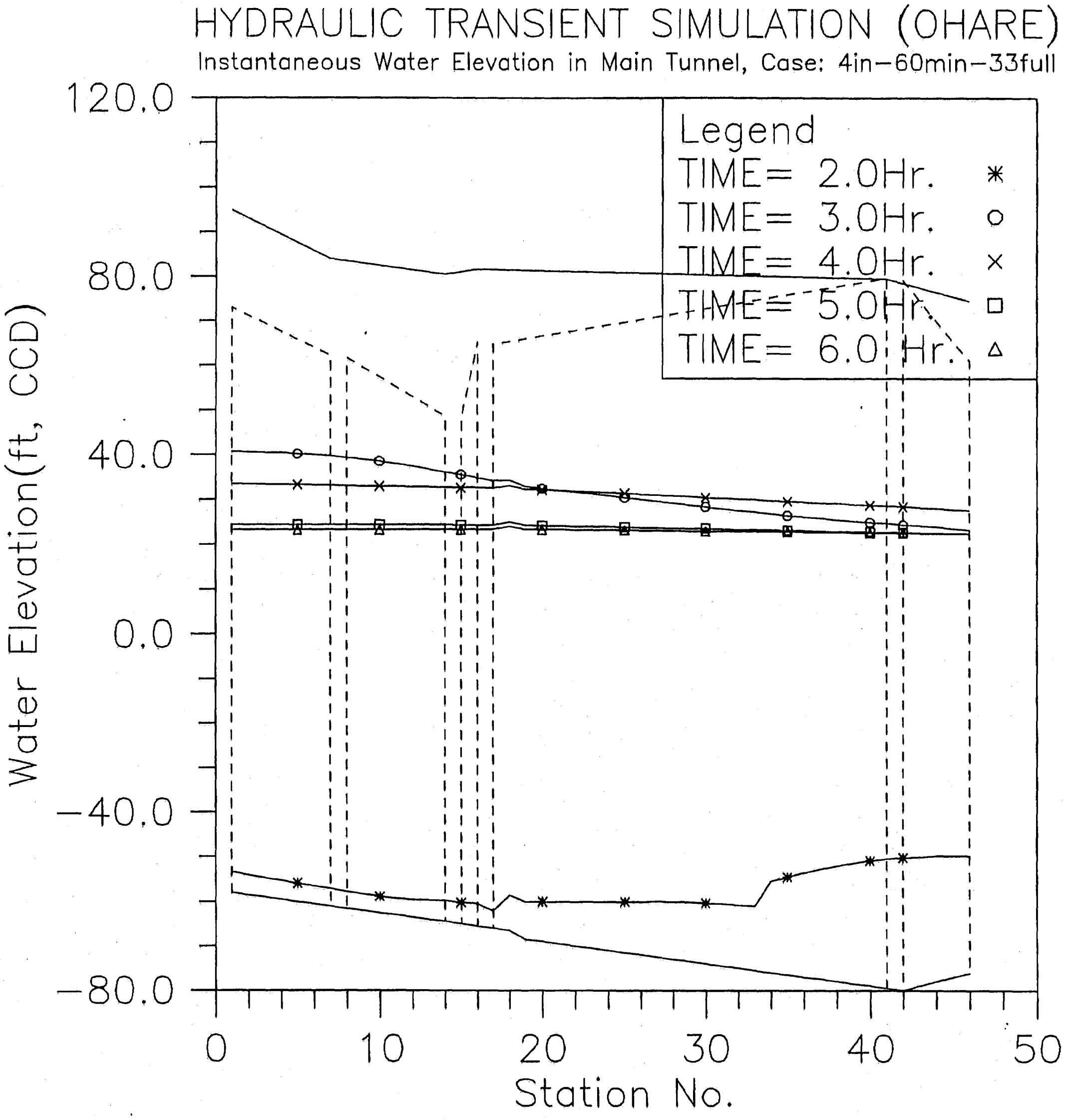

Fig. 55 Instantaneous water elevations in the main tunnel from DS-1 to the main shaft during 4 in 1 hour storm event, modeling conditions: 33% full initial tunnel condition and gated inflow at DS-8.

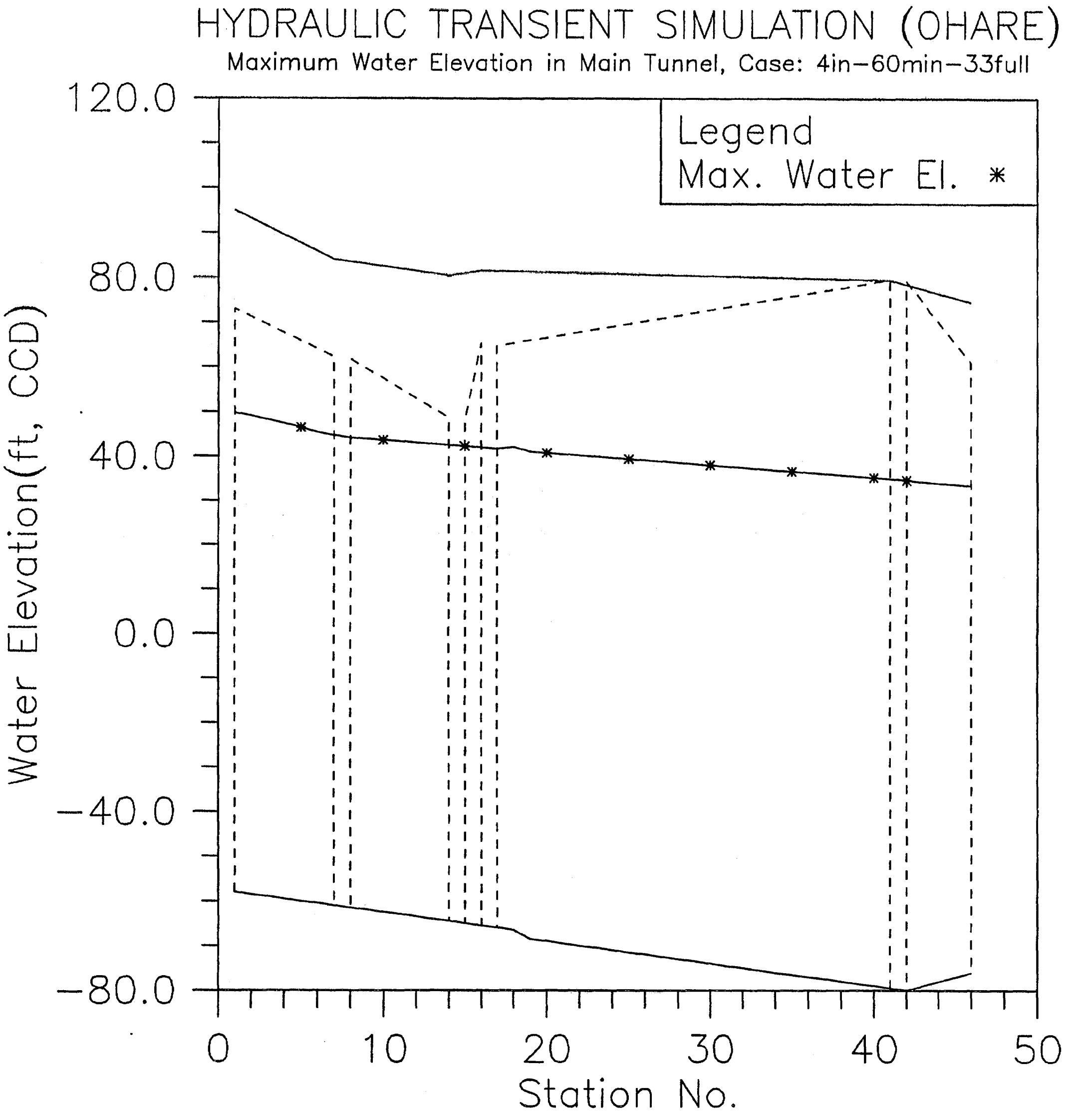

Fig. 56 Maximum water elevations in the main tunnel from DS-1 to the main shaft during 4 in 1 hour storm event, modeling conditions: 33% full initial tunnel condition and gated inflow at DS-8.

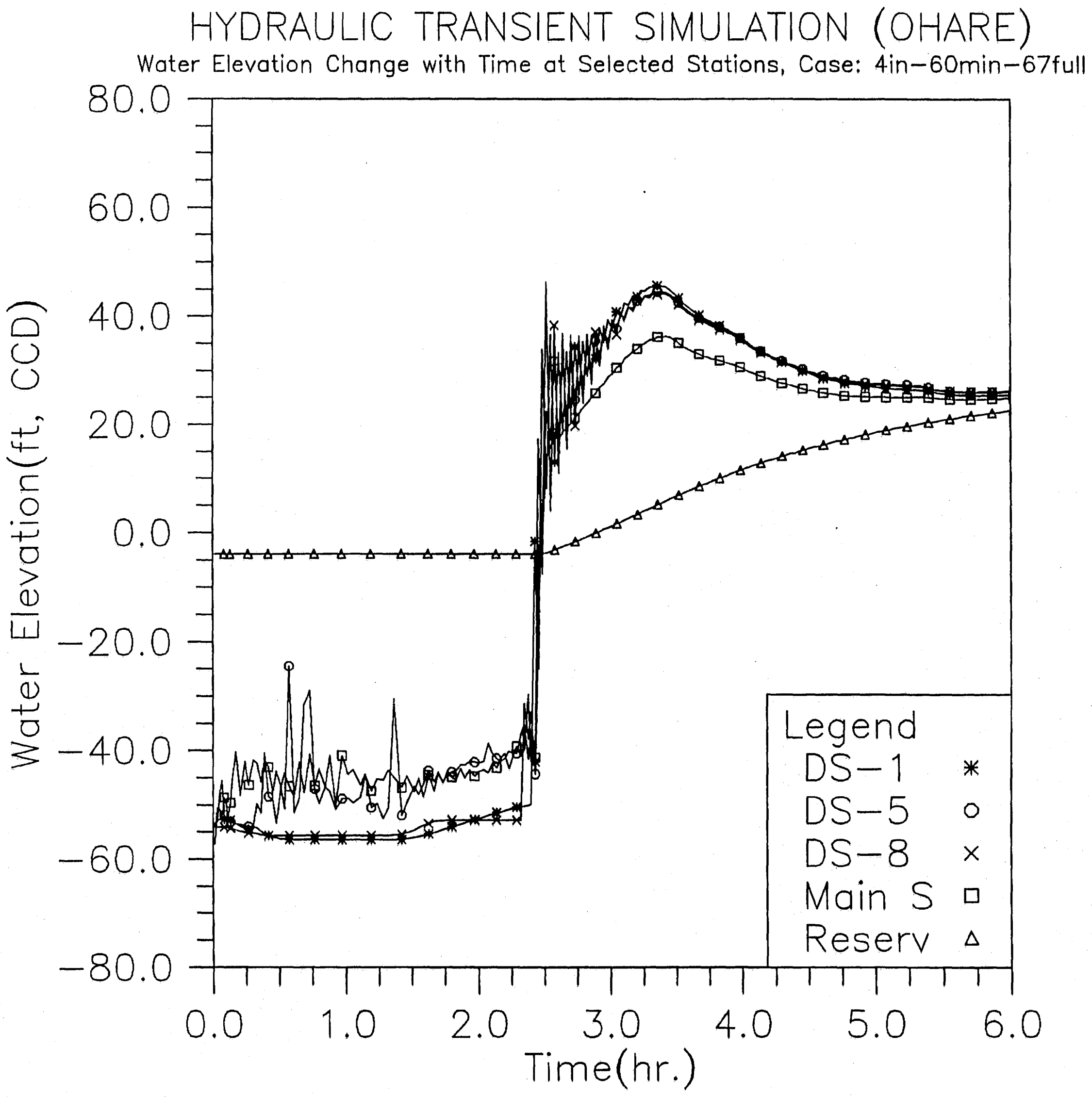

Fig. 57 Water elevation variations with time during 4 in 1 hour storm event at 5 locations (DS-1, DS-5, DS-8, main shaft and reservoir), modeling conditions: 67% full initial tunnel condition and gated inflow at DS-8.

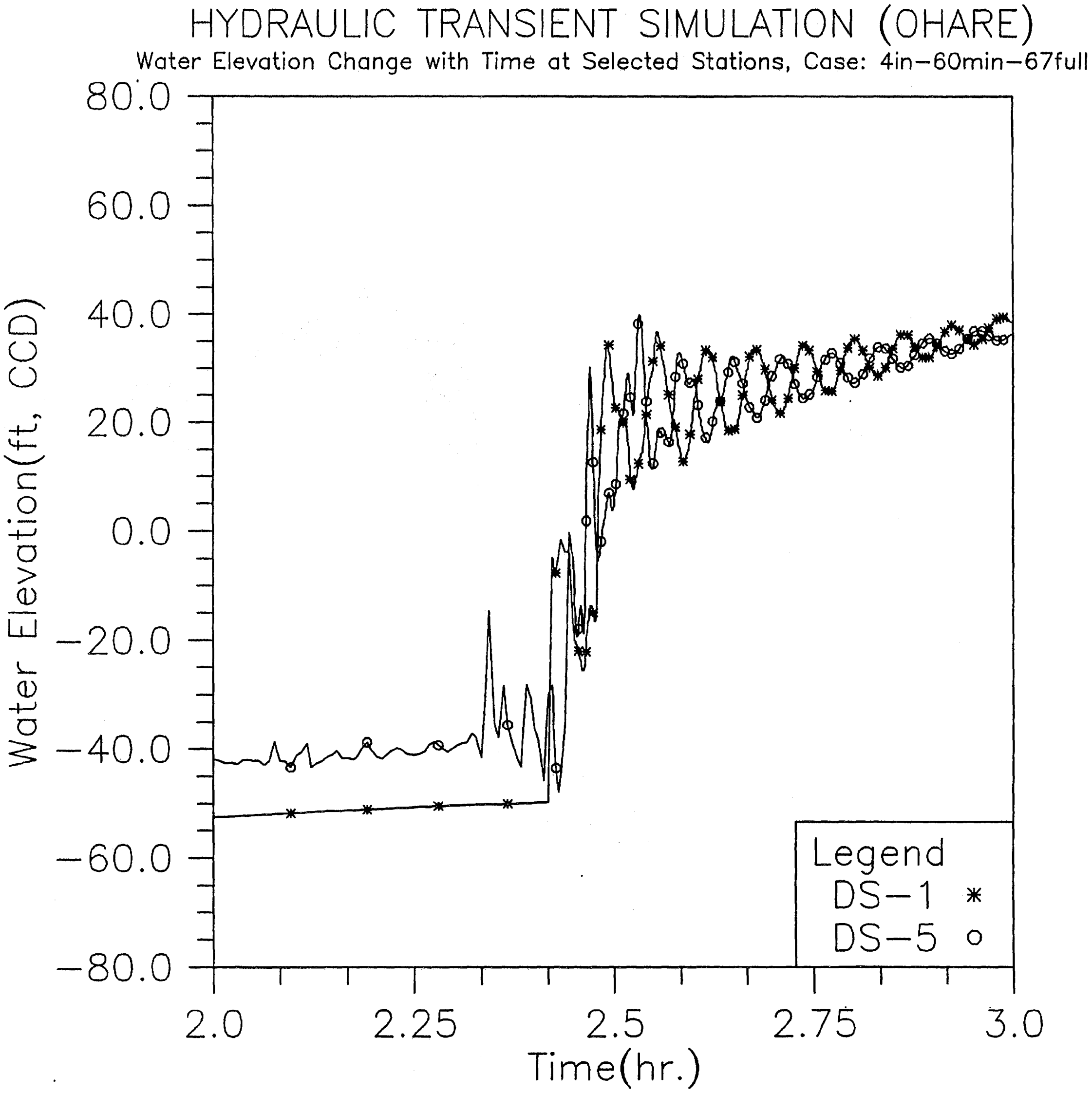

Fig. 58 Detailed water elevation variations with time in the surge process during 4 in 1 hour storm event at 2 locations (DS-1 and DS-5), modeling conditions: 67% full initial tunnel condition and gated inflow at DS-8.

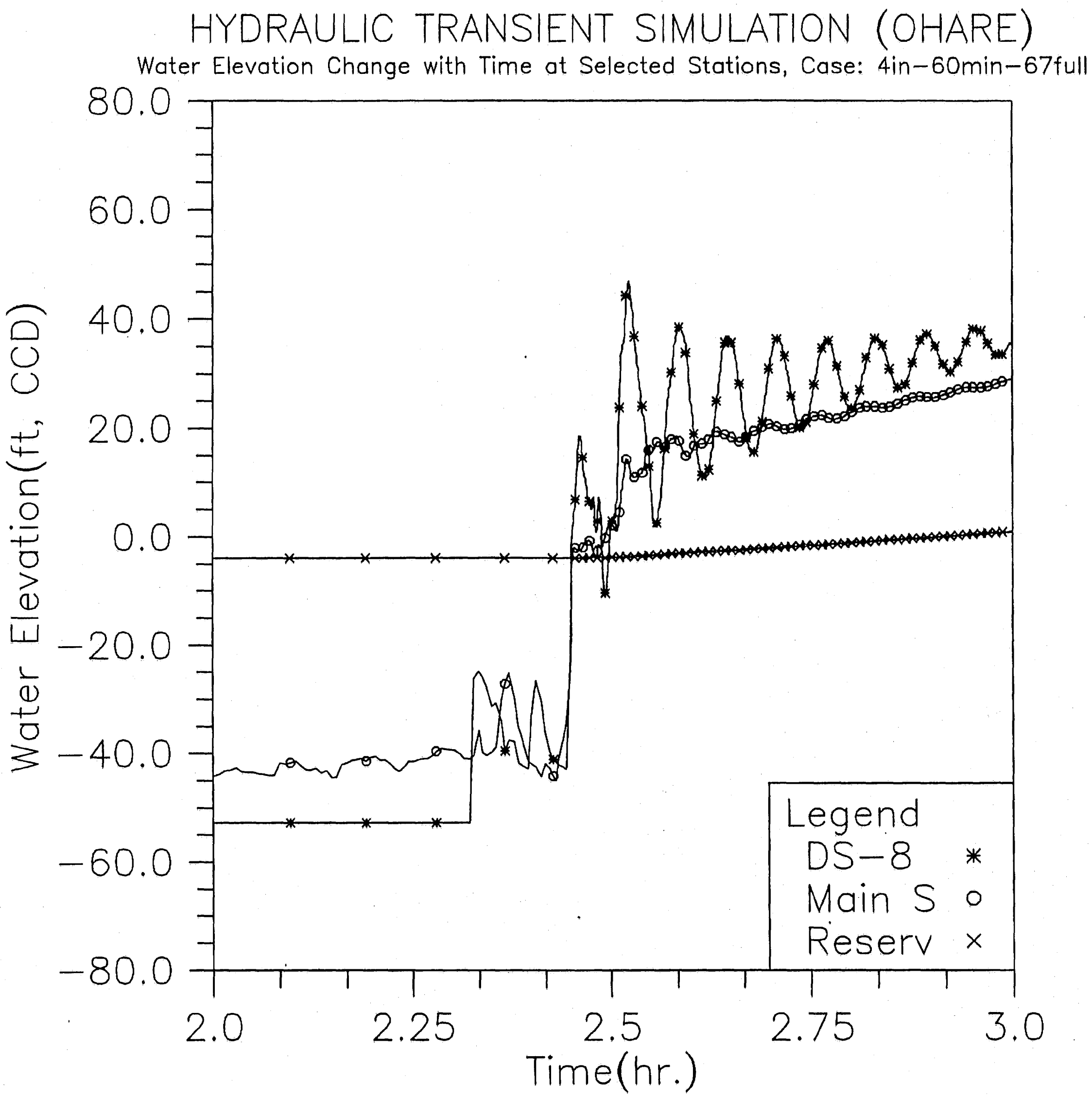

Fig. 59 Detailed water elevation variations with time in the surge process during 4 in 1 hour storm event at 3 locations (DS-8, main shaft and reservoir), modeling conditions: 67% full initial tunnel condition and gated inflow at DS-8.

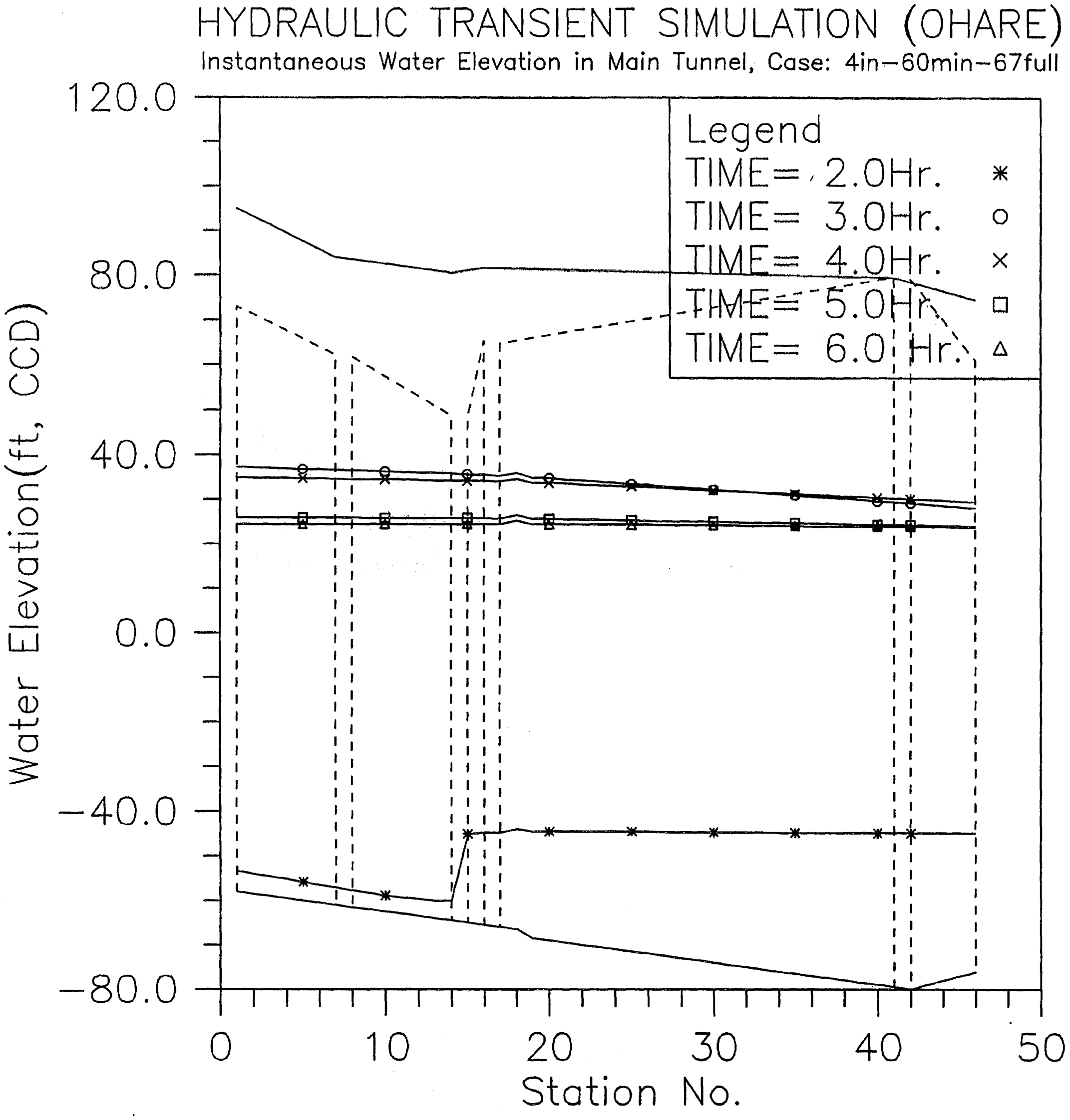

Fig. 60 Instantaneous water elevations in the main tunnel from DS-1 to the main shaft during 4 in 1 hour storm event, modeling conditions: 67% full initial tunnel condition and gated inflow at DS-8.

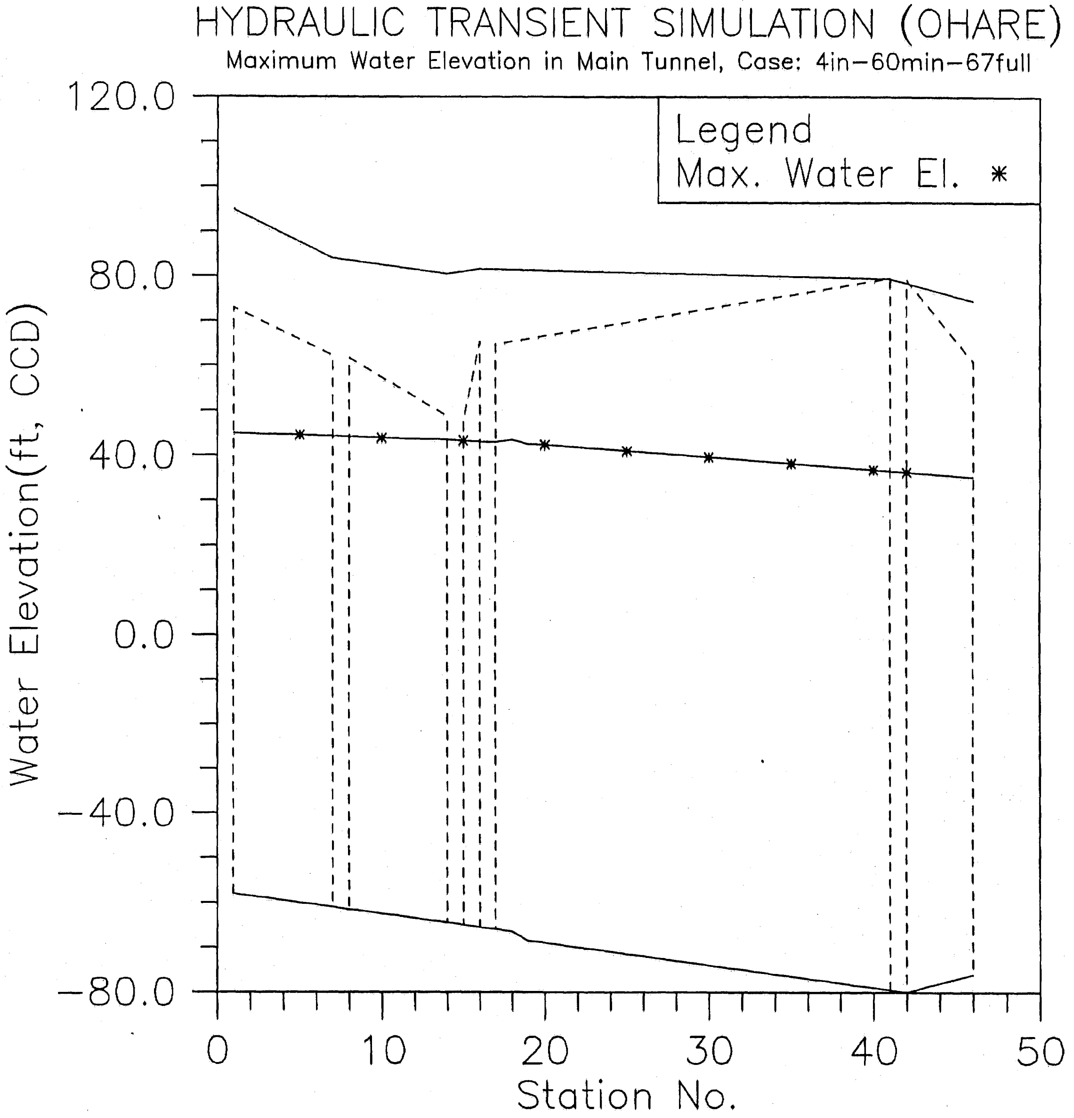

Fig. 61 Maximum water elevations in the main tunnel from DS-1 to the main shaft during 4 in 1 hour storm event, modeling conditions: 67% full initial tunnel condition and gated inflow at DS-8.

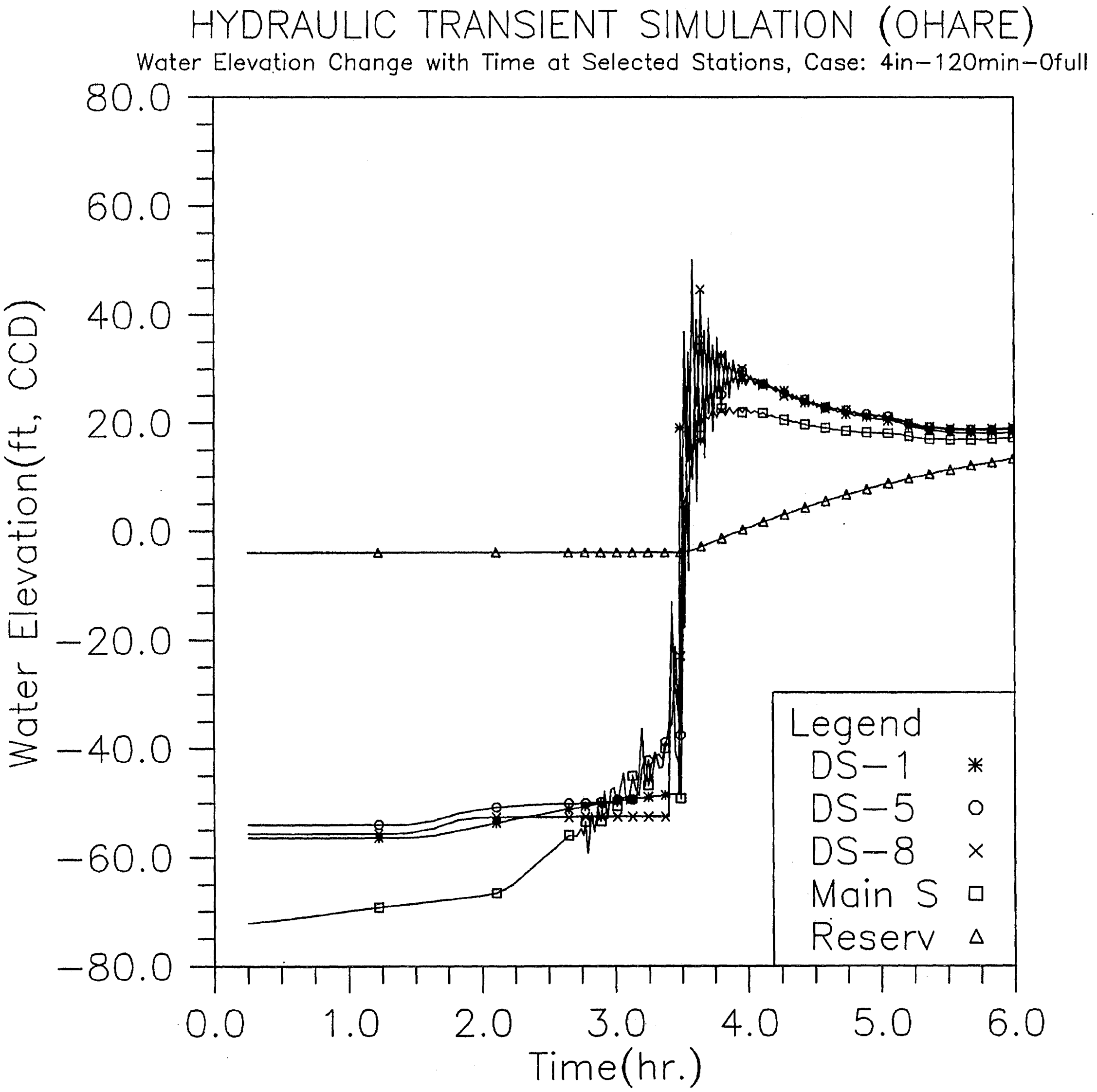

Fig. 62 Water elevation variations with time during 4 in 2 hour storm event at 5 locations (DS-1, DS-5, DS-8, main shaft and reservoir), modeling conditions: empty initial tunnel condition and gated inflow at DS-8.

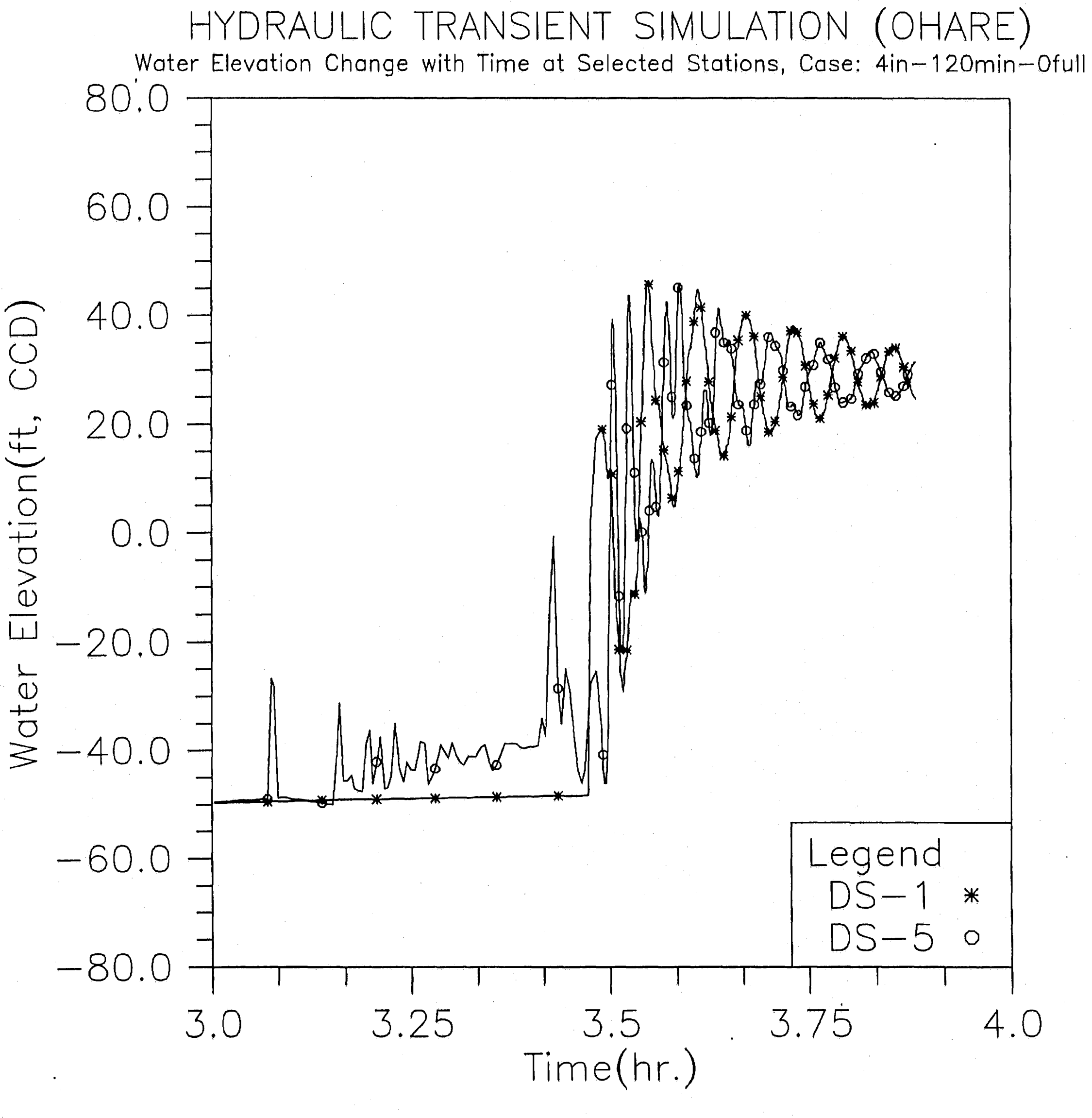

Fig. 63 Detailed water elevation variations with time in the surge process during 4 in 2 hour storm event at 2 locations (DS-1 and DS-5), modeling conditions: empty initial tunnel condition and gated inflow at DS-8.

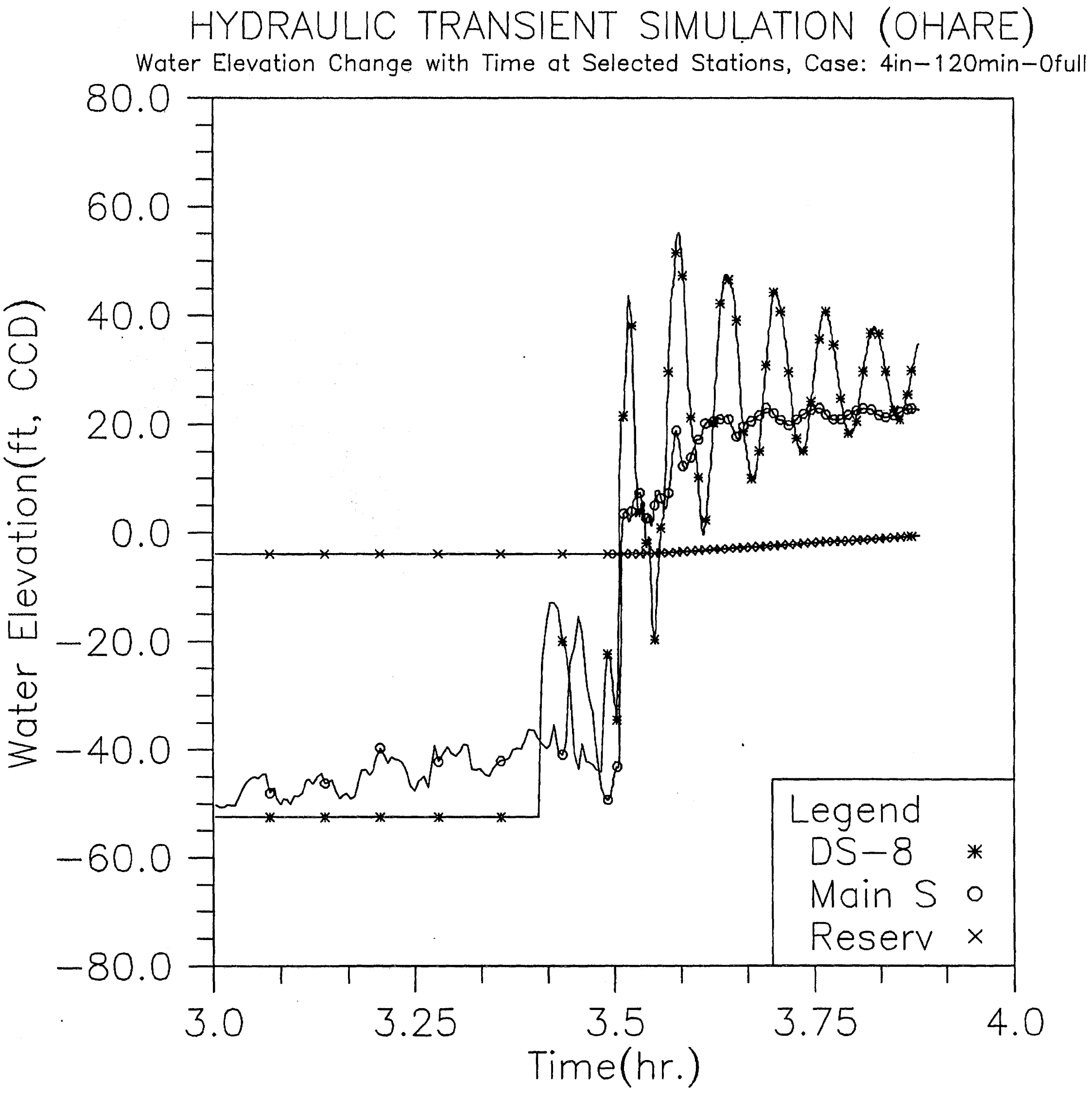

Fig. 64 Detailed water elevation variations with time in the surge process during 4 in 2 hour storm event at 3 locations (DS-8, main shaft and reservoir), modeling conditions: empty initial tunnel condition and gated inflow at DS-8.

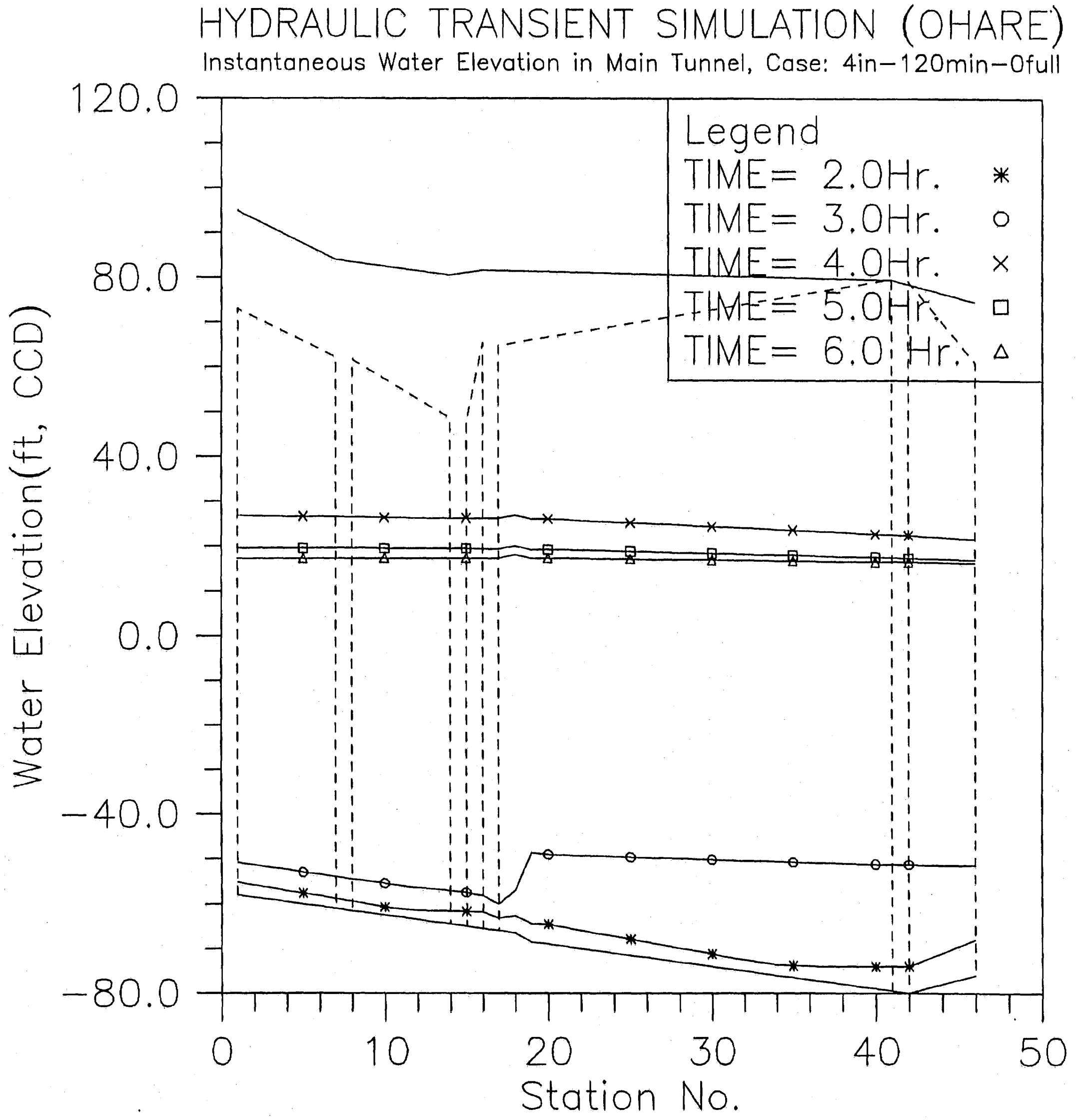

Fig. 65 Instantaneous water elevations in the main tunnel from DS-1 to the main shaft during 4 in 2 hour storm event, modeling conditions: empty initial tunnel condition and gated inflow at DS-8.

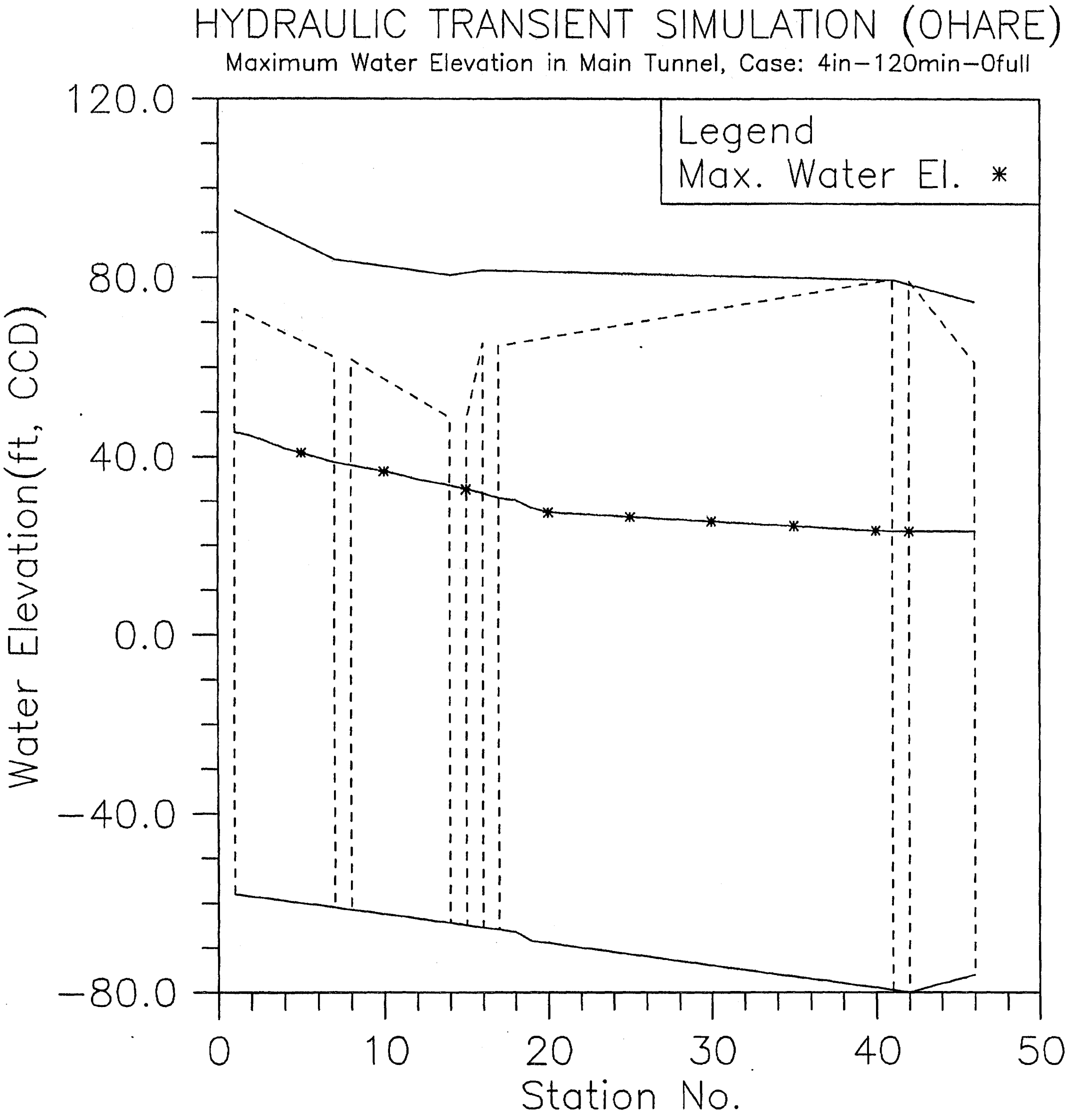

Fig. 66 Maximum water elevations in the main tunnel from DS-1 to the main shaft during 4 in 2 hour storm event, modeling conditions: empty initial tunnel condition and gated inflow at DS-8.

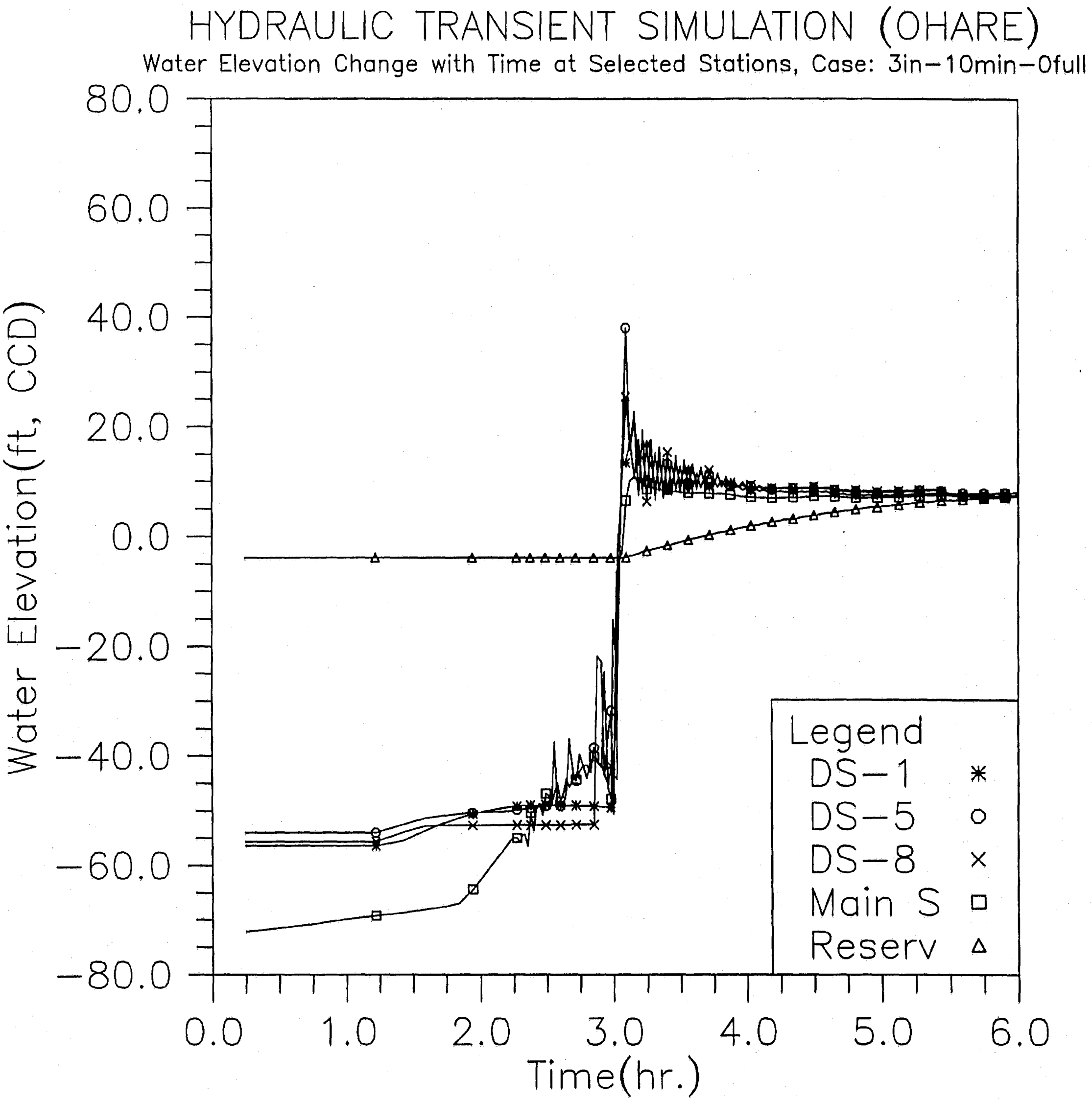

Fig. 67 Water elevation variations with time during 3 in 10 min storm event at 5 locations (DS-1, DS-5, DS-8, main shaft and reservoir), modeling conditions: empty initial tunnel condition and gated inflow at DS-8.

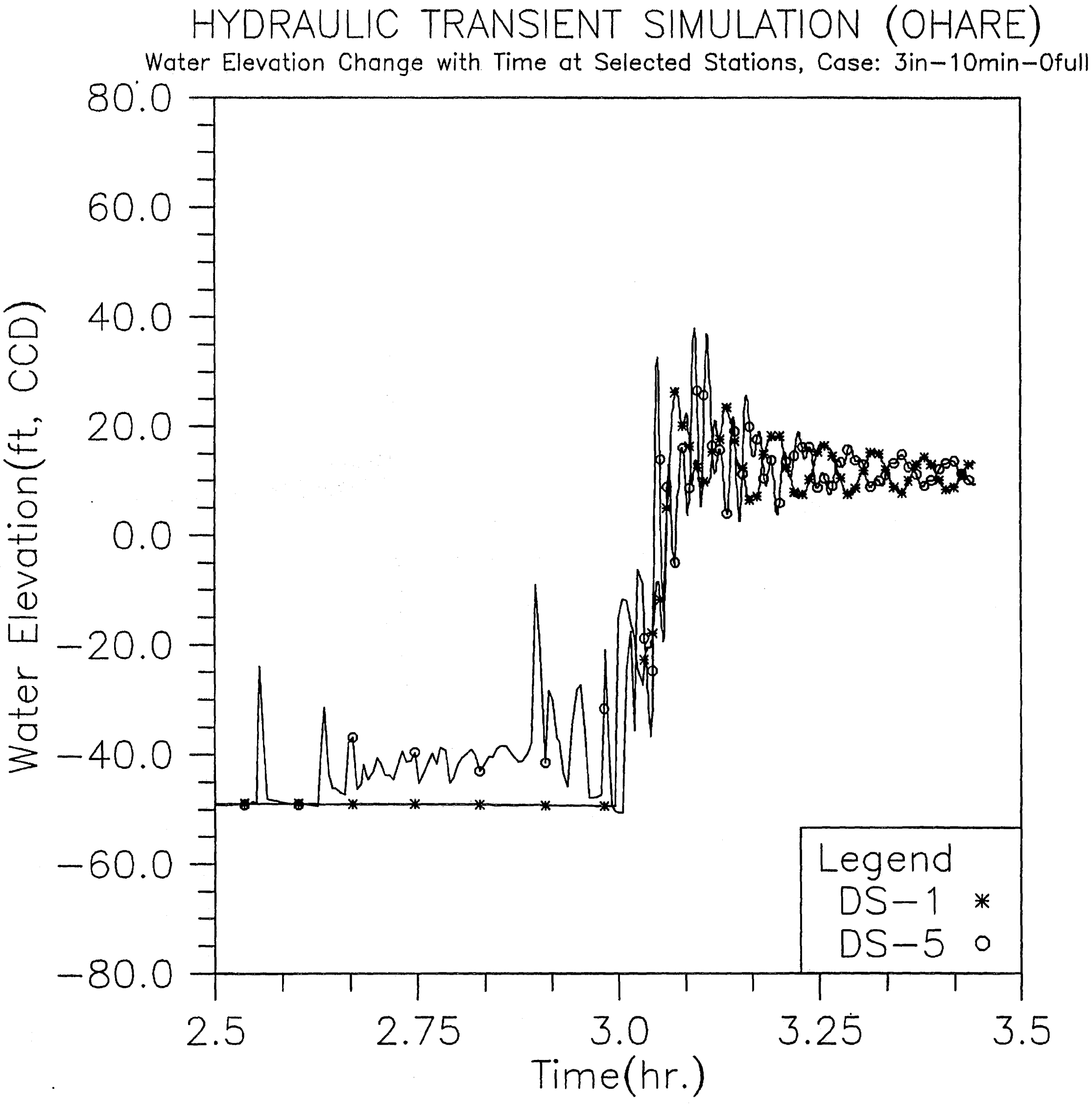

Fig. 68 Detailed water elevation variations with time in the surge process during 3 in 10 min storm event at 2 locations (DS-1 and DS-5), modeling conditions: empty initial tunnel condition and gated inflow at DS-8.

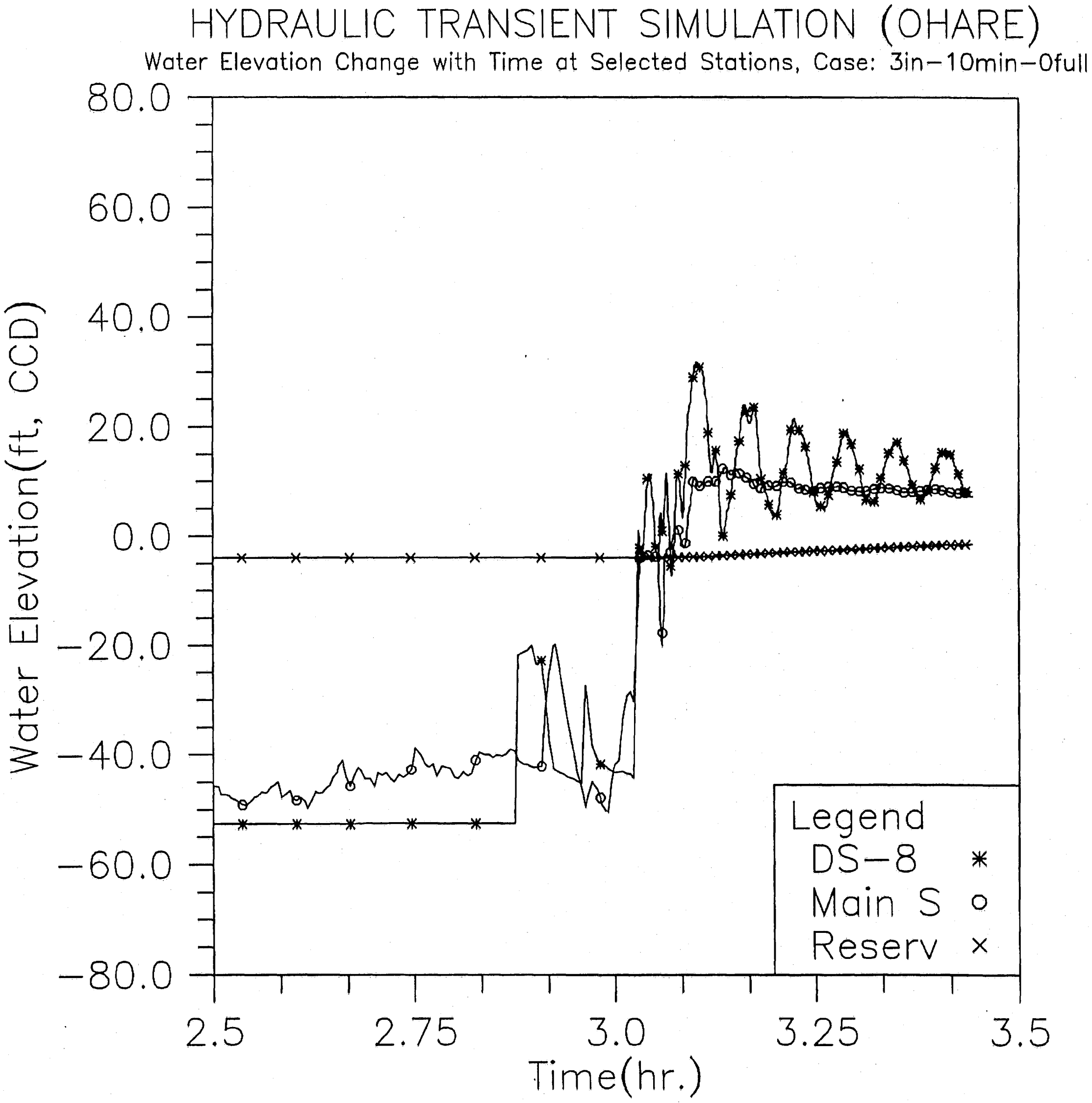

Fig. 69 Detailed water elevation variations with time in the surge process during 3 in 10 min storm event at 3 locations (DS-8, main shaft and reservoir), modeling conditions: empty initial tunnel condition and gated inflow at DS-8.

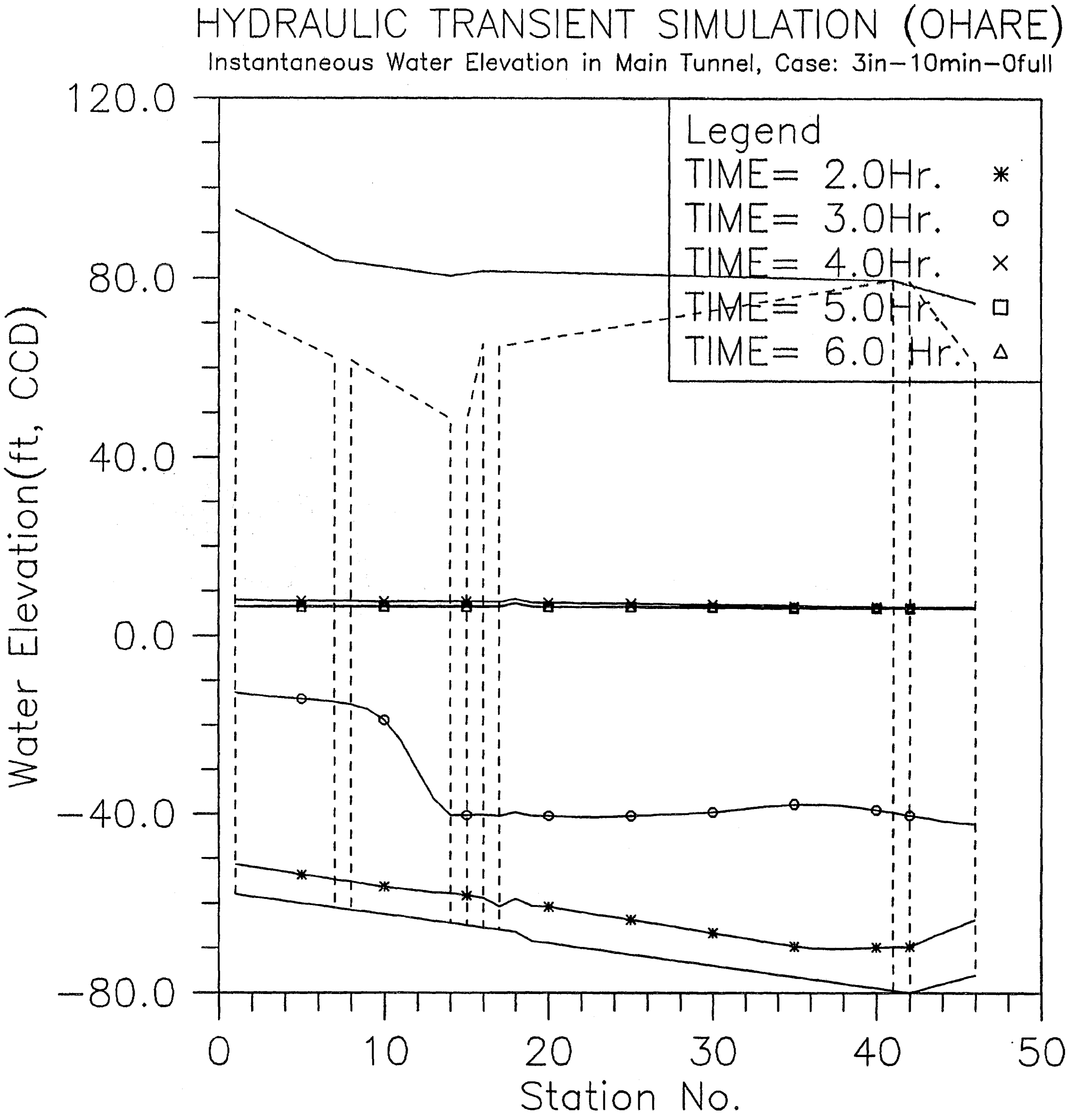

Fig. 70 Instantaneous water elevations in the main tunnel from DS-1 to the main shaft during 3 in 10 min storm event, modeling conditions: empty initial tunnel condition and gated inflow at DS-8.

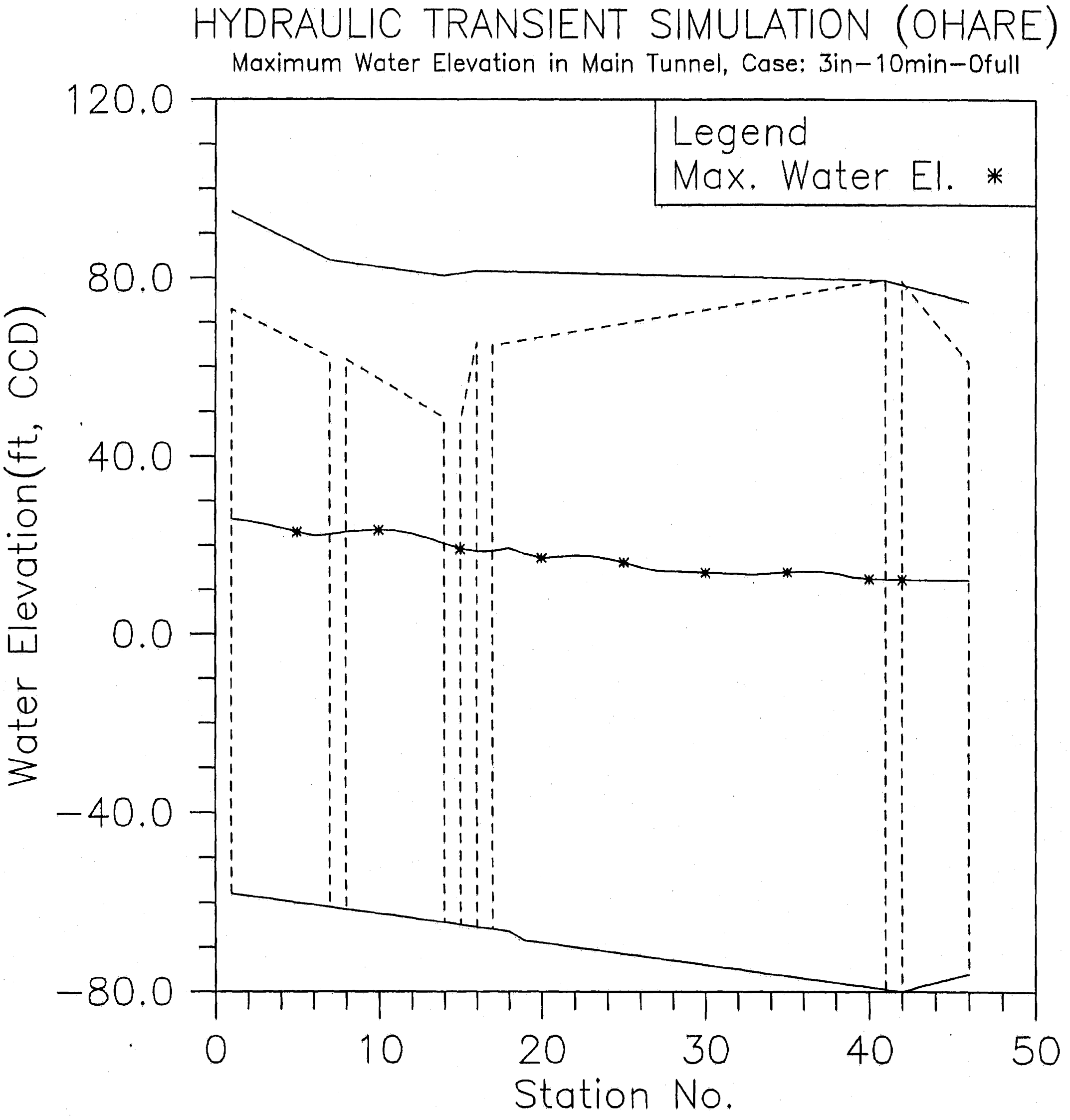

Fig. 71 Maximum water elevations in the main tunnel from DS-1 to the main shaft during 3 in 10 min storm event, modeling conditions: empty initial tunnel condition and gated inflow at DS-8.

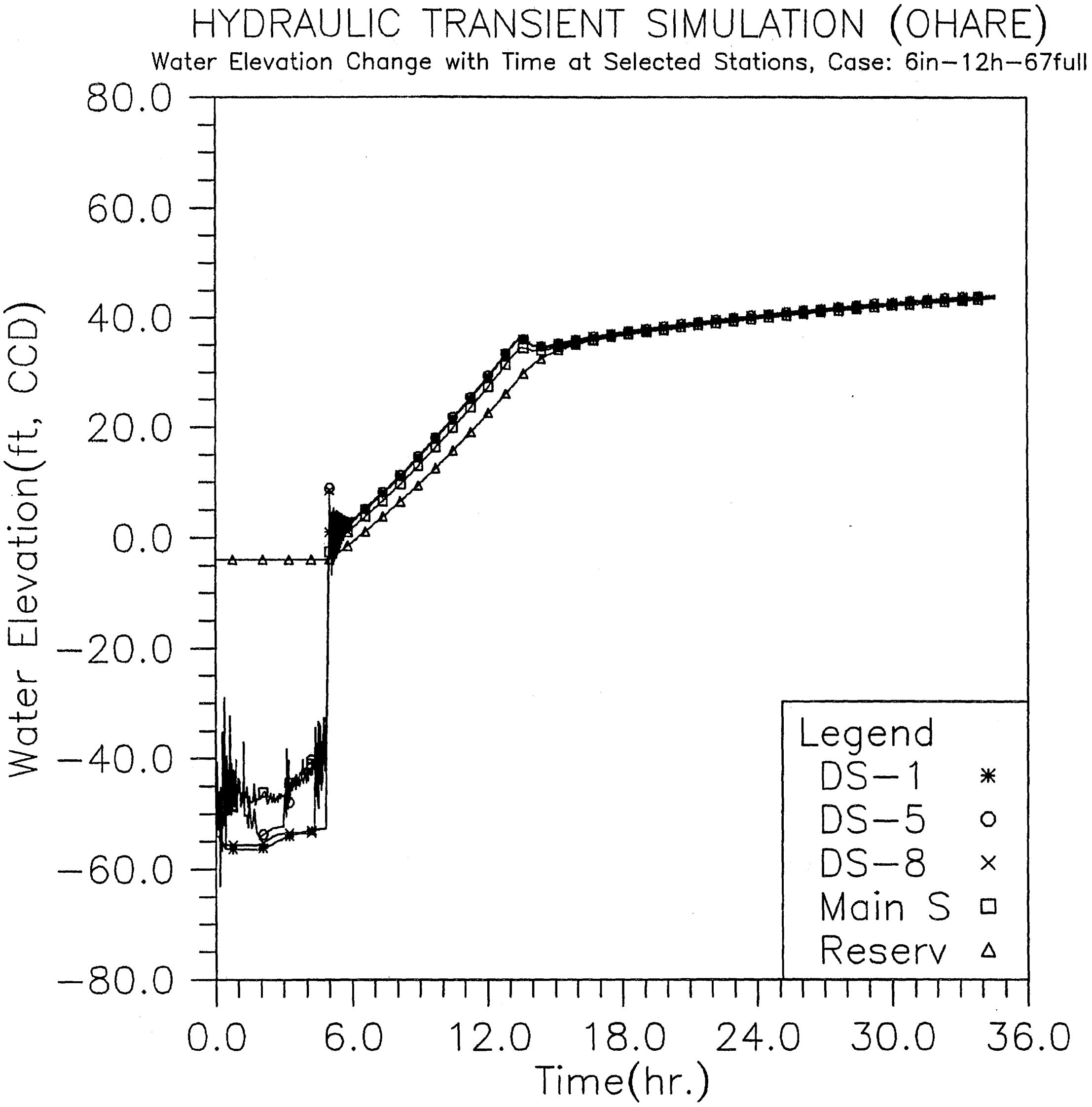

Fig. 72 Water elevation variations with time during 6 in 12 hour storm event at 5 locations (DS-1, DS-5, DS-8, main shaft and reservoir), modeling conditions: 67% full initial tunnel condition and gated inflow at DS-8.

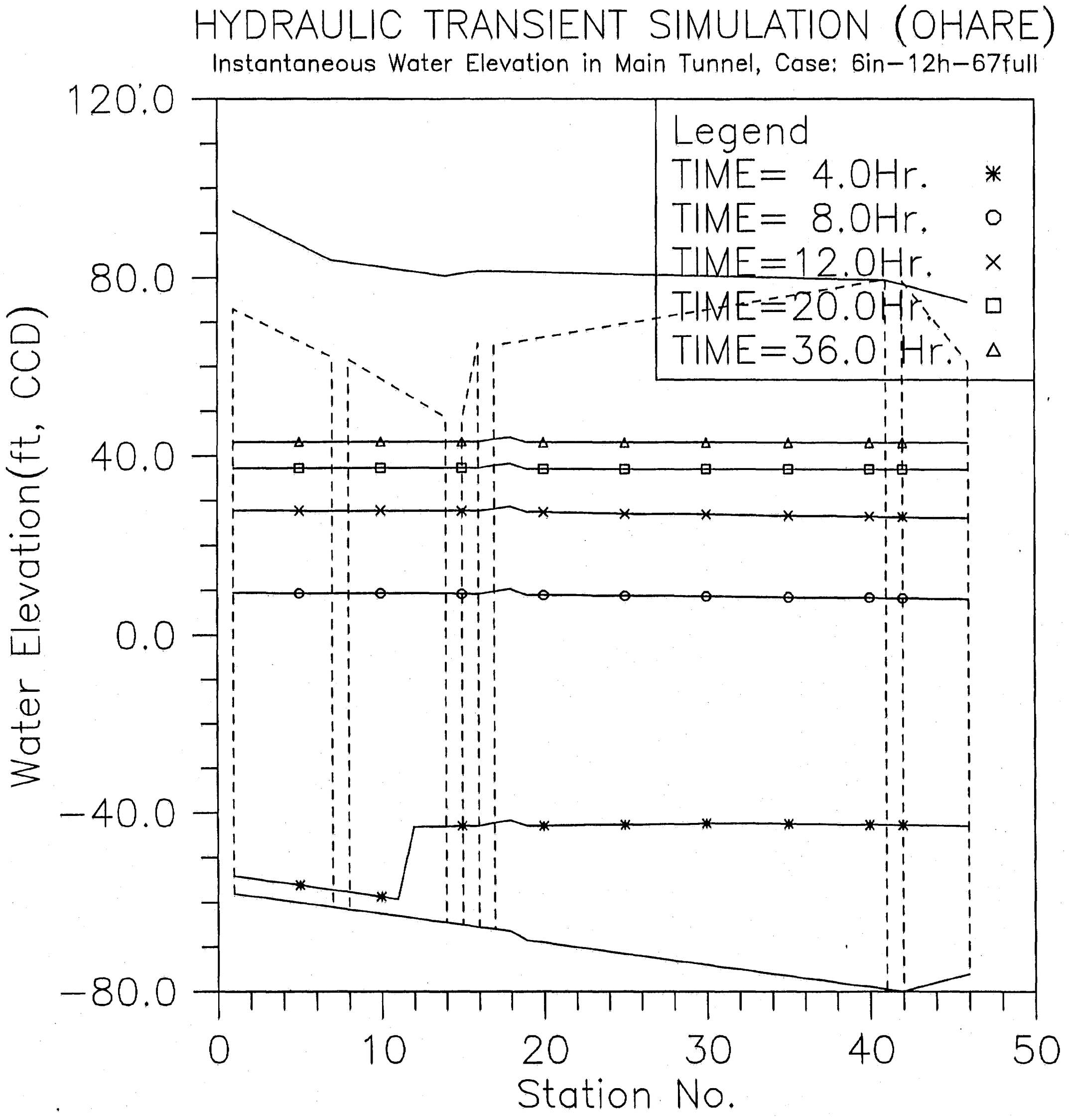

Fig. 73 Instantaneous water elevations in the main tunnel from DS-1 to the main shaft during 6 in 12 hour storm event, modeling conditions: 67% full initial tunnel condition and gated inflow at DS-8.

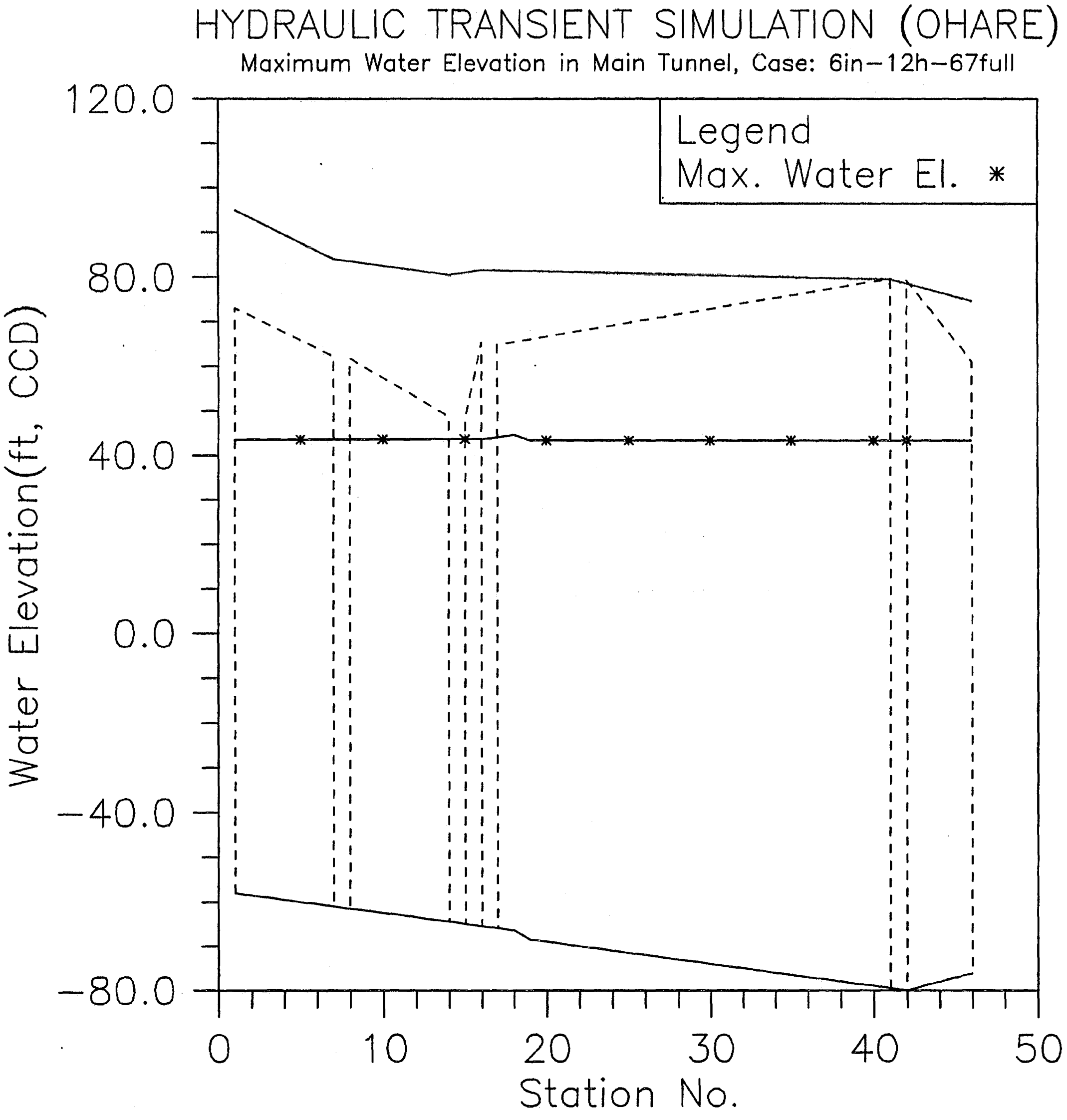

Fig. 74 Maximum water elevations in the main tunnel from DS-1 to the main shaft during 6 in 12 hour storm event, modeling conditions: 67% full initial tunnel condition and gated inflow at DS-8.

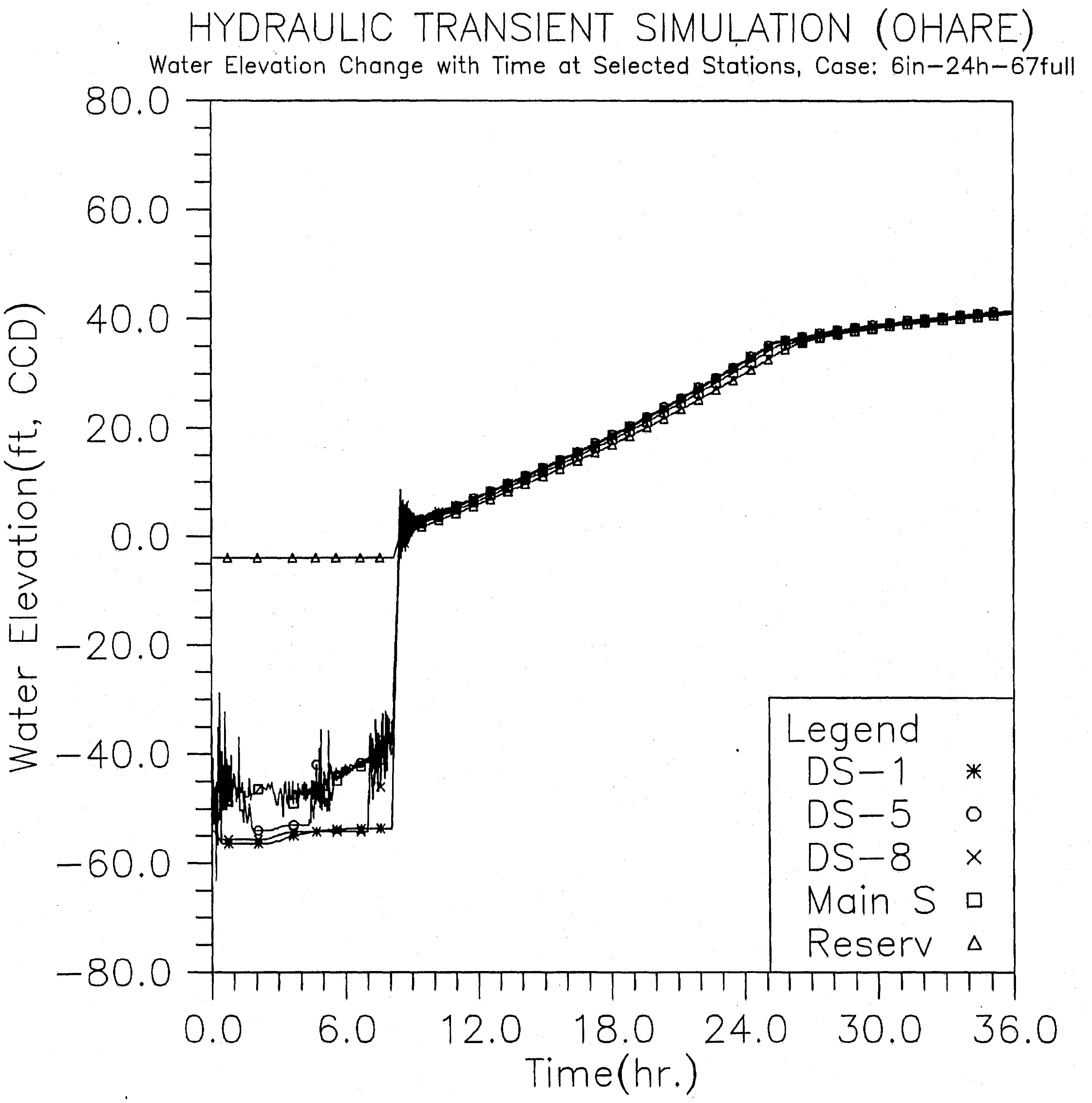

Fig. 75 Water elevation variations with time during 6 in 24 hour storm event at 5 locations (DS-1, DS-5, DS-8, main shaft and reservoir), modeling conditions: 67% full initial tunnel condition and gated inflow at DS-8.

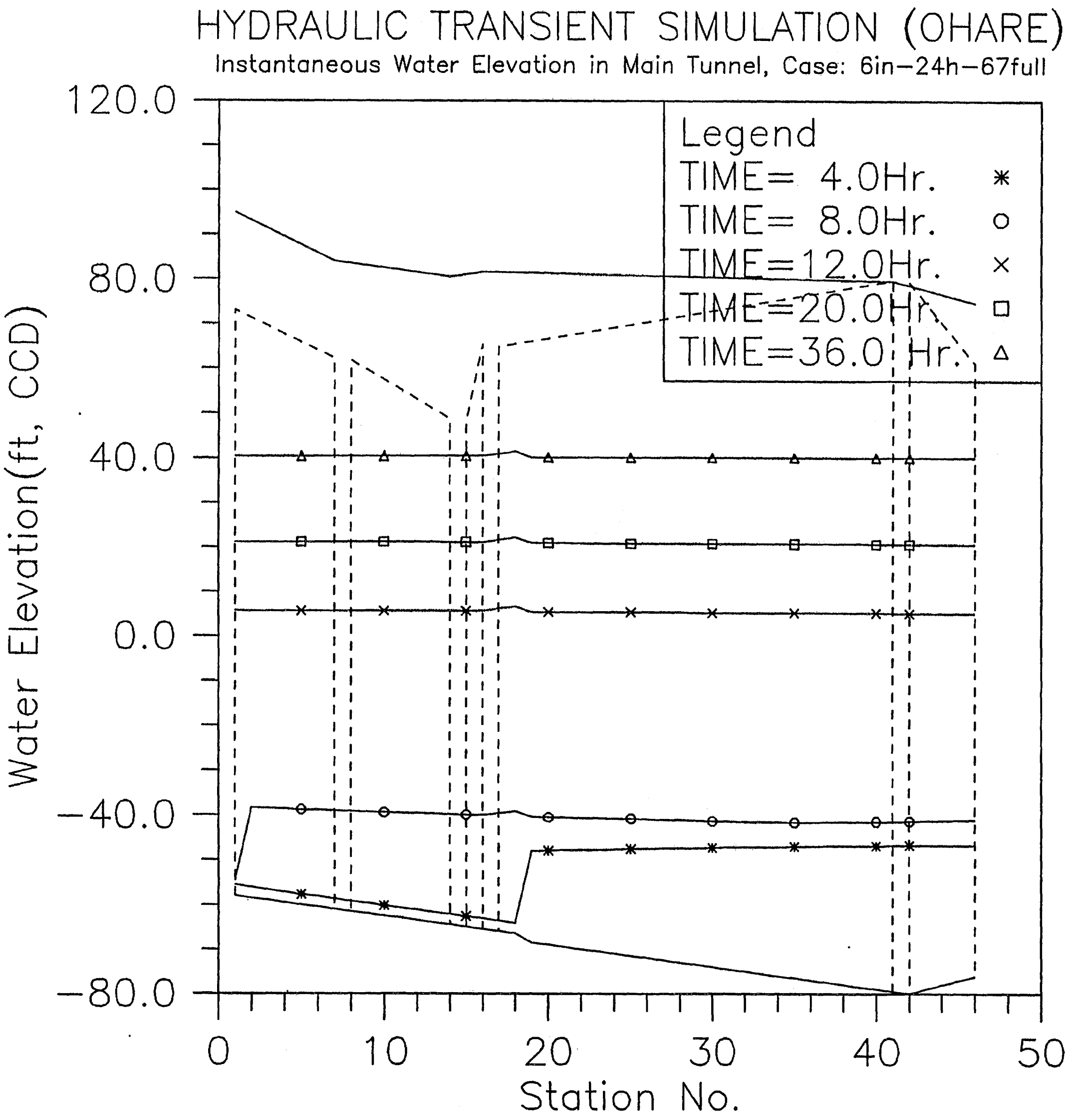

Fig. 76 Instantaneous water elevations in the main tunnel from DS-1 to the main shaft during 6 in 24 hour storm event, modeling conditions: 67% full initial tunnel condition and gated inflow at DS-8.

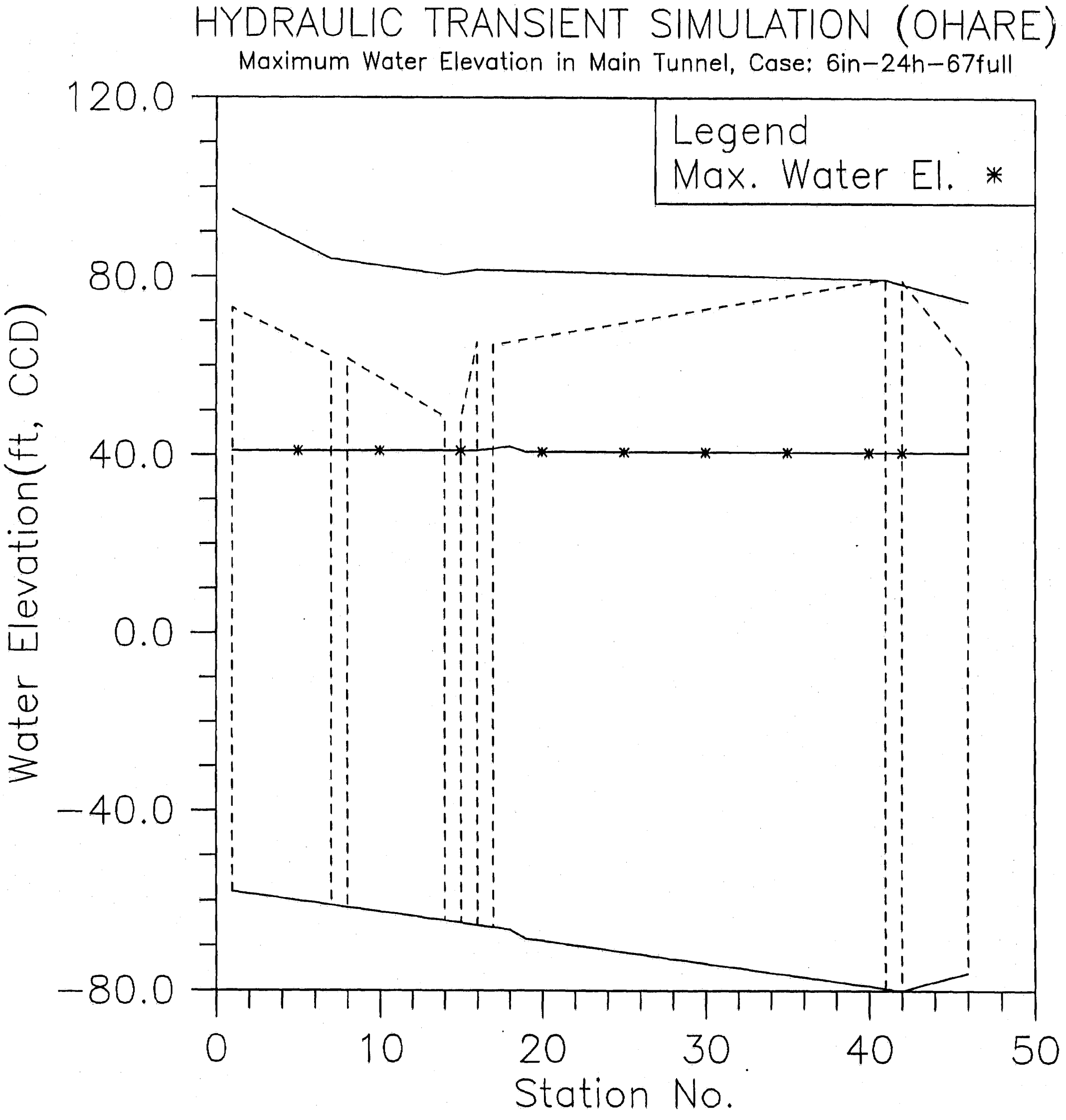

Fig. 77 Maximum water elevations in the main tunnel from DS-1 to the main shaft during 6 in 24 hour storm event, modeling conditions: 67% full initial tunnel condition and gated inflow at DS-8.

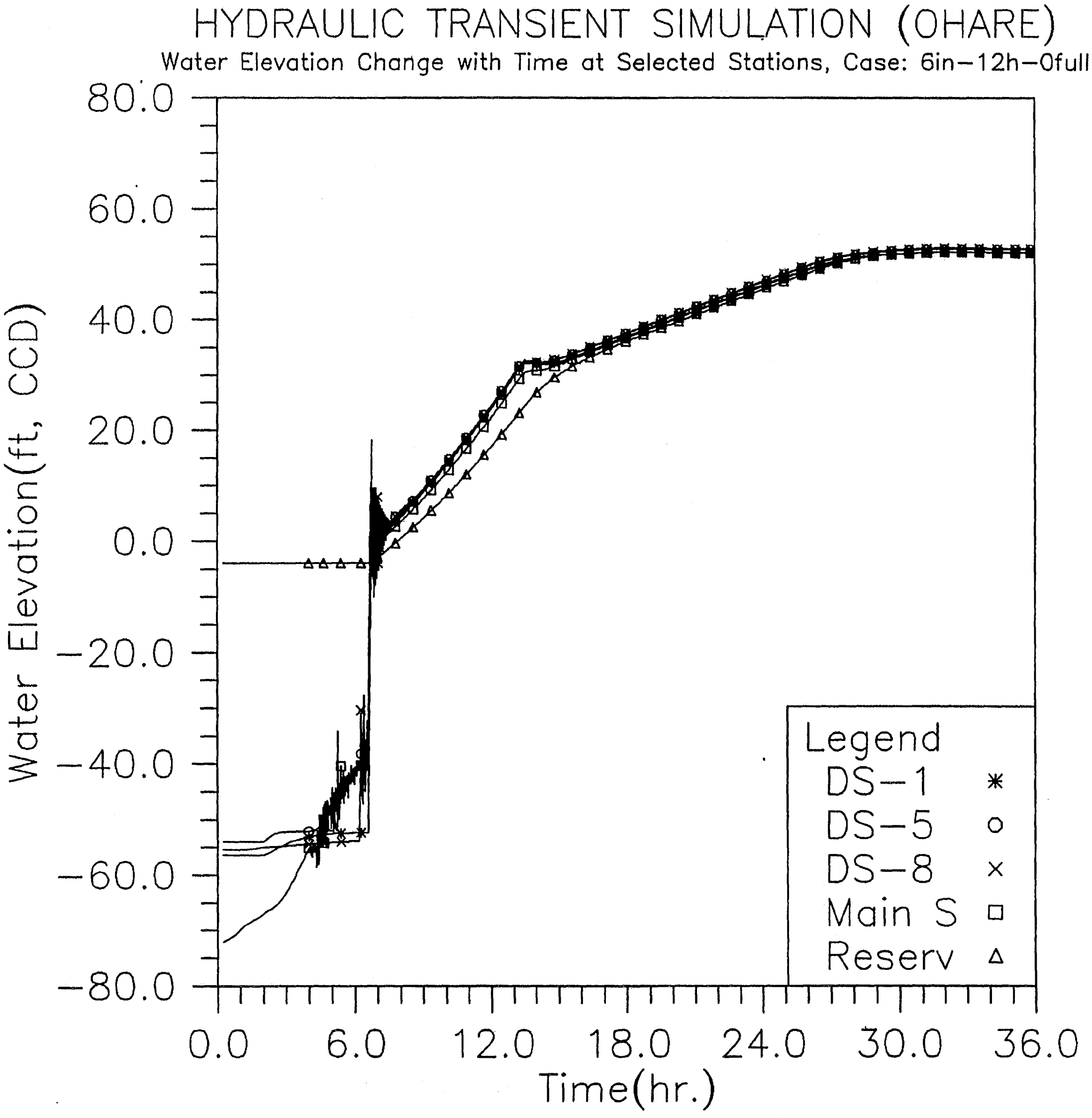

Fig. 78 Water elevation variations with time during 6 in 12 hour storm event at 5 locations (DS-1, DS-5, DS-8, main shaft and reservoir), modeling conditions: empty initial tunnel condition and ungated inflow at DS-8.

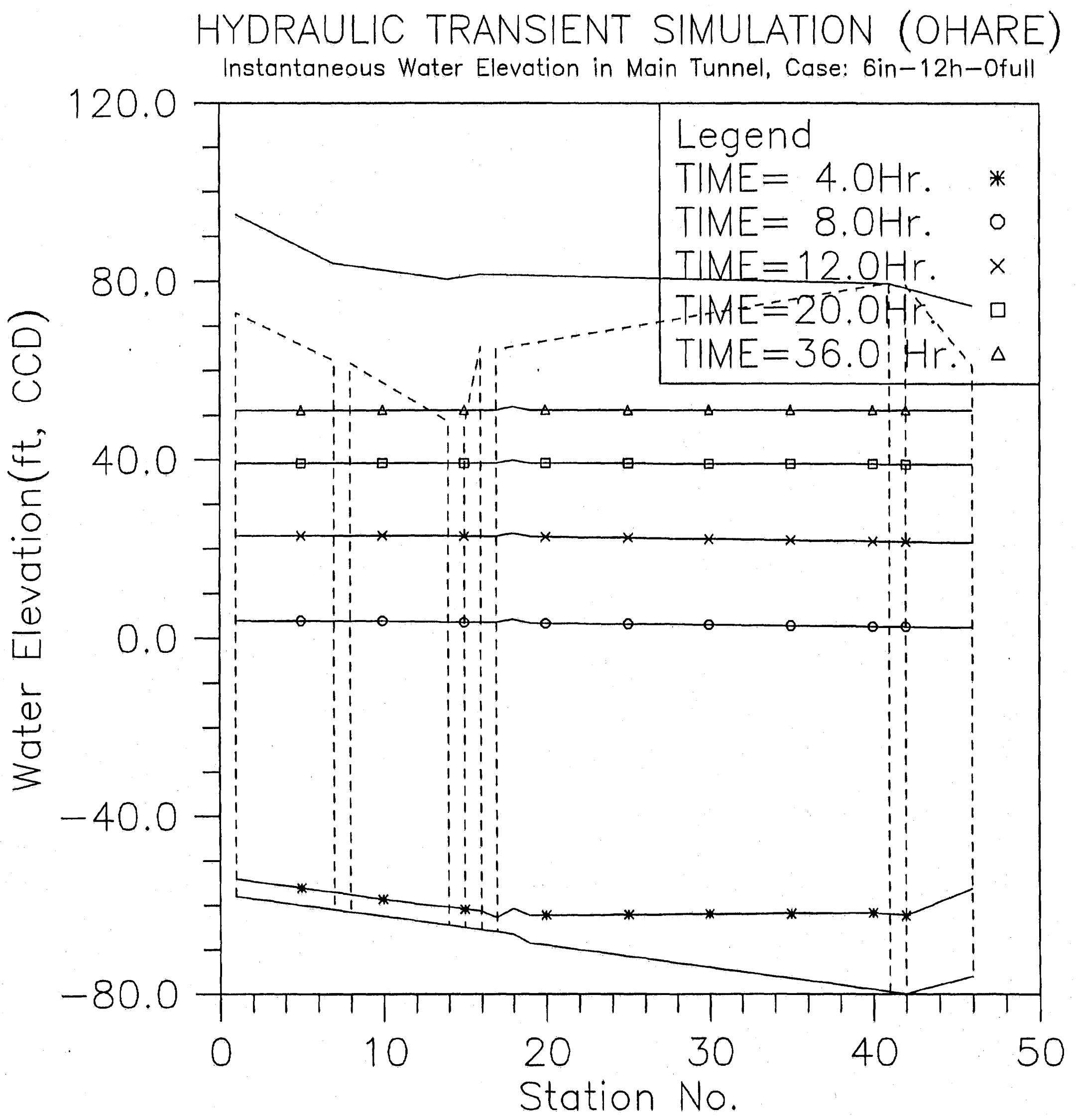

Fig. 79 Instantaneous water elevations in the main tunnel from DS-1 to the main shaft during 6 in 12 hour storm event, modeling conditions: empty initial tunnel condition and ungated inflow at DS-8.

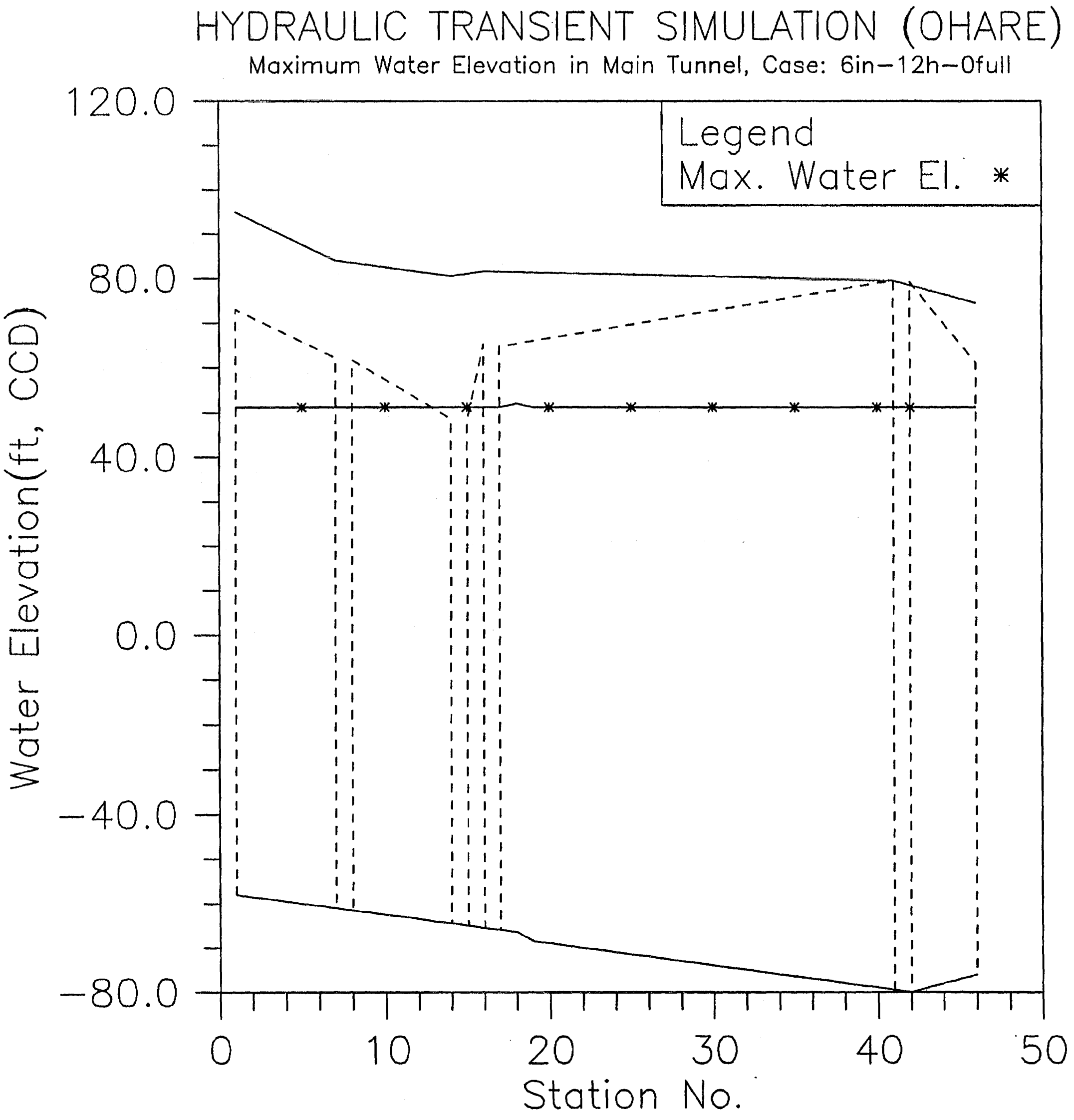

Fig. 80 Maximum water elevations in the main tunnel from DS-1 to the main shaft during 6 in 12 hour storm event, modeling conditions: empty initial tunnel condition and ungated inflow at DS-8.

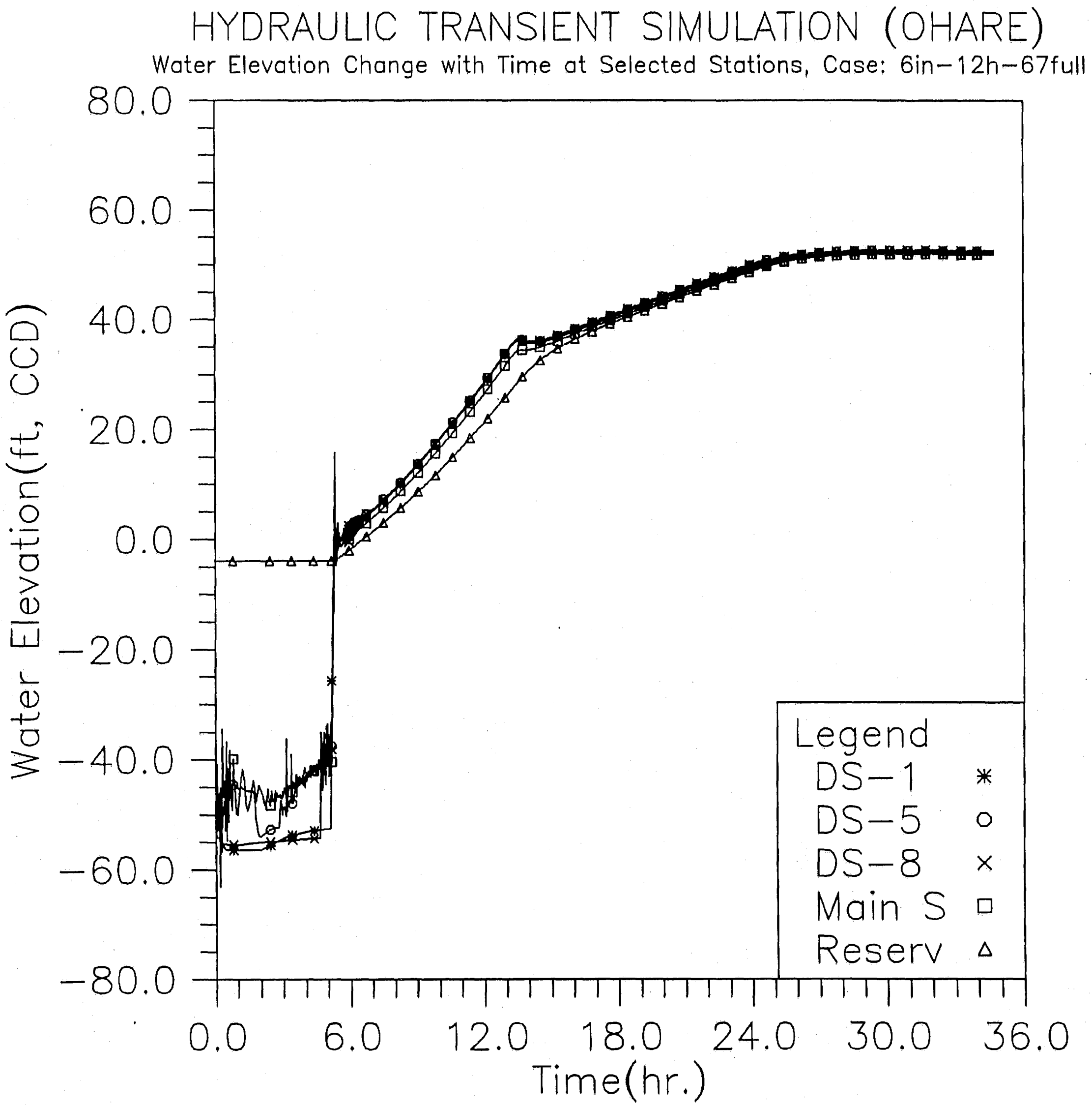

Fig. 81 Water elevation variations with time during 6 in 12 hour storm event at 5 locations (DS-1, DS-5, DS-8, main shaft and reservoir), modeling conditions: 67% full initial tunnel condition and ungated inflow at DS-8.

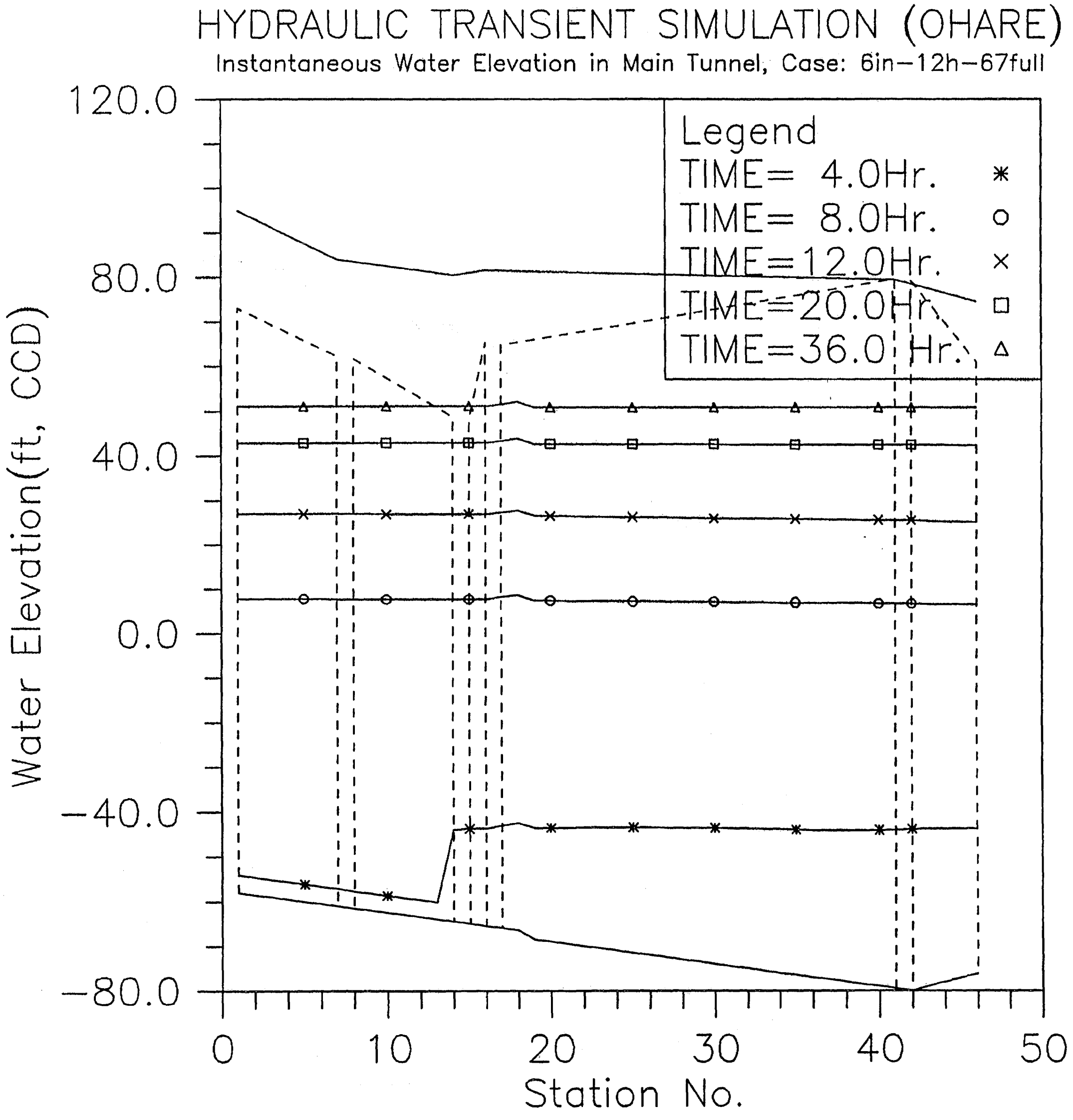

Fig. 82 Instantaneous water elevations in the main tunnel from DS-1 to the main shaft during 6 in 12 hour storm event, modeling conditions: 67% full initial tunnel condition and ungated inflow at DS-8.

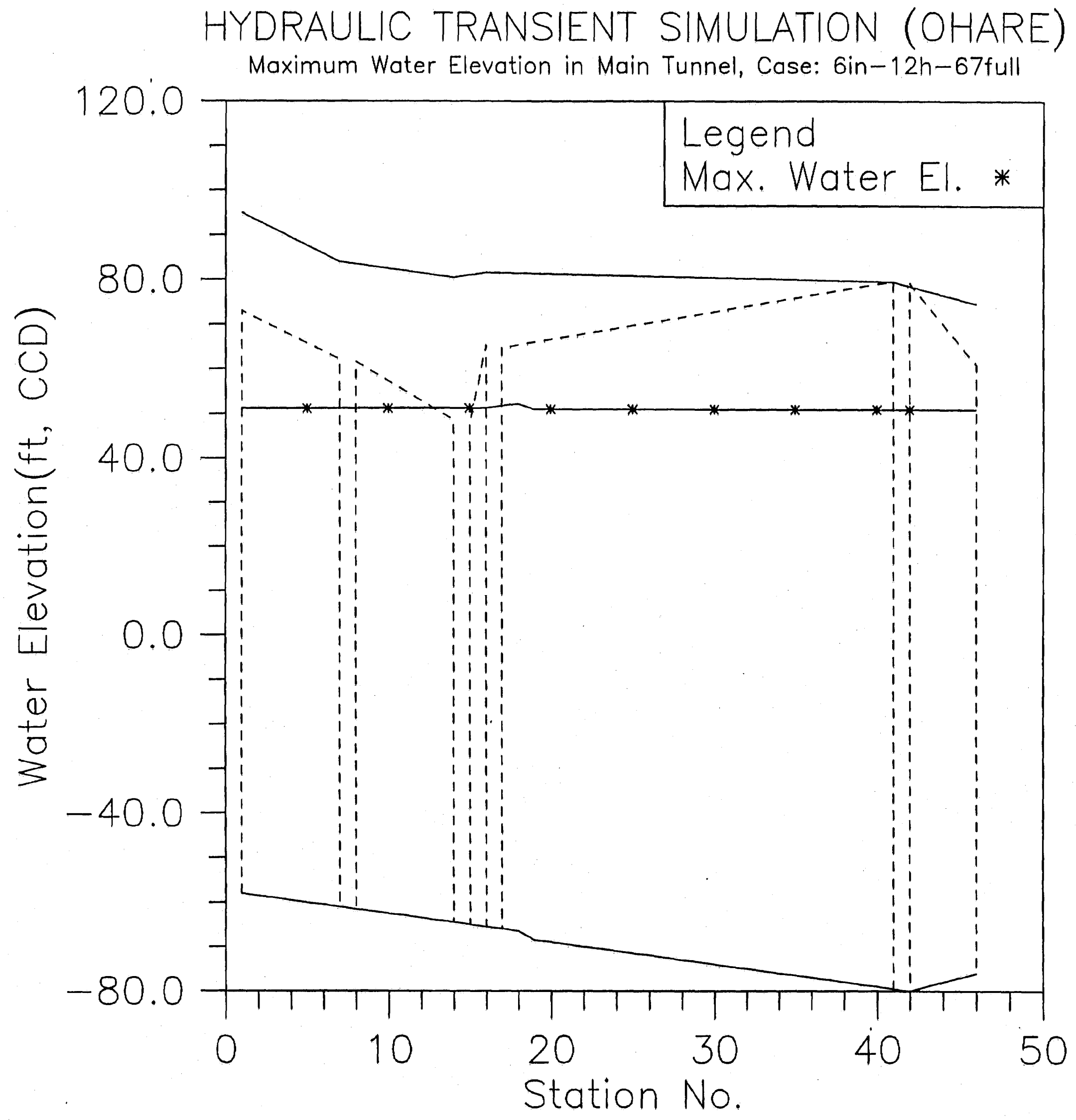

Fig. 83 Maximum water elevations in the main tunnel from DS-1 to the main shaft during 6 in 12 hour storm event, modeling conditions: 67% full initial tunnel condition and ungated inflow at DS-8.

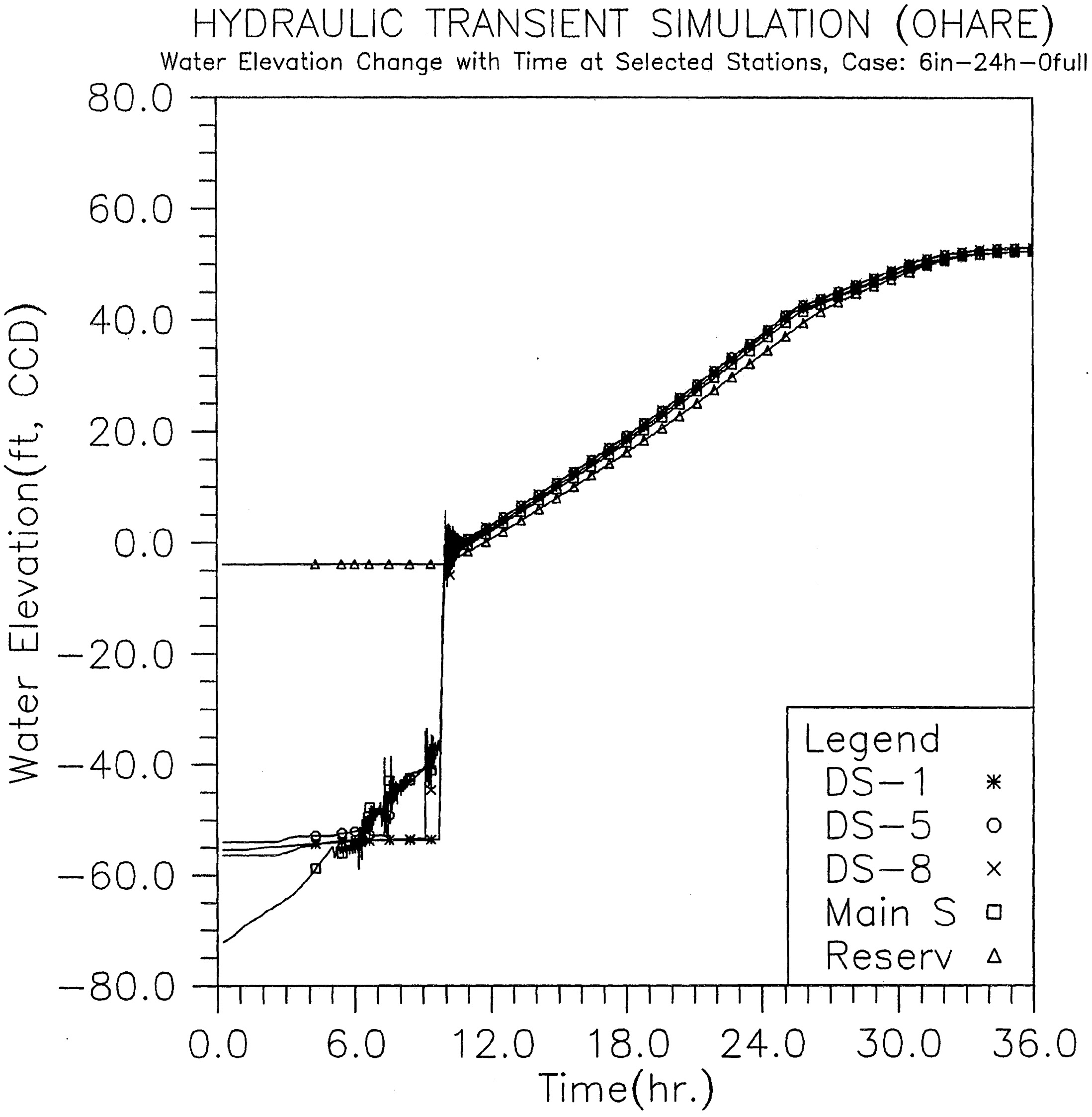

Fig. 84 Water elevation variations with time during 6 in 24 hour storm event at 5 locations (DS-1, DS-5, DS-8, main shaft and reservoir), modeling conditions: empty initial tunnel condition and ungated inflow at DS-8.

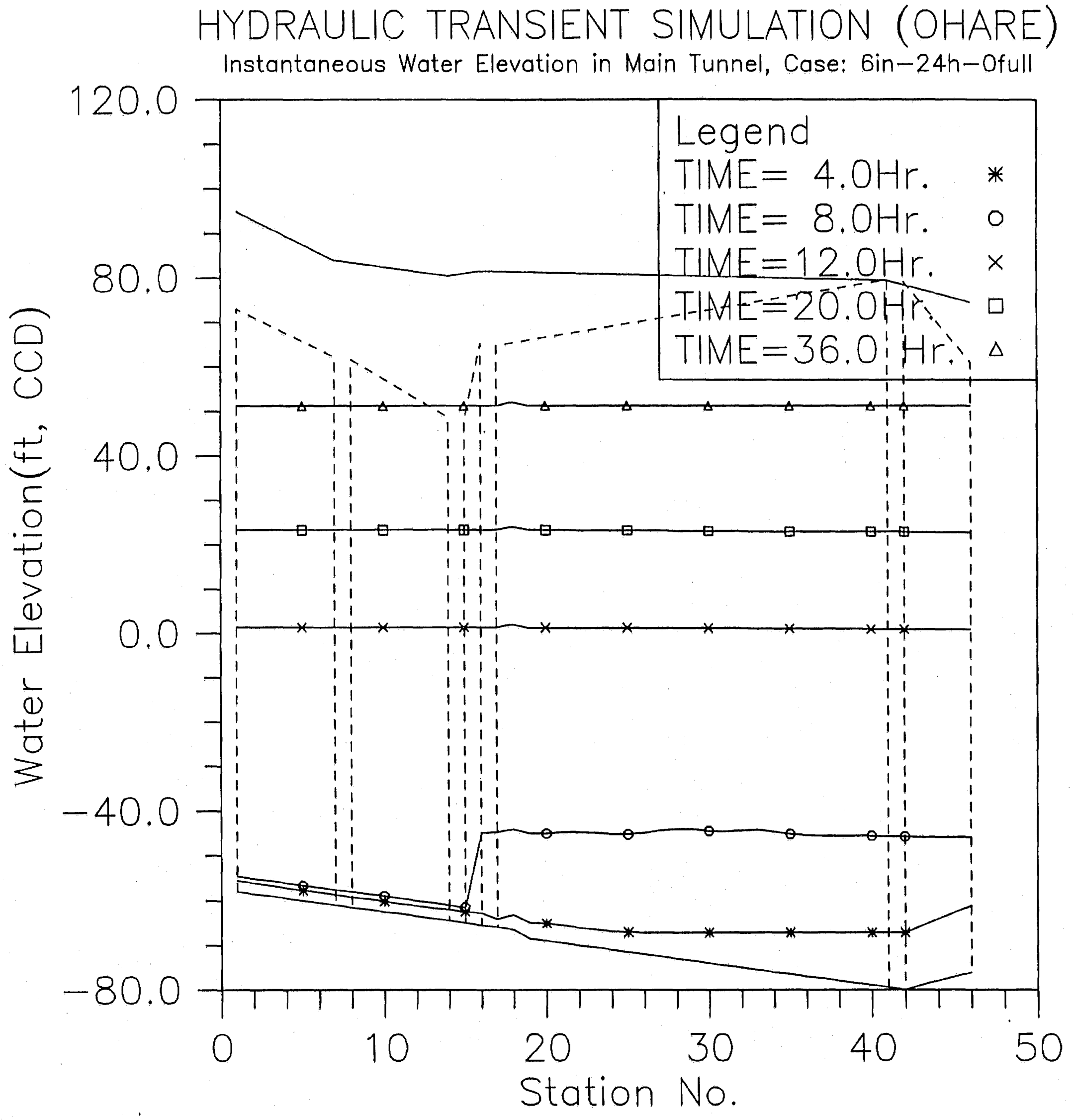

Fig. 85 Instantaneous water elevations in the main tunnel from DS-1 to the main shaft during 6 in 24 hour storm event, modeling conditions: empty initial tunnel condition and ungated inflow at DS-8.

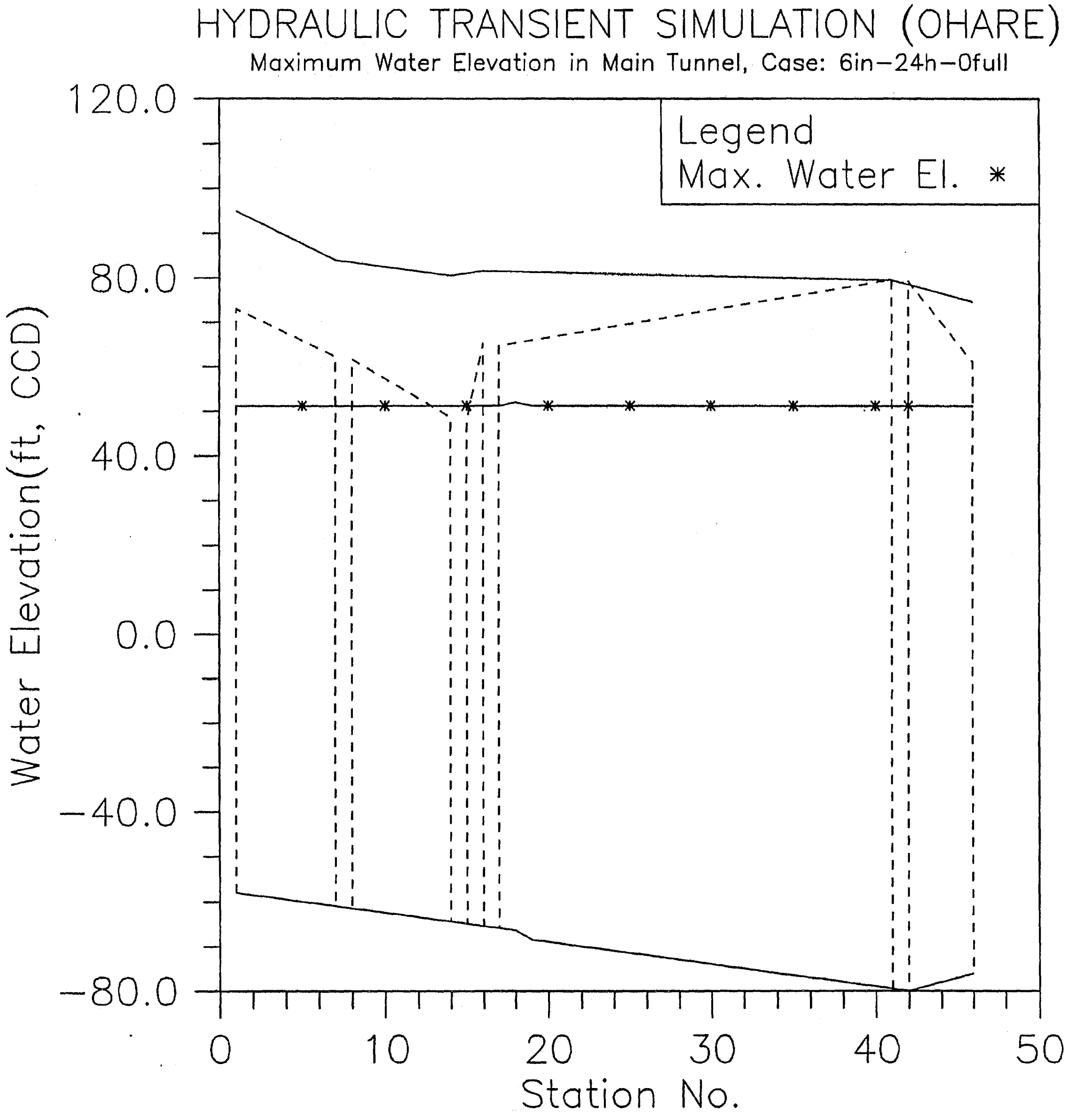

Fig. 86 Maximum water elevations in the main tunnel from DS-1 to the main shaft during 6 in 24 hour storm event, modeling conditions: empty initial tunnel condition and ungated inflow at DS-8.

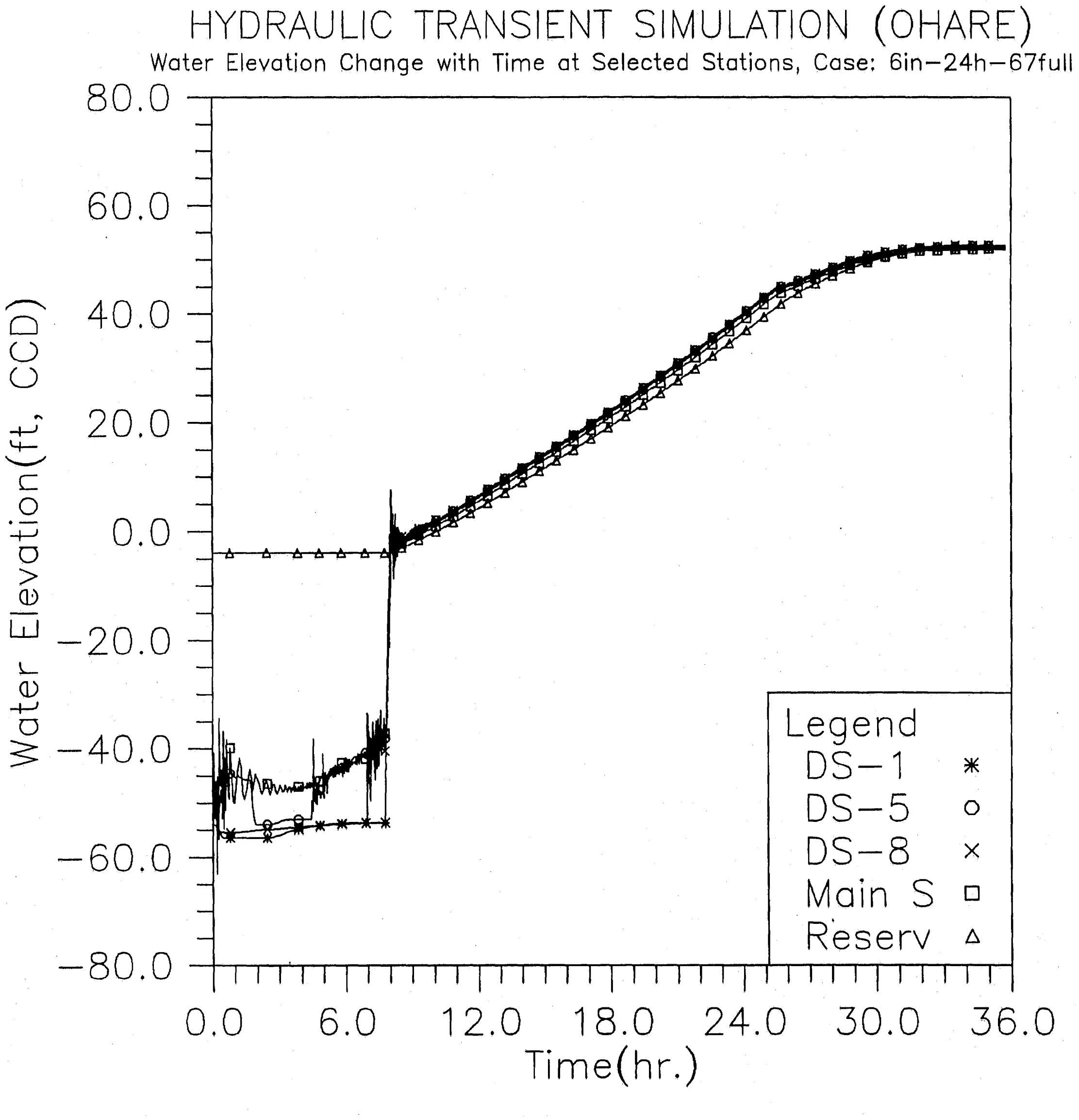

Fig. 87 Water elevation variations with time during 6 in 24 hour storm event at 5 locations (DS-1, DS-5, DS-8, main shaft and reservoir), modeling conditions: 67% full initial tunnel condition and ungated inflow at DS-8.

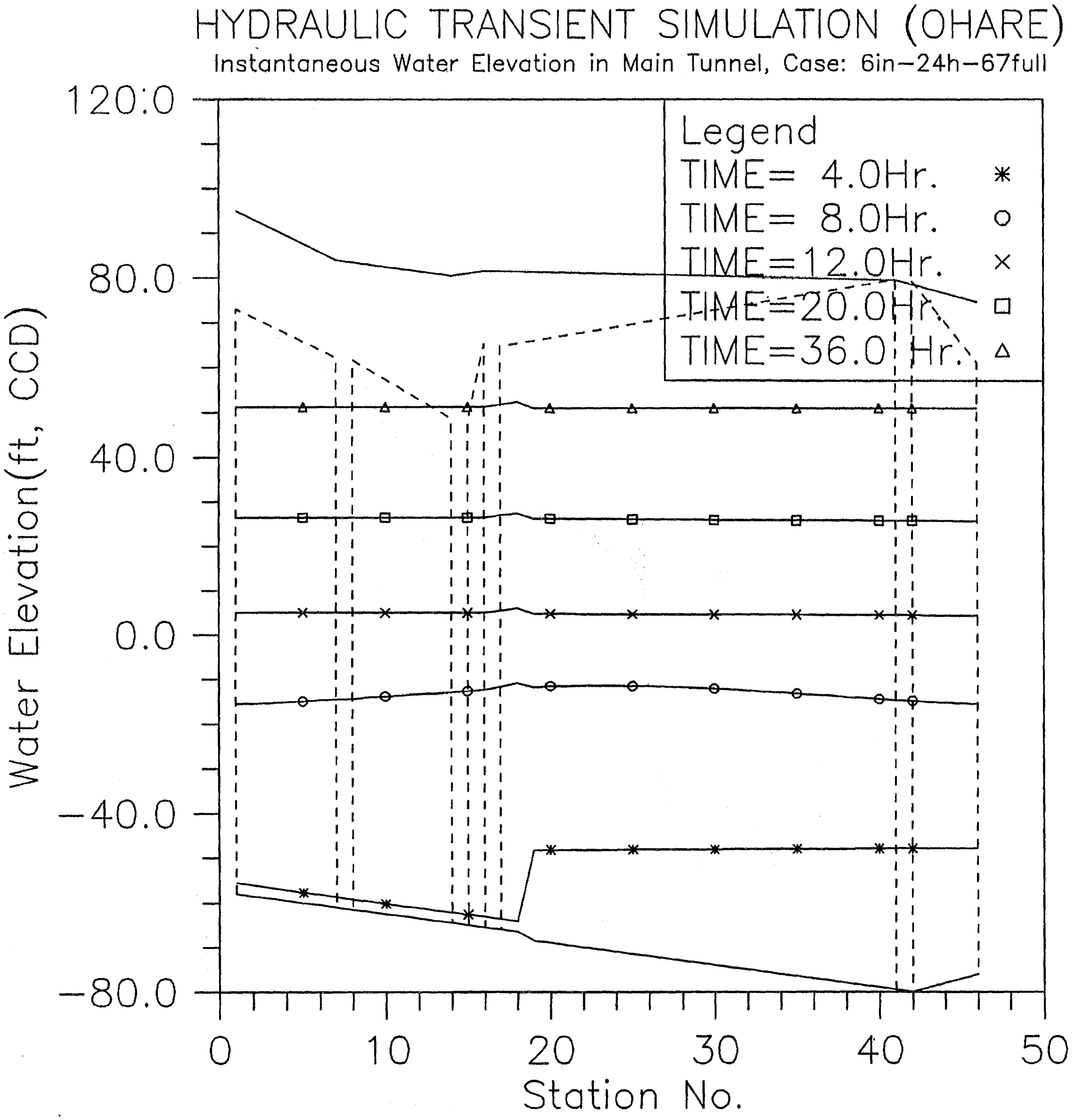

Fig. 88 Instantaneous water elevations in the main tunnel from DS-1 to the main shaft during 6 in 24 hour storm event, modeling conditions: 67% full initial tunnel condition and ungated inflow at DS-8.

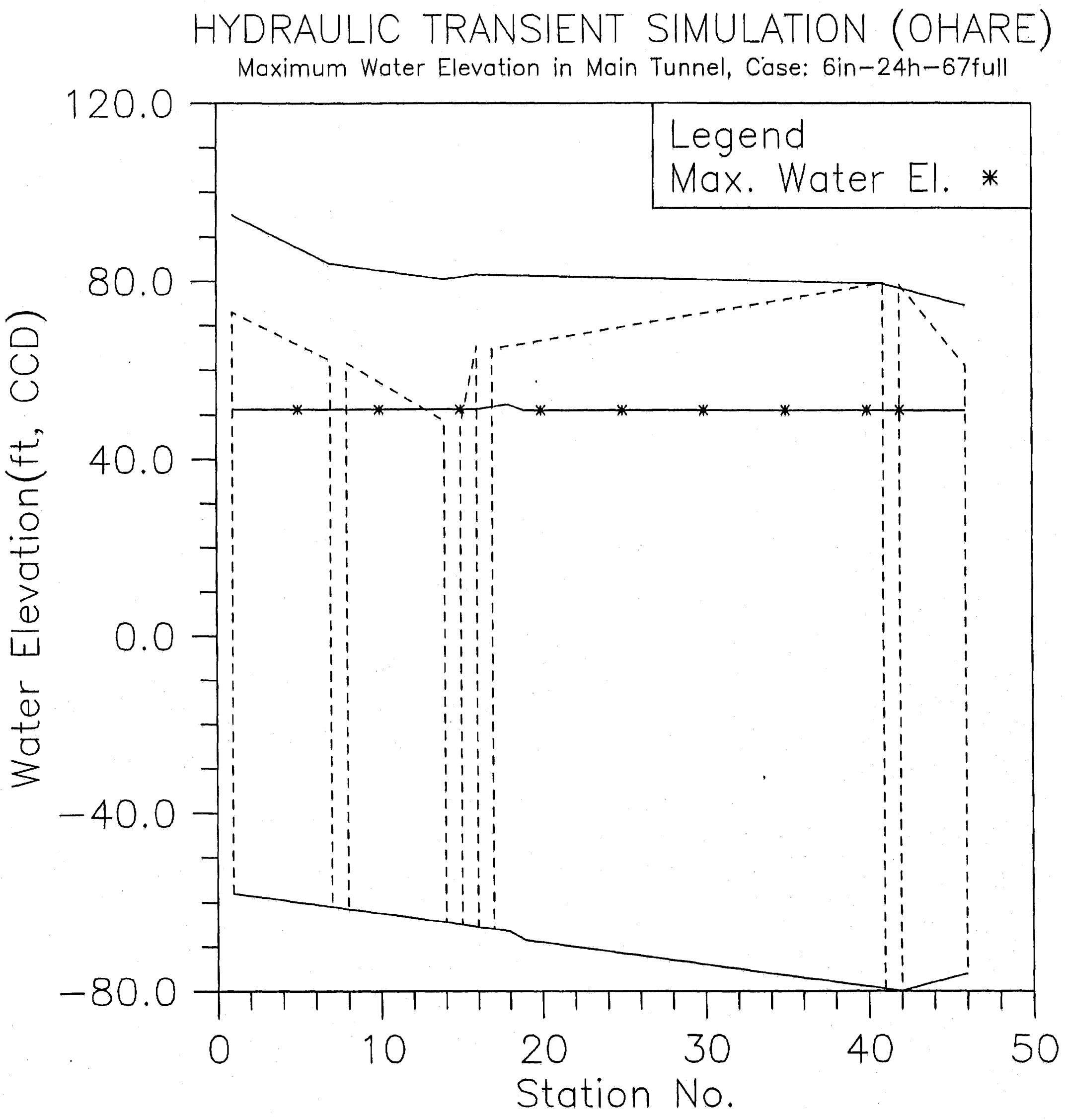

Fig. 89 Maximum water elevations in the main tunnel from DS-1 to the main shaft during 6 in 24 hour storm event, modeling conditions: 67% full initial tunnel condition and ungated inflow at DS-8.

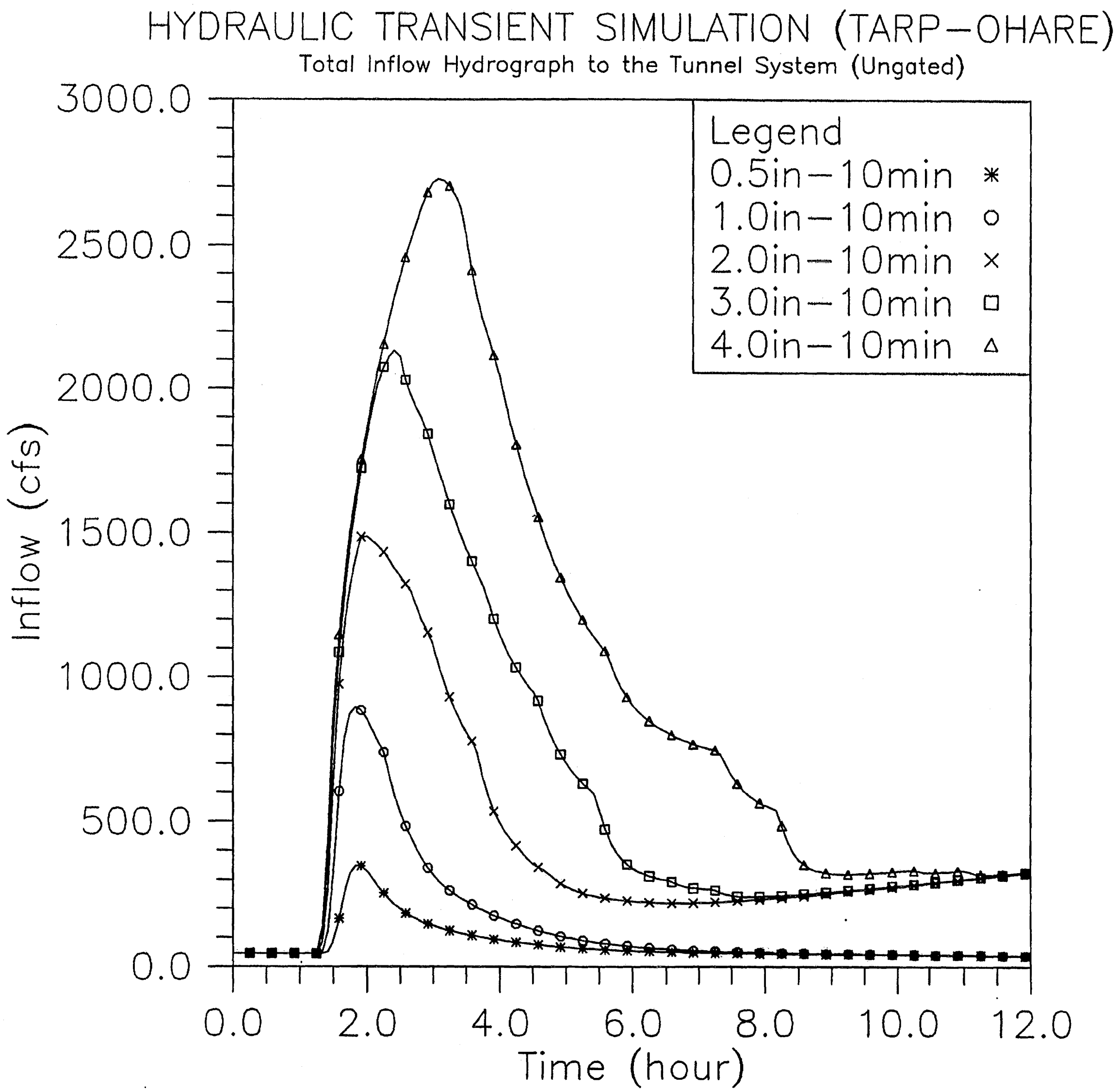

Fig. 90 Total inflow hydrodraphs to the tunnel system for 10 min storm events (combined inflow at DS-8).

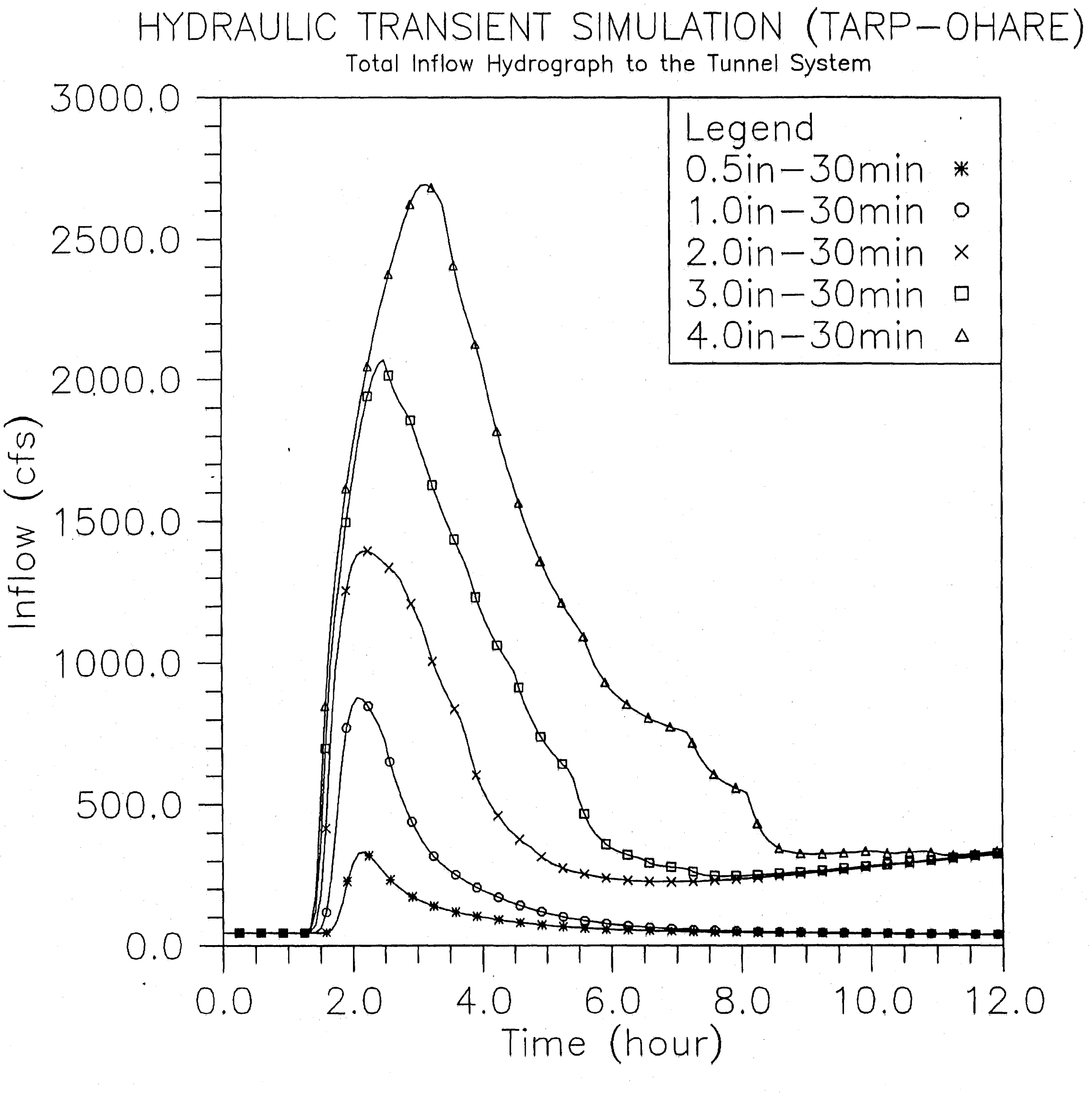

Fig. 91 Total inflow hydrodraphs to the tunnel system for 30 min storm events (combined inflow at DS-8).

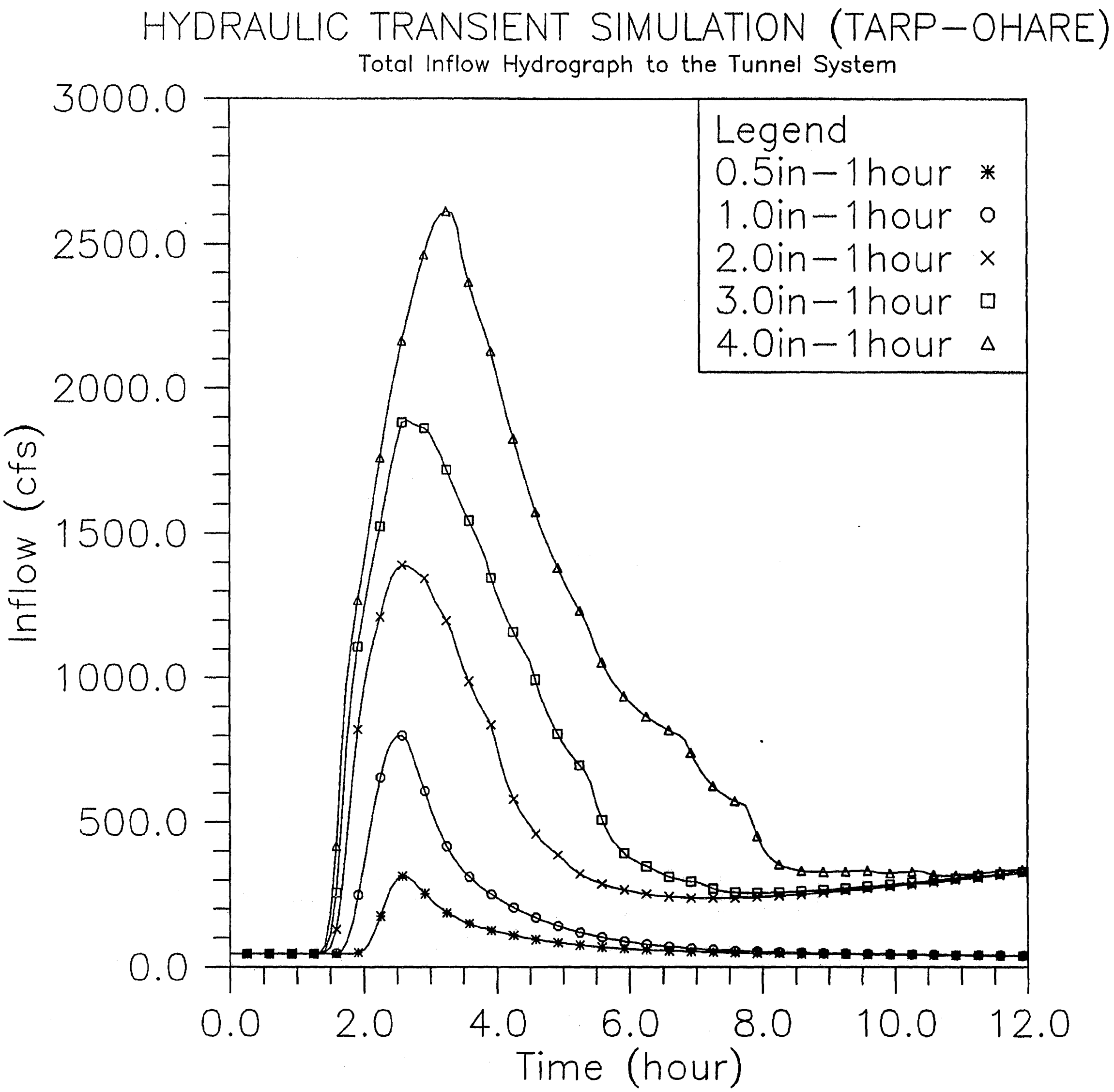

Fig. 92 Total inflow hydrodraphs to the tunnel system for 1 hour storm events (combined inflow at DS-8).

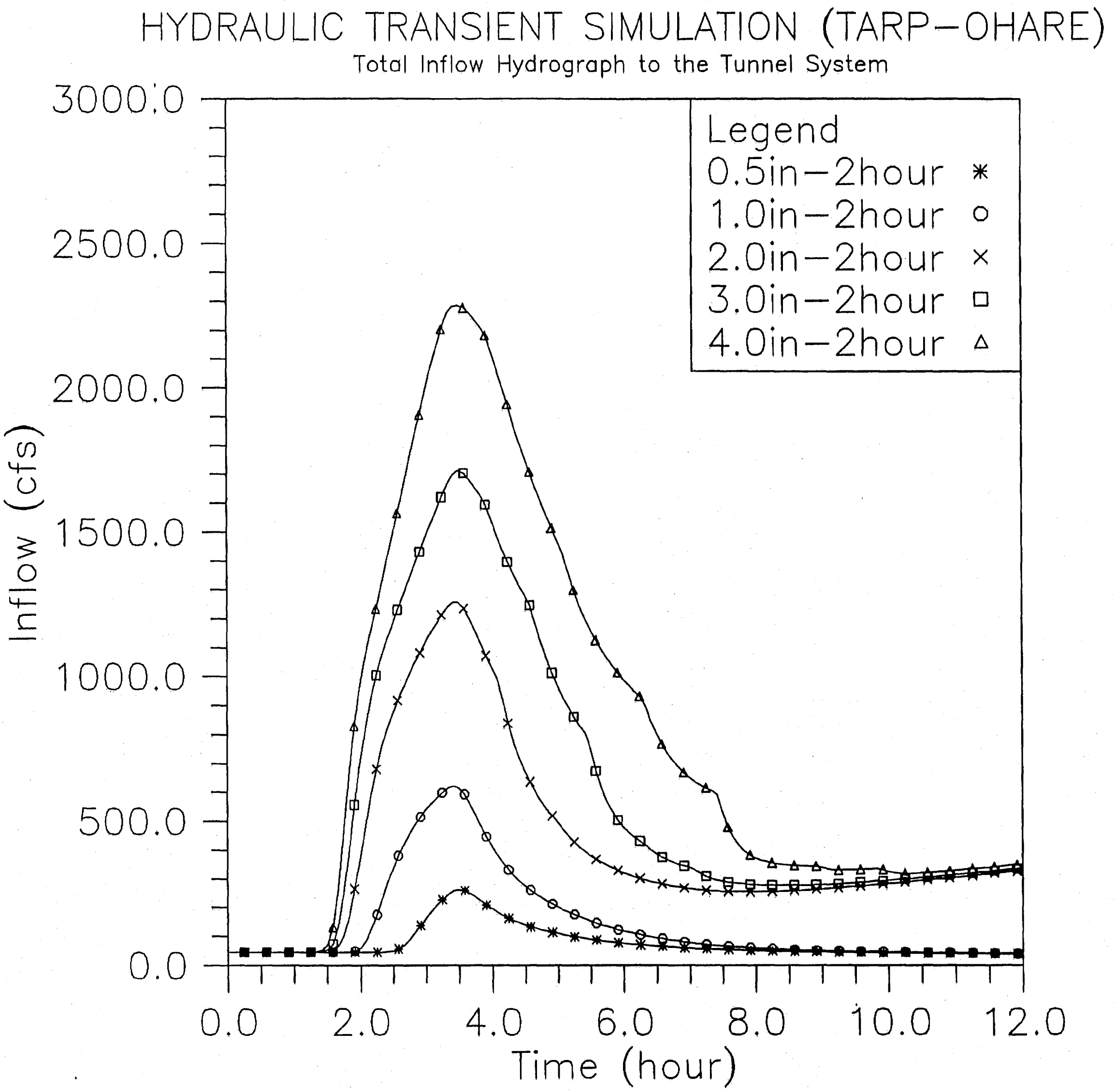

Fig. 93 Total inflow hydrodraphs to the tunnel system for 2 hour storm events (combined inflow at DS-8).

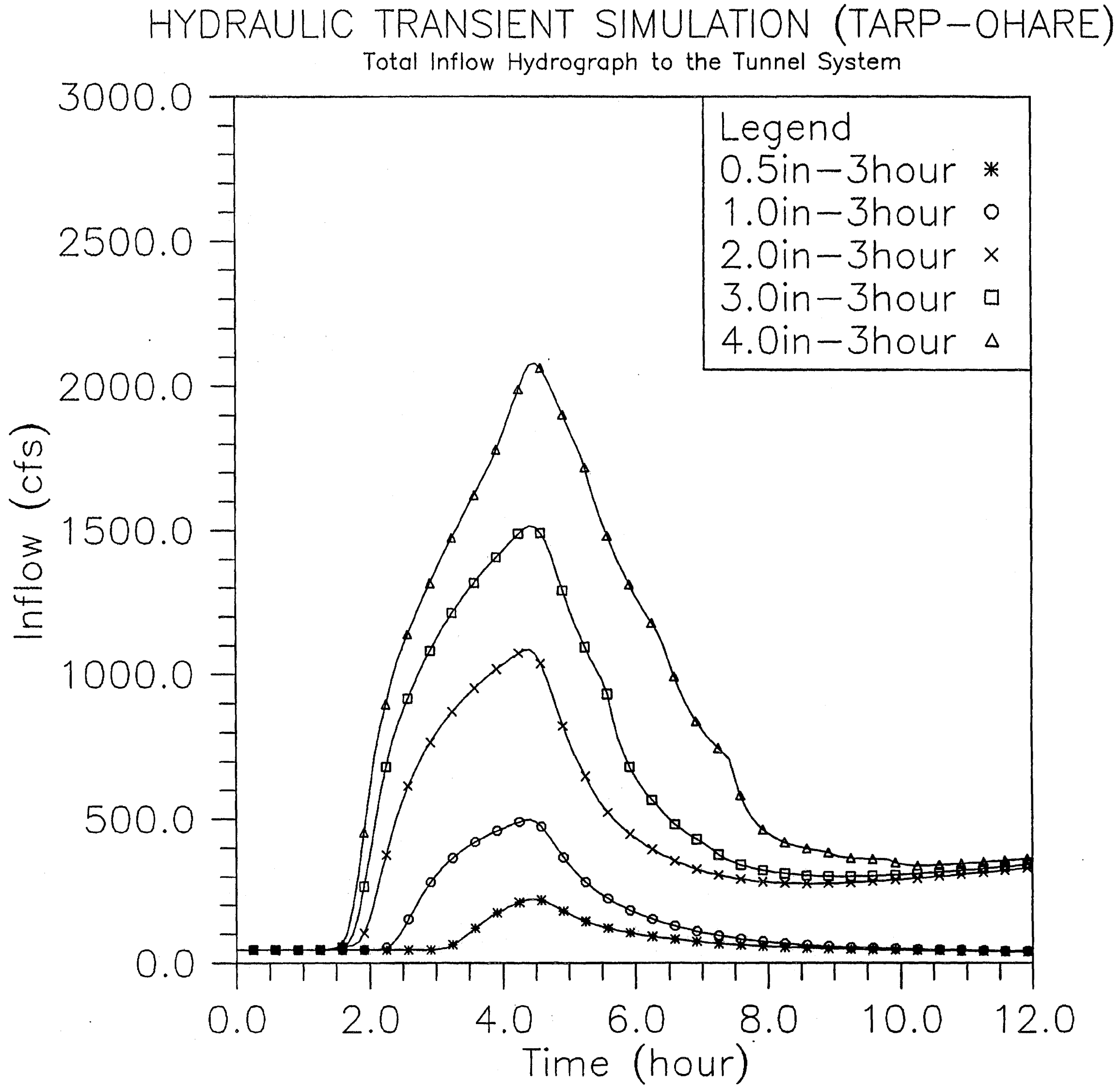

Fig. 94 Total inflow hydrodraphs to the tunnel system for 3 hour storm events (combined inflow at DS-8).

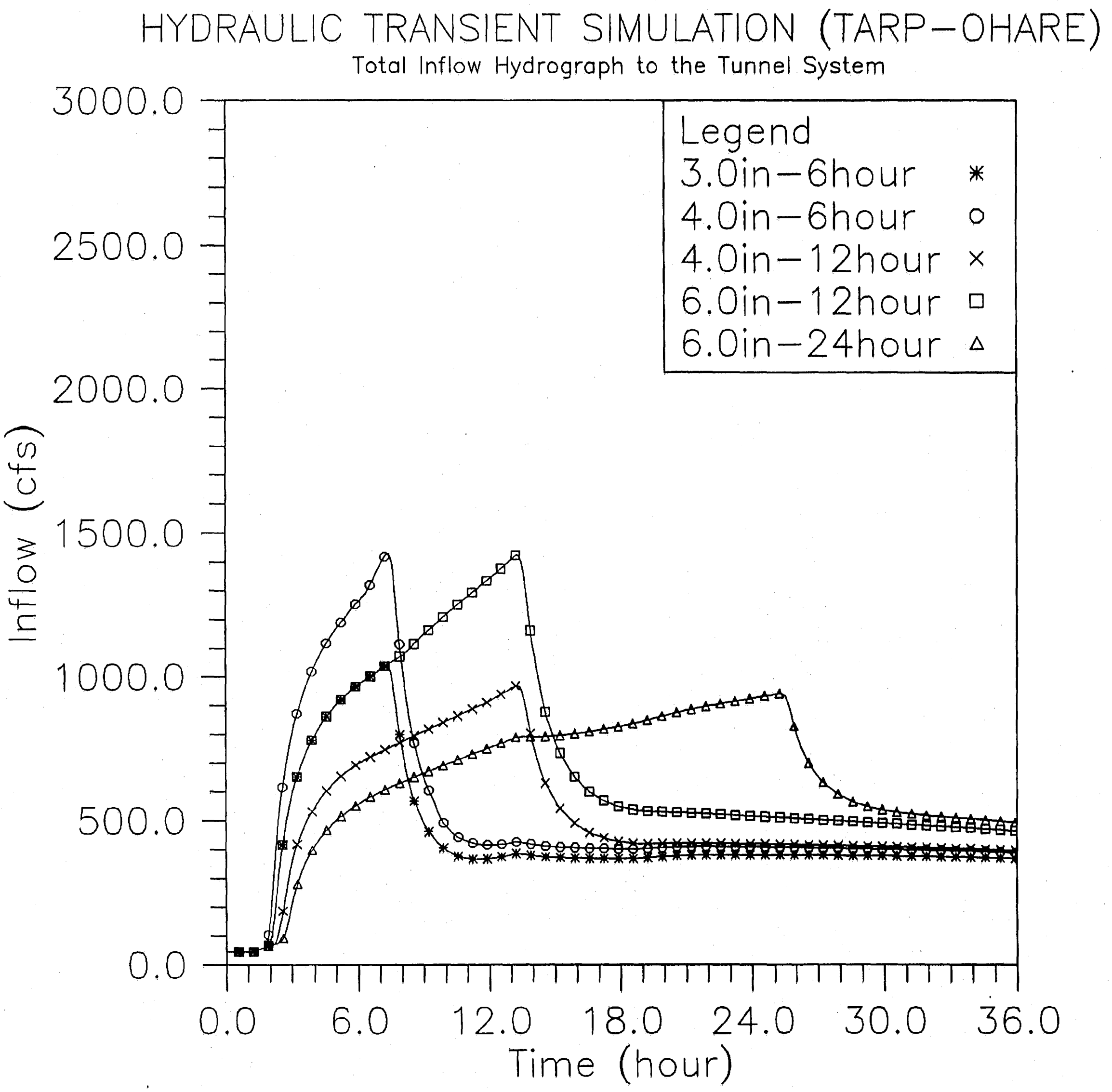

Fig. 95 Total inflow hydrodraphs to the tunnel system for 6 to 24 hour storm events (combined inflow at DS-8).

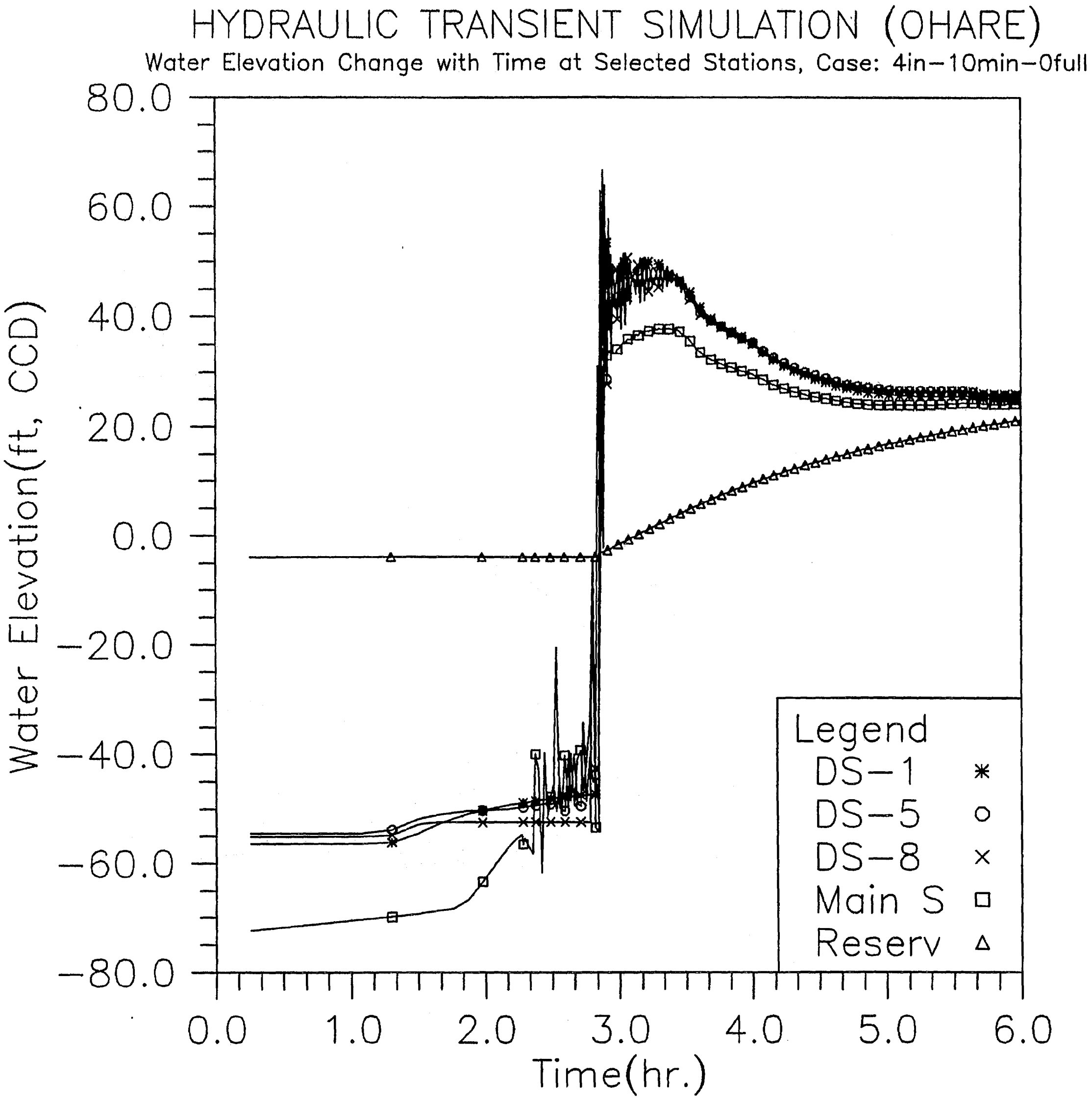

Fig. 96 Water elevation variations with time during 4 in 10 min storm event at 5 locations (DS-1, DS-5, DS-8, main shaft and reservoir), modeling conditions: empty initial tunnel condition, wave speed=400 ft/s, and combined inflow at DS-8.

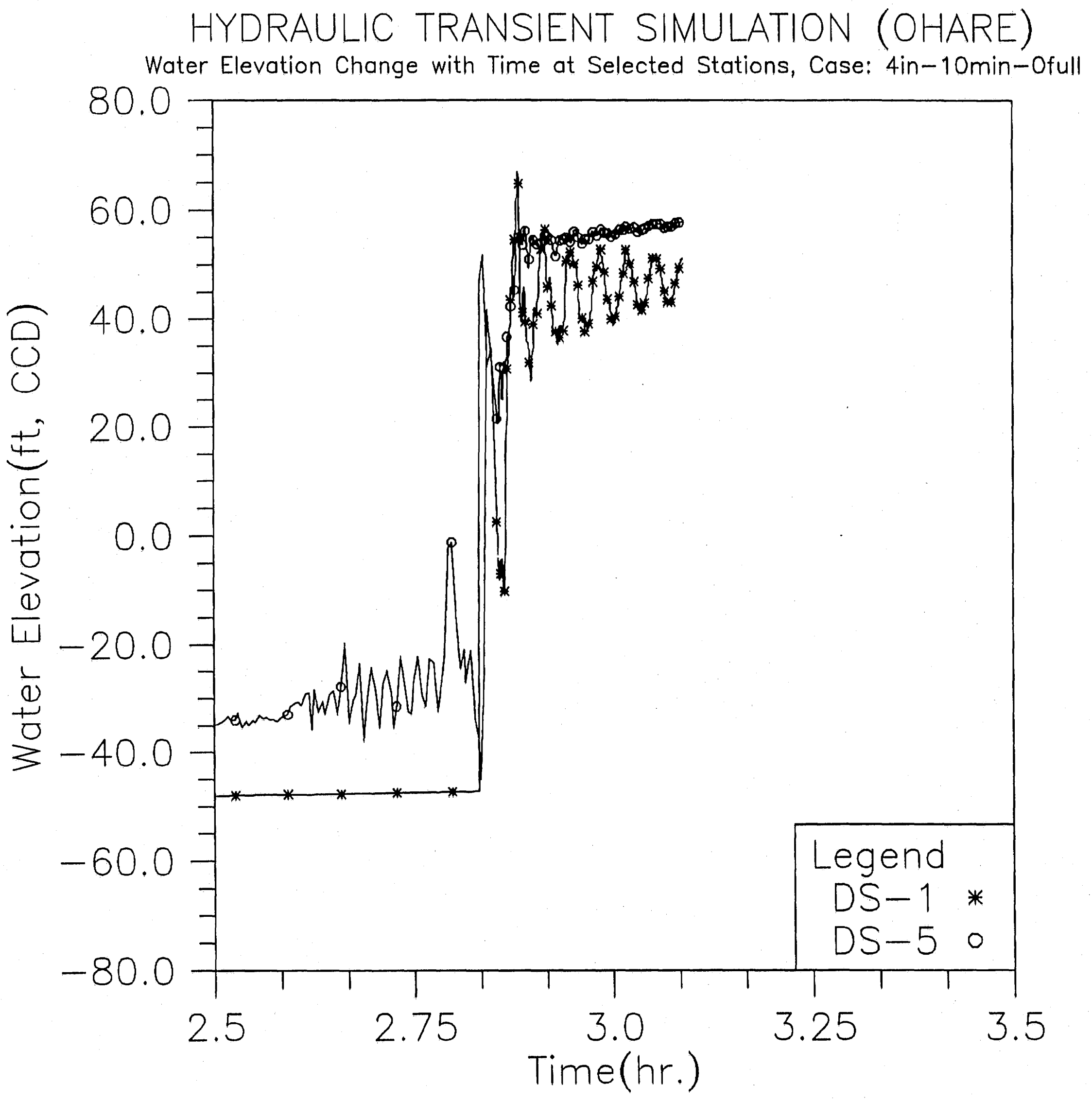

Fig. 97 Detailed water elevation variations with time in the surge process during 4 in 10 min storm event at 2 locations (DS-1 and DS-5), modeling conditions: empty initial tunnel condition, wave speed=400 ft/s, and combined inflow at DS-8.

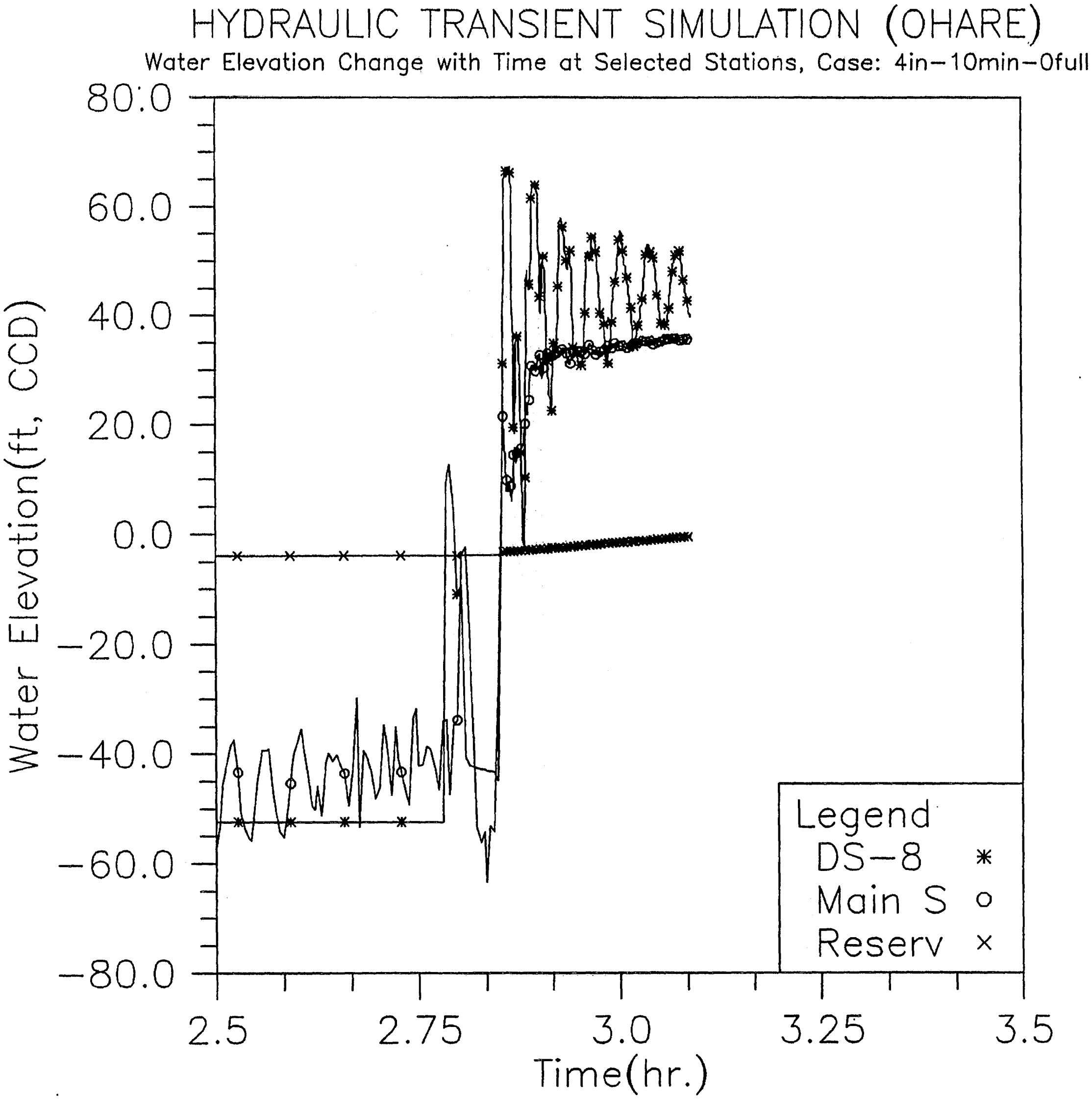

Fig. 98 Detailed water elevation variations with time in the surge process during 4 in 10 min storm event at 3 locations (DS-8, main shaft and reservoir), modeling conditions: empty initial tunnel condition, wave speed=400 ft/s, and combined inflow at DS-8.

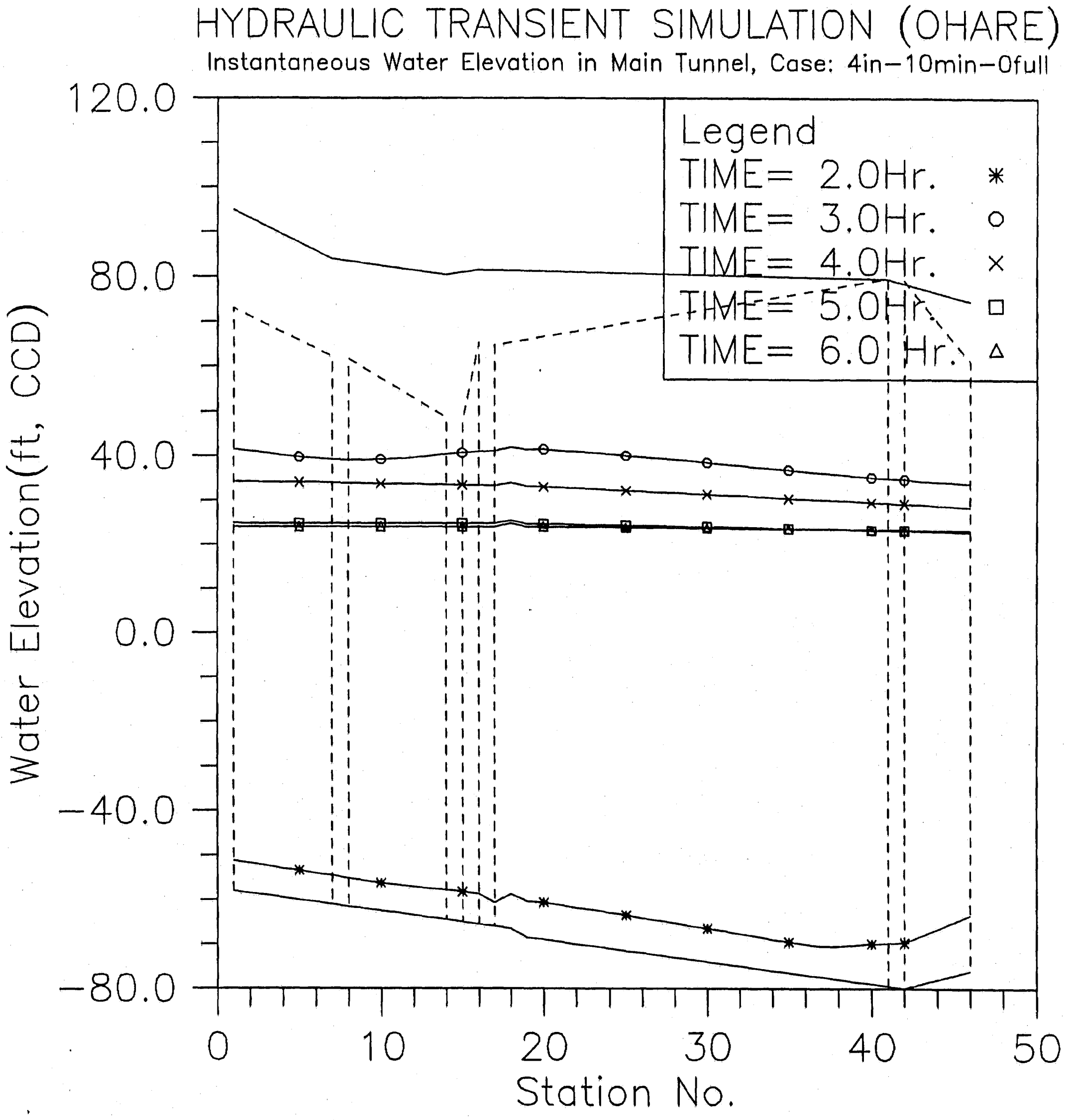

Fig. 99 Instantaneous water elevations in the main tunnel from DS-1 to the main shaft during 4 in 10 min storm event, modeling conditions: empty initial tunnel condition, wave speed=400 ft/s, and combined inflow at DS-8.

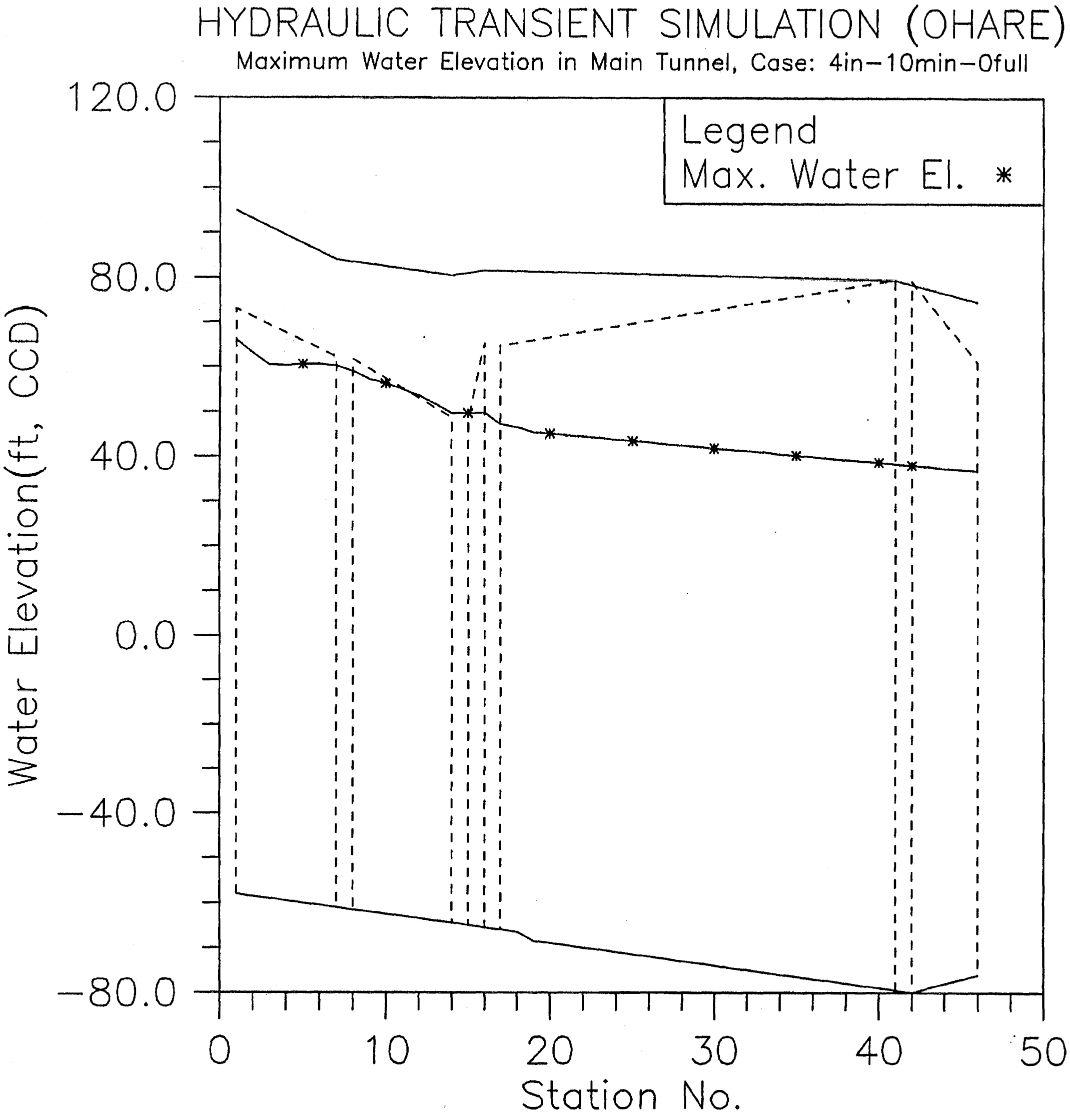

Fig. 100 Maximum water elevations in the main tunnel from DS-1 to the main shaft during 4 in 10 min storm event, modeling conditions: empty initial tunnel condition, wave speed=400 ft/s, and combined inflow at DS-8.

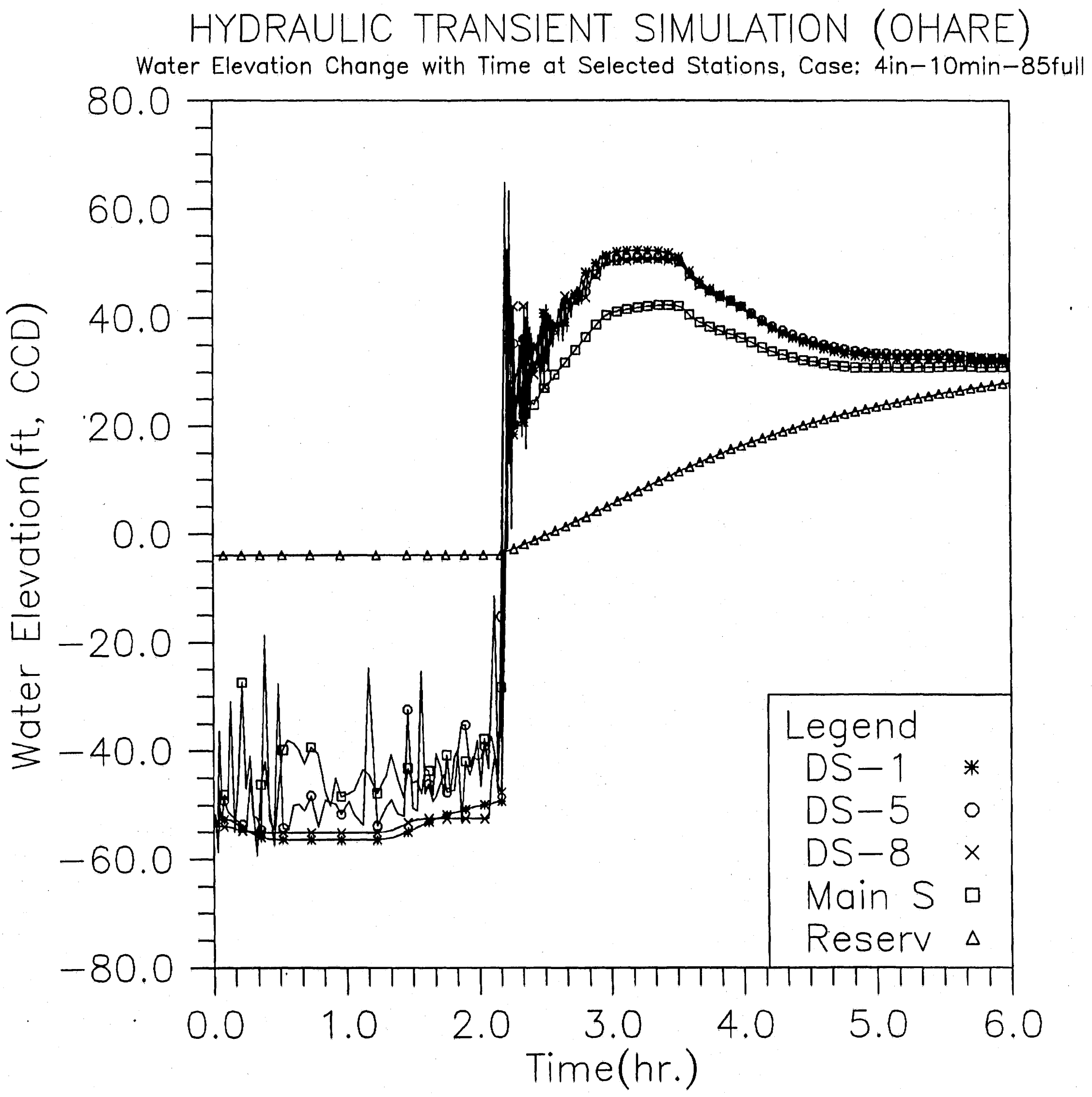

Fig. 101 Water elevation variations with time during 4 in 10 min storm event at 5 locations (DS-1, DS-5, DS-8, main shaft and reservoir), modeling conditions: initially 85% full tunnel condition, wave speed=400 ft/s, and combined inflow at DS-8.

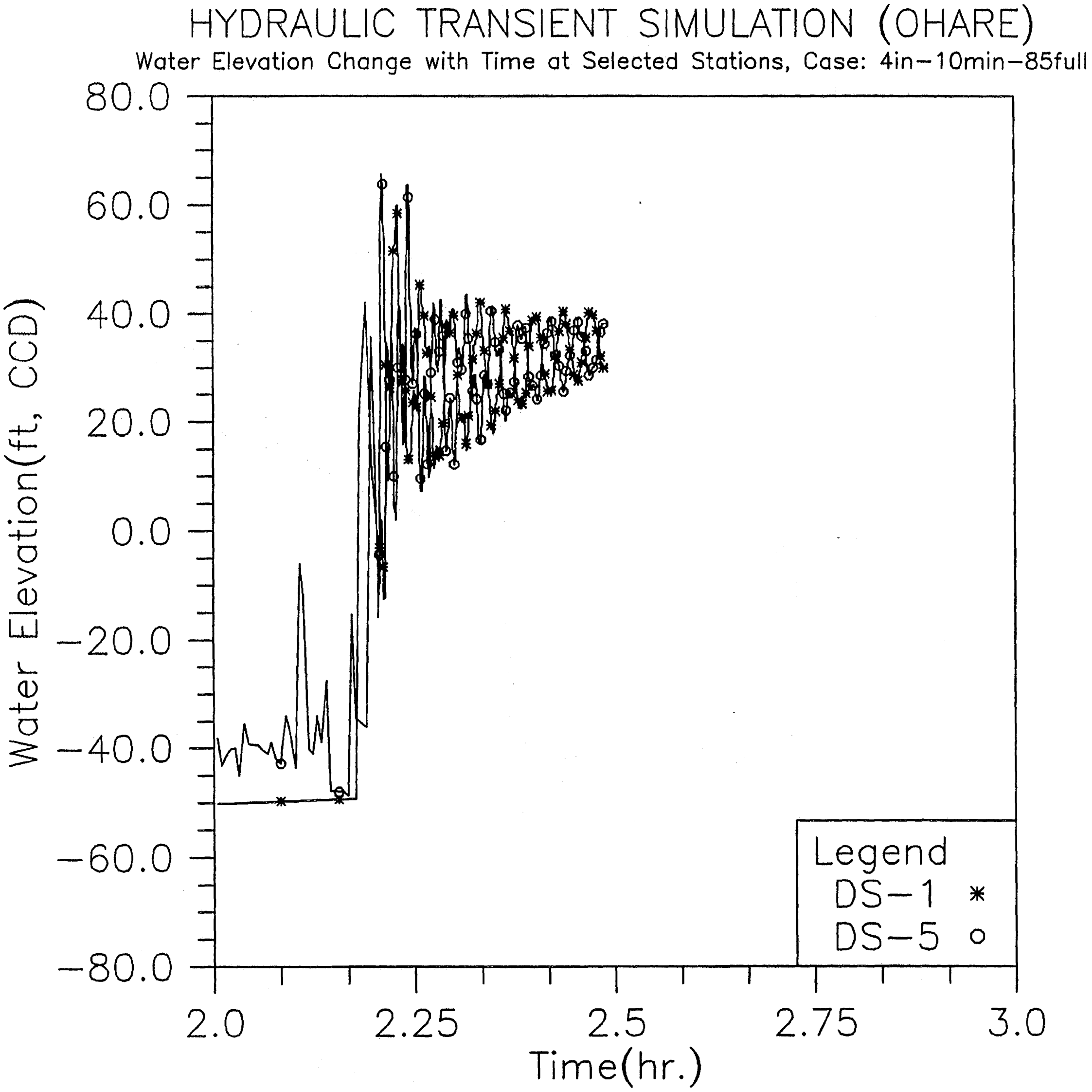

Fig. 102 Detailed water elevation variations with time in the surge process during 4 in 10 min storm event at 2 locations (DS-1 and DS-5), modeling conditions: initially 85% full tunnel condition, wave speed=400 ft/s, and combined inflow at DS-8.

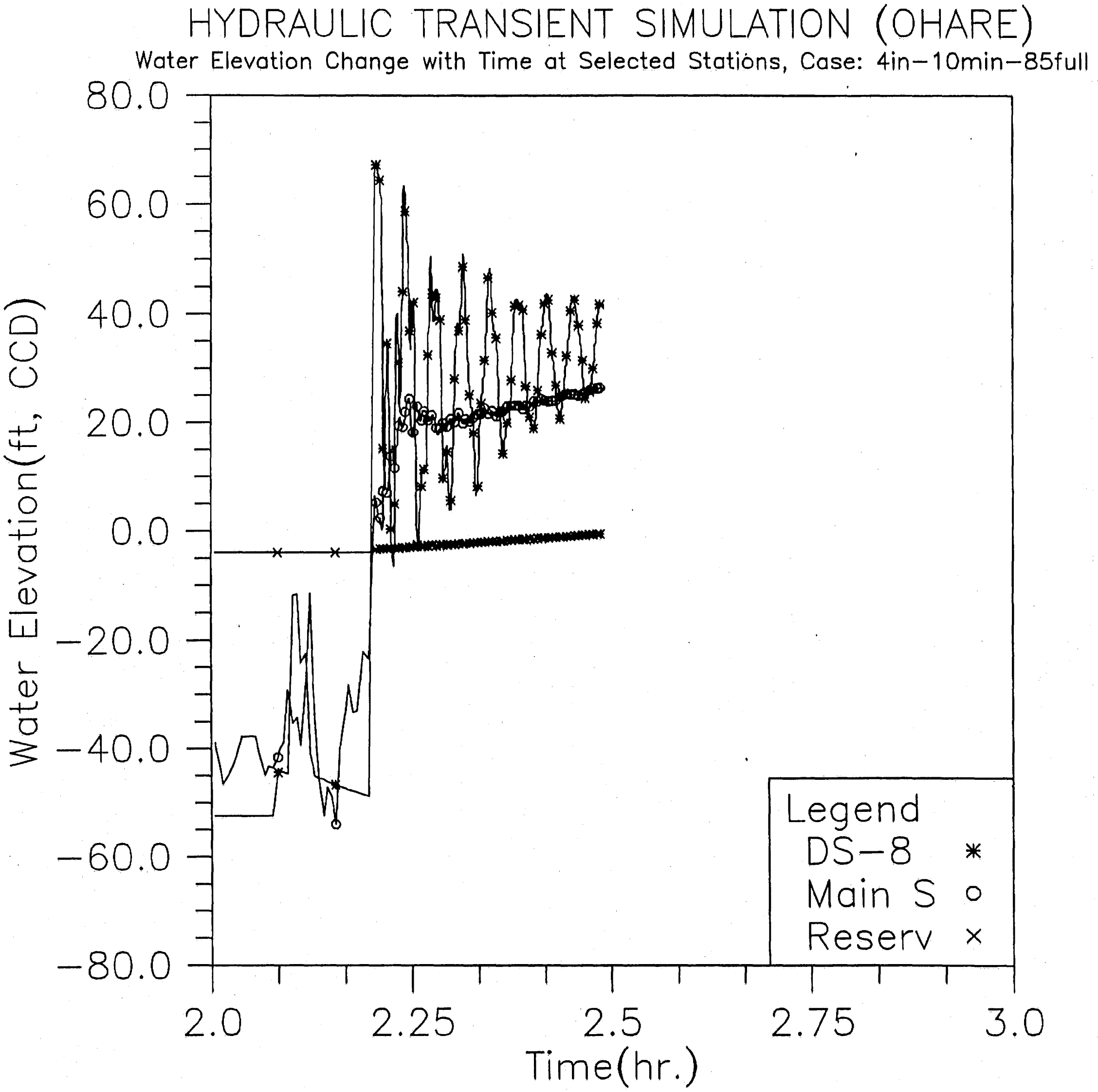

Fig. 103 Detailed water elevation variations with time in the surge process during 4 in 10 min storm event at 3 locations (DS-8, main shaft and reservoir), modeling conditions: initially 85% full tunnel condition, wave speed=400 ft/s, and combined inflow at DS-8.

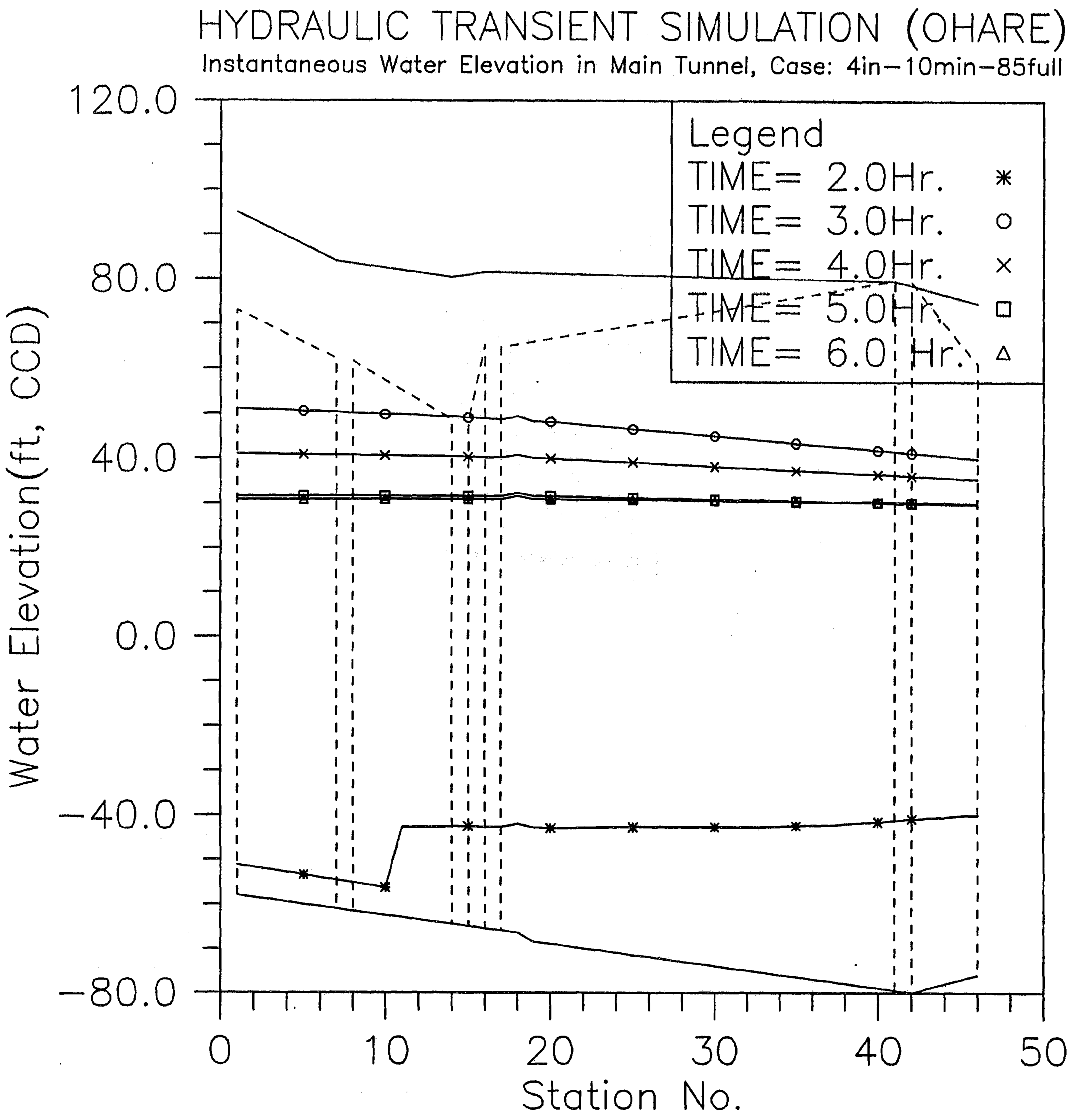

Fig. 104 Instantaneous water elevations in the main tunnel from DS-1 to the main shaft during 4 in 10 min storm event, modeling conditions: initially 85% full tunnel condition, wave speed=400 ft/s, and combined inflow at DS-8.

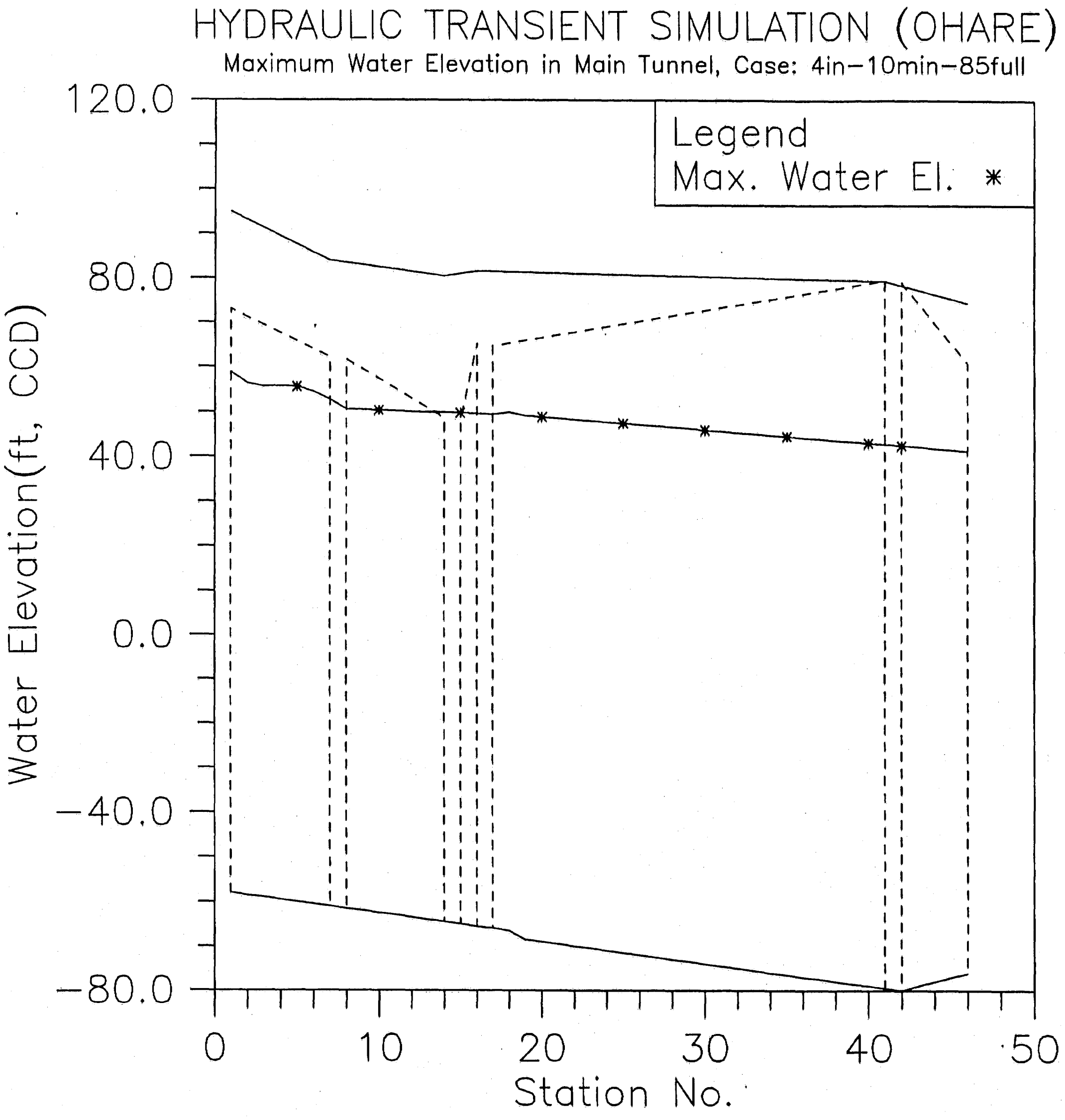

Fig. 105 Maximum water elevations in the main tunnel from DS-1 to the main shaft during 4 in 10 min storm event, modeling conditions: initially 85% full tunnel condition, wave speed=400 ft/s, and combined inflow at DS-8.